Modelling of Neighbourhood Effect in Cities by Coupling Computational Fluid Dynamics and Building Energy Simulation Techniques

Ruijun ZHANG

Department of Architecture and Built Environment

University of Nottingham

This thesis is submitted for the degree of

Doctor of Philosophy

Aug., 2021

ABSTRACT

Building energy simulation (BES) is widely applied to assess indoor comfort and building energy demand, which is reported to encompass a one-third share of the world's energy demand in 2021. There is a range of worldwide accepted building energy simulation packages in hand, such as EnergyPlus ©, Revit©, DOE-2©. These tools comprise series of subroutines to predict the behaviour of systems within the buildings. The calculations in these programs are based on the combination of well-defined laws (i.e., energy and mass balance) and empirical algorithms (e.g., convective heat transfer coefficient). In particular, despite numerous updates over the empirical algorithms of convective heat transfer coefficient (CHTC), the current packages are still considered not proper in representing the local CHTC values in many urban occasions as they simplify the surrounding airflows with homogeneous patterns. Furthermore, it has been reported that the inadequate understanding of outdoor airflow can lead to up to 20 – 40 % error in building energy predictions. This weakness, thus, initiated a subject of the research in the past decades to couple BES with computational fluid dynamics (CFD) tools, which are known for their strengths in airflow modelling, especially in representing the neighbourhood effects in an urban area.

Dynamic coupling of BES to computational fluid dynamics (CFD) techniques are a common strategy to improve the simulation performance. The precedent research of CFD-BES coupling mainly focuses on the indoor environment, but only a few consider the outdoor microclimate conditions. This research aims to investigate the neighbourhood effect on the convection of buildings' exterior surfaces and enhance their presence in the local convective heat transfer coefficient format in building energy modelling.

Among the dynamic coupling strategies, the fully dynamic coupling is understood as computationally intensive and impractical in medium-to-long-term modelling or even short-term (hourly, daily or weekly) modelling of naturally ventilated scenarios on a neighbourhood scale. Therefore, though it

provides a more accurate assessment than the quasi-dynamic approach, it is less popular than the latter one. In this study, frameworks of fully dynamic coupling and virtual dynamic coupling are proposed for short-term and medium-to-long-term (monthly, seasonally or annually) modelling, respectively.

Three case studies are performed for

1) short-term modelling of scenarios with all buildings sealed from outdoors without natural ventilation (sealed scenarios);

2) short-term modelling of scenarios with all buildings under the natural ventilation during the night-time (ventilated scenarios);

3) medium-to-long-term modelling of sealed scenarios.

where ‘sealed’ here means the rooms are sealed from outdoors with the windows closed all the time.

The first case study proves the feasibility of the developed benchmark coupling framework. After that, the second case study expands the framework for application in scenarios of natural ventilation with fast calculations. The last case study provides the virtual dynamic coupling of the CFD and BES with artificial neural network for medium-to-long-term prediction of CHTCs. All case studies are performed in typical hot weather for a simple city community in Los Angeles, U.S.

The results highlight the importance of the neighbourhood effect. For short-term modelling of sealed scenarios, the difference between the prediction of the hourly averaged external convection using the coupling method and that of the standalone conventional BES models is up to 64 %. Furthermore, for short-term modelling of ventilated scenarios, the proposed model substantially reduces the computational cost of the dynamic coupling procedure, taking almost 1/200 of time as the conventional method. Concerning the medium-to-long-term modelling using a virtual dynamic coupling, the predictions of the local CHTCs on the external surfaces are found satisfactory with an accuracy

of 0.88. Moreover, ten is the effective number of days to train the neural network tools for a one-month simulation—the proposed approach saves approximately 2/3 of the required computational time using an ordinary approach.

ACKNOWLEDGEMENT

First of all, I would like to thank my supervisor, Dr. Parham A. Mirzaei, who has been a mentor and guide, in both academy and life, during my years studying in Nottingham. Without his expertise and support, I would have never been succeeded in starting, enjoying, and completing this research. I would also like to thank my second supervisor, Dr. Benjamin M. Jones, for his kind help with the first published paper of my Ph.D. topic. Thanks to the university's Engineering faculty for its financial support of my research project.

I want to extend my gratitude to my lovely friends who have encouraged, motivated, and stood beside me bring joy and love throughout my studying abroad time. Thanks to Lingqiao WU, Conghui DOU, Yaoyao CHEN, Wei GONG, Miaoyuan HUA, and Yanjun WANG. A gratitude is also owed to Dr. Mohammadreza Shirzadi for kindly providing me with a component model for one of my case studies.

Last but not least, I would like to thank my family, parents, and grandparents. None of these would have been possible without their always support.

CONTENTS

ABSTRACT

ACKNOWLEDGEMENT

CONTENTS **i**

LIST OF FIGURES **vi**

LIST OF TABLES **xi**

LIST OF EQUATIONS **xiii**

NOMENCLATURE **xiv**

Chapter 1. INTRODUCTION **1**

1.1. Background 1

1.2. Aims and Objectives 2

1.3. Outline of Works 4

Chapter 2. LITERATURE REVIEWS **5**

2.1. Building Energy Simulation 5

2.1.1. Principles and capability of energy modelling in BES tools 5

2.1.2. Convection algorithms for outside surfaces in ENERGYPLUS 6

2.1.3. Limitations 9

2.2. Computational Fluid Dynamics 9

2.2.1. Researches of CFD modelling 9

2.2.2. CFD climatic modelling 11

2.2.3. Turbulence models 13

2.2.4. Tips from best practice guidelines 13

2.2.5. Limitations 15

2.3. Coupling CFD and BES 15

2.3.1. Coupling strategies 15

2.3.2. Coupling convergence and frequency 17

2.3.3. Current coupling researches 17

2.3.4. Limitations 19

Chapter 3. GENERAL APPROACH 24

3.1. Project Design 24

3.2. Development of General Framework of Coupling CFD and BES 25

3.3. Geometric Design of Coupling Model 28

3.3.1. Benchmark model for the CFD field 28

3.3.2. Benchmark commercial building from DoE for the BES field 29

3.3.3. Coupling model design 30

3.4. Communications Between CFD and BES Solvers 32

3.4.1. Matching characteristics of interfaces in two domains 32

3.4.2. Consistent climate conditions in two domains 33

3.5. CFD Modelling 35

3.5.1. Mathematical models 35

3.5.2. Computational domain for validation 38

3.5.3. Computational domain for coupling simulations 40

3.6. BES Modelling 44

3.7. Combination with Artificial Neural Network 46

3.8. Quantified Metrics for Data Analysis 48

Chapter 4. VALIDATION OF CFD MODEL 50

Chapter 5. SHORT-TERM MODELLING OF SEALED SCENARIOS 57

5.1. Framework for Short-term Modelling of Sealed Scenarios 57

5.2. Description of the Case Study 61

5.3. Coupling Simulation Results 62

5.3.1. One-time-step dynamic coupling 62

5.3.2. Sheltering effect inside neighbourhood community 65

5.3.3. Impact of wind patterns on local CHTCs 69

5.3.4. Comparison of embedded CHTC algorithms and coupling method 73

5.4. Summary 76

Chapter 6. SHORT-TERM MODELLING OF VENTILATED SCENARIOS 78

6.1. Concept of Integration of CFD_f – CFD – BES 78

6.2. Framework for Short-term Modelling of Ventilated Scenarios 79

6.3. Description of the Case Study 83

6.3.1. Case specification 83

6.3.2. Outline of interface between CFD_f and CFD models 85

6.4. Boundary Type on Interfaces for CFD 86

6.4.1. Evaluation of the CFD model performance 86

6.4.2. Performance in different layers 89

6.4.3. Impact of wind speed and direction 92

6.4.4. Representation of openings' local parameters 98

6.5. Runtime and convergence benefit 99

6.6. Comparison of stand-alone BES and coupling method 101

6.6.1. Zonal temperatures 101

6.6.2. Neighbourhood effect 103

6.6.3. Total cooling load 103

6.7. Summary 108

Chapter 7. MEDIUM-TERM TO LONG-TERM MODELLING 109

7.1. Framework for Medium-term to Long-term Modelling 109

7.1.1. Simulation period definition 110

7.1.2. Pre-simulation stage 111

7.1.3. Coupling 112

7.1.4. Training 113

7.1.5. Prediction 115

7.2. Description of the Case Study 115

7.2.1. Case specification 115

7.2.2. Options of combination of period-1 and period-2 117

7.3. Performance of Developed Tools for Different Surface Types 117

7.3.1. Performance of ANN tool-d for roof surfaces 119

7.3.2. Performance of different tools 124

7.4. Effective Size of Period-1 124

7.4.1. Forward method 125

7.4.2. Sampling method 126

7.5. Impact of Wind Direction and Wind Speed 128

7.6. Comparison of Energy Simulation by Three Different Methods 134

7.7. Computational Cost Benefits of The Proposed Framework 134

7.8. Summary 135

Chapter 8. CONCLUSIONS AND FURTHER WORK 136

8.1. Summary of The Work 136

8.2. Conclusions 137

8.2.1. For short-term modelling of sealed scenarios 137

8.2.2. For short-term modelling of ventilated scenarios 138

8.2.3. For mid-term to long-term modelling 140

8.3. Furter Work 141

BIBLIOGRAPHY 142

APPENDICES 156

Appendix 1 Bespoke code to update *IDF files, generate journals and check the convergence of the coupling 156

Appendix 2 Test points of AIJ Case C 173

Appendix 3 Names of exterior surfaces in coupling models 175

Appendix 4 ENERGYPLUS *IDF file for short-term modelling of sealed B5 without applying the coupling method 179

Appendix 5 Additional content to ENERGYPLUS *IDF file to apply the new CHTCs from CFD among iterations during the coupling process 195

LIST OF FIGURES

Figure 2-1 Summary of precedent CFD climatic models [51] 12

Figure 3-1 General framework for short-term external coupling 26

Figure 3-2 Distribution of 120 test points of Architecture Institute of Japan Case C 29

Figure 3-3 Benchmark small office model by DoE [85] 30

Figure 3-4 Distribution of nine cubic buildings for the case studies [86] 31

Figure 3-5 Computational domain for CFD [89] 39

Figure 3-6 Computational grids for AIJ-Case-C CFD validation [90] 40

Figure 3-7 Computational grids for a) sealed and b) ventilated scenarios 41

Figure 3-8 Four basic steps of the proposed virtual dynamic method [89] 47

Figure 4-1 3×3 cubic blocks 50

Figure 4-2 Comparison of the normalized local velocities of experimental measurements and CFD simulations over 120 test points [93] 52

Figure 4-3 Plot of normalized velocity versus normalized experimental velocity [93] 53

Figure 4-4 Plot of er of different CFD models (blue box, interquartile range; red horizontal line, median; yellow cross, mean; black bars, minimum and maximum; red cross, outliers) [93] 54

Figure 4-5 Comparison of final models of CFD_f and CFD 55

Figure 5-1 Framework of the coupling BES and CFD for short-term modelling of sealed scenarios 58

Figure 5-2 Transmitting of variables in short-term coupling of sealed scenarios 59

Figure 5-3 Nine-cube ENERGYPLUS model for the sealed scenario [93] 61

Figure 5-4 Convergence of BES-CFD iterative calculations in the first hour of 25th of September [93] 63

Figure 5-5 Iteration numbers for achieving convergence of the hourly basis coupling [93] 63

Figure 5-6 Comparison of building surface temperature contours in the first hour of the test day at a) 1st iteration (by ENERGYPLUS only using DOE-2 algorithm) and b) last iteration (reached convergence after fully dynamic coupling) in 1) southeast and 2) northwest view [93] 64

Figure 5-7 Comparison of qc'' of B1, B2, B3, and B5 exterior surfaces in the 1st hour of the test day [93] 67

Figure 5-8 Standard deviation of the community's convective energy at different surfaces in the 1st hour of the test day [90] 67

Figure 5-9 Comparison of total hourly exterior surface convection energy of buildings calculated by DoE-2 (BES only) and the coupling method [90] 68

Figure 5-10 Gap between the coupled $h*$ and EnergyPlus h of ground floor S1s on B1, B5 and B9 under the impact of different wind patterns of the test day 70

Figure 5-11 Gap between the coupled $h*$ and EnergyPlus h on S1s of three stories of B1 under the impact of different wind patterns of the test day 70

Figure 5-12 Gap between the coupled $h*$ and EnergyPlus h on S1s of three stories of B1 under the impact of different wind patterns of the test day 71

Figure 5-13 Gap between the coupled $h*$ and EnergyPus h on S1s of three stories of B1 along the time of the test day 71

Figure 5-14 Comparison of EnergyPlus h and coupled $h*$on B11S1 when winds come from different angles with a speed of 2.1 m/s on the test day 72

Figure 5-15 Comparison of EnergyPlus h and coupled $h*$on B11S1 when winds come from 230° with different speeds on the test day 72

Figure 5-16 Improvement in qc'' at exterior rough surfaces by the coupling CFD-BES method in the 1st hour of the test day [90] 74

Figure 5-17 Change of CHTCs by coupling method over the results by embedded algorithms in BES [90] 74

Figure 5-18 Total cooling load of nine commercial buildings throughout the test day by different methods [90] 75

Figure 6-1 Schematic of CFD_f – CFD – BES integration 79

Figure 6-2 Framework of coupling CFD_f – CFD – BES for the exterior surface convection with the inclusion of natural ventilation 81

Figure 6-3 Transmitting of variables in short-term coupling of ventilated scenarios 82

Figure 6-4 Nine-cube ENERGYPLUS model for the ventilated scenario [97] 83

Figure 6-5 Fenestration surfaces of the tested buildings 84

Figure 6-6 Flow information transfer from CFD_f to CFD [97] 85

Figure 6-7 Thirty-four vertical test lines' a) positions and b) names 87

Figure 6-8 Twenty-four horizontal test lines' positions and names 88

Figure 6-9 Plots of normalised velocity $UlocalUmet$ by CFD_f and CFD with different interface boundaries 91

Figure 6-10 Average RMSE of $Ulocal/Umet$ in different monitoring layers by four interface boundaries [86] 92

Figure 6-11 Average RMSE of $Ulocal/Umet$ of all monitoring layers under the impact of wind speed $Umet$ [86] 93

Figure 6-12 Average RMSE of $Ulocal/Umet$ of all monitoring layers under the impact of wind angle [86] 94

Figure 6-13 Comparison of velocity contours between a) CFD_f and CFD with b) mass-mass, c) velocity-pressure, d) pressure-pressure and e) velocity-velocity interface boundary conditions [86] 97

Figure 6-14 Plot of residuals of CHTC for every iterative calculation by CFD_f-BES and CFD_f-CFD-BES methods during the 1st hour of the test day [97] 99

Figure 6-15 Iteration numbers to achieve convergence [97] 101

Figure 6-16 Difference of B5's zone temperature computed by the coupling and stand-alone BES methods [97] 102

Figure 6-17 Standard deviation of surface CHTC by stand-alone BES and dynamic coupling method [97] 105

Figure 6-18 Total cooling load of the community throughout the test day [97] 106

Figure 7-1 Schematic of flowchart of the proposed virtual dynamic coupling [89] 110

Figure 7-2 Structure of the neural network [89] 114

Figure 7-3 Simplified model for the medium-term – long-term virtual dynamic coupling 116

Figure 7-4 Final CFD model for medium-term to long-term simulations 116

Figure 7-5 Hourly weather data, including a) air temperature, b) wind speed and c) wind angle) in September of Los Angeles [89] 118

Figure 7-6 Comparisons between the target and the output of ANN tool-d (for the roof surface) developed from none-filtered target for roof surface during the training stage [89] 120

Figure 7-7 Comparisons between the target and the output of ANN tool-d (for the roof surface) developed from filtered target for roof surface during the training stage [89] 120

Figure 7-8 Relative discrepancy er of different methods' prediction compared to the fully dynamic coupling results of the local CHTCs over different surfaces [89] 122

Figure 7-9 Relative discrepancy er of the predictions by ANN tools a-c using forward method for different combination options of period 1 + period 2 [89] 123

Figure 7-10 Relative discrepancy er of the predictions by ANN tools a-c using sampling method for different combination options of period 1 + period 2 127

Figure 7-11 Relative discrepancy er of the predicted local CHTCs at walls, facing different directions for different combination options (period-1+ period-2) [89] 129

Figure 7-12 Occurrence frequency of wind angles in four directions and the associated wind speed at each specific direction [89] 131

Figure 7-13 Comparison of surface temperatures calculated by different methods at 12 pm on 20th Sep., (row 1: southeast view; row 2 northwest view) [89] 132

Figure 7-14 Comparison of the daily cooling energy of period-2 (11th – 30th Sep.) calculated by three different methods [89] 133

LIST OF TABLES

Table 2-1 Summary of some coupling researches 22

Table 3-1 Boundary conditions for CFD domain validation 39

Table 3-2 Boundary conditions of CFD_f and CFD domains for ventilated scenarios 42

Table 3-3 Boundary conditions for modelling of sealed scenarios 44

Table 4-1 Assessment of CFD model performance using three metrics 56

Table 5-1 Wind patterns of the test day 69

Table 5-2 Comparison of daily cooling energy demand by different method 76

Table 6-1 Average FAC2 of all studied scenarios in different monitoring layers [86] 92

Table 6-2 Tendency of average RMSE by four interface types changing with $Umet$ in different monitoring layers [86] 95

Table 6-3 Tendency of average RMSE by four interface types changing with wind angle in different monitoring layers [86] 96

Table 6-4 Average RMSE of representing parameters at opening surfaces (interfaces) by CFD [86] 98

Table 6-5 Runtime of every iterative calculation by CFD_f-BES and CFD_f-CFD-BES methods for the 1st hour of the test day [97] 100

Table 6-6 Hourly total cooling loads of the community calculated by different methods 107

Table 7-1 Performance information of the developed ANN tools for different surfaces [89] 121

Table 7-2 er of local CHTC between the coupling results and the predictions by developed ANN tool and BES-only (embedded algorithm) for different combination options of period 1 and period 2 [89] 125

Table 7-3 Selected samples for corresponding combination option 126

Table Appx. -1 Coordinates of 120 test points for AIJ Case C 173

Table Appx. -2 List of building exterior surfaces' names 175

LIST OF EQUATIONS

Eqn. 1)	6	*Eqn. 26)*	36
Eqn. 2)	7	Eqn. 27)	37
Eqn. 3)	7	Eqn. 28)	37
Eqn. 4)	7	Eqn. 29)	37
Eqn. 5)	7	Eqn. 30)	37
Eqn. 6)	7	Eqn. 31)	43
Eqn. 7)	8	Eqn. 32)	43
Eqn. 8)	8	Eqn. 33)	47
Eqn. 9)	8	Eqn. 34)	48
Eqn. 10)	8	Eqn. 35)	48
Eqn. 11)	32	Eqn. 36)	48
Eqn. 12)	33	Eqn. 37)	48
Eqn. 13)	33	Eqn. 38)	49
Eqn. 14)	33	Eqn. 39)	49
Eqn. 15)	34	Eqn. 40)	51
Eqn. 16)	34	*Eqn. 41)*	114
Eqn. 17)	34	*Eqn. 42)*	128
Eqn. 18)	35		
Eqn. 19)	35		
Eqn. 20)	35		
Eqn. 21)	35		
Eqn. 22)	35		
Eqn. 23)	36		
Eqn. 24)	36		
Eqn. 25)	36		

NOMENCLATURE

Symbol	Term	Unit
A	Surface area	m^2
a	Constants	
$a_{i,n}$	Output of a network layer	
b	Constants	
$b_{i,n}$	Bias in transfer function	
$C_{1,2,3\varepsilon}$	Turbulence model discharge coefficients	
C_p	Specific heat capacity	J/ ˚C·kg, J/K·kg
C_t	Turbulent natural convection constant	$W/m^2K^{4/3}$
C_μ	Dimensionless $k-\varepsilon$ model constant	
D_{ri}	Material roughness index	
$D_{q_{hr}}$	Allowed relative deviation of hit rate	
d	Destination element/neuron	
E	Total energy of unit mass of fluid	J/kg
E_r	Radius of the Earth	m
E_{ri}	Material roughness index	
e_r	Relative error	
$FAC2$	Fraction of predictions within a factor of two of observations	
F_{ri}	Material roughness index	
$f_{i,n}()$	Transfer function in a neuro	
G_b	k term by the buoyancy	$kg·m^2/s^3$
G_k	k term by the mean velocity gradient	$kg·m^2/s^3$
$\vec{g}$	Gravitational force component	
H	Object height	m

H_b	Additional height to the troposphere	m
h	Combined convective and radiative heat transfer coefficient	W/m^{2}K
h_c	Convective heat transfer coefficient	W/m^{2}K
h_f	Forced component of h_c	W/m^{2}K
h_j	Sensible enthalpy of spices	J/mol
h_n	Natural component of h_c	W/m^{2}K
h_s	Sensible heat	J/kg
h^*	Virtual h_c for ENERGYPLUS	W/m^{2}K
I_z	Turbulence intensity	
i	Surface index	
$\bar{J}_j$	Diffusion flux of spices	mol/m^3·s
K_{eff}	Effective thermal conductivity coefficient	W/K·m
K_t	Thermal conductivity coefficient	W/K·m
k	Turbulence kinetic energy	J/kg
L	Object length	m
L_a	Air temperature gradient within troposphere	K/m
$\dot{M}$	Mass flow rate	kg/s
N	Number of objects	
o	Observations	
P	Pressure	Pa
P_r	Surface perimeter	m
Pr_t	Turbulent Prandtl number	
p_I	Inputs of network	
p	Predictions	
Q_{others}	Heat gain from people, lights, equipment, infiltration, etc.	W
$Q_{extract}$	Heat extracted from the surface	W
q_c''	Convective heat flux	W/m^2

q_{hr}	Hit rate	
R^2	Adjusted determination coefficient	
R_f	Surface roughness multiplier	
S_k	Sink/source for k	kg·m^2/s^3
S_ε	Sink/source for ε	kg/m·s^4
s	Number of stories	
sr	Source element/neuron	
T	Temperature	K
T_a	Air temperature	K, ˚C
T_b	Air temperature at ground level	˚C
T_g	Ground temperature	˚C
T_s	Surface temperature	K, ˚C
t	Time	s
U	Flow speed	m/s
U^*	Time-averaged instantaneous scalar velocity	m/s
u	Dimensionless fluctuating component	
u_τ	Friction velocity	m/s
u'_z	RMS of the velocity fluctuations	m/s
W	Object width	m
W_f	Adjuster of surface direction	
$W_{q_{hr}}$	Threshold of absolute deviation of hit rate	
$w^i_{d,sr}$	Layer weight of network	
$\bar{X}$	Mean of dataset of parameter X	
Y_M	Dilatation dissipation	kg·m^2/s^3
Y_i	Predict data	
y^+	Turbulence metric	
y^*	Turbulence metric	

$y^{\tilde{*}}$	Turbulence metric	
y_P	Distance between the wall and near-wall node *P	m
z	Altitude of surface centroid	m
z_s	Z-score	
α	Exponent of wind speed profile	
ΔT	Temperature difference	K
ΔT_{room}	Mean room temperature	˚C
Δt	Time step	s
Δ	Site boundary layer thickness	m
ε	Turbulence dissipation rate	m^2/s^3
μ_t	Eddy viscosity	kg/m·s
Σ	Tilt from the horizon	°
ρ	Density	kg/m^3
σ_k	Turbulence Prandtl number for k	
σ_X	Standard deviation of dataset of parameter X	
σ_ε	Turbulence Prandtl number for ε	
$\bar{\bar{\tau}}_{eff}$	Deviatoric stress tensor	J/m^3
τ_w	Wall shear stress	kg/m^2

Subscripts

i, j, k	Three-dimensional component/object index

Chapter 1. INTRODUCTION

1.1. Background

Total world energy demand has kept growing for decades and is projected to continue for over 30 years. U.S. Energy Information Administration (EIA) indicated a 47 % increase in total marketed energy to that 601 quadrillion British thermal units (Btu) in 2020 would be achieved in 2050 [1]. Among all delivered energy, the building sector consumes a share of almost one-third currently [2], and the worldwide demand keeps increasing by 1 % and 1.1 % annually through 2020 to 2050 for residential and commercial uses, according to the projection of [1]. The main growth of demand in homes is contributed by emerging regions (like China and India) where strong economic and population growth occurs. Similarly, the increase rate of the commercial sector in these regions is almost doubled that in developed regions, 1.8 %/year comparing to 0.5 %/year respectively. The share of building sector is around 40 % in many developed countries, such as the U.S., the U.K. and in most EU countries [3], [4].

It was put forward that urban density and spatial dispersion had a key impact on energy use in statistical research [5]. The growth of energy demand of the built environment is expected to occur in countries with an emerging market economy [1] attributable to rapid and continuous urbanization projected up to 2030 [6]. With populations shifting from rural to urban locations, more attention should be placed on reducing the energy demand of buildings, especially in the urban context. In particular, a better understanding and assessment of building energy demands in cities can help decision-makers to propose appropriate regulations for indoor and outdoor environments and aid urban planners in the design and modification of cities. Comprehensive modelling tools capable of considering the complexity of urban morphologies and dynamic neighbourhood environments, known as the neighbourhood effect, are then required.

There are many simulation packages capable of modelling building energy demands, such as EnergyPlus, Revit, DOE-2, and eQUEST. They calculate heating/cooling loads by simultaneously solving mass and energy conservation equations for a finite number of zones [7]. The finite regions are relatively large in consequence. Convection is an important mechanism of heat transfer at a building's exterior whose effect can be two to three times larger than the radiant transfer [8]–[10]. Simplified outdoor airflow models have reported errors of 20 – 40% when predicting total building energy demand while up to 95 % for indoor natural ventilation behaviours [11], [12]. Predictive errors in the calculation of convective heat transfer are related to the improper capture of local dynamic wind gradients.

Current building energy simulation (BES) tools use an empirical convective heat transfer coefficient (CHTC), which is often not accurate enough for a specific case, especially in complex urban contexts where the neighbourhood effect shapes the microclimate around a building. Instead, the algorithms embedded within them treat building clusters the same way as an isolated building. This is because they were developed through specific in-situ measurements [12], and so they are unable to increase account for variations in urban morphologies.

Computational fluid dynamics (CFD) techniques can solve the conservation laws at a small scale and are known for their strength in modelling airflows. CFD has been widely applied to environmental studies of different scales, from indoor climates to district and city communities [13]–[15].

1.2. Aims and Objectives

Microclimate in cities is complex and case sensitive considering the sheltering effect between a group of buildings. An evident shortage of current BES tools in presenting neighbourhoods is related to the local airflow, which can be reflected in the convection around buildings. The coupling, or integration, of CFD and BES techniques can compensate for the limitations of BES and offer a more proper assessment of the built environment in cities in terms of

sheltering effect. Here, CFD is used to discretise the fluid domain and BES to discretise the building energy demand calculation [16]. According to the literature reviews, most of current studies using coupling models are focused on the indoor environment. Moreover, applying these tools in scenarios with natural ventilation remains challenging due to the high computational burden. The attempt of medium-to-long-term usage of the coupling concept is rare and lacks reflection of deviations inside the neighbourhood.

Therefore, this research aims to investigate the neighbourhood effect on the convection of buildings' exterior surfaces and enhance their presence in the format of local parameters around/of buildings (e.g., exterior surface's convective heat transfer coefficient) in building energy modelling. Frameworks of coupling CFD and BES techniques to assess building energy in the neighbourhood-scale context are proposed for different scenarios applications.

The staged objectives of this project are:

1) reviewing precedent research to find out the gaps in the topic of urban microclimate modelling in BES and CFD fields and to build up knowledge about BES, CFD, and integrations of both domains. creating valid models for modelling the simple city community.

2) creating valid models for modelling the simple city community.

3) developing frameworks of coupling BES and CFD tools for buildings' exterior convective heat transfer coefficients in different scenarios, including short-term (hourly, daily or weekly) simulations of buildings with/without natural ventilation and medium-to-long-term (monthly, seasonally or annually) simulation of buildings without natural ventilation. The frameworks are tested in three case studies.

4) analysing the results of created coupling models to investigate the improvement in performance of reflecting neighbourhood effect.

1.3. Outline of Works

This research includes the following chapters (linking to the objectives) to approach these aims:

- Chapter 2: Review of research and technical reports of building energy simulation, computational fluid dynamics, microclimate modelling, and the coupling of CFD and BES. This links to Objective 1.

- Chapter 3: General approach to couple CFD with BES, create model and evaluate the performance. This links to Objectives 2 and 3.

- Chapter 5: Case study of short-term modelling of sealed scenarios where all buildings are only ventilated by mechanical systems. This links to Objectives 3 and 4.

- Chapter 6: Case study of short-term modelling of ventilated scenarios where all buildings execute hybrid ventilation strategy, night-purging cooling indeed. This links to Objectives 3 and 4.

- Chapter 7: Case study of medium-/long-term modelling of sealed scenarios where only selected target building participate the coupling calculation. This links to Objectives 3 and 4.

At the end of the research, the main conclusions of three case studies are summarised and further work to this research is put forward.

Chapter 2. LITERATURE REVIEWS

2.1. Building Energy Simulation

2.1.1. Principles and capability of energy modelling in BES tools

Building energy modelling has rapidly evolved from the early basic methods ('indicative', 'application limited', and 'difficult to use') to the modern advanced tools ('predictive', 'generalized', 'handbook oriented',' full CAD integration', and 'easy to use') with hundreds of programs been developed over the past few decades [12], [16]. Crawley et al. provided a survey to comprehensively compare the most common twenty packages, such as DOE -2.1E, EneryPlus, ESP-r, eQUEST, TRNSYS, and reported their work [12], [17]. The comparison was conducted in fourteen categories of software capabilities. EneryPlus and TRACE offered the most available options of convection algorithm at outside surfaces, while the code with the most flexible methods to calculate interior-surface convection categorised as 'Zone load' was IES <VE>. Some vendors embedded CFD module in their packages (including ESP-r, IES <VE>, and TAS), however, almost exclusively focused on resolving ventilation and intra-zonal convection fields as demonstrated by [18]–[20].

Most state-of-art BES tools calculate the energy budget with given weather data profiles by executing sets of subroutines simultaneously for intra-constructional heat transfer, plant systems, inter-space air movement, occupancy, control systems, and other mechanisms [21]. A network of finite-difference nodes is employed in the BES tools to present the various components of discretised building [22]. Multiple nodes can be placed through each component, while heat balance equations are written for each node to be resolved iteratively with temporal and spatial continuity. It was pointed out that treating each zone as a single node responding to the assumption of a well-mixed indoor environment adopted by BES tools could cause a potential error in heat, air, and moisture (HAM) assessments [23]. Most BES codes calculate room heating/cooling load by solving the following equation for indoor air [24]:

$$\sum_{i=1}^{N} q_c'' A_i + Q_{others} - Q_{extract} = \frac{\rho V_{room} C_p \Delta T_{room}}{\Delta t} \quad \text{Eqn. 1)}$$

where N and i are the numbers of enclosure surfaces and the index, respectively. q_c'' (W/m^2) is convective heat flux at interior surface; A (m^2) is the surface area; Q_{others} (W) represents the heat gains from people, lights, equipment, infiltration, etc. ρ (kg/m^3) and C_p (J/kg·˚C) are air density and specific heat capacity, respectively. V_{room} (m^3) is the room volume, ΔT_{room} (˚C) is mean room air temperature difference through the time step Δt (s). $Q_{extract}$ (W) is the heat extracted from the space (the load).

Any change of miscellaneous microclimate can be reflected in airflow around the building in consequence. Therefore, investigations about the methods current BES programs used to calculate the heat transfer, particularly the convection component, at exterior surfaces are demanded. In BES programs, the heat balance at exterior surfaces works between convection, radiation (including short-wave and long-wave radiation), and conduction [25]. The most BES tools selected several empirical convection correlations from massive models (partially reviewed in [8]) and applied them to construction outside surfaces. EnergyPlus, showing its strong capability in exterior convection in the comparative survey [12], [17], is selected to solve the BES domain in this research.

2.1.2. Convection algorithms for outside surfaces in EnergyPlus

The available options of outdoor convection in EnergyPlus include TARP, SimpleCombined, MoWiTT, DOE-2, and Adaptive Convection Algorithm [25]. Different correlations of the exterior convective convection coefficient, h_c (or combined convection and radiation heat transfer coefficient, h) used by these algorithms are presented as follows.

- SimpleCombined calculates the h (W/m^{2}K) from the local wind speed U_z (m/s) at the altitude of specific surface centroid z (m) via:

$$h = D_{ri} + E_{ri}U_z + F_{ri}{U_z}^2 \quad \text{Eqn. 2)}$$

where D_{ri}, E_{ri}, and F_{ri} are roughness indexes of material.

- TARP (Thermal Analysis Research Program) algorithm considers the h_c (W/m^{2}K) as the sum of forced component h_f (W/m^{2}K) and natural component h_n (W/m^{2}K):

$$h_{c,ext} = h_f + h_n \quad \text{Eqn. 3)}$$

The forced component is calculated by:

$$h_f = 2.537 W_f R_f \left(\frac{P_r U_z}{A}\right)^{1/2} \quad \text{Eqn. 4)}$$

where R_f is the surface roughness multiplier; for windward surface, W_f equals to 1 while the value is halved (0.5) for the leeward surfaces facing the direction ±100º from normal incidence. P_r (m) and A (m^2) are the perimeter of the surface and its area, respectively.

Three factors (surface orientation (upward or downward), surface tilt from the horizontal, Σ (˚), and temperature difference between the surface and ambient air, $\Delta T = T_{a,z} - T_s$, need to be identified so that the natural convection component can be determined via:

$$h_n = \begin{cases} 1.3|\Delta T|^{1/3} & if\ \Delta T = 0\ or\ \Sigma = 90 \\ \dfrac{9.482|\Delta T|^{1/3}}{7.283 - |cos\Sigma|} & if \begin{cases} upward\ and\ \Delta T < 0 \\ downward\ and\ \Delta T > 0 \end{cases} \\ \dfrac{1.810|\Delta T|^{1/3}}{1.382 + |cos\Sigma|} & if \begin{cases} upward\ and\ \Delta T > 0 \\ downward\ and\ \Delta T < 0 \end{cases} \end{cases} \quad \text{Eqn. 5)}$$

- MoWiTT computes the h_c by:

$$h_c = \sqrt{[C_t(\Delta T)^{1/3}]^2 + \left[a{U_z}^b\right]^2} \quad \text{Eqn. 6)}$$

where C_t is the turbulent natural convection constant = 0.84 W/m^{2}K$^{4/3}$ while a and b are constants depending on the relative orientation of the surface to normal incidence of wind (Leeward or Windward).

- DOE-2 algorithm calculates the h_c for different surface types (smooth or less smooth) via:

- for smooth surfaces (e.g., glass): $$h_c = \sqrt{{h_n}^2 + \left[a{U_z}^b\right]^2} \quad \text{Eqn. 7)}$$

for less smooth surfaces: $$h_c = (1 - R_f)h_n + R_f\sqrt{{h_n}^2 + \left[a{U_z}^b\right]^2} \quad \text{Eqn. 8)}$$

where R_f is the surface roughness multiplier that is 2.17, 1.67, 1.52, 1.13, 1.11, and 1.00 for roughness indices of 1 to 6, respectively, representing very rough to very smooth surfaces. The constants *a* and *b* depend on the relative orientation of the surface to the normal incidence of wind. For windward surfaces, the constants *a* and *b* are 3.26 W/(m^{2}K(m/s)^b) and 0.89, respectively, and 3.55 W/(m^{2}K(m/s)^b) and 0.617 for leeward surfaces. h_n is the natural convective heat transfer coefficient, which is determined in [25] as follows:

for $\begin{cases} upward\ and\ T_{a,z} - T_s < 0 \\ downward\ and\ T_{a,z} - T_s > 0 \end{cases}$: $$h_n = \frac{9.482\left|T_{a,z} - T_s\right|^{1/3}}{7.283 - |cos\Sigma|} \quad \text{Eqn. 9)}$$

for $\begin{cases} upward\ and\ T_{a,z} - T_s > 0 \\ downward\ and\ T_{a,z} - T_s < 0 \end{cases}$: $$h_n = \frac{1.810\left|T_{a,z} - T_s\right|^{1/3}}{1.382 + |cos\Sigma|} \quad \text{Eqn. 10)}$$

where Σ is the surface tilt from the horizon.

- The adaptive convection algorithm for the outside surface in EnergyPlus encompasses many developed correlations. Exterior surfaces were classified into four categories: Roof Stable, Roof Unstable, Vertical Wall Windward, and Vertical Wall Leeward, depending on the wind direction and direction of surrounding heat flow and associated buoyancy; so that correlations grouped in corresponding categories can be assigned to surfaces.

Besides, the vendor also offers approaches to edit the surface convection coefficients on outside surfaces manually. EnergyPlus was designed to override convection coefficients by the algorithms with assigned user-defined correlations on selected surfaces. All these options can be specified for the entire model or assigned to any selected surface to determine the coefficient.

2.1.3. Limitations

The way current BES tools calculate the outside surface convection has several limitations, including:

- The outdoor ambient environment is simplified with no access to solve the specific conditions for individuals. For example, the air temperature at a given height is treated the same throughout the site, leading to inevitable misestimation of the actual scenarios.

- The impact of building sheltering effect on external convection is neglected. There is no involved reflective parameter to the urban morphologies in the embedded algorithms for outside surface convection, which means current BES tools treating a group of constructions would be the same as that used for isolated buildings.

2.2. Computational Fluid Dynamics

2.2.1. Researches of CFD modelling

Computational Fluid Dynamics technology has been widely applied to solving urban-/neighbourhood-scale problems, including:

- Pedestrian wind comfort and safety [26]–[31]. Baskaran and Kashef (1996) [26] ran CFD simulations to visualize the flow field around the isolated and grouped buildings. Blocken, Janssen, and van Hooff (2012) [27] undertook a case study at the Eindhoven University of Technology to explore the pedestrian winds. Bady et al. (2011) [28] investigated the impact of building geometry on the flows in street canyons. Ramponi et al. (2015) tested different urban densities with street canyon properties [29]. Like these,

most studies of this topic were inclined to investigated various scaled problems isothermally; others simplified the temperature of constructions by assuming deviation to ambient air temperature [30], [31].

- *Pollution dispersion* [32]–[38]. Like those concerning pedestrian wind comfort and safety, most of the studies of pollution dispersion ran isothermal simulations (such as investigations of different turbulence models [32], [35], pollution source positions [33], weather conditions [34], boundary condition [38]); temperature field was only considered in limited studies. Haghighat and Mirzaei simulated the pollution dispersion with non-isothermal surfaces [36] and tested the pollution removal effectiveness in pedestrians [37].

- *Cross ventilation* [14], [39]–[46]. The CFD studies of cross ventilation were processed isothermally [14], [39]–[45] and non-isothermally [46], mostly isothermally, which could be caused by the high computational cost of using intensely fine meshes. In addition, the calculation domain of cross ventilation studies could be interior spaces only or integrated indoors and outdoors. Typically, the model with integrated indoor and outdoor spaces for cross ventilation simulation consists of millions of cells which would bring the challenge of a high burden, especially when targeting a group of buildings rather than isolated. Tong, Chen, and Malkawi (2016) [39] determined the Influence Region according to the flow rate accuracy in neighborhood scale with the target building under the cross ventilation. The created model contained 2-11 million cells. Shirzadi, Mirzaei, Naghashzadegan (2018) [14] enhanced the cross-ventilation modelling by developing an adaptive discharge coefficient for turbulence model. The mesh had 1-2 million cells. Their improved model was expanded to over 4 million cells and then applied to the highly-packed urban area [40]. King et al. (2017) [42] compared the single-side ventilated and cross-ventilated buildings in isolated and sheltered scenarios, with meshes of 4 million and 16 million cells, respectively. Peren, van Hooff, and Ramponi (2015) [43] investigated the impact of roof geometry on cross ventilation of isolated building with meshes of 2-2.7 million cells. van Hooff, Blocken, and

Tominaga (2017) [44] compared the cross-ventilation modelling using RANS and LES turbulence models against the experiment. The mesh they employed contained 1.8 million cells. Micallef, Buhagiar, and Borg (2016) [45] modelled a case study of cross-ventilated room in a courtyard building and tested the influence of the courtyard height. There were two buildings modelled by meshes of 3 million cells.

- *Urban heat island effect* [15] and *others* like the impact of obstacles' geometry on airflows [47], [48], model setups [49], novel climatic models [34], [50], etc.

2.2.2. CFD climatic modelling

To approach dynamic microclimate analysis in an urban area, computational models should be flexible in responding to stochastic winds from different directions.

There are mainly three kinds (in aspect of model shapes) of climatic modelling implemented for urban climate studies, as summarized in *Figure 2-1*.

The rectangular model (see *Figure 2-1a*) was widely employed in most of previous studies, mainly for steady-state simulations. There are more available empirical instructions for this model. It is preferred in concise mesh size. However, the advantage vanishes when applying it to the scenarios of non-parallel winds. Some researchers raised concerns about interferences between its inlet and outlet boundaries in the extremely oblique winds [34], [50]. For long-term simulations, several model generations with specific considerations for each domain are required. Moreover, the information transmission between different domains solving dynamic scenarios can cause a potential error.

Solazzo, Vardoulakis, and Cai (2011) [34] developed an innovative method to overcome the interferences issue in the highly-inclined wind by rotating the dish with buildings on it with fixed inlet/outlet boundaries (see *Figure 2-1b*). This model provides the most succinct size in oblique winds. It was designed

to convert the long-term simulation into a mathematical calculation adding up the occurrence-frequency averaged impact of pre-set climate scenarios. Steady-state evaluations need to establish a database for all the possible climatic alternatives at the selected site, which increased the manual and computational burden in repetitive modelling for different scenarios. In addition, the neglected connectivity between scenarios may cause the potential error, and the impact would accumulate with the extension of the examination period.

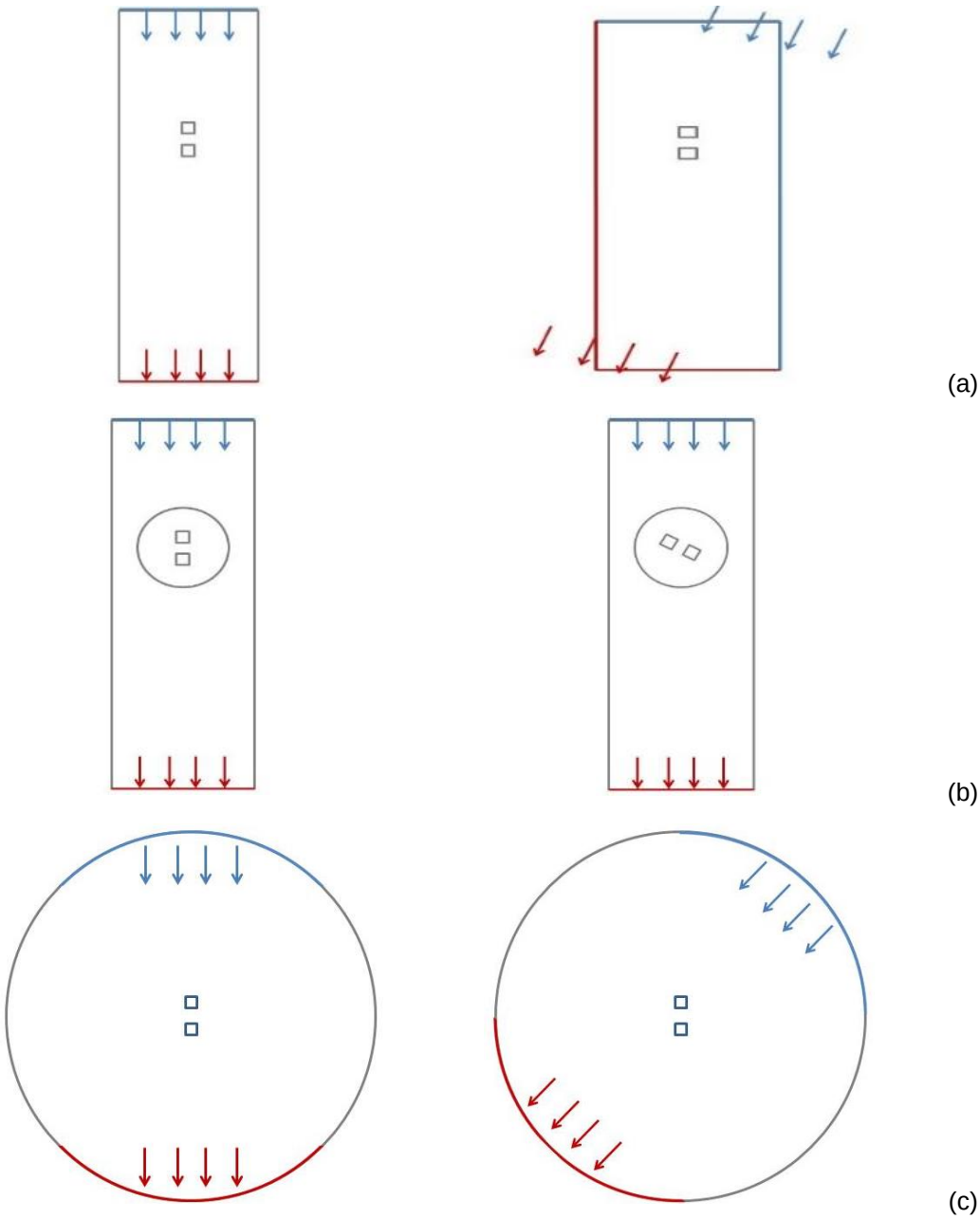

Figure 2-1 Summary of precedent CFD climatic models [51]

Mirzaei and Carmiliet (2013) [50] (see *Figure 2-1c*) proposed the almost directionally independent circular model. This approach can assess stochastic winds by a single model and relieve the burden of repetitive generations. Also, it eliminates the connectivity concerns in the other two models. However, regional control and special meshing techniques are required to prevent the mesh size from becoming too large.

2.2.3. Turbulence models

Many theories have been developed to model the turbulence of flow, including Direct Navier-Stokes (DNS), Large Eddy Simulation (LES), and Reynolds Average Navier-Stokes (RANS), etc. [52]. LES and DNS have delivered more accurate simulations of urban flow with compromised high computational costs [32], [53]. As the most common option, the RANS model is preferable in terms of the simulation burden; however, its delivered representation of airflow in the canopy layer, particularly the wake flow, was not as good [35], [54]. There are different physical models available for the RANS scheme, including Standard (STE), Realized (RLZ), Renormalization-group (RNG) $k-\varepsilon$, and Reynolds-stress (RMS) [35]. It was found in previous researches that among these RANS models, STE was the most used for pedestrian wind and plume dispersion modelling. In contrast, the least used one was RMS. the results by RLZ were the least accurate comparing to experimental measurements, while RNG was found as the optimum [35]. The COST (European Cooperation in the Scientific and Technical Research) group suggested not applying STE to solve wind engineering problems with high simulation accuracy requirements.

2.2.4. Tips from best practice guidelines

Some helpful tips from Best Practice Guidelines (BPG) [54], [55] by two famous institutions, AIJ (Architecture Institution of Japan) and COST, are summarised in this section.

The size of the studied building determines the size of the entire computational domain. One important factor used in domain extension specification is a blockage, defined as the ratio of the projected area of a building (lying in flow

direction) on a vertical plane to free vertical section area of the whole domain. The CFD community has reached a consensus on maximum blockage as 3 % so that the airflow is presented from artificially accelerated velocity as compressed by small free regions. However, a more rigorous recommendation is made by mainstreams suggesting 1.5 % blockage.

The distance between the site lid and building roof ranges from $4H$ to $10H$ (where H represents the height of the tallest building), giving various blockage values for single building studies. In extensive field simulations for multiple building groups, domain height should be six times the height of tallest constructions (H_{max}). With 1.5 % blockage, the distance from the object region to the site lateral boundaries are $5H$ while $6H$ to the top of the domain. The wind tunnel, where the experiment is taken as a benchmark for CFD model validation, should be designed with no larger than 10 % blockage. Moreover, it is highlighted that air from the inlet boundary $5H$ away from the object encounters the building should get $15H$ downstream extent to depict the fully developed wake flow better.

BPGs recommended hexahedral cells rather than tetrahedral cells as mitigated truncation error by the former. The former type can also achieve a smoother iterative convergence and lower convergence criteria. However, tetrahedral cells are more flexible in the demonstration of complex geometries. A layer with prism cells is usually drawn as a pedestal at solid boundaries in a domain with tetrahedral elements to improve accuracy.

The worst domain resolution is regulated with a minimum of ten cells on each building dimension to elaborate the separation effect on flows by solid windward corners. The inflation ratio of adjacent cells should be maintained no larger than 1.3. The grids are always in a non-uniform arrangement to conserve mesh size, but denser near solid boundaries with a stretching ratio controlled less than 1.3 compared to adjacent elements. BPGs suggested arranging at least three cells below the evaluation level (typically, 1.5 – 2 m above the ground). For the model independency test, the initial mesh should be refined at least twice with a volume increasing ratio of 3.4, equivalently 1.5

for each dimension. However, a smaller ratio of around 1.2 for each side was used in the precedent studies.

2.2.5. Limitations

CFD is powerful in airflow modelling. However, the investigations of airflow in cities are primarily isothermal as firstly thermal properties of building surfaces as the boundary conditions are required to start the calculations and the secondly expected high computational burden to model naturally ventilated spaces with extremely fine meshes. The determination of building surface temperature as the boundary condition can be from the site measurement or simulation of building energy.

2.3. Coupling CFD and BES

The coupling, or integration, of CFD and BES techniques can compensate for their individual limitations and offer a more accurate assessment of the built environment. Here, CFD is used to discretise the fluid domain and BES to discretise the building energy demand calculation [16].

2.3.1. Coupling strategies

In general, there are two methods of coupling CFD and BES tools, known as *internal* and *external* coupling [56].

The internal coupling, also seen as sub-routinization, expands the existing program to cover both techniques. However, the developed code needs to be rewritten to achieve the extra functions. Also, it is computationally expensive as the mismatching time step size required to perform the dynamics in fluid and solid fields [57], [58]. The former takes few seconds while the latter takes hours. Furthermore, convergence may occur due to the stiffness difference between fluid and solid fields [58]. Therefore, the application of this approach was limited in precedent research [59].

Conversely, external coupling is a more widely used method, perhaps because BES and CFD techniques are each well developed, albeit separately. More

accurate predictions of building energy demand can be obtained by using the advantages of each tool. This approach overcomes the stiffness problem of internal coupling. Fluid and solid can be solved in different time scales. Moreover, it is easier to optimize the features of a particular domain individually rather than expand them functionally. This approach has been applied to most precedent research.

External coupling can be processed statically or dynamically. The terms ‘static’ and ‘dynamic’ represent the behaviour of data handshaking between two programs: the dynamic method calculates using updated inputs throughout the run time, whereas the static method processes the data exchange with fixed input [57].

Dynamic strategies processing the data exchange at every step are proposed for the cases where both programs intensely require the real-time boundary conditions to deliver the solutions. Four concepts were introduced into the dynamic approach: one-time-step coupling, quasi-dynamic coupling, full dynamic coupling, and virtual dynamic coupling [60]. One-time-step coupling achieves mutually consistent results (‘converged’) solutions in two programs by an iterative process within a single time step. It was suggested to dealing with conditions where there are significant turning points of weather or load. Assessment of building budget is primarily projected through a more extended period (daily, monthly, seasonal and annual) rather than a single time step. Thereby, the latter three methods can be adopted. Quasi-dynamic coupling contains series of one-step processes in every time step. At the end of each time step, the output of one program is transferred to the other program as its boundary conditions of the next time step. The fully dynamic method is finer coupling to the quasi-dynamic approach that convergence must be reached in each time step before moving to the next. Therefore, it is more computationally expensive. The virtual dynamic coupling can be a good strategy for long-term analysis due to the moderate modelling burden. It collects data from a bunch of the one-time-step dynamic coupling results for different scenarios. It then deduces regression equations to be embedded into the BES program for the calculation of energy consumptions.

2.3.2. Coupling convergence and frequency

Some boundary conditions of BES and CFD in coupling are obtained from each other. With iterative handshaking, the variables are updated until becoming stable. Five groups of exchanged information (including T_s with h and T_a, T_s with nominal h, T_s with q_c'', q_c'' with h and T_{air}, and q_c'' with nominal h) between BES and CFD domains are evaluated in convergence, stability, and speed [60]. For interior surfaces' coupling, the most proposed method for indoor coupling is BES provides inside surface temperature for CFD while CFD feeds back the surface convective heat transfer coefficient and air temperature to BES. The unique solution of the coupled model was proved to exist [24].

It was put forward that the surface coupling (external coupling) can overcome its drawback in accuracy comparing to the fully integrated (internal coupling) with a fine-enough time step size. The frequency of 4 – 10 iterations between programs was specified as expected to get converged indoor modelling. For instance, the time step of surface coupling should be set as 6 – 15 minutes to reach a similar accuracy by fully integrated approach processing at an interval every hour [60].

2.3.3. Current coupling researches

Previous applications of the external coupling of CFD and BES tools, mainly use the former three strategies of dynamic coupling (one-time-step, quasi dynamic, and fully dynamic), focus on both interior [7], [22], [24], [58], [61]–[64] and exterior surfaces [65]–[69].

This research focused on the coupling on exterior surfaces. Mochida et al. [64] used the cross-ventilation rate, estimated by site-scale CFD simulation, as the input for the BES analysis. Although their CFD domain covered the outdoor environment, the main change in BES occurred inside the room due to the updated ventilation rate. However, there was no significant improvement of the exterior CHTC. Nikko et al. [67] proposed wind factors to modify the wind profiles in the BES domain. The factors depended on the local terrain and urban morphologies. However, they did not differentiate between surfaces or

buildings because the weather data was applied uniformly to each object in the BES domain. Yi and Feng [65] and Malys, Musy, and Inard [66] used CFD to improve surface CHTC for BES. Some of these studies were designed for specific cases and did not generally reflect various and random urban morphologies [64], [66], [67]. Also, many of the executed couplings [64], [65], [67] between tools lack an iterative process that improves predictive accuracy.

In BES-CFD coupling studies, the interest region of the CFD domain for natural ventilation modelling was mainly defined in three ways:

- *Indoor-only*. For example, Barbason and Reiter (2014) [70] executed quasi-dynamic coupling for a two-storey house with space discretised. Hong, Lee, and Kim (2017) [71] simulated the energy consumption of a classroom in Seoul using the coupling CFD – BES method.

- *Hybrid indoor-outdoor*. For example, Wang and Wong (2009) [72] applied a one-time-step coupling on cross-ventilated room's interior surfaces. Kim et al. (2013) [73] compared different modelling methods by testing the naturally ventilated residential building. Zhang et al. (2013) [68] conducted an eight-day simulation of ventilated scenarios with both interior and exterior surfaces involved in coupling.

- *Regional decomposition (multi-scale modelling / nesting technique)*. There are very limited cases using regional decomposition approach [64].

The indoor-only method is somewhat restricted as it is difficult to define the boundary conditions at the opening surfaces for CFD simulations without considering the influence of the surrounding environment. The hybrid indoor-outdoor model provides the complete picture of airflow as sheltering effect in the city area is involved besides the indoor environment. However, this approach typically requires a high-resolution mesh (high number of cells) [44]–[46], [73], [74] and much longer calculation time. Also, so long as iterative calculations are required in a dynamic coupling simulation [57], [75], the burden would be extremely high to execute the CFD calculations of a hybrid

indoor-outdoor model. The regional decomposition method defines two (or multiple) regions in different scales. It uses one region's output at the interfaces (where the different-scale parts share the information) to facilitate modelling the other region. This method takes less time and lowers computational cost than the hybrid indoor-outdoor method, and it provides a more accurate outcome than the indoor-only method provided.

Mochida et al. [64] employed the regional decomposition method. They created two models, one (denoted as R1) was used to model the whole study domain, and the other (denoted as R2) to cover only a near-field region around buildings. R2 was treated as a non-isothermal model to carry out a precise calculation with boundary conditions extracted from the results of R1, which was processed isothermally with a less computational burden.

Only a few studies employed the virtual dynamic method. For example, Qin et al. (2012) [76] employed a neural network program trained by CFD results and then replaced CFD in the iterative coupling process when communicating with BES. At the same time, the modelling was performed for interior surfaces. Yi and Malkawi (2012) [77] developed an artificial neural network (ANN) model from the results of CFD and then the predictions of local weather conditions were passed to BES for long-term assessment of building performance. An optimized building form could be selected on this basis.

Table 2-1 summaries some coupling researches in seven aspects: the position of coupling interfaces, the ventilation type, employed programs of both domains, the exchanged variables (from BES to CFD and reversely), coupling strategy and the length of simulation period.

2.3.4. Limitations

The gaps of current studies of coupling CFD and BES are explored as:

- The precedent researches of CFD-BES coupling mainly focused on the indoor environment but only a few to communicate with outdoor microclimate. As discussed before, the current BES tools use empirical

correlations for outside surface convective heat transfer coefficient with neglected sheltering effect by the neighbouring constructions [78]. Therefore, the energy demand assessment's potential enhancement by applying the coupling technique to building outside surfaces.

- Though fully dynamic coupling is the most accurate way, the quasi-dynamic coupling is the most popular option. Particularly for scenarios with natural ventilation, the intense computational burden restricted the application of fully dynamic coupling. Therefore, a novel way to fast process fully dynamic coupling for naturally ventilated spaces is required.

- As the main driver of the growth in building energy in the next thirty years is from the emerging countries [79], where rising population and rapid urbanization are occurring, increasing attention is paid to the city-scale energy studies. Therefore, when long-term urban energy modelling, valid virtual dynamic coupling seems the only practical option. Furthermore, adjusting the weather data would be homogeneously assigned to the exterior surfaces in building energy models - meaning that no difference from surface to surface would be expressed despite significant vertical gradients.

  This implies that it is vital to provide a direct specification of convection conditions for all envelope surfaces in a city using metamodels such as regression or advance models. There are some studies aimed to improve the regression functions of CHTC to enhance their accuracy. For example:

  Zhang, Gan, and Mirzaei (2019) [80] developed a regression function for the local CHTC of a specific building integrated photovoltaics (BIPV) surface. They tested the BIPV in designed scenarios of wind speeds, wind angles, solar radiations, air temperatures, and arrangement of BIPVs to get the dataset of local CHTC. It should be, however, highlighted that although such CHTC regression metamodels could be helpful in some specific scenarios, the complexity of urban environment increases difficulties of the implementation of metamodels in urban areas as not only

weather conditions, but also the urban morphology (arrangement of buildings) [81], [82].

In summary, applying a dynamic coupling method for exterior surfaces is limited. Therefore, attempts are required to focus on the usage for different scenarios, including sealed buildings where spaces are controlled by mechanical ventilation without windows opened and the naturally ventilated buildings. Strategies are needed to provide fast simulation simultaneously with proper presentation, especially for naturally ventilated buildings always associated with highly dense meshes. Further, practices of enhancing neighbourhood effect in the medium-to-long-term modelling by virtual dynamic coupling are also in demand. Currently, the virtual dynamic coupling is used to improve the weather profiles, which would be assigned to the site homogeneously, ignoring the deviation by sheltering effect in cities.

Hence, advanced models such as artificial neural networks (ANN) seem preferable over regression models as they have been successfully applied in many fields of building services, including control of humidity [83], control of intelligent lighting [84], and optimization of building designs [85], etc.

Table 2-1 Summary of some coupling researches

Authors	Ref.	Interface position	Natural ventilation ?	Programs (BES + CFD)	From BES to CFD	From CFD to BES	Coupling strategy	Period
Negrao	[7]	interior	yes	TRNSYS +/	T_s	Q + flow rate	fully dynamic	short-term
Beausoleil-Morrison	[22]	interior	yes	ESP-r +/	T_s/h_c	h_c	quasi-dynamic	short-term
Zhai and Chen	[24]	interior	no	EnergyPlus +MIT-CFD	Different types were tested.		short-term	
Fan, Hayashi, and Ito	[61], [62]	interior	no	TRNSYS +Fluent	$q + T$	$T + U$	fully dynamic	short-term
Gijón-Rivera et al.	[63]	interior	no	ESP-r/TRNSYS + FORTRAN	h_c	h_c	one-step static	short-term
Mochida et al.	[64]	interior	yes	TRNSYS +/	/	flow rate	one-step static	short-term
Yi and Feng	[65]	interior+ exterior	no	EnergyPlus +Fluent	T_s	h_c	quasi-dynamic	short-term
Malys, Musy, and Inard	[66]	exterior	no	SOLENE +CODE_STURNE	/	/	/	mid-term
Nikkho et al.	[67]	exterior	no	EnergyPlus +OpenFOAM	/	weather data	virtual dynamic	long-term
Zhang et al.	[68]	Interior + exterior	yes	EnergyPlus +Fluent	T_s	$h_c + T_a$ + flow rate	quasi-dynamic	mid-term
Shen and Wang	[69]	exterior	no	EnergyPlus +Gambit	T_s	h_c	quasi-dynamic	short-term

Barbason and Reiter	[70]	interior	yes	TRNSYS +Fluent	$T_a + T_s$	$T_z + T_s$	quasi-dynamic	short-term
Hong, Lee, and Kim	[71]	interior	yes / no	EnergyPlus + STAR-CCM+	/	flow rate	one-step static	short-term
Wang and Wong	[72]	interior	yes	ESP-r +Fluent	T_s + flow info. @ openings	h_c	one-time-step dynamic	short-term
Kim et al.	[73]	interior	yes	EnergyPlus + NA	T_s	*h* (airflow rate)	quasi-dynamic	short-term
Qin et al.	[76]	interior	no	DeST +/	T_s	q_c''	virtual dynamic	long-term
Yi and Malkawi	[77]	interior	/	/	/	weather data	virtual coupling	long-term

Chapter 3. GENERAL APPROACH

3.1. Project Design

This research is proposed to base on simulations. As aiming to develop a framework, this research was following the inductive research process. The external coupling strategy was adopted in this project to use of the strength of current CFD and BES tools.

Mutually consistent geometrical models were created in the BES and CFD domains with coherence in the boundary name.

The investigations would consider buildings with natural and mechanical ventilation to provide frameworks for applying the coupling method in different scenarios. Those with only mechanical ventilation were denoted as sealed scenarios. The term 'sealed' means the buildings are isolated from outdoors and are ventilated using a mechanical system with all windows closed so no natural ventilation occurs. In contrast, the natural ventilation scenarios referred to those where the windows of buildings were opened.

Firstly, a simple framework of coupling CFD and BES was put forward for short-term fully dynamic simulation. In this study, the building surface temperatures (T_S) of the energy model, and the convective heat transfer coefficients (h_c) of the CFD model, are the variables exchanged between the CFD and BES domains. The buildings were tested using a fully dynamic approach to ensure that convergence was guaranteed each time step. Here, convergence is a unique solution shared by both domains. For this study, both domains achieved the same (or with only a slight difference in) convective heat flux ($q_c^{''}$) on outdoor surfaces in every time step before moving to the next time step. A simple sealed case study was undertaken to test and assess the performance of the proposed framework. Besides the sealed case, the model was expanded to execute natural ventilation scenarios (in this study, night flushing cooling using cool air to precool the spaces during the night-time was

employed.) that integrate different scales of CFD and BES. The fully dynamic coupling was considered not feasible for medium-term to long-term simulation due to its demand of extremely intense computational time and burden. A framework of virtual dynamic coupling that combined CFD, BES, and artificial intelligence was developed and investigated to load medium/long-term energy modelling effectively and efficiently.

In this research, all energy modelling used EnergyPlus 8.7©, CFD simulation used Ansys Fluent 19.1© and CFX 19.1©, and bespoke code was written in MATLAB R2018a©. EnergyPlus used a text input file with a format of *.IDF.

3.2. Development of General Framework of Coupling CFD and BES

A schematic of the general external coupling process for short-term building energy demand assessment is presented in *Figure 3-1*. This framework aims to improve the assessment of the energy demand of any building or community by using the localised convective characteristics from CFD calculations instead of BES's embedded algorithms. In general, information required by the framework includes:

- site information, including location, terrain, and orientation of buildings, etc.
- building form, including building type, building dimensions, ventilation mechanism and opening positions, etc.
- calculation operations, including date, run period, iterative number limit, etc.
- meteorological data, including solar radiation, wind speed, ambient temperature, wind angle, ground temperature, sunset time, and other weather conditions.

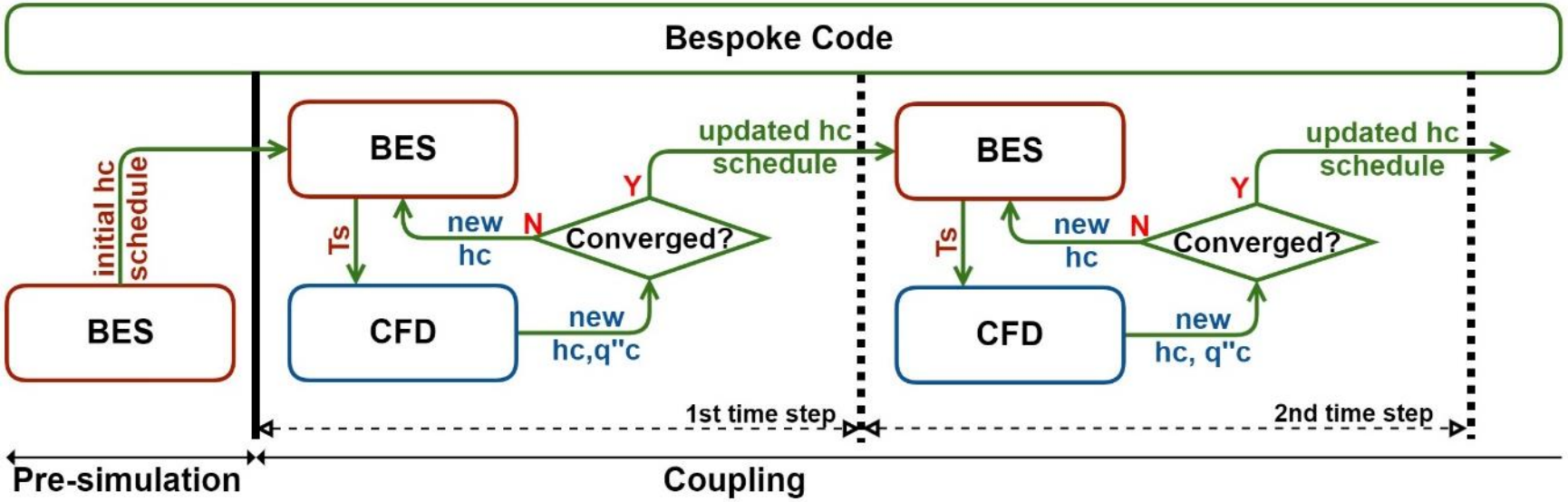

Figure 3-1 General framework for short-term external coupling

To consider the time lag phenomenon of thermal calculations, a pre-simulation is run for a defined period (from a few hours to several days) before the simulation period. The latter stage may benefit from an initial guess by the pre-simulation. Therefore, in the pre-simulation stage, the convective heat transfer calculations are made by the BES using its embedded algorithms; here, those of EnergyPlus. Edited schedules of default convective heat transfer coefficient values for all surfaces are then added to the BES input file. Also, the BES's CHTC calculation method is amended to 'customization' or 'schedule' instead of the empirical algorithms used to start the dynamic simulation.

The core of the dynamic simulation is the iterative calculations shared between the CFD and BES domains at each time step (shaded in blue in *Figure 3-1*). Here, T_s is forwarded by the BES to the CFD model as a boundary condition. The CFD then returns h_c to the BES via bespoke code. Within each time-step of the simulation period, the h_c schedules and T_s are updated during every iteration until convergence is achieved. It is noteworthy that the CFD domain runs a quasi-dynamic simulation, which means that the boundary conditions are fixed for the transient flow at every time step. An appropriate residual criterion should be assigned for the reference variable. The reference variables can separately be T_s for BES and h_c for CFD, alternatively using q_c'' in either domain. If the residual meets the required criterion after two continuous iterations, the loop ends, and the calculation progresses to the next time-step. Otherwise, iterative calculation continues.

Convergence of the coupling process can be determined by two methods. The first is when the residual of T_s by BES or h_c by CFD between two iterations reaches a threshold. The second method is to achieve acceptable difference in q_c'' between two domains. In this study, both methods were employed. The convergence criterion for each time-step of the coupling process was set to three orders of magnitudes for both T_s and h_c (h^* indeed as explained in *Section 3.4.1*, see *Eqn. 13*) in sealed scenarios or two orders of magnitudes for q_c'' in ventilated scenarios. However, the convergence criterion was altered to two orders of magnitudes if the number of iterations for a single time-step exceeded 20 and was deemed an acceptable compromise between prediction

accuracy and computational time and cost. The residuals were determined using the average error between two sequential iterations. As EnergyPlus only accepts user-defined *CHTC* for non-fenestration surfaces, all of the iterative analysis and results given in the following sections are based on exterior walls and roofs.

The detailed frameworks are developed based on this general framework for different scenarios, including the sealed and ventilated scenarios. The information is provided in corresponding chapters.

Appendix 1 shows the bespoke code written in MATLAB for assigning the surface temperature from the BES field as the boundary condition in Fluent, the new CHTCs in EnergyPlus and check the convergence of the coupling process.

3.3. Geometric Design of Coupling Model

3.3.1. Benchmark model for the CFD field

The configuration of the CFD model needs to be validated against empirical data before being applied to the coupling method. The experiments by the Architectural Institution of Japan (AIJ) [83] provided data measured in a wind tunnel for a range of cuboids and layouts. Its *Case C* consisted of nine small cubes (their dimensions $W \times L \times H$ are 0.2 m × 0.2 m × 0.2 m) arranged in a 3 × 3 array and represented a simple city community. It was selected as the benchmark for the CFD model validation. The aspect ratio of every street canyon in Case C was unity.

The AIJ placed 120 test points 0.02 m above the ground to monitor the local air velocity within the street canyons of this simple city block. The distribution of 120 points is presented in *Figure 3-2*. The coordinates of each test points are given in *Appendix 2*.

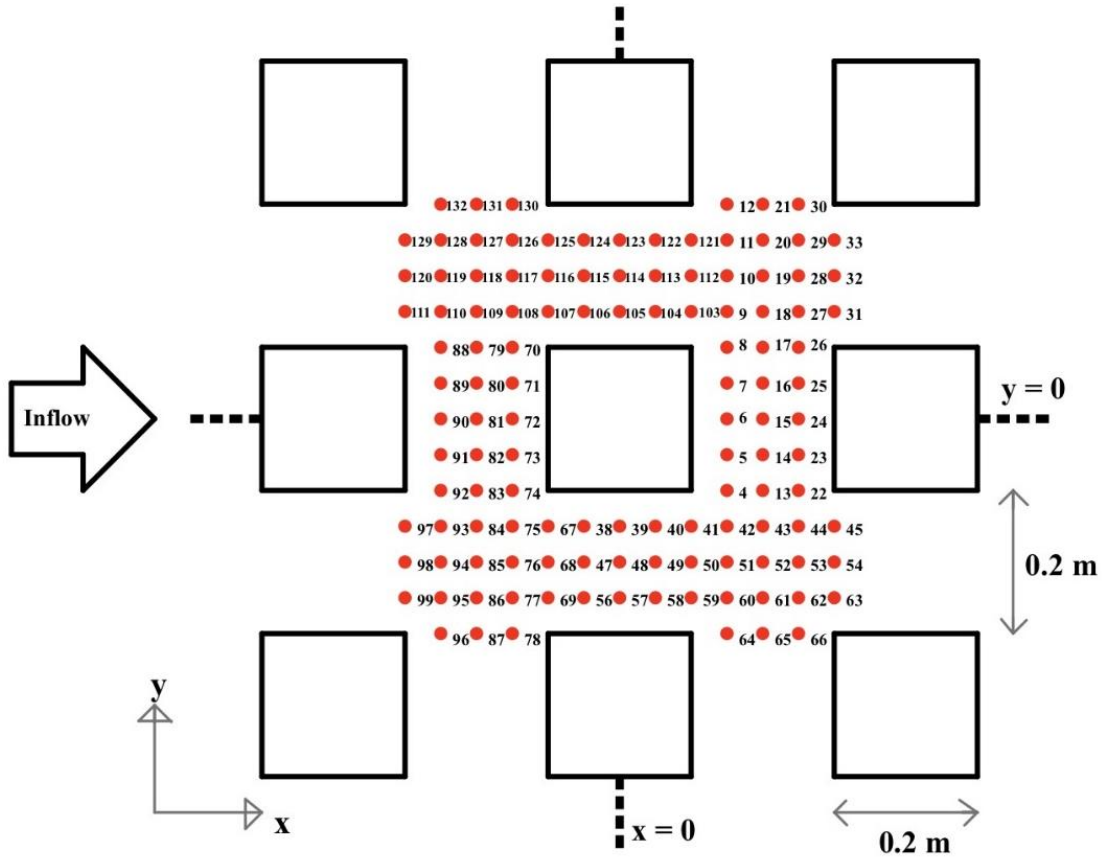

Figure 3-2 Distribution of 120 test points of Architecture Institute of Japan Case C

3.3.2. Benchmark commercial building from DoE for the BES field

It is difficult to find suitable buildings that are geometrically matching with the AIJ Case C. An alternative method is to use an existing model of a similar scenario and then amend it to obtain equivalent performance. In this study, a benchmark building was developed from a small office model provided by U.S. Department of Energy (DoE) [84], [85], as presented in *Figure 3-3*.

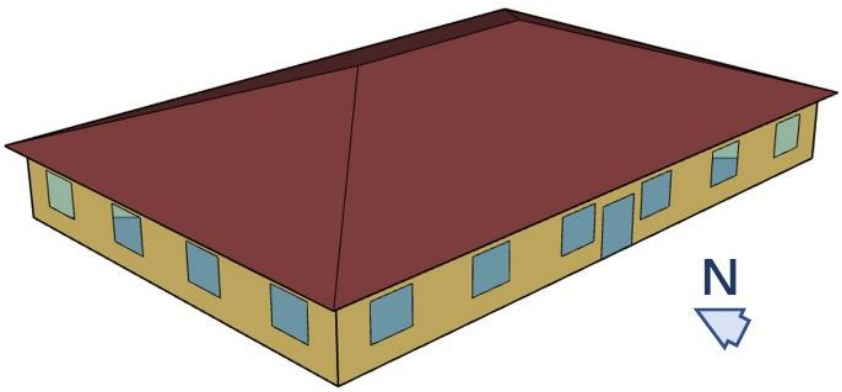

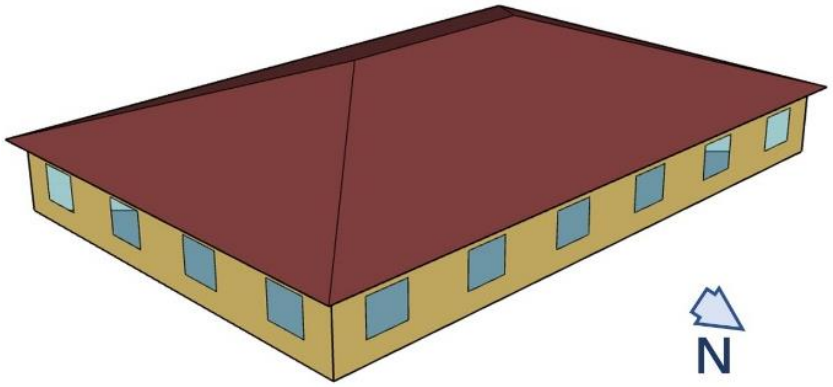

Figure 3-3 Benchmark small office model by DoE [85]

The building consists of an attic space and five offices laid out so that one office forms a central core room surrounded, on all sides, by the other four offices. The window to wall ratio is 24.4 % for the building's south-facing front façade (where the entrance door is situated; see *Figure 3-3*) and 19.8 % for the other walls. The door height is 2.13 m, windows occupy 39.7 % of the wall in the horizontal dimension and 50 % of the vertical dimension. Windows are located 0.9 m above ground level. The door width is 6.6 % of the wall width.

3.3.3. Coupling model design

In this project, the coupling model was a small street community consisting of nine cuboid commercial buildings ($L \times W \times H = 10\ \mathrm{m} \times 10\ \mathrm{m} \times 10\ \mathrm{m}$) in a 3 × 3 array. The distance between any two buildings was determined as 10 m. The shape and dimension of buildings were adjusted to achieve a homologous geometry similar to the Case C of the Architectural Institution of Japan (AIJ) [83]. The aspect ratio of every street canyon inside the community is 1, which agrees with the aspect ratio of Case C of AIJ.

Each building is divided into three storeys and the heights of the floors are 3.4 m, 3.3 m, and 3.3 m from the bottom of the building to the top. Windows are situated on the south and north façades of each floor to facilitate cross-ventilation and have the same window to wall ratio used in the benchmark case, which is 19.8 % with 39.7 % in horizontal and 50 % in vertical directions. In addition, every building has an entrance door on the south façade. The door has a height of 2.13 m which is the same as that in the reference benchmark

BES model, but its width is 1 m because using the 6.6 % of the wall width gave a width that is too narrow. Moreover, the buildings are oriented to the south to optimize energy conservation and indoor comfort. *Figure 3-4* shows the distribution of newly developed EnergyPlus model for the case studies and provide a view of nine buildings indexed from B1 in the southwest to B9 in the northeast. Unlike the sealed scenario, when the buildings are under natural ventilation, the windows on top two floors are divided into two even parts.

Each surface was denoted using the format: storey number-surface type-surface orientation. The letters S, W, D, and R represent walls, windows, doors, and roofs. Then, orientation is counted counter-clockwise from due south as 1. Finally, combining with the building index, the name of each surface is determined (e.g., B11S2 denotes the east wall on the ground floor of B1). In ventilated scenarios, the lower half of the top two floors' windows is denoted as W1 while the upper part as W2, as seen in *Figure 6-5*. Only the W1s are openable for a designed period. The full list of building surfaces is provided in *Appendix 3*.

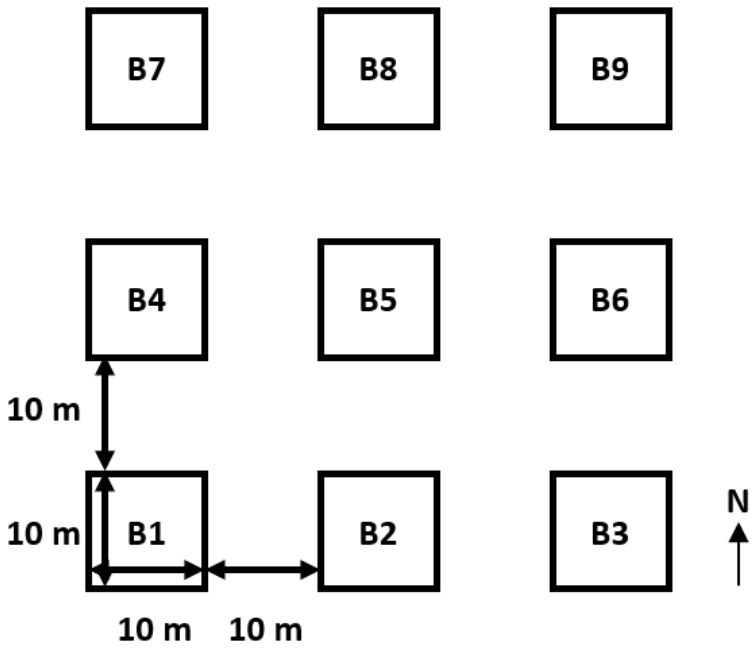

Figure 3-4 Distribution of nine cubic buildings for the case studies [86]

3.4. Communications Between CFD and BES Solvers

Mutually consistent geometrical models were created in the BES and CFD as the essential coupling condition. The geometrical details were described in *Section 3.3.3*. The communication between CFD and BES domains depended on the matching characteristics of interfaces and the consistent climatical models. For the former aspect, firstly, it requires determining the interfaces for the coupling process, and then the parameters exchanged on corresponding interfaces. The boundary conditions of the CFD domain in the coupling process need to be updated according to the weather data. Therefore, the CFD boundaries' flow velocity, turbulence, and temperature were featured as the vertical profiles using the same algorithm as EnergyPlus.

3.4.1. Matching characteristics of interfaces in two domains

The coupling strategy focused on the outdoors in this study; thus, the coupling interfaces between BES and CFD domains were placed merely at the buildings' exterior surfaces. All wall surfaces and roof surfaces participated in the iterative calculation during the coupling process, that BES provided surface temperature for CFD while CFD improved the convective heat transfer coefficients in BES.

The concept of convective heat transfer coefficient, h_c (W/m^{2}K), is expressed based on a relation between the convective heat flux, q_c'' (W/m^2), and temperature difference between the solid boundary and its surrounding fluid as known as the Newton's law of cooling:

$$q_c'' = h_c(T_s - T_a) \qquad \text{Eqn. 11)}$$

where $T_{a,s}$ (°C) is the surrounding ambient air temperature, respectively.

The value of h_c used by the CFD tool is a function of the temperature difference between the solid surface, T_s (°C), and the adjacent fluid flow, $T_{a,s}$ (°C). However, EnergyPlus calculates the surface convective heat transfer

using $T_{a,z}$ (°C), which is considered to have a fixed value at a particular height for any given weather data. The principle of the coupling process is to achieve a unified convective heat flux,q_c'', in both tools. Therefore, the parity is achieved by equating the two terms:

$$q''_{c,CFD} = h_c(T_s - T_{a,s}) = h^*(T_s - T_{a,z}) = q''_{c,BES} \quad \text{Eqn. 12)}$$

where h^* is a virtual h_c that works as an *adapter* to helps EnergyPlus estimate the same convection as the CFD model. It is given by

$$h^* = \frac{q''_{c,CFD}}{(T_s - T_{a,z})} \quad \text{Eqn. 13)}$$

In an iterative process (see *Figure 3-1*), it can be also presented as:

$${h_{i+1}}^* = \frac{q''_{c,CFD_i}}{(T_{s_i} - T_{a,z})} \quad \text{Eqn. 14)}$$

where i specifies the current iteration index.

The glass surfaces (including windows and doors) were treated differently. The temperature of glass surfaces would be transmitted from the BES side to the CFD side; however, no convective heat transfer coefficient on glass surfaces in BES would be updated throughout the whole process.

3.4.2. Consistent climate conditions in two domains

The validated CFD model was enlarged 50 times to match the BES domain's size and to represent the neighbourhood of the coupling procedure. In addition, the grids were amended slightly to capture different surfaces on buildings' facades. After these, the CFD domain solved the temperature equation in the Reynolds Averaged Navier-Stokes (RANS) scheme. Rather than the steady-state modelling in the validation stage, semi-transient CFD simulations were executed in the coupling stage. Weather and boundary conditions were updated hourly rather than the steady-state modelling in the validation stage. The flow velocity and turbulence features derived from experimental data were

replaced by vertical wind profiles using the same algorithm as EnergyPlus. In EnergyPlus, the vertical profile of the local wind speed, U_z (m/s), for neutral atmospheric boundary layer (ABL) modelling is set based on a power-law profile regarding to the altitude, z (m), as follows:

$$U_z = U_{met}\left(\frac{\delta_{met}}{z_{met}}\right)^{\alpha_{met}}\left(\frac{z}{\delta}\right)^{\alpha} \quad \text{Eqn. 15)}$$

where α is a dimensionless exponent and δ (m) is the boundary layer thickness at the site. Both parameters depend upon the local terrain type. The subscript '*met*' refers to those data collected at the meteorological station. Default values of z_{met}, δ_{met}, and α_{met} are 10 m, 270 m, and 0.14, respectively.

In EnergyPlus, the embedded equation for the decrease in air temperature with altitude in the troposphere is:

$$T_{a,z} = T_b + L_a\left(\frac{E_r z}{(E_r + z)} - H_b\right) \quad \text{Eqn. 16)}$$

where L_a (K/m) is the air temperature gradient throughout the troposphere and is always $L_a = -0.0065$K/m. E_r (m) is the radius of the Earth with a value of 6356km. H_b (m) allows the boundary layer to be extended above the troposphere, which is unnecessary here and so is always zero. $T_{a,z}$ (°C) and T_b (°C) are the local air temperatures at altitude z (m) and at ground level, respectively. The latter can be determined from the meteorological air temperature ($T_{a,z\,met}$, °C) measured at height z_{met} (m) using:

$$T_b = T_{a,z\,met} - L_a\left(\frac{E_r z_{met}}{(E_r + z_{met})} - H_b\right) \quad \text{Eqn. 17)}$$

Here, $T_{a,z\,met}$ is normally measured at z_{met} =1.5 m above ground level.

The vertical velocity and temperature gradients at the CFD inlet boundary (see in *Figure 3-5*), are determined by (*Eqn. 15 - Eqn. 17*) , so that both tools have the same profiles. The following equations are used to calculate the local turbulence kinetic energy, k (J/kg), and the turbulence dissipation rate, ε

(m^2/s^3), at z in the vertical profile of the dimensionless turbulent intensity, I_z where:

$$I_z = \frac{u'_z}{U_z} = 0.1\left(\frac{z}{\delta}\right)^{-\alpha-0.05} \quad \text{Eqn. 18)}$$

The boundary layer thickness, δ (m), depends on the local terrain, and is δ =460 m in a city [25]. The corresponding power law exponent is α =0.33 for a city, and u'_z (m/s) is the root mean square of the velocity fluctuations in the stream-wise direction:

$$k_z = \frac{{u'_{u,z}}^2 + {u'_{v,z}}^2 + {u'_{w,z}}^2}{2} \cong \frac{3}{2}{u'_z}^2 = \frac{3}{2}(I_z U_z)^2 \quad \text{Eqn. 19)}$$

$$\varepsilon_z = C_\mu^{1/2} k_z \frac{U_{ref}}{z_{ref}} \alpha \left(\frac{z}{z_{ref}}\right)^{\alpha-1} \quad \text{Eqn. 20)}$$

where C_μ is the dimensionless $k-\varepsilon$ model constant taken as C_μ =0.09. The '*ref*' subscript indicates reference conditions, where U_{ref} and z_{ref} are set using meteorological data.

3.5. CFD Modelling

3.5.1. Mathematical models

The governing equations of the RANS scheme for the steady modelling are, for continuity and momentum, respectively:

$$\frac{\partial \rho}{\partial t} + \frac{\partial}{\partial x_j}\left(U_j\right) = 0 \quad \text{Eqn. 21)}$$

$$\frac{\partial}{\partial t}\left(\rho u_j\right) + \rho U_j \frac{\partial}{\partial x_j}\left(U_i\right) = -\frac{\partial P}{\partial x_i} + \frac{\partial}{\partial x_j}\left[\mu\left(\frac{\partial U_i}{\partial x_j}\right) + \left(-\rho\overline{u_i u_j}\right)\right] + \rho\vec{g} \quad \text{Eqn. 22)}$$

Where ρ (kg/m^3) is the fluid density, t (s) is the time, U (m/s) is the mean flow velocity, u is the dimensionless fluctuating component of U, P (Pa) is the fluid pressure, μ is the dimensionless molecular viscosity, $\rho\vec{g}$ is the term reflecting

the gravitational force, and the $-\rho\overline{u_i u_j}$ term is the Reynolds stress tensor, which can be determined by the eddy viscosity assumption:

$$-\rho\overline{u_i u_j} = \mu_t\left(\frac{\partial U_i}{\partial x_j}+\frac{\partial U_j}{\partial x_i}\right)-\frac{2}{3}\delta_{ij}\left(\mu_t\frac{\partial U_k}{\partial x_k}+\rho k\right) \quad \text{Eqn. 23)}$$

where μ_t (kg/m·s) is the eddy viscosity.

In this study, the $k-\varepsilon$ model, which solves transport equations for k and its dissipation rate, is used to calculate μ_t by

$$\mu_t = C_\mu\rho\frac{k^2}{\varepsilon} \quad \text{Eqn. 24)}$$

where C_μ is a constant.

Standard method was selected to solve the $k-\varepsilon$ model. This turbulence model is widely used in similar studies due to its low computational burden when compared to the more accurate Large-Eddy Simulation (LES) method. The transport equations of k and ε using the standard $k-\varepsilon$ (SKE) model are [87]:

$$\frac{\partial}{\partial t}(\rho k)+\frac{\partial}{\partial x_i}(\rho k U_i)=\frac{\partial}{\partial x_j}\left[\left(\mu+\frac{\mu_t}{\sigma_k}\right)\frac{\partial k}{\partial x_j}\right]+G_k+G_b-\rho\varepsilon-Y_M+S_k \quad \text{Eqn. 25)}$$

$$\frac{\partial}{\partial t}(\rho\varepsilon)+\frac{\partial}{\partial x_i}(\rho\varepsilon U_i) = \frac{\partial}{\partial x_j}\left[\left(\mu+\frac{\mu_t}{\sigma_\varepsilon}\right)\frac{\partial\varepsilon}{\partial x_j}\right]+C_{1\varepsilon}\frac{\varepsilon}{k}(G_k+C_{3\varepsilon}G_b)-C_{2\varepsilon}\rho\frac{\varepsilon^2}{k}+S_\varepsilon \quad \text{Eqn. 26)}$$

where G_k (kg·m^2/s^3) and G_b (kg·m^2/s^3) are generated k terms by the mean velocity gradient and buoyancy, respectively. σ_k and σ_ε denote the turbulent Prandtl number for k and ε, respectively; Y_M (kg · m^2/s^3) is the dilatation dissipation, S_k (kg·m^2/s^3) and S_ε (kg/m·s^4) are additional source or sink terms for k and ε, respectively; $C_{1\varepsilon}, C_{2\varepsilon}$ and $C_{3\varepsilon}$ are constant values.

The default values for the standard k−ε model constants used in Fluent are given as $C_\mu =$ 0.09, $C_{1\varepsilon} =$ 1.44, $C_{2\varepsilon} =$ 1.92, $\sigma_k =$ 1.0, σ_ε =1.3 [87].

The energy equation can be also written as:

$$\frac{\partial}{\partial t}(\rho E) + \frac{\partial}{\partial x_i} U_i(\rho E + P) = \frac{\partial}{\partial x_j}\left[K_{eff}\frac{\partial T}{\partial x_j} - \sum_j h_j \bar{J}_j + \left(\bar{\bar{\tau}}_{eff} U_i\right)\right] + S_h \quad \text{Eqn. 27)}$$

$$E = h_s - \frac{P}{\rho} + 0.5U^2 \quad \text{Eqn. 28)}$$

where E (J/kg) represents the total energy of the fluid, T (K) is the flow temperature, and h_s (J/kg) is the sensible heat of the fluid. h_j (J/mol) and $\bar{J}_j$ (mol/m^3·s) are the sensible enthalpy and the diffusion flux of the spices j, and the term involving the deviatoric stress tensor $\bar{\bar{\tau}}_{eff}$ (J/m^3) represents the viscous heating. K_{eff} (W/K·m) is the coefficient of the effective thermal conductivity, in standard $k-\varepsilon$ model it is defined as follows:

$$K_{eff} = K_t + \frac{C_p \mu_t}{Pr_t} \quad \text{Eqn. 29)}$$

where K_t (W/K·m) is the coefficient of the thermal conductivity, C_p (J/K·kg) is the thermal capacity of the fluid and Pr_t is the turbulent Prandtl number with a default value of 0.85.

The vertical profiles of the inflow velocity (U_z), kinetic energy (k_z), and turbulence dispersion rate (ε_z) should rest with the experimental measurement for validation modelling or climatic models for coupling calculations.

Standard wall function was respectively applied to the models to solve the near-wall region conditions with turbulence metrics of 30 < y^* < 300. The standard wall function calculates y^* using the below equation:

$$y^* \equiv \frac{\rho C_\mu^{0.25} k_P^{0.5} y_P}{\mu} \quad \text{Eqn. 30)}$$

where k_P (m^2/s^2) is the turbulent kinetic energy at the near-wall node *P which is placed at a distance of y_P (m) from the wall.

3.5.2. Computational domain for validation

A directionally independent cylindrical model proposed by Mirzaei and Carmiliet [47] was employed to capture the stochastic winds, as shown in *Figure 3-5*. According to the best practice given by the COST as summarised in *Chapter 2*, the computational domain had the dimensions of $5H$ and $15H$ in the vertical and horizontal planes, respectively. Here, H is the height of the target object and is $H = 0.2$ m. The inflation ratio of continuous cells was maintained so that it was no larger than 1.2. Hybrid meshes, which helped to minimize the computational cost of the coupling process, were generated using the multi-zonal pave method in Fluent 19.1©. A dense layer of structured hexahedral grids was drawn around the buildings, while a coarse layer of structured grids was created towards laterals of the site domain. An unstructured buffer layer linked two structured layers with a smooth transition. This meshing strategy was aimed at reducing the computational cost with little sacrifice on accuracy [88]. *Figure 3-6* shows the buffer layer filled with dense unstructured hexahedral cells. The perimeter of circle was evenly divided into 16 parts, so that the domain boundaries can capture different wind directions at intervals of 22.5 °; see *Figure 3-5*. Four meshes consisting of 130,968, 159,469, 198,627, and 233,766 cells, were created with a refinement ratio of 1.1 in each dimension following the COST recommendations [52]. The four meshes created with increased model size are hereon denoted m1, m2, m3 and m4.

The vertical profiles of the inflow velocity (U_z), the kinetic energy (k_z), and the turbulence dispersion rate (ε_z) were obtained from the AIJ wind tunnel measurements. The energy equations were not activated as the validation modelling was isothermal. A standard function was applied as the wall treatment. All of the equations were solved by the SIMPLE algorithm. The pressure equation was discretized using a *second order* scheme while the rest used the *second order upwind* method. Convergence was achieved below six orders of magnitude for all equations, except for the continuity equation, which was $<5 \times 10^{-6}$.

Table 3-1 Boundary conditions for CFD domain validation

Boundary	Type	Setups
Ground, Building surfaces, Non-inlet/outlet laterals	Wall	No-slip
Inlet	Velocity inlet	Components specified velocity method: Velocity components: x and y component from vertical profiles by AIJ k and ε from vertical profiles by AIJ
Outflow	Pressure outlet	Gauge pressure = 0pa k and ε from the verticals profile
Sky	Symmetry	/

Table 3-1 shows the boundary condition set for AIJ-Case-C CFD validation.

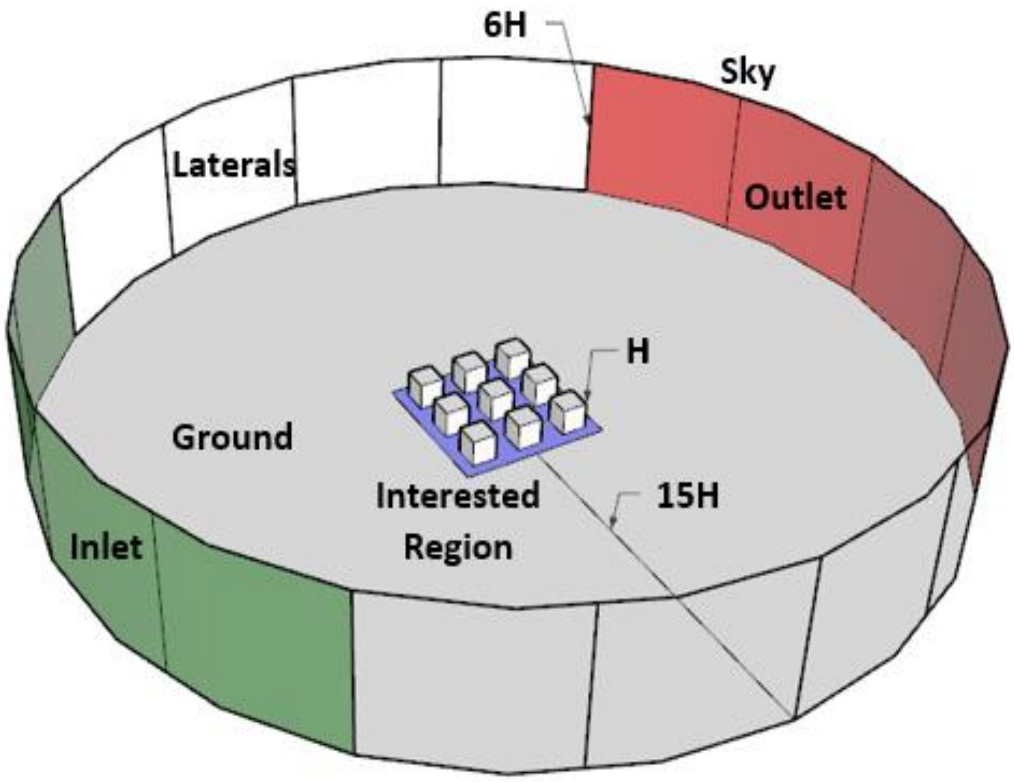

Figure 3-5 Computational domain for CFD [89]

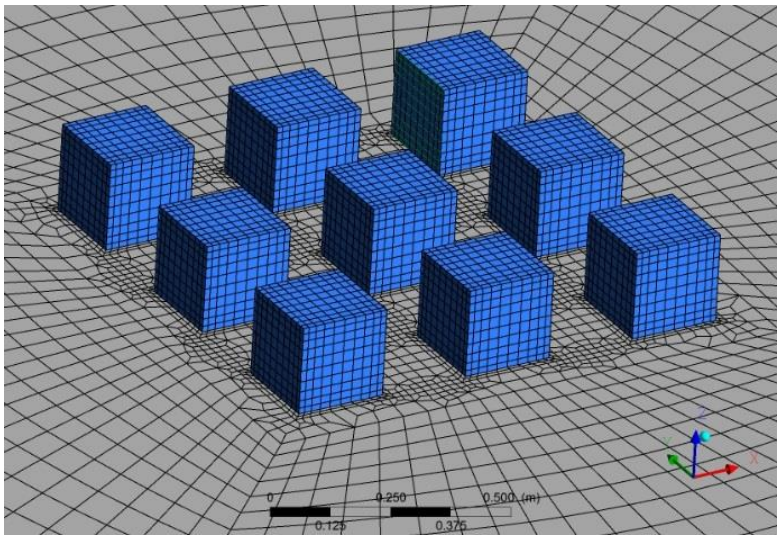

Figure 3-6 Computational grids for AIJ-Case-C CFD validation [90]

3.5.3. Computational domain for coupling simulations

The grids of the validated model were amended slightly (without or with little change on the layer for boundary flow) to capture the different surfaces, e.g., the structure of floors, the windows, and the doors. *Figure 3-7a* shows the mesh for short-term sealed scenario modelling.

Two models of different densities were used to demonstrate areas of two scales for modelling ventilated scenarios. The one with finer grids was named CFD_f, while the other with coarser grids was CFD (similar to that used for short-term sealing-scenario modelling). The CFD_f model was developed from a validated model proposed by Shirzadi et al. [39], while the CFD model (see in *Figure 3-7b*) was based on the validated model of AIJ Case C presented in *Section 3.5.2*.

The benchmark model for CFD_f was validated against measurements of wind tunnel experiments conducted at Niigata Institute of Technology as reported by Tominaga and Blocken [91]. The building model had dimensions of 0.16 m × 0.16 m × 0.2 m for width, depth, and height, and it was subject to cross-ventilation through two openings on the opposite walls. Eight similar structures surrounded the target building with the exact dimensions in a community with an urban area density of $C_A = \frac{\text{built area}}{\text{plan area}} = 0.25$, the same as that of AIJ case C and the designed coupling model. The valid configuration of CFD_f referred to

the work of Shirzadi et al. [39], who achieved a prediction error of flow rate of 7 % by using a calibrated $k-\varepsilon$ model. According to this calibrated model, the modified values of coefficients in *Eqn. 25* and *Eqn. 26* were changed to $C_\mu = 0.141$, $C_{1\varepsilon} = 1.50$, $C_{2\varepsilon} = 3.20$, $\sigma_k = 1.0$ and $\sigma_\varepsilon = 0.294$ for the CFD_f calculations.

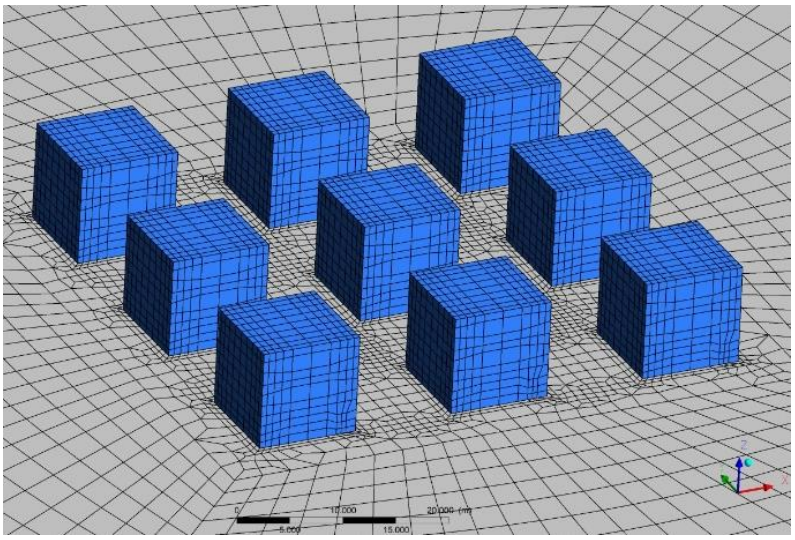

(a)

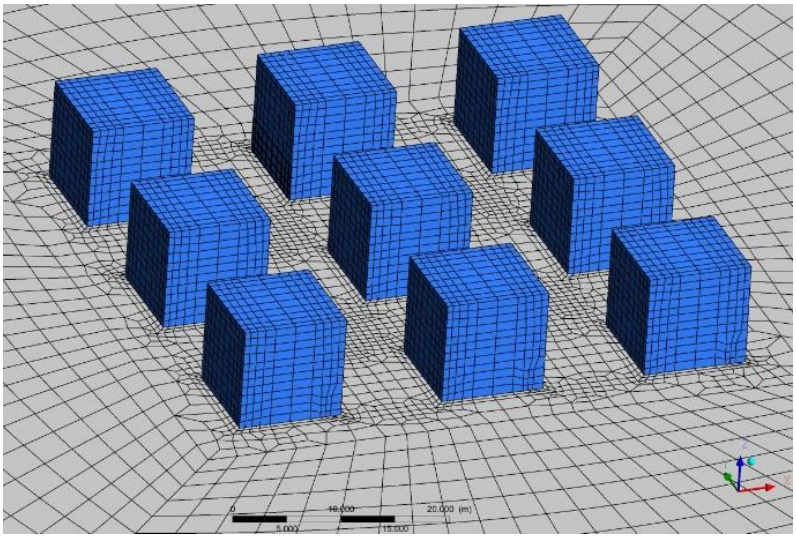

(b)

Figure 3-7 Computational grids for a) sealed and b) ventilated scenarios

The final CFD_f model for the case study contains approximately 7.5 million cells. Several strategies were applied to reduce the calculation load. They were, firstly, running CFD_f isothermally in only the pre-simulation stage. Then, CFD passed the boundary conditions to the coarser domain, CFD, to participate in the iterative calculations. The CFD domain was designed to have merely an indoor environment (it contains only 130K cells), however, with the

capability of representing the microclimate around naturally ventilated buildings. The transferred information includes airflow mass rate ($\dot{M}$), velocity (U), pressure (P), kinetic turbulence energy (k) and turbulence dissipation rate (ε). The appropriate boundary types for CFD to receive the flow information from CFD_f were investigated and discussed in *Chapter 6*. The modelling of CFD_f was executed by CFX 19.1©.

Table 3-2 Boundary conditions of CFD_f and CFD domains for ventilated scenarios

Boundary	Type	CFD_f	CFD
Ground	Wall	No-slip Constant surface temperature: T_g from the weather data	
Solid building envelopes	Wall	No-slip Constant temperature: T_s from BES (fixed)	No-slip Constant temperature: T_s from BES (updated)
Other walls	Wall	No-slip, Smooth wall Adiabatic	
Sky	Symmetry	/	
Inlet (Cylinder)	Velocity inlet	Velocity magnitude and direction: magnitude vertical profile U_z from the weather data, direction specified by x, y components Temperature: vertical profile $T_{a,z}$ from the weather data Turbulence: vertical profiles of k_z and ε_z	
Outflow (Cylinder)	Pressure outlet	Gauge pressure = 0 Pa Temperature: vertical profile $T_{a,z}$ from the weather data Turbulence: vertical profiles of k_z and ε_z	
Ventilating windows	Velocity inlet/outlet	/	To be investigated

*T_g is the ground temperature from weather data.

Table 3-2 elaborates the boundary conditions assigned for the CFD_f and CFD domains. The SIMPLE algorithm was used to solve the RANS equations for CFD, and the default embedded algorithm in CFD_f was the COUPLED

algorithm. All the equations were solved through the *second order* transient schemes. The standard and scalable wall treatments were employed for CFD and CFDf domains, respectively, to match their requirements of solving the boundary layers according to the sizes of their first layer cells. The scalable wall function adds a limiter in the calculation of the turbulence metrics so that y^* in *Eqn. 30* is replaced with $y^{\tilde{*}}$:

$$y^{\tilde{*}} = max\,(y^*, y^*_{limitation}) \quad \text{Eqn. 31)}$$

where $y^*_{limitation}$ = 11.225. In CFX, the scalable wall function is defined based on y^+:

$$y^+ \equiv \rho u_\tau y/\mu \quad \text{Eqn. 32)}$$

where u_τ (m/s) is the friction velocity defined as $u_\tau = \left(\frac{\tau_w}{\rho}\right)^{0.5}$ and τ_w (kg/m^2) represents the wall shear stress. The y^+ of CFDf was within the range of 10 to 300. The convergence criteria were set at 10^{-4} for both CFDf and CFD domains.

For sealed scenarios, in no matter short-term or long-term assessments, the near-wall region was processed with the standard wall function while the y^* was maintained between the range of 30 – 300 so that the log-law could be assumed to be valid for the mean velocity. The *second order* method was employed to solve the discretization equation of pressure whilst other quantities were solved by *second order upwind* method under the SIMPLE scheme. During the coupling simulation, the convergence criteria for CFD were set as 10^{-4}. *Table 3-3* demonstrates the boundary conditions of the CFD field for the sealed scenarios' calculations.

More information of the models for different scenarios is described in detail in corresponding chapters.

Table 3-3 Boundary conditions for modelling of sealed scenarios

Boundary	Type	Setups
Building envelopes	Wall	No-slip Constant temperature: T_s from BES
Ground	Wall	No-slip Constant surface temperature: T_g from the weather data
None-inlet/outlet laterals and Sky	Wall	No-slip Adiabatic
Inlet	Velocity-inlet	Velocity magnitude and direction: magnitude vertical profile U_z from the weather data, direction specified by x, y components Temperature: vertical profile $T_{a,z}$ from the weather data Turbulence: vertical profiles of k_z and ε_z
Outlet	Pressure-outlet	Gauge pressure = 0 Pa Temperature: vertical profile $T_{a,z}$ from the weather data Turbulence: vertical profiles of k_z and ε_z

*T_g is the ground temperature from weather data.

3.6. BES Modelling

The BES models for coupling were developed from the benchmark model described in *Section 3.2.2*, whose configurations were considered calibrated, as they were used in an officially published model.

The buildings are occupied between 7 a.m. to 9 p.m. on weekdays, except for national holidays. The percentage occupancy increases to 95 % at 9 a.m. There is a one-hour lunch break between 12 p.m. and 1 p.m. when 50 % of the occupants stay in the building. Occupancy decreases to 30 % at 5 p.m. and then to 10 % at 7 p.m. The operative temperature is maintained between 21 - 24 °C during occupied hours and between 15.6 - 26.7 °C at all other times according to the benchmark building.

The algorithm for the outside surface convection used by the benchmark model was DOE-2, which calculated the convective heat transfer coefficient through the following equations [25], as introduced in *Section 2.1.2*:

for smooth surfaces (e.g., glass): $$h_c = \sqrt{{h_n}^2 + \left[a{U_z}^b\right]^2} \quad \text{Eqn. 7)}$$

for less smooth surfaces: $$h_c = (1 - R_f)h_n + R_f\sqrt{{h_n}^2 + \left[a{U_z}^b\right]^2} \quad \text{Eqn. 8)}$$

where R_f is the surface roughness multiplier that is 2.17, 1.67, 1.52, 1.13, 1.11, and 1.00 for roughness indices of 1 to 6, respectively, representing very rough to very smooth surfaces. The constants *a* and *b* depend on the relative orientation of the surface to the normal incidence of wind. For windward surfaces, the constants a and b are 3.26 W/(m^{2}K(m/s)^b) and 0.89, respectively, and 3.55 W/(m^{2}K(m/s)^b) and 0.617 for leeward surfaces. h_n is the natural convective heat transfer coefficient, which is determined in [25] as follows:

for $\begin{cases}\text{upward and } T_{a,z} - T_s < 0\\ \text{downward and } T_{a,z} - T_s > 0\end{cases}$: $$h_n = \frac{9.482\left|T_{a,z} - T_s\right|^{1/3}}{7.283 - |cos\Sigma|} \quad \text{Eqn. 9)}$$

for $\begin{cases}\text{upward and } T_{a,z} - T_s > 0\\ \text{downward and } T_{a,z} - T_s < 0\end{cases}$: $$h_n = \frac{1.810\left|T_{a,z} - T_s\right|^{1/3}}{1.382 + |cos\Sigma|} \quad \text{Eqn. 10)}$$

where Σ is the surface tilt from the horizon.

Besides assigning the same building construction materials, the operating condition of BES field in these buildings was functionally similar to the benchmark case but was simplified. For example, the ideal load of the air system was used instead of the complex PSZ-air conditioning units with a gas furnace system (used in the reference model) for simplification and conservation of computational cost.

The case study site was selected to be in Los Angeles, U.S., where the weather data shows that 25th September is the hottest workday of the year there. Therefore, regarded as the representative of a hot period, 25th September was selected as the test day for short-term simulation while the

whole month of September was selected as the test period for long-term simulation.

Hourly weather data from the online database was used to assess the indoor environment in the commercial building. At the preliminary design stage, the DOE-2 algorithms were applied to calculate the outside-surface convection coefficients for a few hours on the day before the test day (e.g., 24th September in short-term modelling) and for the initial guesses of each hour of the test period (e.g., 25th September in short-term modelling).

The *Appendix 4* provides the original ENEGYPLUS' *IDF files of the example case of short-term sealed buildings without applying the coupled CHTCs (denoted as the BES-only method). To keep it concise, the *IDF file in the appendix would only show B5 among nine buildings rather than all of them. During the iterative calculation of the coupling process, information on new CHTC from the CFD domain would be applied to the EnergyPlus by creating new schedules and specifying the determination method of CHTC for each surface, as shown in *Appendix 5*. An example is the last iteration (2nd) at 12 pm on the test day in the appendix. Again, only B5 is presented.

3.7. Combination with Artificial Neural Network

Figure 3-8 presents four stages of the proposed virtual dynamic method, including (1) preliminary simulation (denoted as pre-simulation), (2) coupling, (3) training and (4) prediction stages. The data for training of the neural network were generated during the first two stages. As discussed in *Section 3.4.1*, the adjusted values (h_c^*) were collected and assessed instead of the real local CHTCs from the CFD side in the coupling process. Amongst the whole process, the BES tool worked at all stages except the training step, whilst the CFD tool worked only at the coupling stage. A bespoke code was further developed to connect all steps with an artificial neural network (ANN) package in the training stage. The developed ANNs were then used to predict future CHTCs to be inserted into BES for medium/long-term simulation.

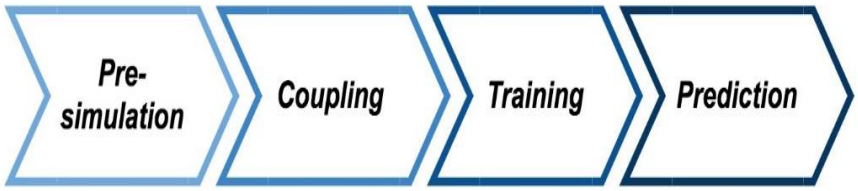

Figure 3-8 Four basic steps of the proposed virtual dynamic method [89]

In order to reduce the computational load of long-term simulation, the target building was identified instead of focusing on the whole interest region. The iterative calculations were only be executed on the target buildings' exterior surfaces.

The ANNs were projected to predict the target buildings' converged CHTCs from local environmental parameters and the thermal performance of the local surface. In general, the input of the neural network consists of

- the normalized meteorological parameters (including solar radiation, wind speed, and direction),
- the zone temperature of spaces in surrounding buildings,
- the difference between the initial temperature of the target building's exterior-surface (estimated by BES with the embedded CHTC algorithms) and the corresponding ambient air temperature (at a level by the altitude of the centroids of surfaces calculated through *Eqn. 16*).

In this study, the normalization of meteorological parameters was computed by Z-score values so that the parameters of weather conditions would be scaled to data with a mean value of 0 and a standard deviation of 1 by the below equation:

$$z_s = \frac{(X - \bar{X})}{\sigma_X} \qquad \textit{Eqn. 33)}$$

where z_s is the Z-score, $\bar{X}$ and σ_X are the mean and standard deviation of dataset of parameter X, respectively.

3.8. Quantified Metrics for Data Analysis

Four dimensionless metrics were introduced to quantify the performance of the computational model, including the relative error (e_r), the root mean square error (*RMSE*) of the relative error, the hit rate (q_{hr}) and the fraction of predictions within a factor of two of observations ($FAC2$). These metrics are used to compare the experimental (observed and denoted as o) and numerical (predicted and denoted as p) values of a given variable for all N data points. The relative error and its root mean square error are given by

$$e_r = \frac{1}{N}\sum_{i=1}^{N}\left|\frac{p_i - o_i}{o_i}\right| \quad \text{Eqn. 34)}$$

$$RMSE = \sqrt{\frac{1}{N}\sum_{i=1}^{N}\left(\frac{o_i - p_i}{oi}\right)^2} \quad \text{Eqn. 35)}$$

where i denotes the index of samples, ranging from 1 to N.

The hit rate is given by

$$q_{hr} = \frac{1}{N}\sum_{i=1}^{N} n_i \ with \ n_i = \begin{cases} 1 \ for \ \left|\frac{p_i - o_i}{o_i}\right| \le D_{q_{hr}} \ or \ |p_i - o_i| \le W_{q_{hr}} \\ 0 \ \ else \end{cases} \quad \text{Eqn. 36)}$$

where $D_{q_{hr}}$ is the allowed relative deviation. The threshold for the absolute deviation ($W_{q_{hr}}$) is related to the experimental uncertainty, which can be estimated from the engineering data, by the equipment manufacturer, or empirically from other experiments that use the same experimental method [92]. In this study, the thresholds for $D_{q_{hr}}$ was set as 0.25, following COST [52], and $W_{q_{hr}}$ was set as 0.03 [96].

FAC2 is considered to be one of the most robust methods because it excludes *the* high influence of extreme outliers [55], [97]. *FAC2* can be determined by:

$$FAC2 = \frac{1}{N}\sum_{i=1}^{N} n_i \ with \ n_i = \begin{cases} 1 \ if \ \ 0.5 \le \frac{p_i}{o_i} \le 2.0 \\ 0 \ \ else \end{cases} \quad \text{Eqn. 37)}$$

A model that shows a perfect agreement to an experiment would have q_{hr} and *FAC2* equal to 1. Hanna and Chang [97] claimed that a model with *FAC2* over 0.5 would be *good enough* whereas COST [55] required a no-less-than 0.66 hit rate for a successful velocity-field validation.

In long-term virtual dynamic coupling, the metrics, two more metrics were used for checking the developed prediction tool: one was the mean square error (*MSE*) and the other was the adjusted determination coefficient (R^2):

$$MSE = \frac{1}{n}\sum_{i=1}^{n}(o_i - p_i)^2 \qquad \textit{Eqn. 38)}$$

$$R^2 = 1 - \frac{\sum(o_i - Y_i)^2}{\sum(o_i - \bar{o})^2} \qquad \textit{Eqn. 39)}$$

The value of R^2 is within the rage of 0-1 while a larger value for them can be assumed as a better fitting to the target values

Chapter 4. VALIDATION OF CFD MODEL

This chapter provides the validation of airflow model in CFD field. The airflow model was validated using the AIJ Case C experimental data [86][86][86]. The Case C consists of nine cubic blocks measuring 0.2 m by 0.2 m by 0.2 m ($L \times W \times H$), as seen in *Figure 4-1*. These nine cubic blocks are distributed in a 3 × 3 array. The distance between every block is 0.2 m, forming the canyons of an aspect ratio of 1. As described in *Sections 3.3.1* and *3.5.2*, to study the boundary layer effect inside the street canyons, comparisons were made at the set of 120 measurement points located at 0.02 m above the ground as displayed in *Figure 3-2*. Four meshes (having 130,968, 159,469, 198,627, and 233,766 cells and are hereon denoted m1, m2, m3, and m4, respectively) were drawn for the independence test. After obtaining the validated airflow model, it is then applied in sealed scenarios and as the CFD (with coarser grids out of two domains) in ventilated scenarios.

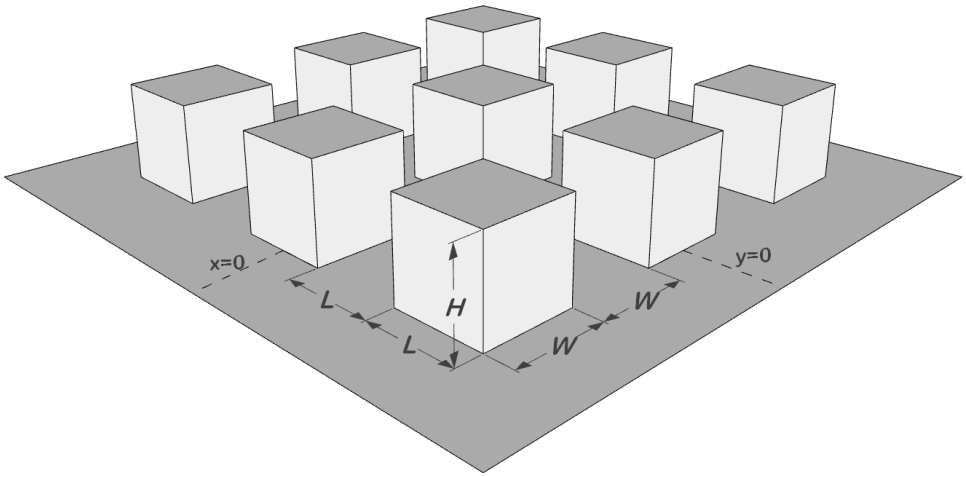

Figure 4-1 3 × 3 cubic blocks

A velocity obtained by CFD prediction was with respect to the time-averaged vector. However, the airflow in the wind tunnel was captured regardless of its direction and the recorded value is referring to the time-averaged instantaneous scalar velocity (U_z^*, m/s). Therefore, the local velocity used by CFD ($U_{z,C}$, m/s) is converted to U_z^* [98]:

$$U_z^* = \sqrt{U_{z,C}^2 + 2k_{z,C}} \quad \text{Eqn. 40)}$$

where $k_{z,C}$ (J/kg) is the local turbulence kinetic energy used by CFD.

The predicted values of U_z^* were compared to the wind tunnel measurements in the format of normalized velocity with respect to the inlet velocity $U_{z,inlet}$ (2.434 m/s) at the test height used in the AIJ Case C scenario.

Figure 4-2 shows the comparison at each sample point. As can be observed, significant discrepancies were observed, particularly close to the blocks in the street canyons. This is due to a failure in, or weakness of, the selected turbulence-model at representing the turbulent kinetic energy in the boundary layer immediately adjacent to the solid cubes [54]. The overestimation of the velocity field by the standard $k-\varepsilon$ turbulence model is well-known and is shown by *Figure 4-3*, where a majority of data points lie above the straight line (with a gradient of unity), which indicates experimental and prediction parity.

Figure 4-4 shows the minimum, maximum, 25th, and 75th percentiles, median, and mean (no considering the outliers that exceed 1.5 times the interquartile range away from the 25th and 75th percentiles) of relative error e_r, and *Table 4-1* quantifies the accuracy of each model by providing the 95th-centile, 5th-centile, median and mean of e_r, the hit rate, and *FAC2*; see *Eqn. 34*, *Eqn. 36* and *Eqn. 37* in *Section 3.8*. The 5th-centile e_r of the models was within 0.005 – 0.020, which was good. The 95th-centile error exceeded 0.3 for each model. However, such poor conditions are considered to be rare and extreme due to the low median value, which was approximately 0.1. The mean error of all created models was around 0.13, which is an acceptable value [50] .

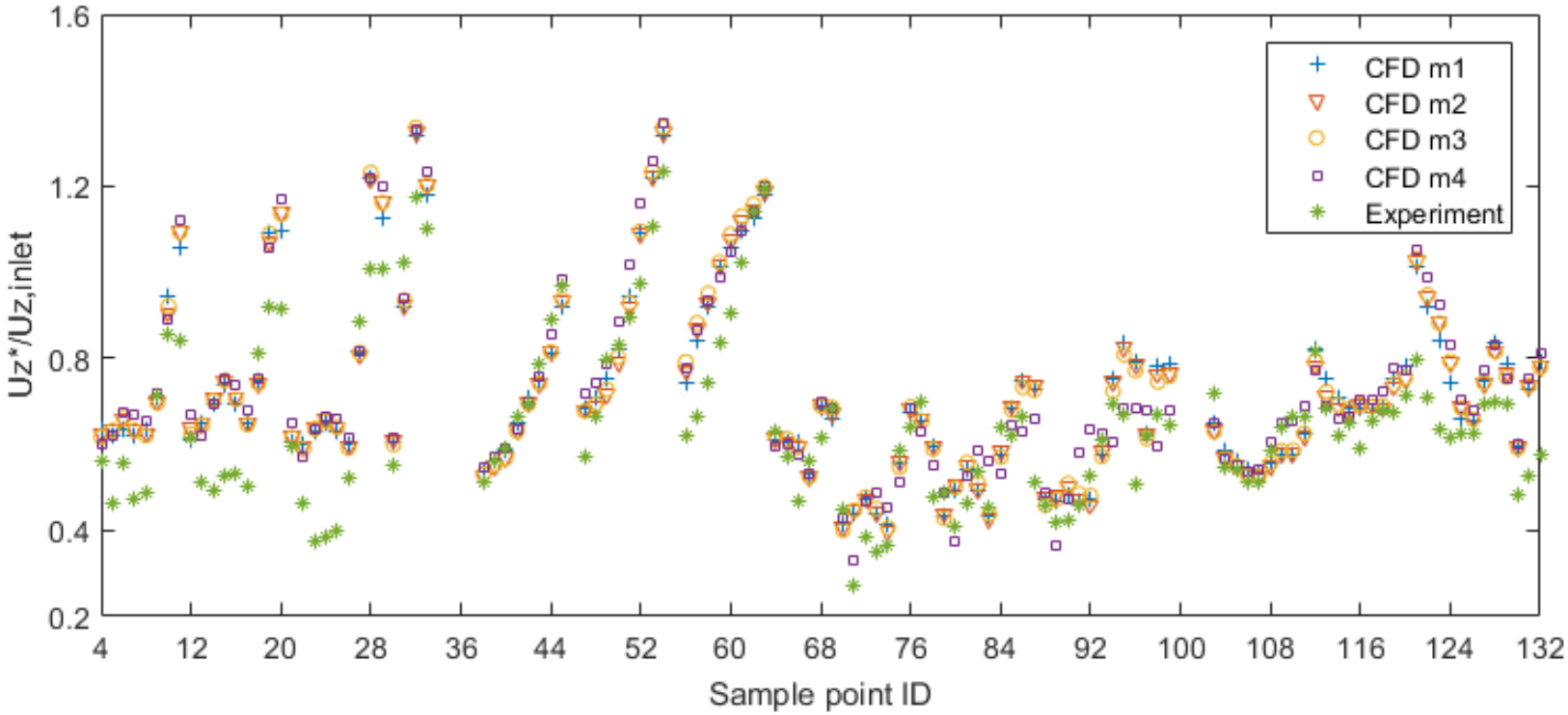

Figure 4-2 Comparison of the normalized local velocities of experimental measurements and CFD simulations over 120 test points [93]

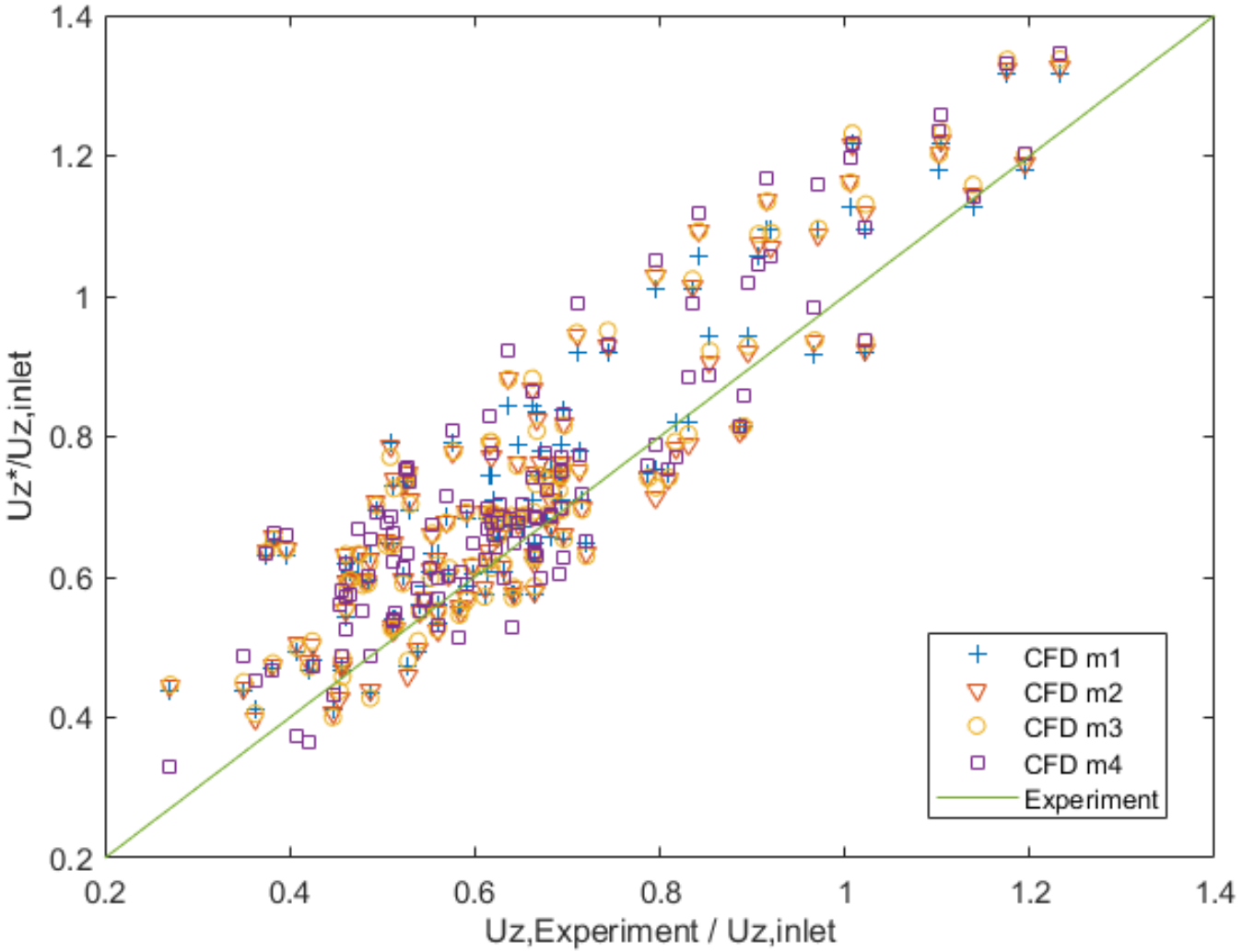

Figure 4-3 Plot of normalized velocity versus normalized experimental velocity [93]

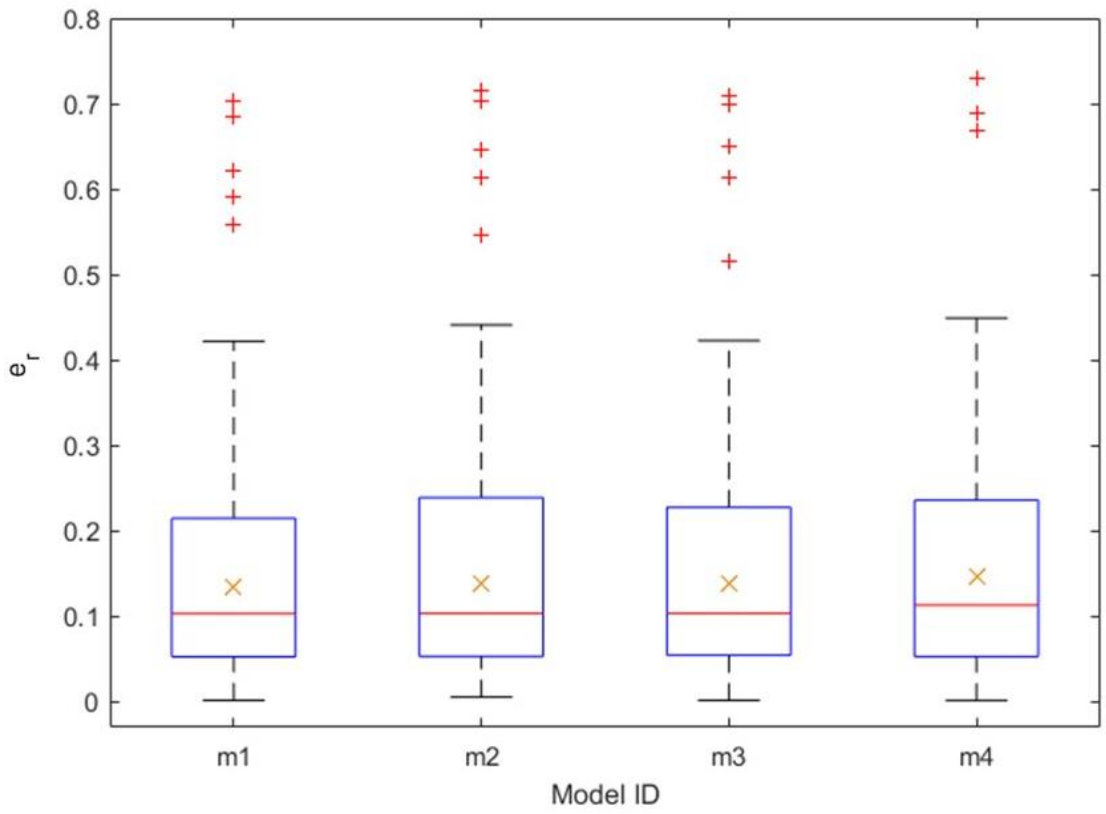

Figure 4-4 Plot of e_r of different CFD models (blue box, interquartile range; red horizontal line, median; yellow cross, mean; black bars, minimum and maximum; red cross, outliers) [93]

Table 4-1 shows that the hit rates for all the models are over 0.77, which is much higher than 0.66 baseline criterion, which COST [55] suggests indicates a successful validation of the mesh; see *Section 3.8*. The *FAC2* values were 1 for all models, suggesting that there was no extreme outlier (half or twice the empirical data) in the predictions. Furthermore, they all surpass the benchmark value of 0.5 proposed by Chang and Hanna [97] as *good enough*. In general, the metrics show that the performance of the four models was similar. This may be because the heights of their first layers' cells are identical. Moreover, the sample points were selected at locations close to ground level, which is also near the location of this first layer wall-function and could be one of the main sources of error besides the turbulence model. The wall y^* (see *Eqn. 30*) of each model was controlled within the range of 30 - 300 for the implemented standard wall-function, as suggested by [99]. The error barely changed with increasing density, which means the meshes were independent.

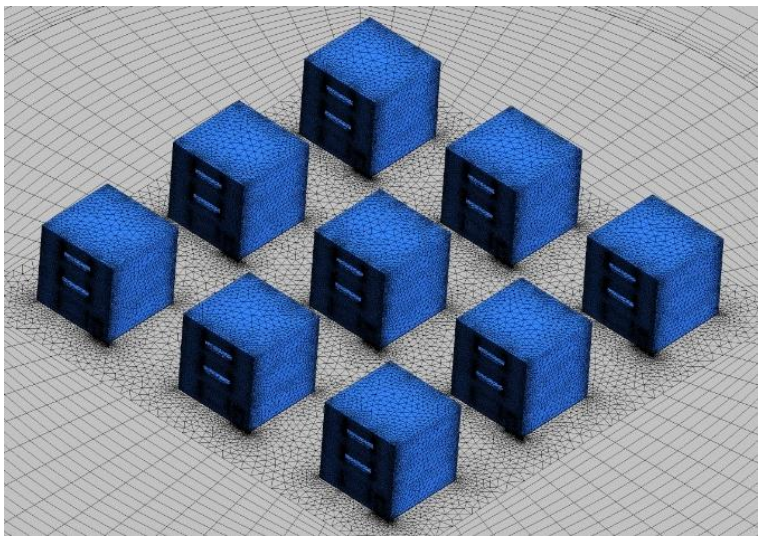

CFD_f

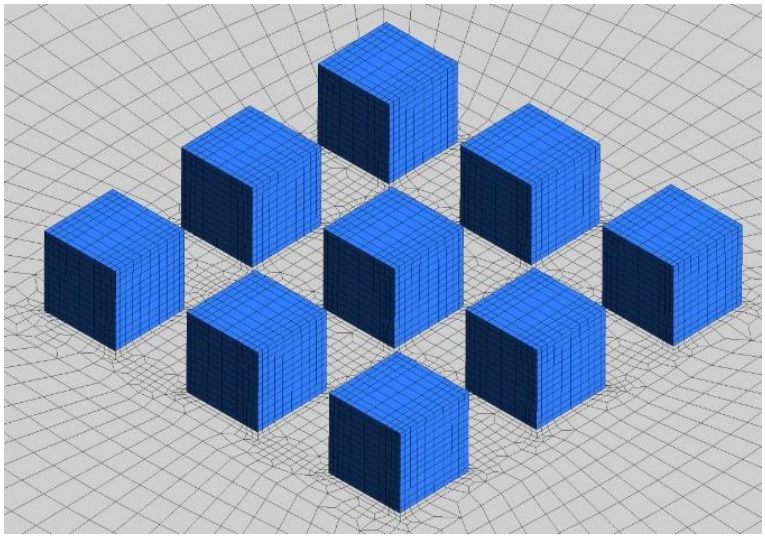

CFD

Figure 4-5 Comparison of final models of CFD_f and CFD

An independence test was also executed after enlarging the validated meh 50 times to the size of the coupling design. Finally, the mesh was refined by adding more layers close to solid boundaries with the size of first layer cells approximately 0.1 m, giving accurate boundary layer assessment by maintaining the *y** [99]. The cell number of refined mesh was over 700 K, more than five times that of the validated model. Comparison of flow velocity at 120 test points (obtained by enlarging the coordinates of the original 120 test points by 50 times, lying in the boundary layer) showed that the mesh without refinement would be sufficient to give accurate flow modelling. The relative error e_r was approximately 0.1 with $FAC2$ of 1. Therefore, considering the computational cost, the mesh without refinement was employed.

These results suggest that model m1 can now be applied to a case study because its predictions are comparable with models m2-4, but it has the benefits of being the smallest and having the lowest computational cost.

Table 4-1 Assessment of CFD model performance using three metrics

Model ID	m1	m2	m3	m4
95th percentile e_r	0.3312	0.3566	0.3569	0.3961
5th percentile e_r	0.0107	0.0168	0.0152	0.0056
Median e_r	0.1026	0.1003	0.0938	0.1104
Mean e_r	0.1338	0.1385	0.1379	0.1456
Hit rate, q_{hr}	0.792	0.783	0.775	0.783
FAC2	1.000	1.000	1.000	1.000

After the validation stage, the mesh was enlarged 50 times to represent the neighbourhood of the coupling procedure. CFD_f (with finer grids out of two domains) in ventilated scenarios, it was developed from the validated airflow model developed by Shirzadi et al. [42] (as explained in *Section 3.5.3*). It was reported that the relative error of the airflow rate decreased from 1.01 by the standard $k-\varepsilon$ model to 0.07 by the calibrated $k-\varepsilon$ model (which solved the turbulence equations *Eqn. 25* and *Eqn. 26* using modified coefficients: $C_\mu = 0.141$, $C_{1\varepsilon} = 1.50$, $C_{2\varepsilon} = 3.20$, $\sigma_k = 1.0$, and $\sigma_\varepsilon = 0.294$). The final CFD_f consists of over 7M cells (see *Figure 4-5*).

Chapter 5. SHORT-TERM MODELLING OF SEALED SCENARIOS

This chapter provides the process of applying the fully dynamic coupling of CFD and BES method into the short-term energy demand assessment of sealed scenarios when the windows of all tested buildings are closed throughout the simulation. First, a detailed framework of the short-term modelling of sealed scenarios is developed. Then it is tried out in a case study on the hottest workday (25th September) in Los Angeles, the U.S. Finally, the performance of the proposed coupling method is analysed in representing the neighbourhood effect in city communities.

5.1. Framework for Short-term Modelling of Sealed Scenarios

Supplementary to the general framework introduced in *Section 3.2*, *Figure 5-1* demonstrates the developed framework of fully dynamic external coupling for the short-term assessment of sealed scenarios. As explained in *Section 3.2*, the simulation was divided into two stages: pre-simulation (also called preliminary design stage) and dynamic coupling.

There are three objectives in the pre-simulation stage:

- to prepare the CFD and BES model according to the designed building form (e.g., the building type, the building dimensions, ventilation mechanisms, building surfaces), and relative weather data input files to be applied in the CFD field in climatic boundaries format (performed by *Eqn. 15*, *Eqn. 16*, *Eqn. 19*, and *Eqn. 20*).

- to record the initial CHTCs calculated by the embedded algorithm (DOE-2 in this study) in BES.

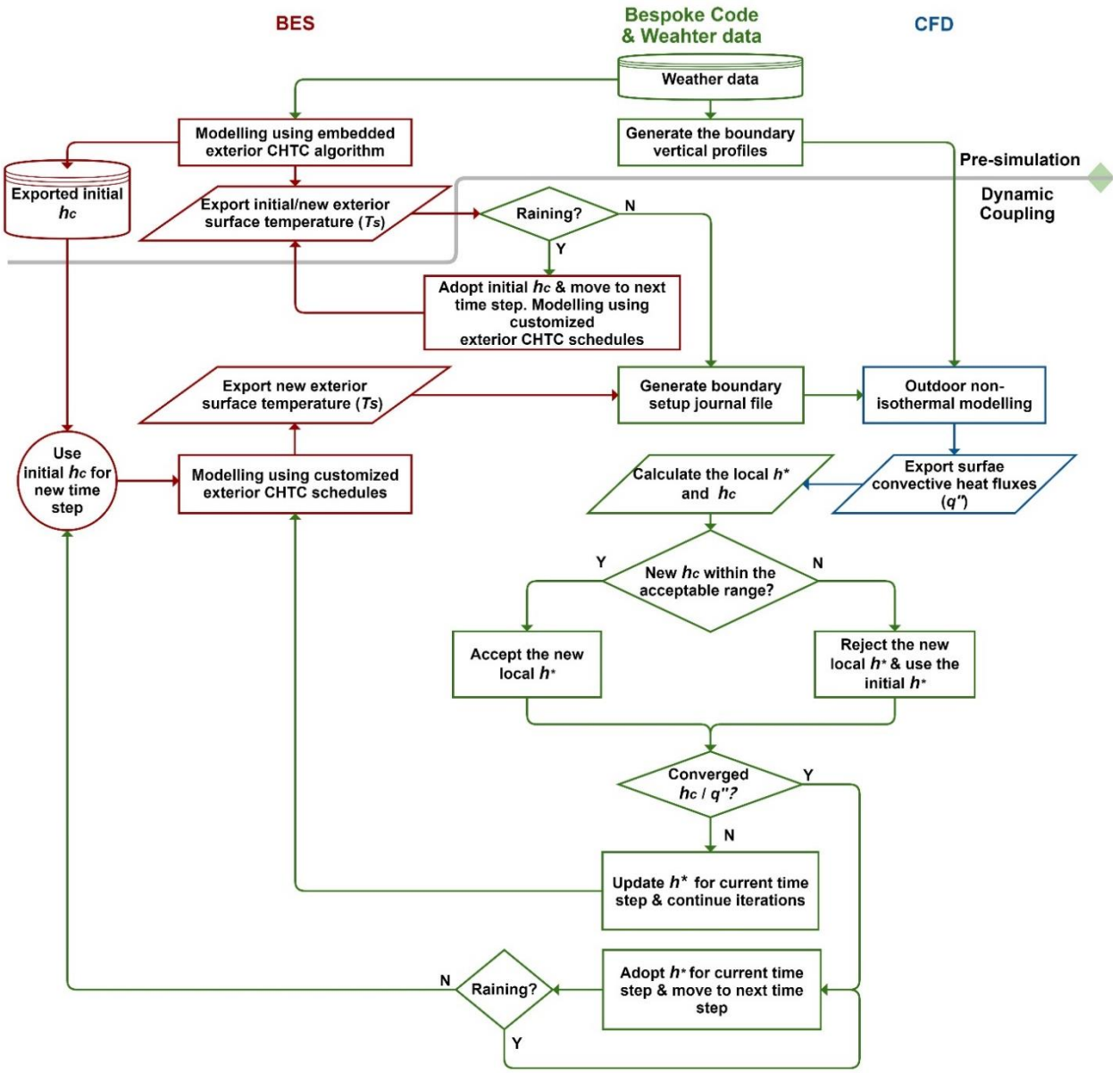

Figure 5-1 Framework of the coupling BES and CFD for short-term modelling of sealed scenarios

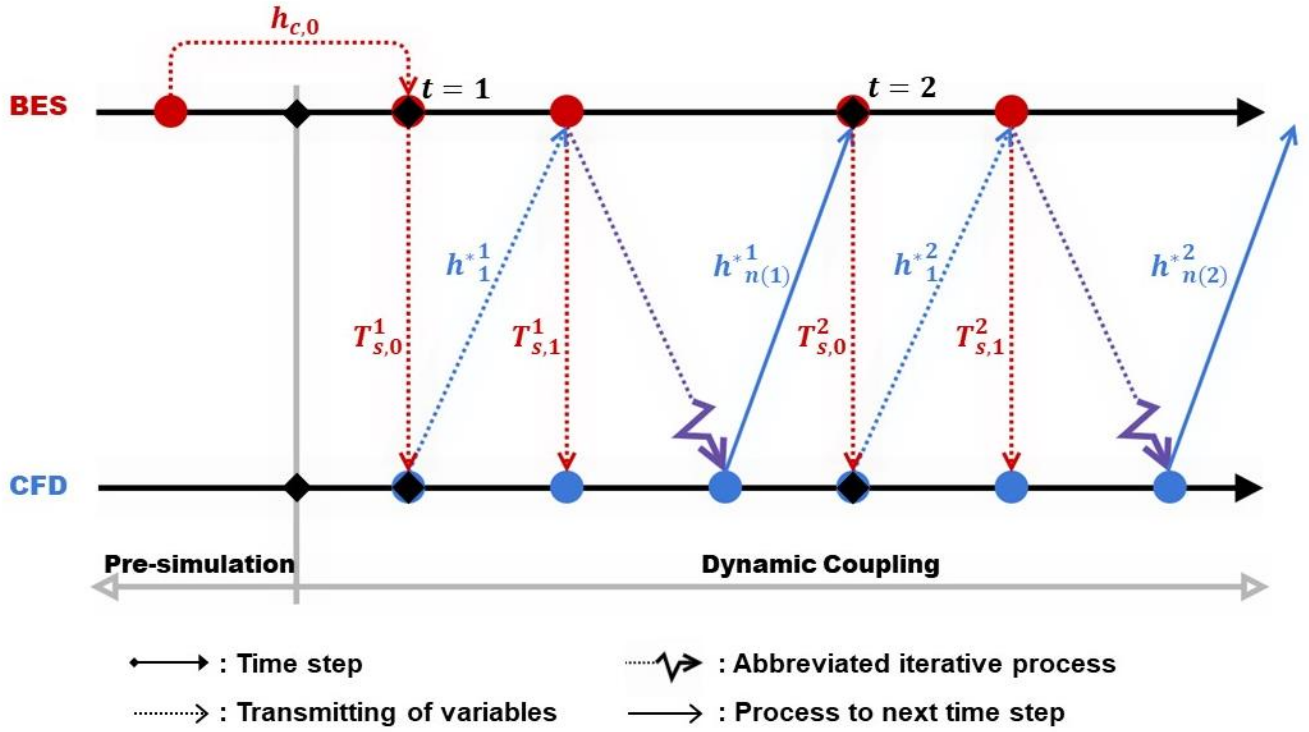

Figure 5-2 Transmitting of variables in short-term coupling of sealed scenarios

- to ensure the time-lag effects in thermal calculations are included by recording the thermal parameters (hereon, CHTCs) of a few hours before the test day. In this study, 6 hours before the test day were considered.

When the pre-simulation stage is completed, the dynamic coupling stage starts with the loop process between CFD and BES domains with the assistance of custom code. Bespoke code is used to transfer customized inputs and meteorological data between the CFD and BES modules. The code passes all configurations to the BES as an input file in a standard format. It generates another file with a set of commands for the CFD module to set up its boundary conditions, such as wind's vertical velocity and turbulence profiles. The raining status is checked at the beginning of each time step to decide whether the coupling process is activated. As the surfaces are assumed to be wet covered by water for raining hours, the CHTC of exterior surfaces is set as 1000 W/Km^2 in EnergyPlus. Therefore, the coupling process would be skipped when it is raining. Meteorological data are applied to the BES tool directly. In contract, the data are transferred into journal file format by the bespoke code to be read into the CFD tool to capture the same vertical wind profile as the BES.

There was no precedent of acceptance range of coupled values of CHTCs of exterior surfaces. However, according to the CIBSE Guide C [99], the exterior CHTCs for insulated surfaces can range up to 40 at a wind speed of 10 m/s. A reasonable range can then be guessed and assigned accordingly higher to cover the whole ranges of wind speed and the impact of deviation in local air temperature used to calculate h and h^*. The other way would be referring to the acceptance range of interior surfaces CHTCs, which were set to be within the range of 0.2 – 5 [100] or 0.1 – 10 [56] empirical CHTCs. Such based-on-empirical value range has not yet been established for exterior surfaces; thus, the range can be loosened slightly considering the more complex exterior environment when applying to outdoors. In this case study, the obtained h^* were considered not out of reasonable range (no more than ten times of CHTC empirical values); thereby, they were accepted. *Figure 5-2* visualizes the variables' transmitting process in the short-term coupling of sealed scenarios. In this figure, the subscripts i and the superscripts t for exchanging variables

${h^*}_i^t$ and $T_{s,i}^t$ represent the current iteration number and time step number, respectively. Thus, when i reaches n, it means the convergence (determined as when the changing of T_s by BES or h_c by CFD becomes stable) between two domains is achieved.

5.2. Description of the Case Study

A fully dynamic coupling simulation was run for the hottest workday, the 25th of September in Los Angeles. The daily temperature ranges from 18.1 °C to 34.1 °C. Sunset is at 6 p.m., after which there is no solar radiation until sunrise the following day. All buildings were sealed from the outdoors without any natural ventilation. Therefore, none of the windows would be opened during the simulation time, which means the fenestration surfaces should be treated as a 'wall' boundary in the CFD field. According to the model design principles introduced in *Section 3.3.3*, the model for short-term coupling of sealed scenarios was drawn as displayed in *Figure 5-3*. Each building was oriented to the due south. In BES field, these nine buildings were operated following the setups illustrated in *Section 3.6*. Furthermore, in *Section 3.5.3*, the computational model of the CFD domain is provided.

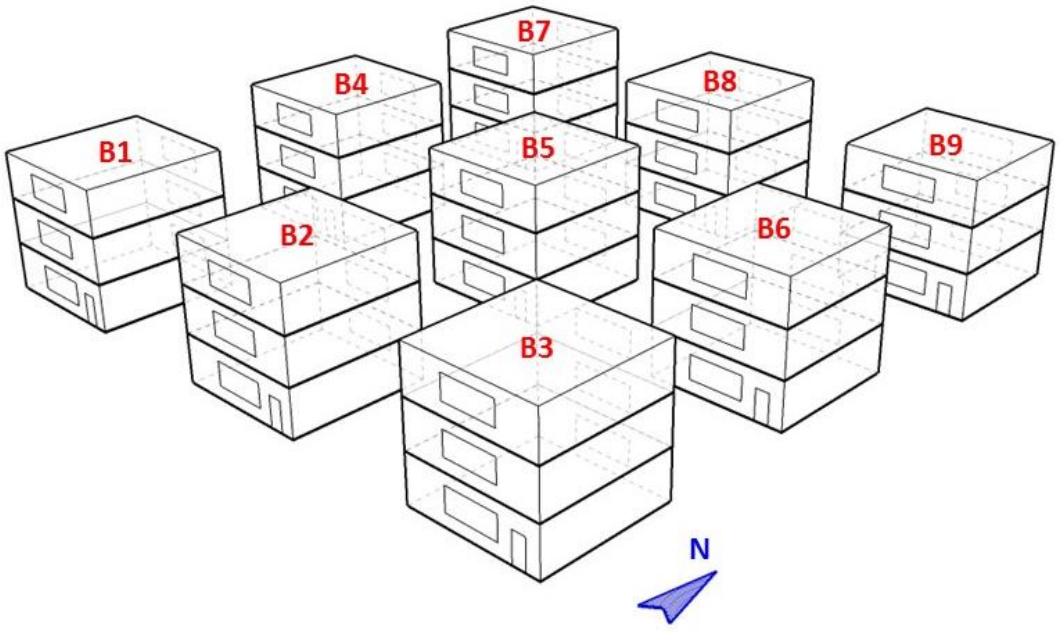

Figure 5-3 Nine-cube EnergyPlus model for the sealed scenario [93]

5.3. Coupling Simulation Results

5.3.1. One-time-step dynamic coupling

Fully dynamic coupling is a combination of a series of the one-step-time dynamic couplings. In this study, a daily simulation was performed that contains 24 one-step-time couplings.

Figure 5-4 shows the residuals of T_s and h^* for the first hour of the 25th of September as an example of the convergence process. The first hour of a day is within the night period when there is no need to consider the impact of solar radiation. The residuals are displayed logarithmically to base 10 to aid interpretation. According to meteorological data, the ambient air temperature is 19.4 °C, and the prevailing wind direction is from 50 ° (clockwise from due North) at a speed of 3.1 m/s.

In this time step, the average convective heat energy gained by the exterior surfaces (including all fenestration surfaces) are changed by approximately 64 %. The average change of the daily community convective energy is found to exceed 82 %. *Figure 5-6* compares the initial surface temperature contours of each building with the fully converged contours. It shows that higher T_s are predicted using the coupled method. Also, the fully converged results clearly show the discrepancies inside the community due to the sheltering effect.

Figure 5-5 provides the number of iterations used to achieve convergence between two domains for each hour. The residual criterion between two programs for each time-step is guaranteed to be $<1 \times 10^{-3}$. However, some situations could occur where the convergence criterion needs to be relaxed when the residuals decline slowly with regular temperature oscillations and fail to approach the level of 1×10^{-3} within 20 iterations. Then, the criterion is increased to 1×10^{-2} to minimize computational time.

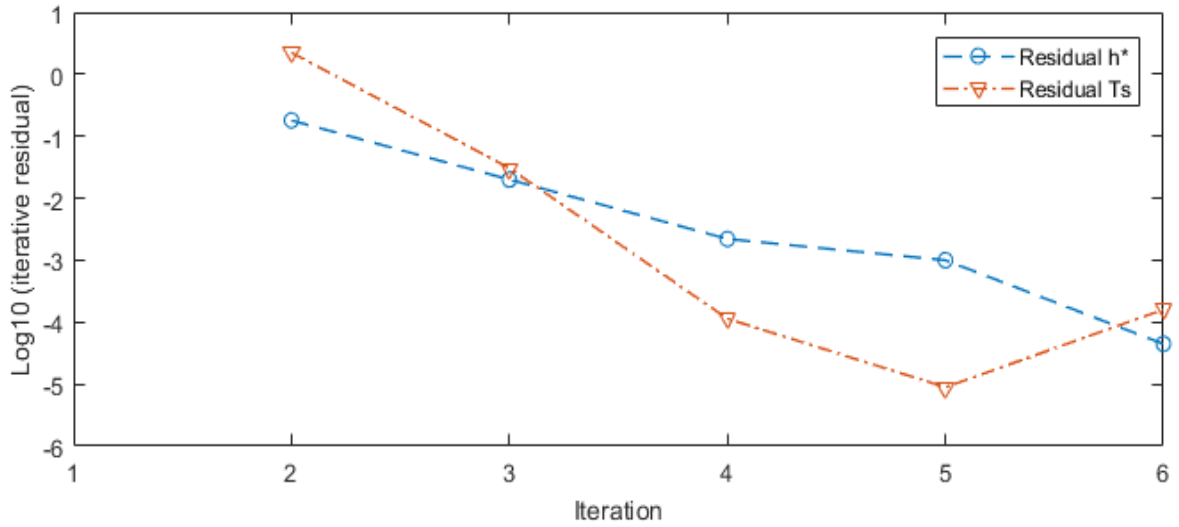

Figure 5-4 Convergence of BES-CFD iterative calculations in the first hour of 25th of September [93]

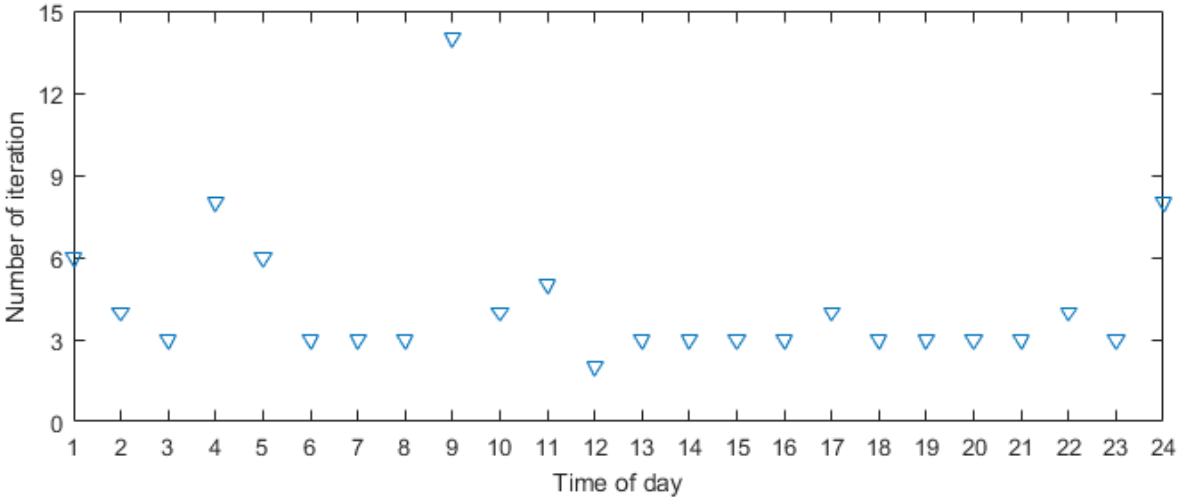

Figure 5-5 Iteration numbers for achieving convergence of the hourly basis coupling [93]

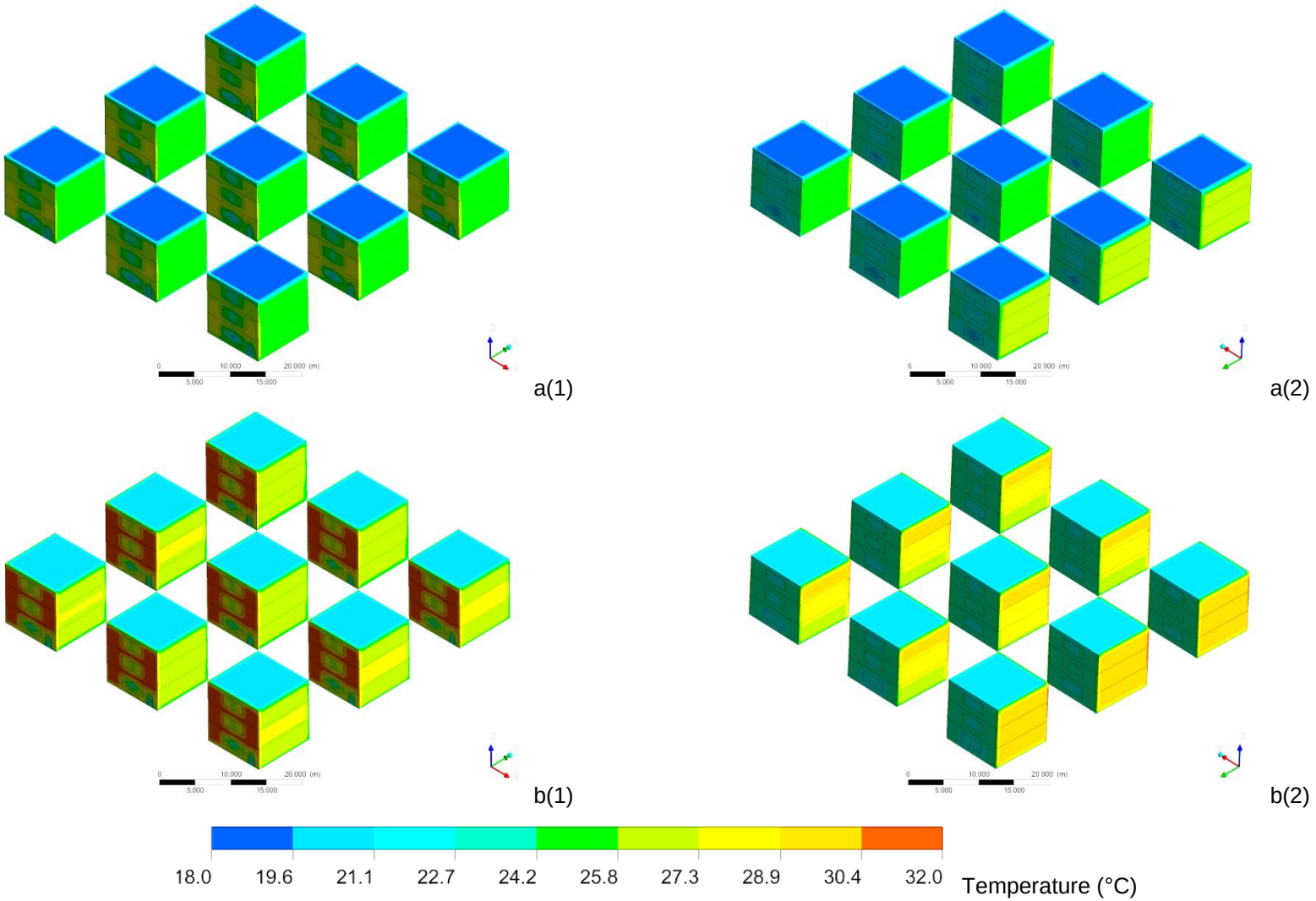

Figure 5-6 Comparison of building surface temperature contours in the first hour of the test day at a) 1st iteration (by EnergyPlus only using DOE-2 algorithm) and b) last iteration (reached convergence after fully dynamic coupling) in 1) southeast and 2) northwest view [93]

5.3.2. Sheltering effect inside neighbourhood community

In EnergyPlus, the effect of the wind direction is taken into account by classifying walls as either windward or leeward, even in some advanced algorithms, such as TARP, MoWiTT and DOE-2. The differences between the buildings' energy estimations caused by sheltering effect are small when calculated by these algorithms. Using an airflow analysis produced by CFD, this aspect can be significantly improved. We now use the buildings denoted B1, B2, B3 and B5 (see *Figure 5-3*). as case study examples during the first hour of the simulation, when the wind comes from northeast. Here, B3 is the windward building, B1 is the farthest building from the wind source and B5 is located in the centre of the array; see *Figure 5-3*.

Figure 5-7 shows the rate of convective heat gain per unit area of each surface for the first hour of the day when the influences of solar radiation and shadow distribution can be eliminated. Each surface is denoted using the format: storey number-surface type-surface orientation. Here, S and R represent walls and roofs, respectively. Then, orientation is counted counter-clockwise from due south as 1 (e.g. 1S2 denotes the east wall on the ground floor). In general, there are no significant discrepancies between the initial values of q_c'' used by EnergyPlus for surfaces on the selected four buildings facing in the same direction. The average standard deviation of q_c'' obtained by the coupled method for each surface of the nine buildings is 0.805, which is much lower comparing to 4.393 obtained for the converged coupling results during the first hour of the day. The latter value enhances the representation of the sheltering effect between the neighbourhood blocks as seen in *Figure 5-7* and *Figure 5-8*.

Figure 5-8 clearly shows a much higher standard deviation for the community q_c'' using the coupled method than that obtained using the DOE-2 algorithm embedded in EnergyPlus. The sheltering effect is clearest at S2 (east surface) on each floor obtained by the coupled method and is less dominant in S4 (west surface). In addition, the standard deviations of q_c'' at S1, S2 and S3 at each floor are very similar, but only that for S4 is found to be higher when calculated

by EnergyPlus. In contrast, clear differences can be seen in the results obtained by the coupled method.

Figure 5-9 compares the total hourly convective energy of each building's exterior surface during the simulation day predicted using DOE-2 and the coupling method. The dash lines indicate the DOE-2 algorithm and are clearly very concentrated while the reasons for the discrepancies are unclear. There was a sudden trough at noon, caused by the following reasons. First, among all the surfaces that can be lit by the sun, the area of S2 and S4 were larger than S1. At noon, the direct solar radiation was coming from due south. Therefore, the S2 and S4 were in the shadows, leading to lower Ts and temperature differences between Ts and the ambient air on the two surfaces. Besides the impact of temperature on the local convective heat transfer coefficient, the wind direction and wind speed also play essential roles. The convective heat transfer coefficient at leeward would be lower and less sensitive to the wind direction. As the wind came from due East at noon, there were more surfaces sheltered and considered leeward, which can also account for the part of the reason for the trough's occurrence.

Figure 5-16 shows the maximum, minimum, median and average prediction enhancements of q_c'' for each building during the first hour of the simulation day. The change in q_c'' for an individual surface can be up to 313 %. All the mean values are larger than the corresponding median values for each building, which means that most surfaces have been changed by a higher value than the mean.

In general, the convection energy of windward buildings (B3, B6 and B9) are more sensitive to the proposed coupling method. During this hour, the average improvement of q_c'' at exterior rough surfaces is approximately 74%. Although there is no direct access to amend the CHTC values of fenestration surfaces, they are modified somehow due to the improved values for the facades they are located in.

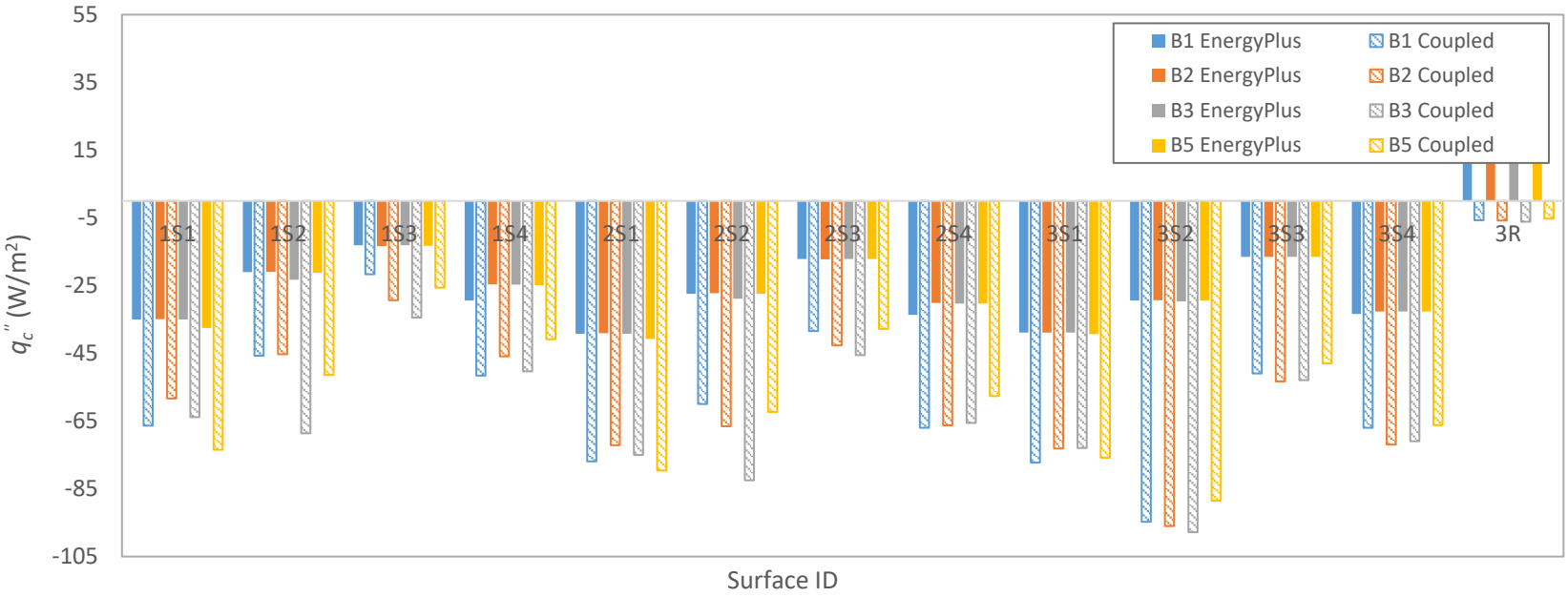

Figure 5-7 Comparison of q_c'' of B1, B2, B3, and B5 exterior surfaces in the 1st hour of the test day [93]

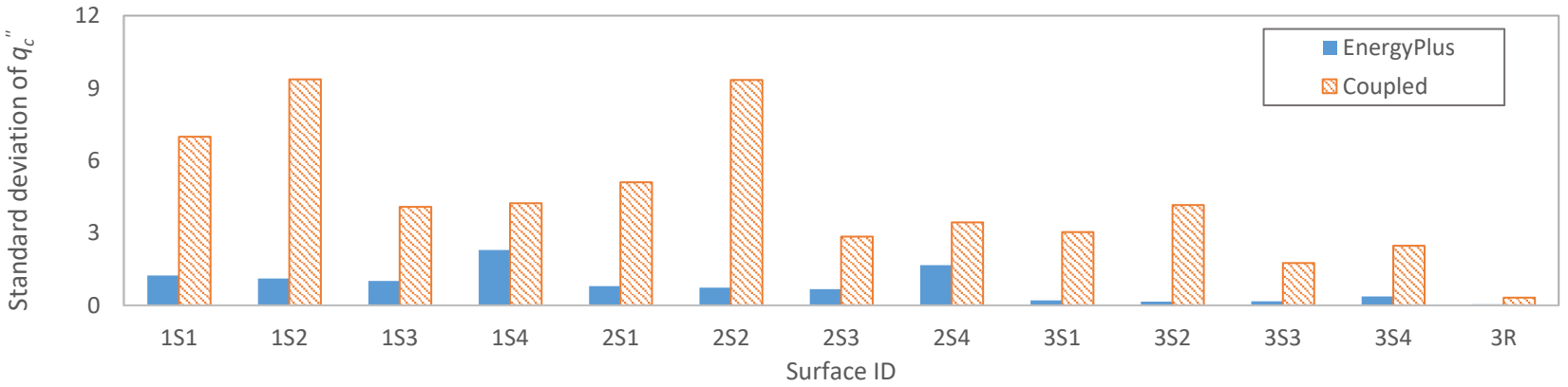

Figure 5-8 Standard deviation of the community's convective energy at different surfaces in the 1st hour of the test day [90]

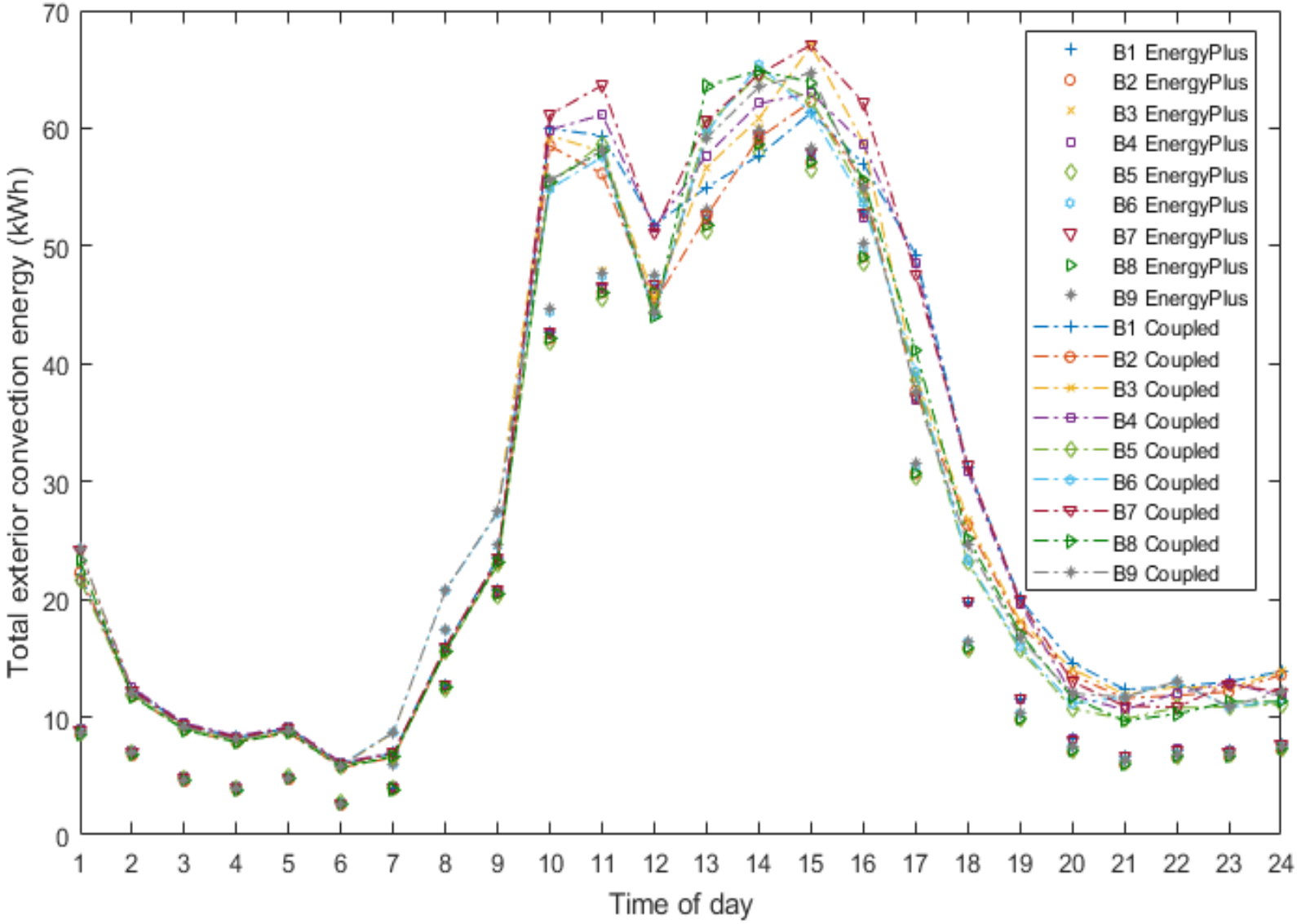

Figure 5-9 Comparison of total hourly exterior surface convection energy of buildings calculated by DoE-2 (BES only) and the coupling method [90]

5.3.3. Impact of wind patterns on local CHTCs

1. The wind patterns of the test day are provided in *Table 5-1*, including the wind speed and wind direction of each hour. In addition, comparisons of CHTCs on the following surfaces were conducted to investigate the impact of wind patterns on local CHTCs: south surfaces of the ground floor of B1, B5 and B9 (seen in *Figure 5-10*);

2. south surfaces of three stories of B1 (seen in *Figure 5-11*);

3. different surfaces of the ground floor of B1 (seen in *Figure 5-12*).

Table 5-1 Wind patterns of the test day

Time of day	**1**	**2**	**3**	**4**	**5**	**6**	**7**	**8**
Wind speed (m/s)	3.1	2.6	2.1	2.1	2.1	1.5	1.5	2.1
Wind direction (°)	50	70	70	80	100	70	140	10
Time of day	**9**	**10**	**11**	**12**	**13**	**14**	**15**	**16**
Wind speed (m/s)	2.1	4.1	4.1	4.6	5.2	5.7	5.7	5.7
Wind direction (°)	350	230	260	270	260	230	240	240
Time of day	**17**	**18**	**19**	**20**	**21**	**22**	**23**	**24**
Wind speed (m/s)	4.6	3.1	3.1	2.6	2.1	2.6	2.1	2.1
Wind direction (°)	250	230	230	220	170	150	230	220

Figure 5-10 - *Figure 5-12*, present the gap between the coupled h^* and the original h by DOE-2 algorithm in EnergyPlus against the wind speeds and wind directions. As can be observed from the figures, the impact of wind patterns on local CHTC is irregular, though there seems to be a relatively regular reflection when considering only the height difference (seen in *Figure 5-11* and *Figure 5-13*). Focusing on the scope of the gaps, more significant differences

are found caused by the different orientations of surfaces, followed by the position of the building and the last the height of the surface.

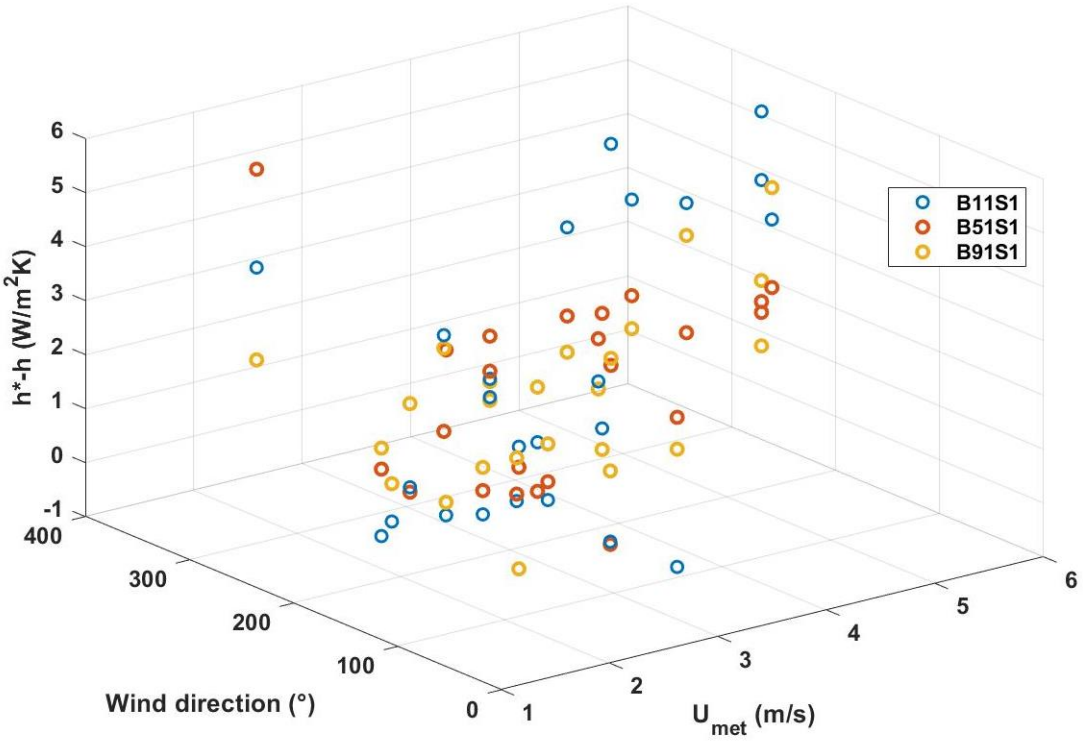

Figure 5-10 Gap between the coupled h^* and EnergyPlus h of ground floor S1s on B1, B5 and B9 under the impact of different wind patterns of the test day

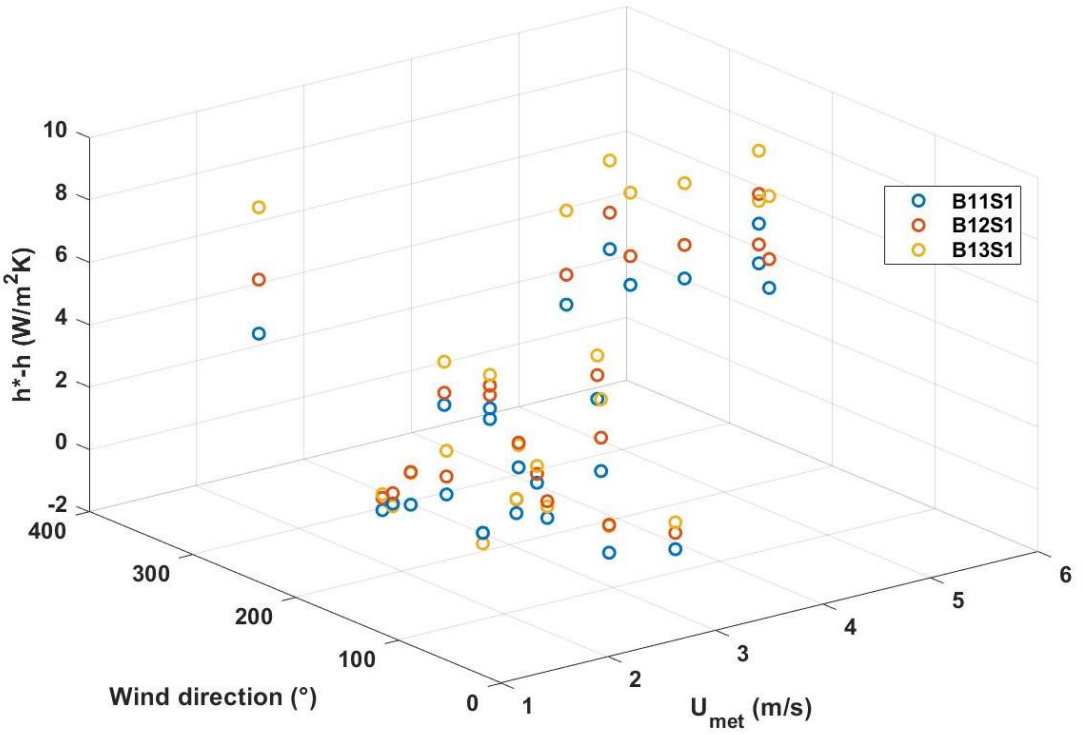

Figure 5-11 Gap between the coupled h^* and EnergyPlus h on S1s of three stories of B1 under the impact of different wind patterns of the test day

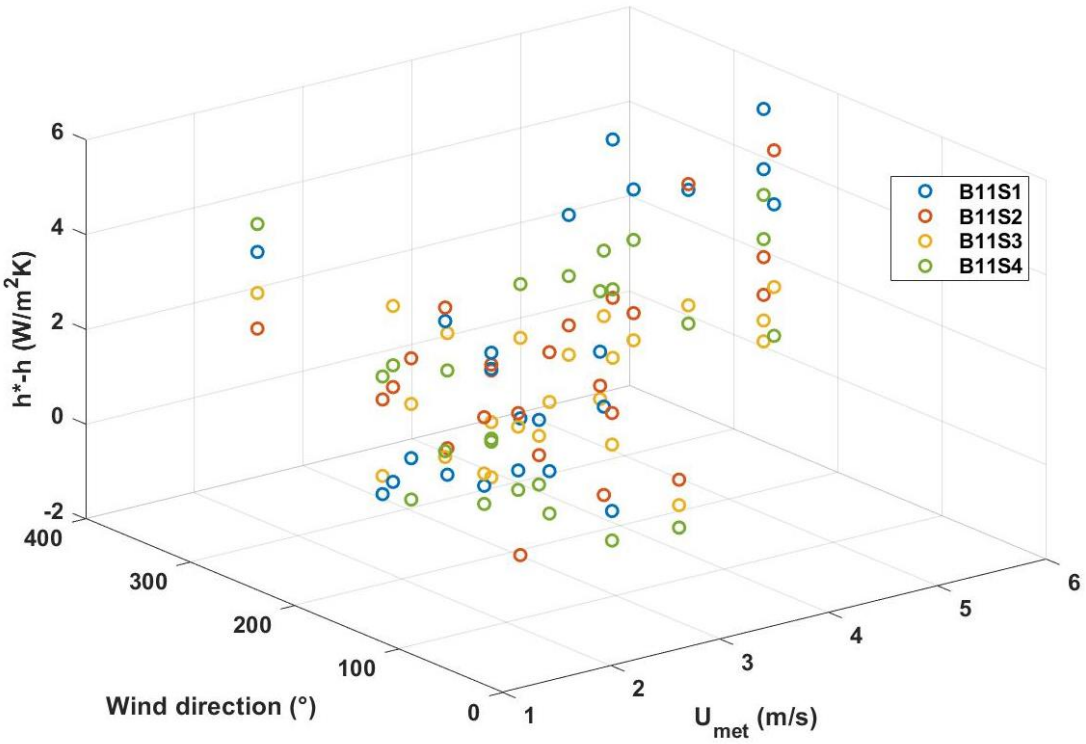

Figure 5-12 Gap between the coupled h and EnergyPlus h on S1s of three stories of B1 under the impact of different wind patterns of the test day*

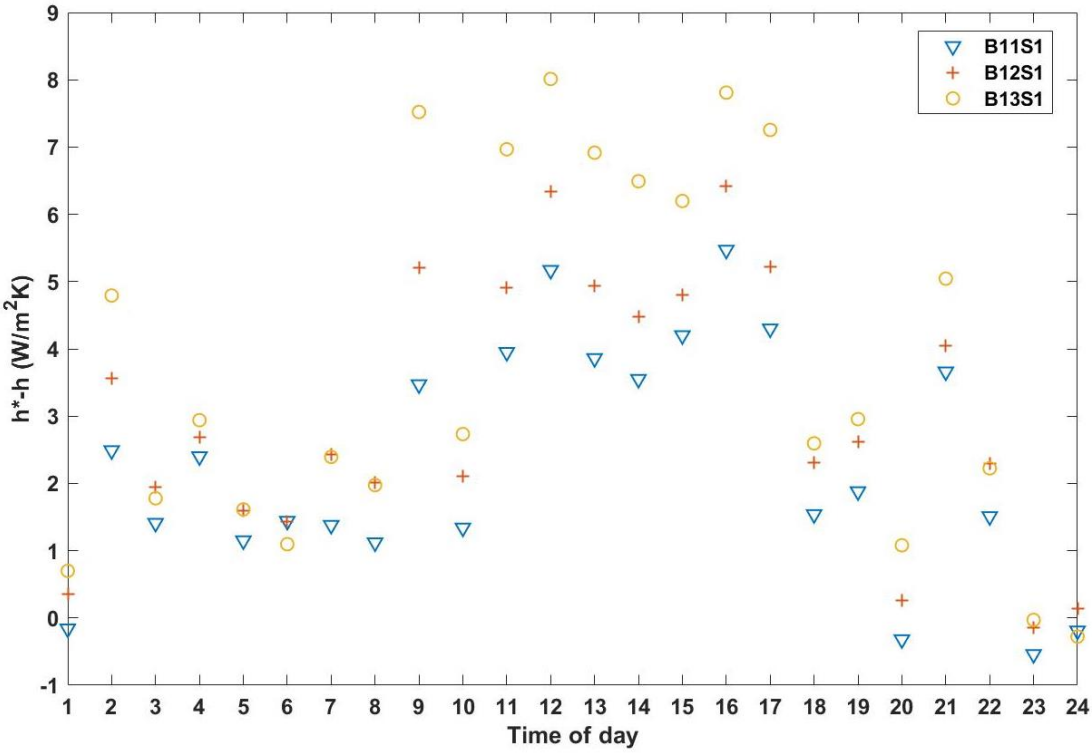

Figure 5-13 Gap between the coupled h and EnergyPus h on S1s of three stories of B1 along the time of the test day*

For most hours of the test day, the gap is smallest on the bottom floor, increasing with the height, as seen in *Figure 5-13*. However, there are several hours this trend is disrupted. The occurrence of these hours seems not only related to the wind pattern. For example, when the wind speed is 2.1 m/s, the trend along height is not reflected during the hours No. 3, 5, 8, and 24 with the wind directions of 70°, 100°, 10°, and 220°, respectively; however, the trend is tenable in hours 4, 9, 21, and 23 with wind directions of 80°, 350°, 170°, and 230°, respectively. The underlying rule for this phenomenon is not intuitive nor merely described as a regulation of wind patterns.

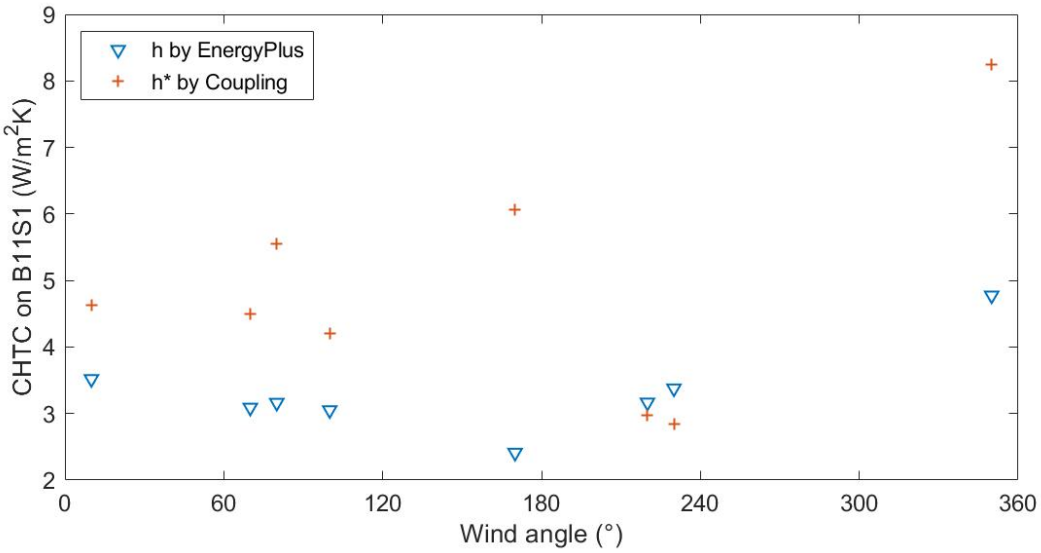

Figure 5-14 Comparison of EnergyPlus h and coupled h^* on B11S1 when winds come from different angles with a speed of 2.1 m/s on the test day

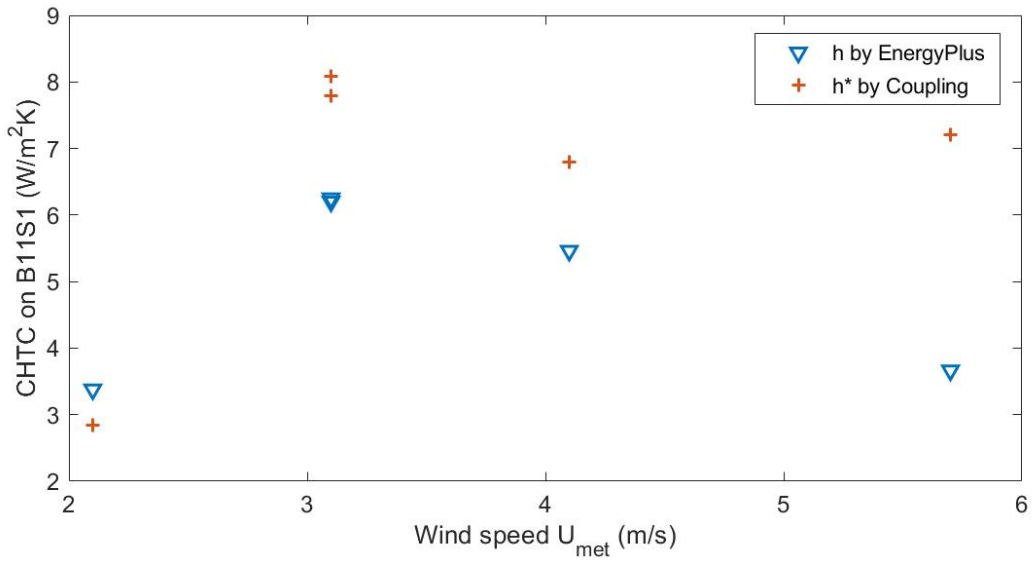

Figure 5-15 Comparison of EnergyPlus h and coupled h^* on B11S1 when winds come from 230° with different speeds on the test day

To see the impact of wind patterns on the CHTC on a specific surface, for example, B11S1, *Figure 5-14* and *Figure 5-15* compare the h by EnergyPlus and h^* by coupling method with the change of wind angles at a speed of 2.1 m/s and change of wind speed at an angle of 230°, respectively. It is evident that the h^* or the gaps between h and h^* are determined merely by the wind patterns. The distributions of h^* in the plot are more dispersive than h, with irregular gaps, especially for the impact of wind angles. In *Figure 5-15*, when the wind comes from 230° with a speed of 3.1 m/s, two h values almost overlap. However, an apparent deviation between two h^*can be located, meaning that there are other factors impacting. Therefore, a more complex relationship between the CHTCs and the microclimate should be discovered rather than applying a correction factor according to the wind patterns to existing algorithms' results.

5.3.4. Comparison of embedded CHTC algorithms and coupling method

After completing the fully dynamic coupling for the simulation day, the newly created dynamic CHTC profiles are compared to those obtained using the algorithms embedded in EnergyPlus, including DOE-2, TARP, MoWiTT, SimpleCombined and the Adaptive model.

Figure 5-17 shows the average change of the CHTC throughout the simulation day for each building by percentage. The deviation from SimpleCombined is much higher than the others, especially for buildings B5, B6, B8 and B9. The highest discrepancy between the SimpleCombined CHTC and the coupled CHTC of an individual surface throughout the test day is over 521 %. The absolute average discrepancy between the SimpleCombined and the coupled results is up to 7.95 W/m^{2}K. DOE-2 is found to provide the most similar predictions to the coupled model while the daily average discrepancy is approximately 1.60 W/m^{2}K. The average difference in the DOE-2 model is approximately 20 % and is the lowest. The highest is by SimpleCombined at 169 %, whilst the differences of TARP and MoWiTT are quite similar, at 28 % and 30 %, respectively.

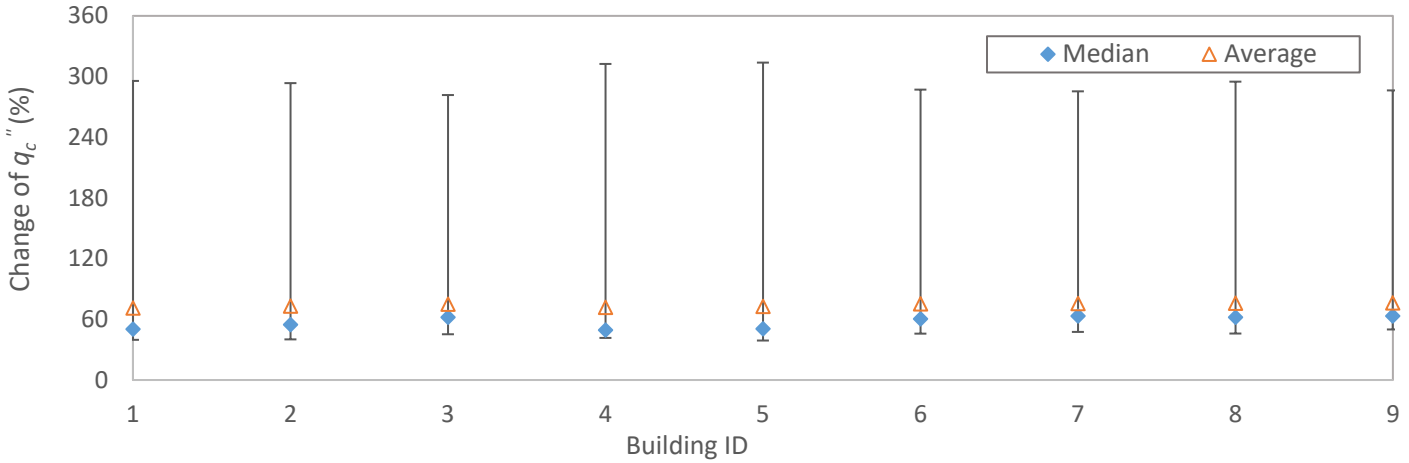

Figure 5-16 Improvement in q_c'' at exterior rough surfaces by the coupling CFD-BES method in the 1st hour of the test day [90]

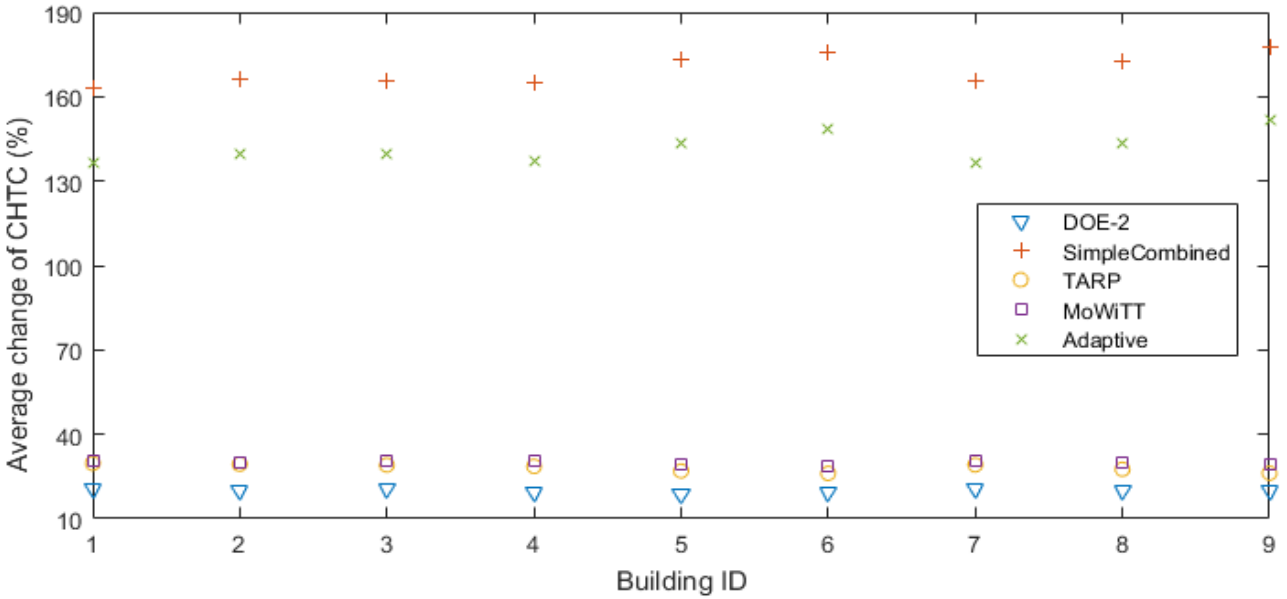

Figure 5-17 Change of CHTCs by coupling method over the results by embedded algorithms in BES [90]

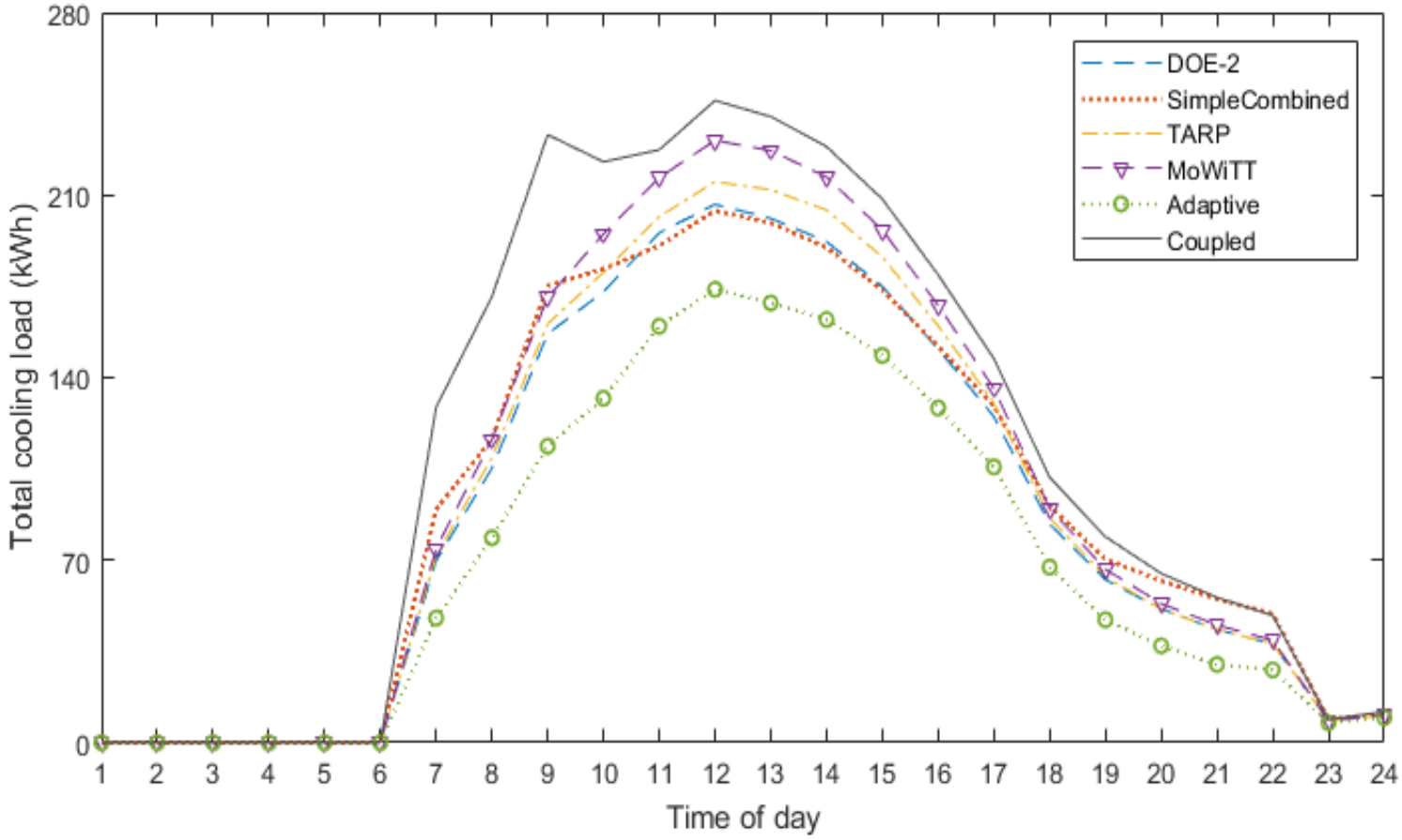

Figure 5-18 Total cooling load of nine commercial buildings throughout the test day by different methods [90]

Figure 5-18 presents a comparison of the total cooling demand of the nine buildings between the embedded EnergyPlus algorithms and the coupled BES-CFD model. *Table 5-2* gives the daily energy demand predicted by the different methods.

Table 5-2 Comparison of daily cooling energy demand by different method

Cooling demand (kWh)	DOE-2	SimpleCombined	TARP	MoWiTT	Adaptive	Coupled
	2048.7	2149.3	2132.5	2261.4	1646.0	2603.9

All of the algorithms underestimate the demand when compared to the coupled model. The MoWiTT provides the closed predictions to the coupled method, but the smallest difference in the daily cooling demand is approximately 343 kWh. The largest difference is seen for the Adaptive model and is 958 kWh. Large differences can be observed from 7 a.m. to 10 a.m. when the wind blows from 140 °, 10 °, 350 ° and 230 °. During this period, the coupled results are up to twice those estimated by the Adaptive model where a clear deviation between the coupled method and the other algorithms can be seen.

5.4. Summary

This chapter provides the approach of fully dynamic coupling for short-term modelling of sealed scenarios. The key findings in this chapter are:

- An analysis of an example hour during a test day shows that this coupling method can change the prediction of a building community's outdoor q_c'' by approximately 74 %. The prediction of hourly exterior convection energy is changed by over 64 % (including fenestration surfaces).

- Even with the best matching DOE-2 model, there is a 20 % difference in the daily average amendment of the CHTC.

- All EnergyPlus embedded algorithms are found to underestimate the cooling load of the case study buildings.

- BES's weakness in representing the neighbourhood effect is proved.

Chapter 6. SHORT-TERM MODELLING OF VENTILATED SCENARIOS

This chapter investigates simulating the community where buildings are under natural ventilation using the external fully dynamic coupling. The main challenge of modelling ventilated buildings is that the computational burden would be extremely high to execute the CFD calculations of a hybrid indoor-outdoor model, especially in a coupling assessment. Therefore, a novel method for fast modelling ventilated buildings is proposed in this chapter. *Section 6.2* a provides a framework of the proposed method. After determining the appropriate interface types between two CFD models with different scales, a case study is provided to check the feasibility and benefits of the proposed method. The case study is taken for the hottest workday in Los Angeles, with the flush precools of all nine cubic buildings in the tested community during the night-time.

6.1. Concept of Integration of CFD_f – CFD – BES

Cross-ventilation is one of the essential natural ventilation techniques that can be applied in many climates and seasons. It works through heat removal by placing two or multiple openings at opposite or adjacent facades of a building. One of its applications is the night-flush cooling, which removes the heat from the building mass during the night and early morning, so the targeted space can be pre-cooled for the next day. However, the coupling strategy of BES and CFD domains needs to be upgraded before applying it to natural ventilation cases.

CFD technique can help to perform the airflow within or around a naturally ventilated building. The applications can be sorted through the interest regions: indoor-only, hybrid indoor and outdoor, and regional decomposition (considering the domain in multiple scales). The first one does not suit the assessment of the outdoors. Moreover, according to the *Section 2.3.3*, the

hybrid indoor and outdoor model usually has an extremely high resolution, which makes it impractical or unfeasible to participate in a fully dynamic coupling with BES that iterative calculations are run until the convergence is reached achieved. Therefore, the regional decomposition uses the nesting technique to become an attractive choice due to its modulated burden.

The airflow is processed with the CFD field divided into two parts, one containing the whole domain of both indoor and outdoor spaces with fine grids, and the other contains only an outdoor domain with coarse grids. The fine mesh was denoted as CFD_f, and the coarse one was denoted as CFD (with similar mesh density as that in *Chapter 5*). Only CFD would communicate continuously with the BES field throughout the simulation. CFD_f acts in an off-line mode where it was run only once at the beginning of the simulation to provide the information at interfaces, but no further participation took place. *Figure 6-1* shows the relationships of CFD_f, CFD, and BES in the integration. The interfaces between different domains are illustrated in following *Section 6.2*.

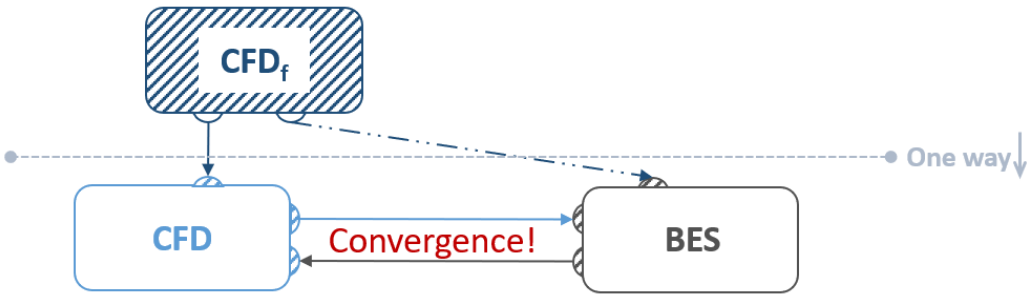

Figure 6-1 Schematic of CFD_f – CFD – BES integration

6.2. Framework for Short-term Modelling of Ventilated Scenarios

Figure 6-2 shows the schematic of the proposed coupling CFD_f – CFD – BES method for an energy demand assessment of buildings while the effect of natural ventilation is taken into account. This framework is extended from a benchmark framework proposed in *Chapter 5*, which consists of two main CFD and BES components linked with a custom code. The embedded algorithm in BES domain calculates the initial CHTC values in the preliminary stage for subsequent iterative calculations. When entering the dynamic

simulation stage, convection control function of BES is then altered to 'user input' mode to receive updated results from CFD. Buildings are simulated using a fully dynamic approach that ensures a convergence between CFD and BES in exterior surfaces' convection for each time-step. The BES and CFD domains should achieve a similar convective heat flux (q_c'') with an acceptable small difference (e.g., less than 10^{-2} in this study) at the outdoor surfaces in every time-step before moving to the next one.

Now, an additional CFD_f component is included in the framework to enable the simulation of natural ventilation. Also, the bespoke code is modified as an interlink station between three domains and the weather data, building, and site information. While CFD_f model consists of a high-resolution grid for indoor and outdoor domains, CFD consists of a coarse grid for only the outdoor domain. Inflow and outflow boundaries should be inserted for the ventilation surfaces of the buildings in CFD as deletion of its indoor part. The setups of these boundaries are obtained from the CFD_f simulation at the beginning. Therefore, the whole process can be divided into preliminary off-line simulation and dynamic online simulation.

Pre-simulation is implemented for a relatively short period (a few hours) before the simulation day. As the results of CFD_f are fixed throughout the iterative dynamic stage, the CFD_f domain only participates in this stage as an offline component. Its simulation period includes natural ventilation time (e.g., purging time including the night and the early morning when the space is unoccupied or relatively empty). The mass flow rates through the ventilated rooms from CFD_f are given to the BES, while the flow patterns from CFD_f are passed to CFD at the opened ventilation surfaces.

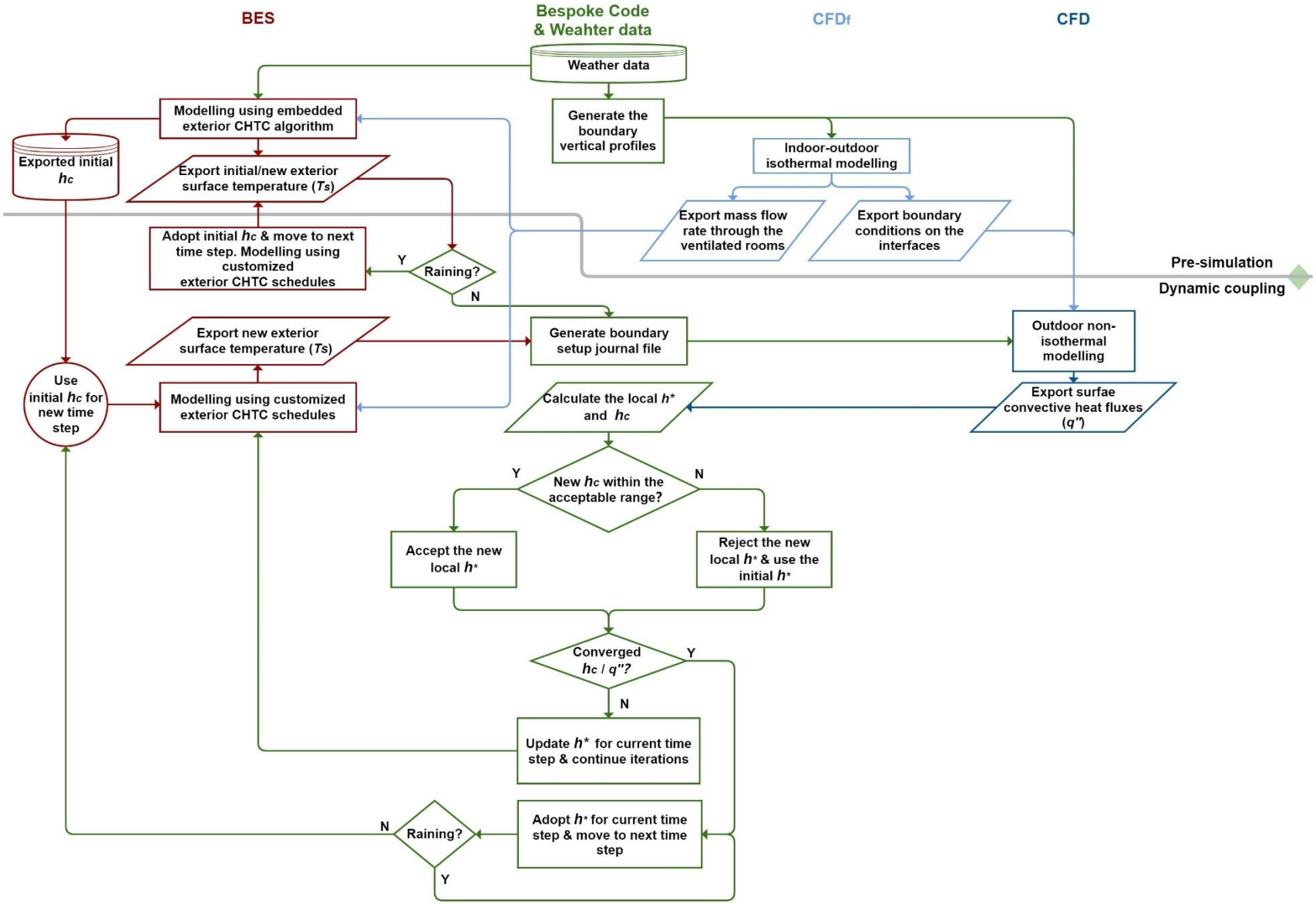

Figure 6-2 Framework of coupling CFDf – CFD – BES for the exterior surface convection with the inclusion of natural ventilation

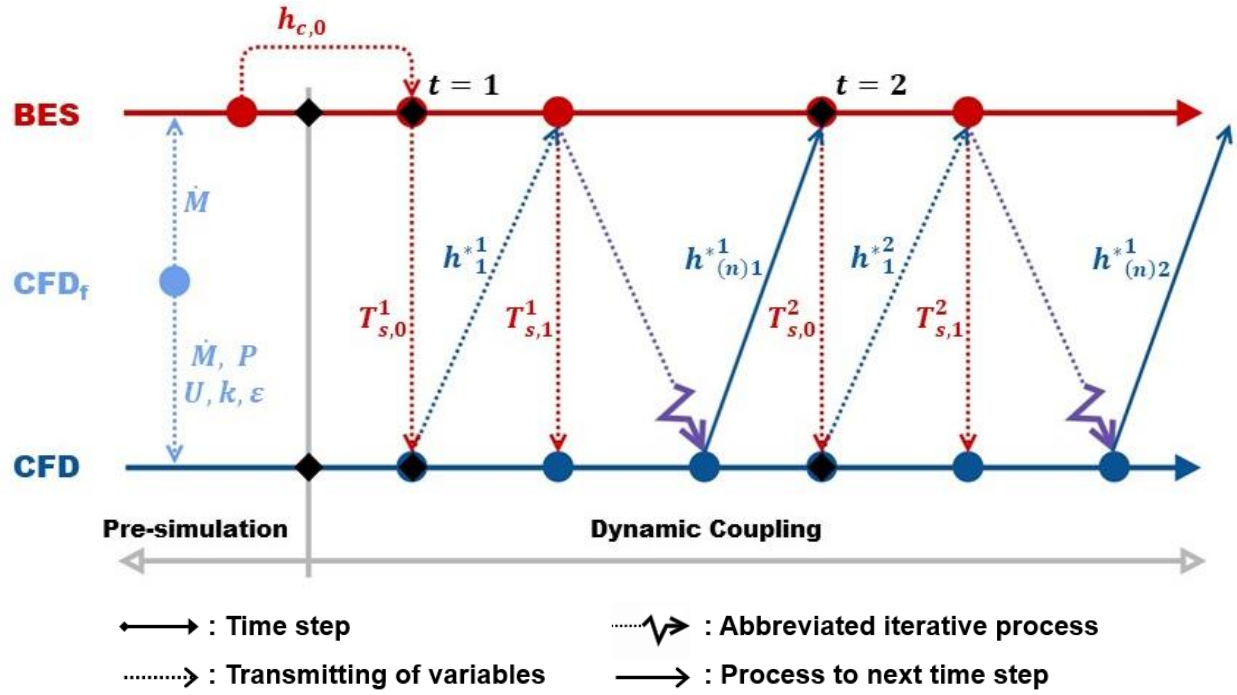

Figure 6-3 Transmitting of variables in short-term coupling of ventilated scenarios

The information is accepted as the boundary conditions for CFD to model the microclimate without indoor environment. The information includes mass flowrate ($\dot{M}$), velocity (U), pressure (P), kinetic turbulence energy (k) and turbulence dissipation rate (ε). In this study, four boundary types were investigated to find out the optimum option for the low-resolution CFD model to represent the microclimate as that simulated by the high-resolution CFD_f model. These boundary types of windows openings included, 1) mass flowrate in and out; 2) velocity inlet with pressure outlet; 3) pressure inlet and outlet and 4) velocity inlet and outlet.

Moreover, the boundary conditions of CFD include following aspects: 1) climatic conditions from the weather data, 2) ventilating opening conditions determined by CFD_f, and 3) other exterior surface conditions (e.g., surface temperatures) provided by BES. *Figure 6-3* shows the transmitting process of variables within all components.

6.3. Description of the Case Study

6.3.1. Case specification

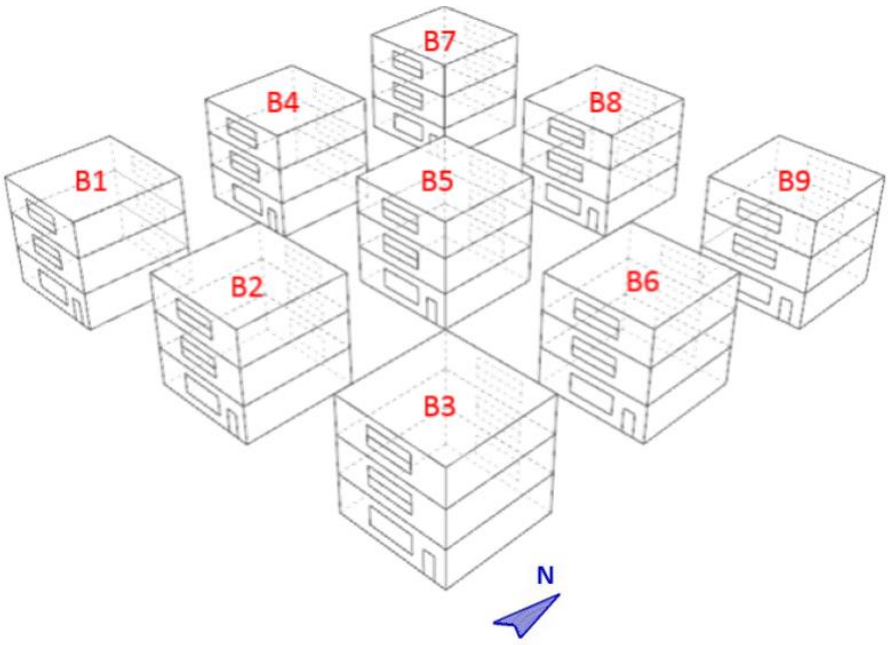

Figure 6-4 Nine-cube EnergyPlus model for the ventilated scenario [97]

Intense cooling is in demand in commercial buildings where insulation is regularly assigned, and high internal heat gain released from occupants, lightings, and other equipment. Therefore, the application of night-purging combined with mechanical ventilation provides a high potential in saving energy for commercial buildings as the space is unoccupied during the night. Thus, scenarios of night-purging were assumed to investigate the use of cool night air to remove and absorb the stored heat from the building as a sink to be utilized for the following diurnal time [98].

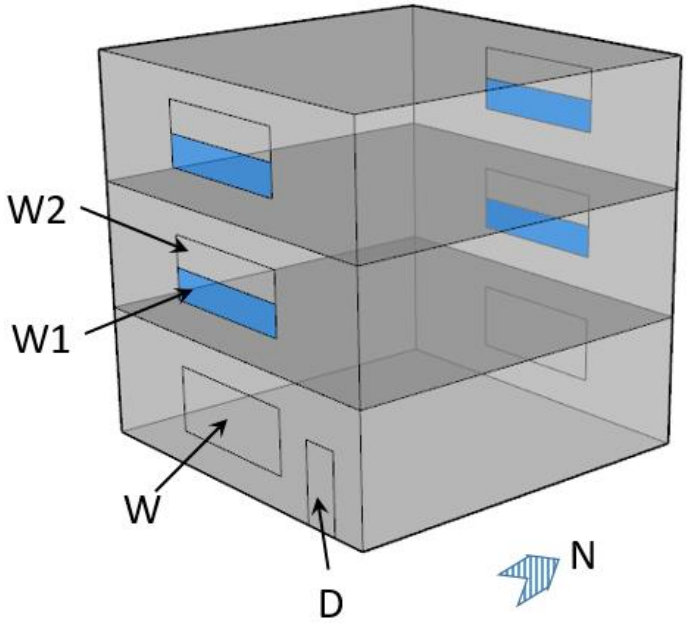

Figure 6-5 Fenestration surfaces of the tested buildings

The windows on the top two layers were divided into two equal parts of W1s and W2s while W1s would be opened for night-purging. The simulation is processed for a typical hot day (September 25th) in Los Angeles, U.S., including 12 hours of purging period (1 a.m. – 6 a.m. and 7 p.m. – 12 a.m.) and 12 hours of mechanical ventilation during the working time when all windows were kept closed. *Figure 6-4* shows the developed model according to the design principles stated in *Section 3.3.3*, and *Figure 6-5* shows the names of the fenestration surfaces of the tested buildings.

6.3.2. Outline of interface between CFD_f and CFD models

The interfaces between CFD_f and CFD models lie on the W1s of each building. During the naturally ventilating time, CFD_f runs the isothermal simulation so that the airflow information at its W1s can be transferred to CFD. When transferring of the flow parameters, an important action is to specify the opening surface as either inlet or outlet boundary in the CFD model. The specification was based on the flow direction. If the relative component (x or y) of flow was towards the indoor space, then the surface was defined as the outlet boundary by the bespoke code as the indoor space was exclusive from the CFD model. The opposite surface was defined as the inlet boundary in this scenario.

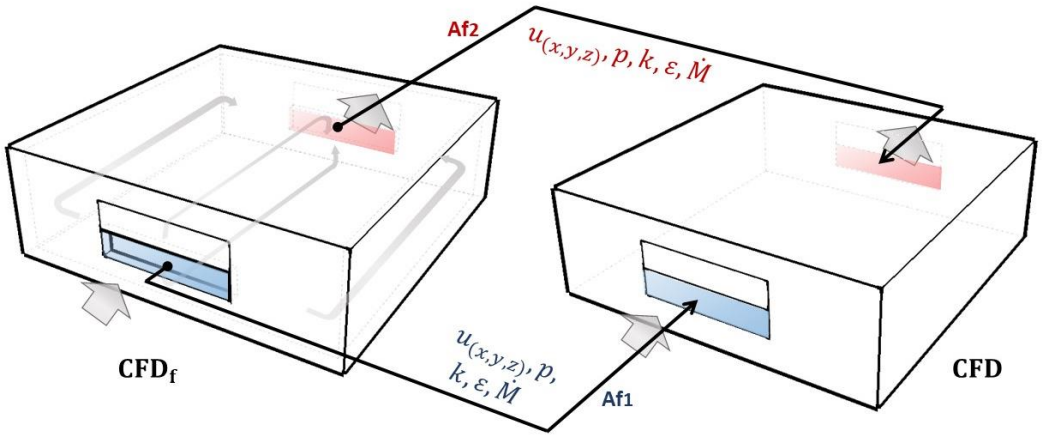

Figure 6-6 Flow information transfer from CFD_f to CFD [97]

CFD was designed to have merely an indoor environment, however, with the capability of representing the microclimate around naturally ventilated buildings. Therefore, to capture the patterns of the flow entering the windows (Af_1) and the flow leaving the windows (Af_2), the flow information obtained in CFD_f was passed to CFD to define the boundaries (see in *Figure 6-6*). In CFD, if the flow direction was pointed towards the interior space, the window boundary should be defined as outflow (Af_1). At the same time, the inflow boundary was assigned to the windows, releasing air to the exteriors (Af_2).

6.4. Boundary Type on Interfaces for CFD

This section demonstrates the selection of boundary types on interfaces for CFD to receive flow patterns from CFD_f and use the information to represent the urban microclimate. The options of boundary types refer to the inlet and outlet boundaries in CFD as defined in *Section 6.3.2*. The four options of boundary types of W1s investigated in this study include:

1) the mass flow rate in and mass flow rate out (denoted as 'mass - mass'),

2) the velocity inlet with pressure outlet (denoted as 'velocity - pressure'),

3) the pressure inlet with pressure outlet (denoted as 'pressure - pressure'), and

4) the velocity inlet and velocity outlet (denoted as 'velocity - velocity').

6.4.1. Evaluation of the CFD model performance

There were thirty-four vertical and twenty-four horizontal lines (as seen in *Figure 6-7* and *Figure 6-8*) created inside the community to monitor the performance of CFD, representing the velocity patterns of CFD_f.

Lines 1 - 16 laid at the centre of street canyons, and lines 17 - 34 were located close to the fenestrations (1 m from the openings), as seen in *Figure 6-7*. The vertical lines, consisting of 30 test points, were drawn from the ground to a level slightly higher than the building roofs (12 m above the ground). Horizontal lines, consisting of 25 test points, were placed at the same height as the centroid of W1s to investigate the influence of the flow from the openings on the urban flow. As seen in *Figure 6-8*, lines 41 - 52 were under the influence of both leeward and windward regions simultaneously, while lines 35 - 40 and 53 - 58 were only within the windward or leeward region. The test points were distributed evenly along the test lines. The performance of the proposed CFD_f -CFD method was examined at three wind speeds (4 m/s, 8 m/s and 16 m/s) and in 5 wind directions (0 °, 22.5 °, 45 °, 67.5 ° and 90 °).

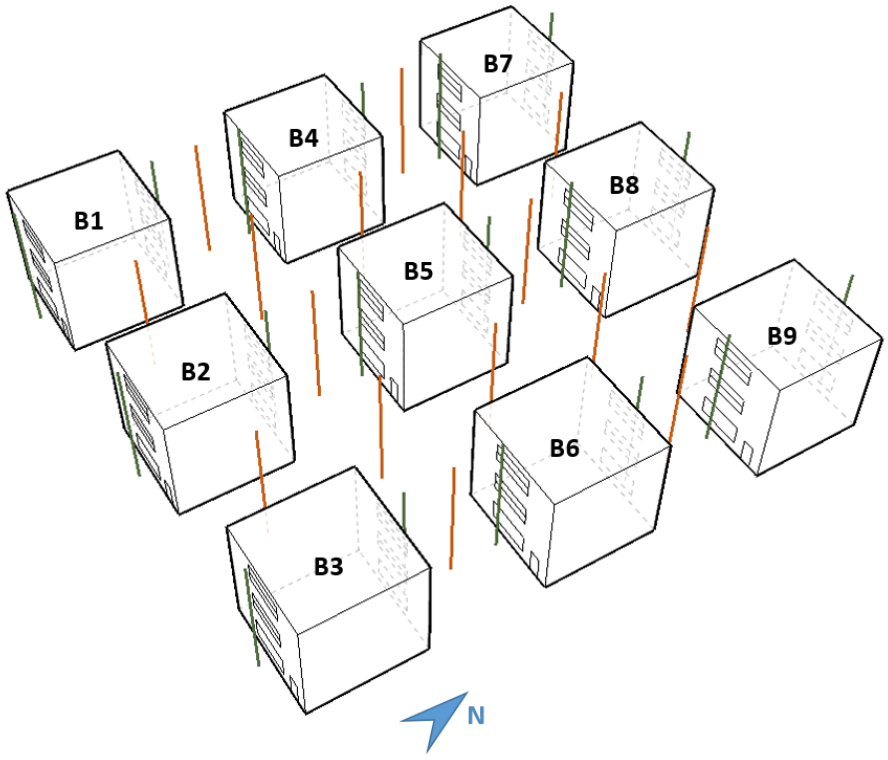

(a)

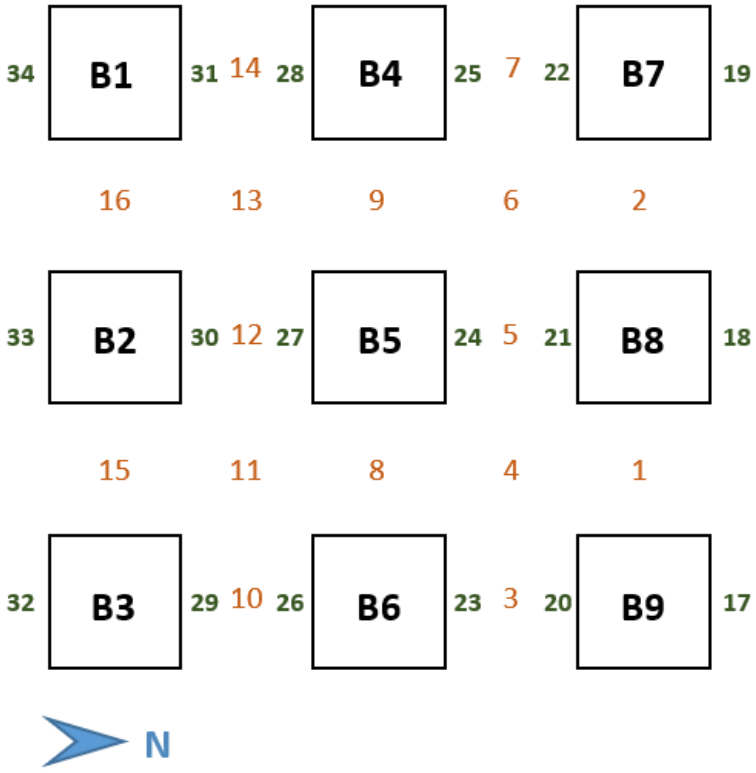

(b)

Figure 6-7 Thirty-four vertical test lines' a) positions and b) names

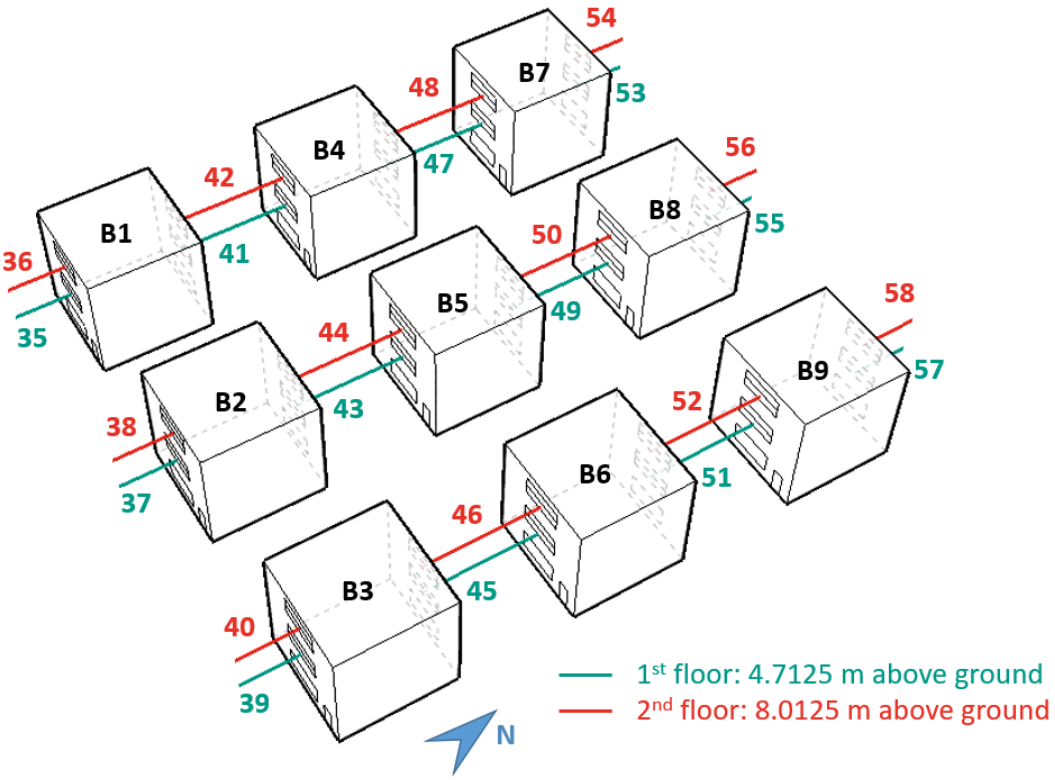

Figure 6-8 Twenty-four horizontal test lines' positions and names

Two metrics were used to evaluate the CFD performance; one was the root mean square error (RMSE, see *Eqn. 35*) of the relative error between observed values (o_i) by CFDf and predicted values (p_i) by CFD. N is the amount of the test points. The other metric was the fraction of the predictions within a factor of two of the observations ($FAC2$, see *Eqn. 37*).

The comparisons of results by CFDf and CFD were provided for:

- the street-canyon layer (denoted as 'SC') where containing lines 1 - 16,
- the close-to-opening layer (denoted as 'CTO') where containing lines 17 - 34,
- the opening-to-environment layer (denoted as 'OTE') where containing lines 35 - 40 and lines 53 - 58,
- the opening-to-opening layer (denoted as 'OTO') where containing lines 41 - 52.

Besides, a low-resolution CFD with an indoor environment (denoted as 'CFD_{in}' having the same cell size as the validated CFD model) was created and tested to weigh the impact of removing the indoor part using the boundary information from CFD_f instead. Furthermore, an independence test has been undertaken by refining CFD_{in} to specify the influence of the model resolution on its accuracy of representing scenes. Whereas the influence of the removal of indoor parts and the refinement of CFD_{in} was found negligible.

6.4.2. Performance in different layers

Figure 6-9 shows the local velocity patterns of the lines (i.e., 5, 24, 55, and 43) around the central building (B5) in four layers (line 5 in SC, line 24 in CTO, 55 in OTE, and line 43 in OTO) when the wind is coming from 0 ° at a speed of 8 m/s. A more considerable discrepancy can be seen at the levels of two openings' positions on the two vertical lines, especially at line 5, which is under the influence of both airflows released from the front building (jet zone) and entering the rear building (breathing zone). Underestimation is observed in CFD by each interface boundary for the CTO layer.

The velocity-velocity option underestimates the local velocity in the SC layer (along line 5). Among four options, the pressure-pressure option provides the best overall prediction on the two vertical lines, followed by the mass-mass, velocity-velocity options. In contrast, the velocity-pressure boundary condition gives the worst representation. However, since the second floor, around 6 m above the ground, the velocity-velocity and mass-mass interfaces surpass the performance of the velocity-pressure and pressure-pressure options. The boundary layer may introduce part of deviations at a lower level in CFD where it is insufficiently or not enough-accurately modelled due to the model's much lower resolution than CFD_f. Deficiency of the pressure-pressure option is observed in the OTO layer. As sample line 55 is located in the leeward region, under such a scenario, the pressure boundary shows a good representation of the airflow conditions in the jet zone. However, when the distance to the window increases, its advantage diminishes until it becomes the worst option comparing to the others. It can be seen in *Figure 6-9d* that the pressure

boundaries (see both the velocity-pressure and pressure-pressure) fail to (or cannot accurately) capture the inhaling flow pattern (breathing zone) in the OTO layer.

Figure 6-10 shows the average RMSE values of the normalized local speeds (to different meteorological speeds with 0 ° incident angle) computed using four boundary options. The worst performance of CFD is found for representing the horizontal distribution of airflow between the buildings. The complexity of the exhaust from the front buildings and the inflow of the rear buildings affects this area and raises the difficulty of accurate descriptions. The figure shows that all mass-mass and pressure-pressure boundary setups perform better than velocity-pressure and velocity-velocity when representing vertical patterns. However, the pressure-pressure option becomes the least precise when considering the horizontal distributions. The most significant difference of RMSE of four interface options is approximately 0.060, occurring in the OTO layer, and it is given between the pressure-pressure and the mass-mass options. Moreover, the pressure-pressure boundary is the least accurate, with an average RMSE value of 0.556 in the OTO layer. Overall, the mass-mass boundary shows the best performance with an average RMSE of 0.408, followed by velocity-velocity of 0.411, followed by velocity-pressure of 0.422. The worst is pressure-pressure, with an average RMSE of 0.428.

Table 6-1 provides the average $FAC2$ values of all studied scenarios including different wind speeds and wind angles for each monitoring layer by four interface boundaries. $FAC2$, which is considered as the most robust metric because it excludes the interference from the extreme outliers, indicates 'good enough' model when the value exceeds 0.5, and ‘perfect' when reaching 1 [94]. Therefore, from the values of $FAC2$, the performances of the four interface options are good, that the values of each layer are above 0.70, and the overall values are found no less than 0.84.

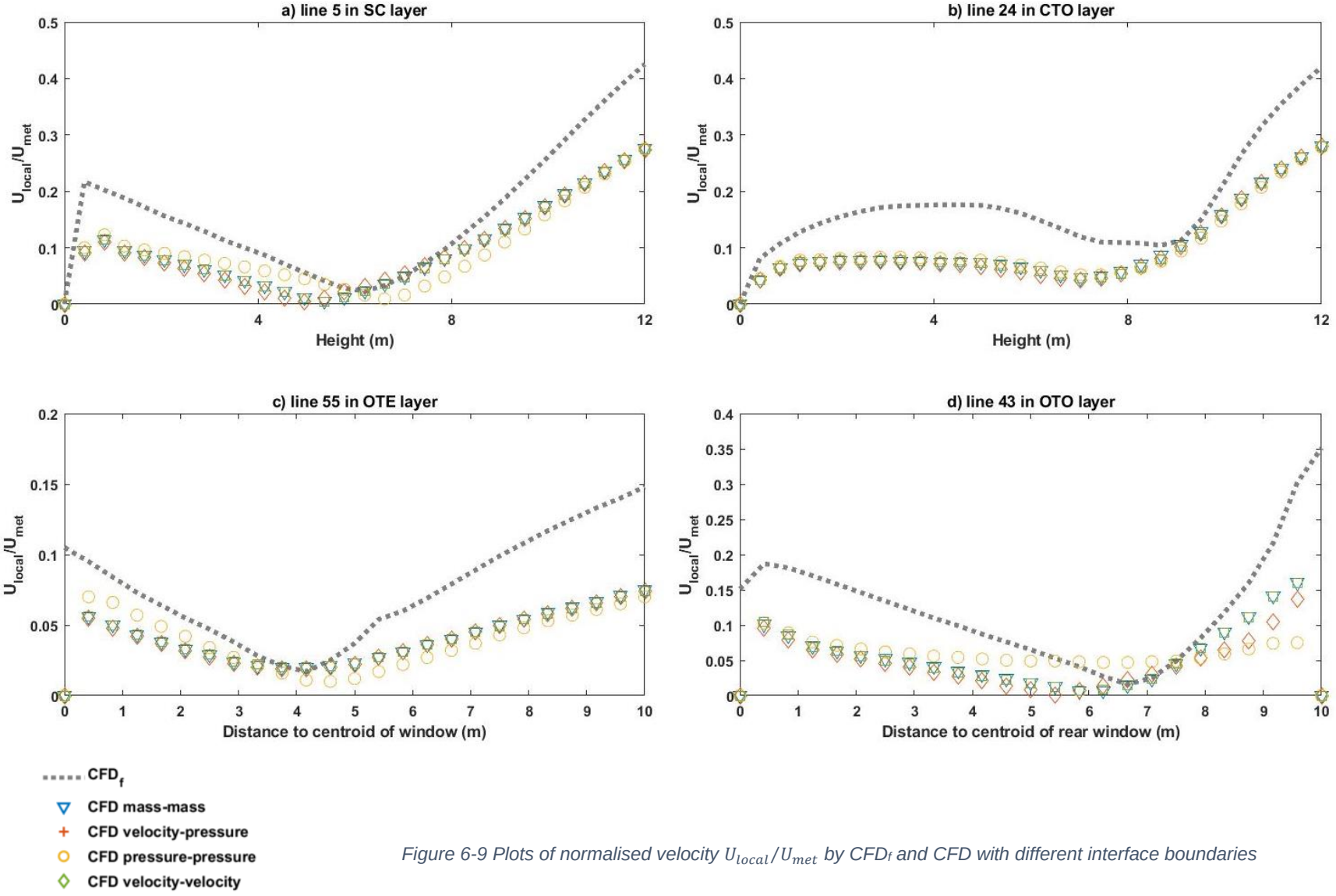

Figure 6-9 Plots of normalised velocity U_{local}/U_{met} by CFD_f and CFD with different interface boundaries

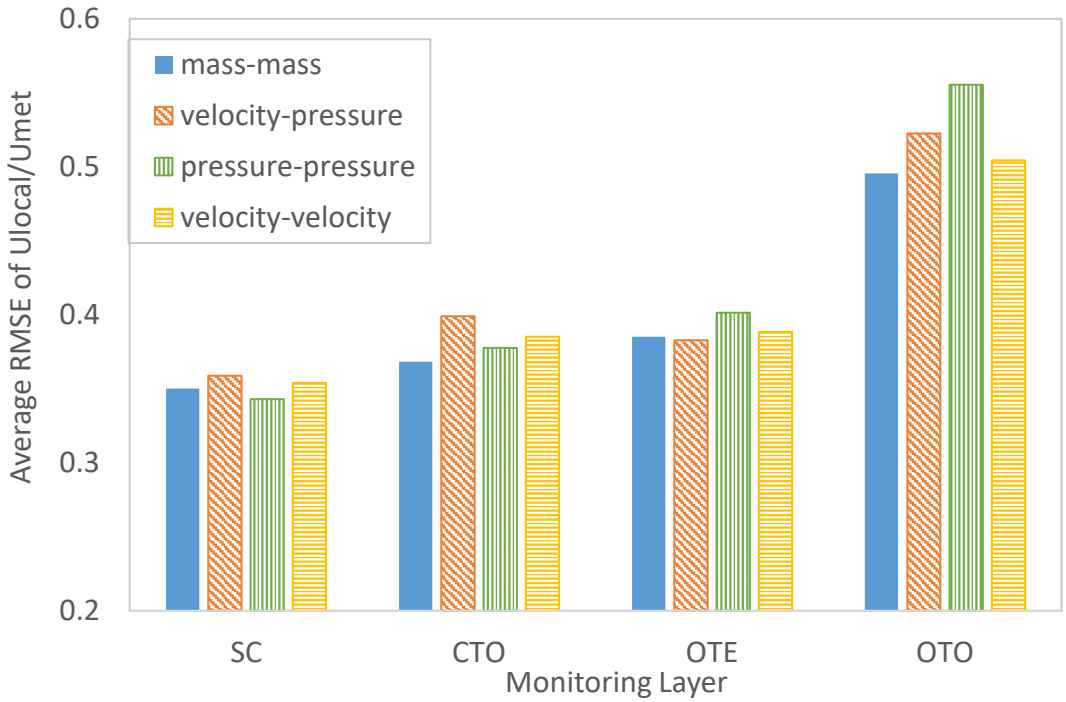

Figure 6-10 Average RMSE of U_{local}/U_{met} in different monitoring layers by four interface boundaries [86]

Table 6-1 Average FAC2 of all studied scenarios in different monitoring layers [86]

Boundary types	mass-mass	velocity-pressure	pressure-pressure	velocity-velocity
SC	0.91	0.91	0.93	0.91
CTO	0.86	0.84	0.87	0.86
OTE	0.90	0.90	0.86	0.89
OTO	0.80	0.75	0.70	0.79
Overall	0.87	0.85	0.84	0.86

6.4.3. Impact of wind speed and direction

The magnitude of wind speed is found influential in the performance of CFD. As seen in *Figure 6-11*, all interface types show a tendency of slow-down growth along with increasing wind speed. Moreover, the advantages of mass-mass and velocity-velocity interfaces at low-to-middle wind speed are clear, while the pressure-pressure is preferable at high speed. *Figure 6-12* reveals

the impact of wind angle on the coupling quality. An apparent low accuracy of CFD occurs when the wind flows in the direction perpendicular and parallel to the windows (that wind angle = 0 °, 90 ° in this case), and the OTO area mainly contributes to this part of the error. In the case of perpendicular wind, the jet and breathing zones intertwine in the OTO layer, while the layer is also affected by the separated flow of the building laterals.

Table 6-2 and *Table 6-3* display the CFD performance tendency along with the increase of the wind speed and wind angle in different monitoring layers. As seen in the table, the CFD model with different interface types performed consistently along with the U_{met} and wind angle within a specific layer, except the OTO. In general, similar tendencies may be interpreted by the impact of different interface boundary conditions, which is not the most important reason for the deviation between the CFD and CFD_f. Instead, the central part of the deviation can be contributed by removing the indoor part, the reduction in resolution, the difference of simulation engine, and the errors in data transfer during coupling.

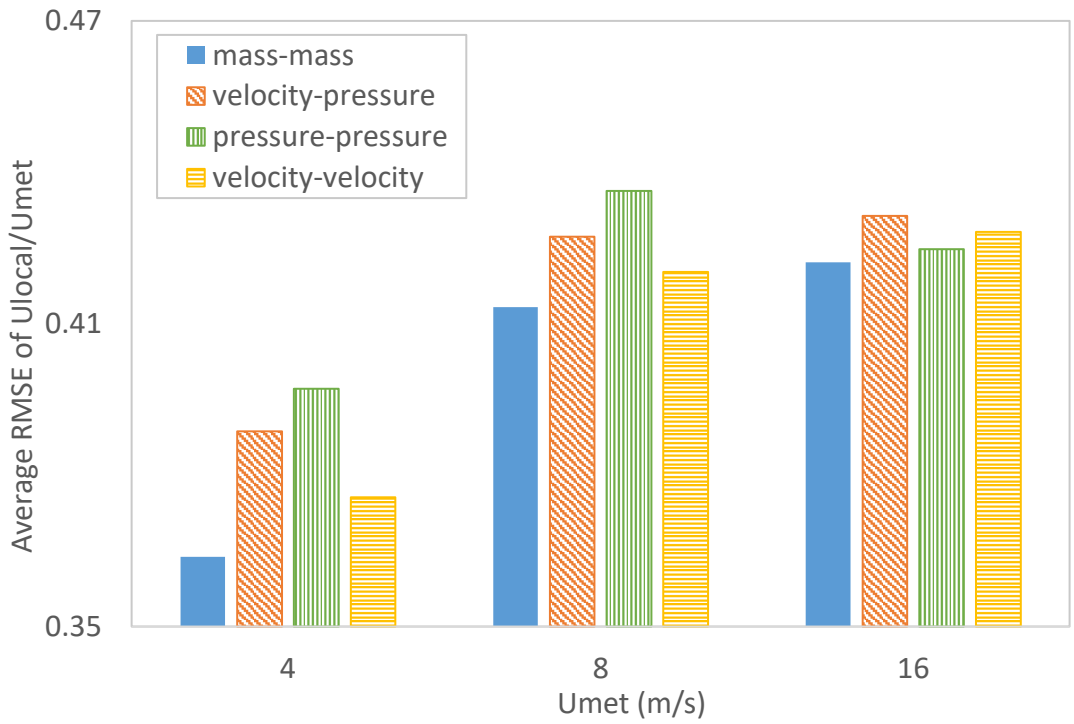

Figure 6-11 Average RMSE of U_{local}/U_{met} of all monitoring layers under the impact of wind speed U_{met} [86]

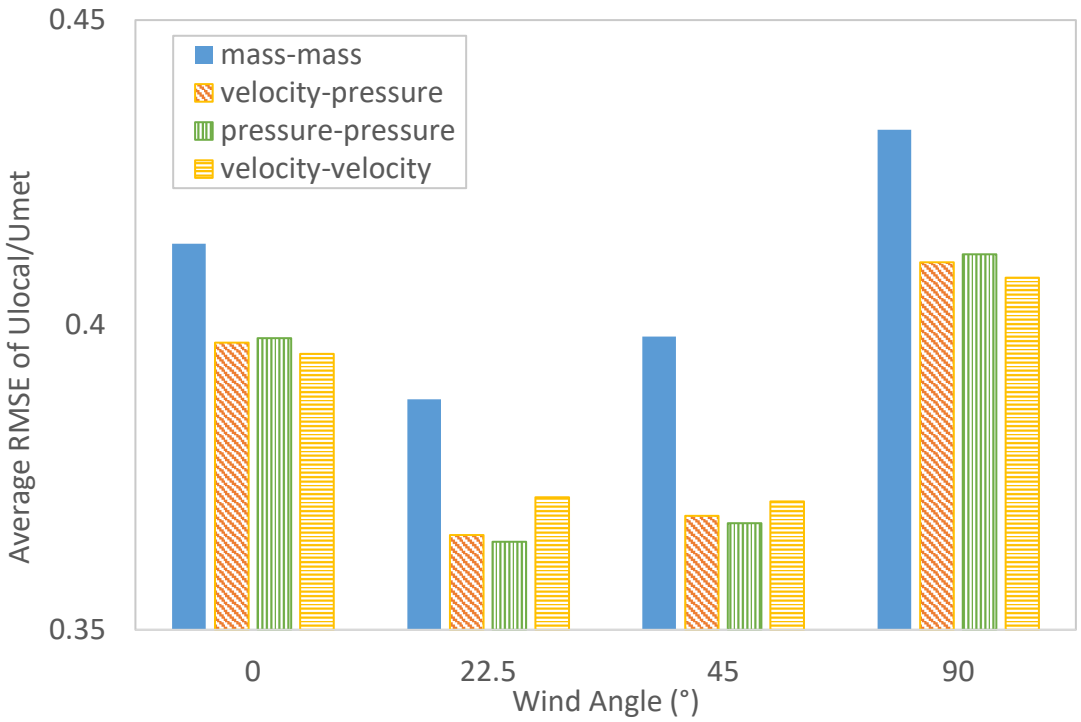

Figure 6-12 Average RMSE of U_{local}/U_{met} of all monitoring layers under the impact of wind angle [86]

In addition, as seen in *Table 6-2* and *Table 6-3*, the influence of the wind speed and wind angle is not linear in each layer, which also indicates the necessity of coupling CFD_f and CFD for specific scenarios. A test by comparing the CFD and CFD_{in} models (which includes the indoor part) has shown that the impact of the removal of indoor is less than 0.01 in RMSE, which proves the feasibility of the proposed coupling method. According to the test, the CFD grid size is quite close to the optimal value for the selected wall function (this is in line with the validation results of the model), as when it is refined, its gap to the CFD_f model would increase. However, the reduction in resolution combined with different wall functions may still be one of the leading causes of deviations. Furthermore, the change in model size is enormous (130K cells compared to 7.5 million cells), so the coarse grids cannot fully reproduce that part of flow information in CFD with very simplified boundary conditions at the interfaces.

Table 6-2 Tendency of average RMSE by four interface types changing with U_{met} in different monitoring layers [86]

Monitoring layer	SC	CTO	OTE	OTO
Impact of inflow velocity magnitude (U_{met}) → increasing U_{met}				
mass-mass	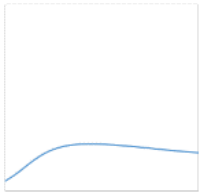		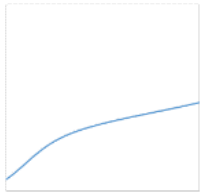	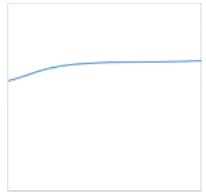
velocity-pressure	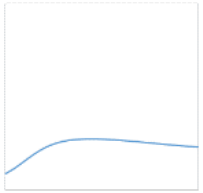		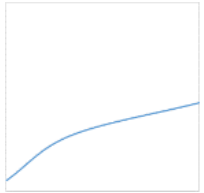	
pressure-pressure	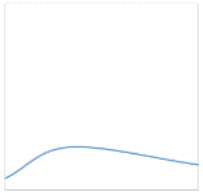	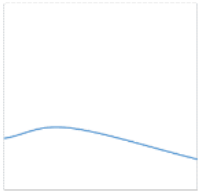	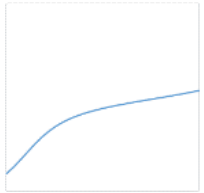	
velocity-velocity	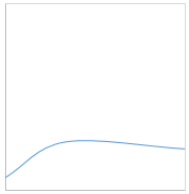	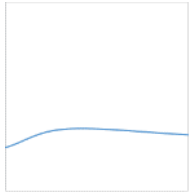	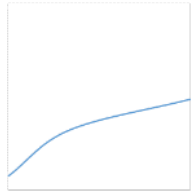	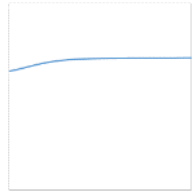

* Vertical axis: rising RMSE in an upward direction

Table 6-3 Tendency of average RMSE by four interface types changing with wind angle in different monitoring layers [86]

Monitoring layer	SC	CTO	OTE	OTO
Impact of inflow direction (wind angle) → increasing wind angle				
mass-mass	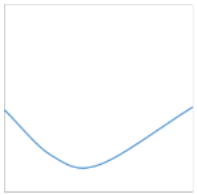	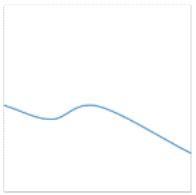	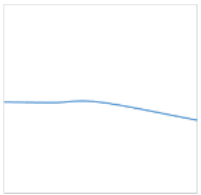	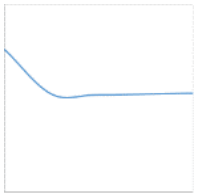
velocity-pressure	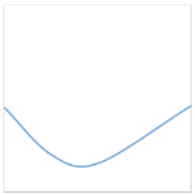	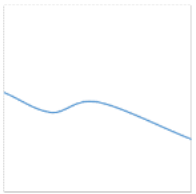	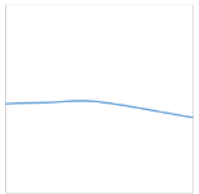	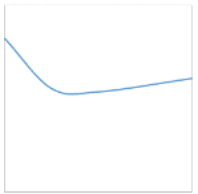
pressure-pressure	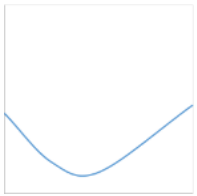	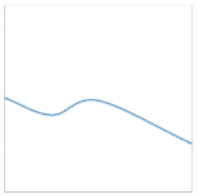	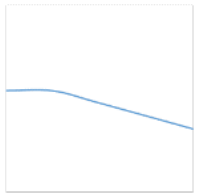	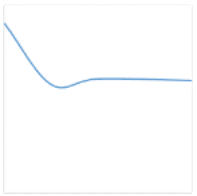
velocity-velocity		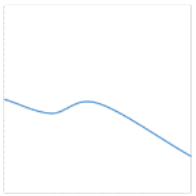	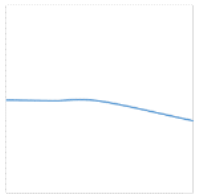	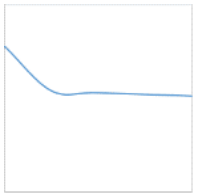

* Vertical axis: rising RMSE in an upward direction

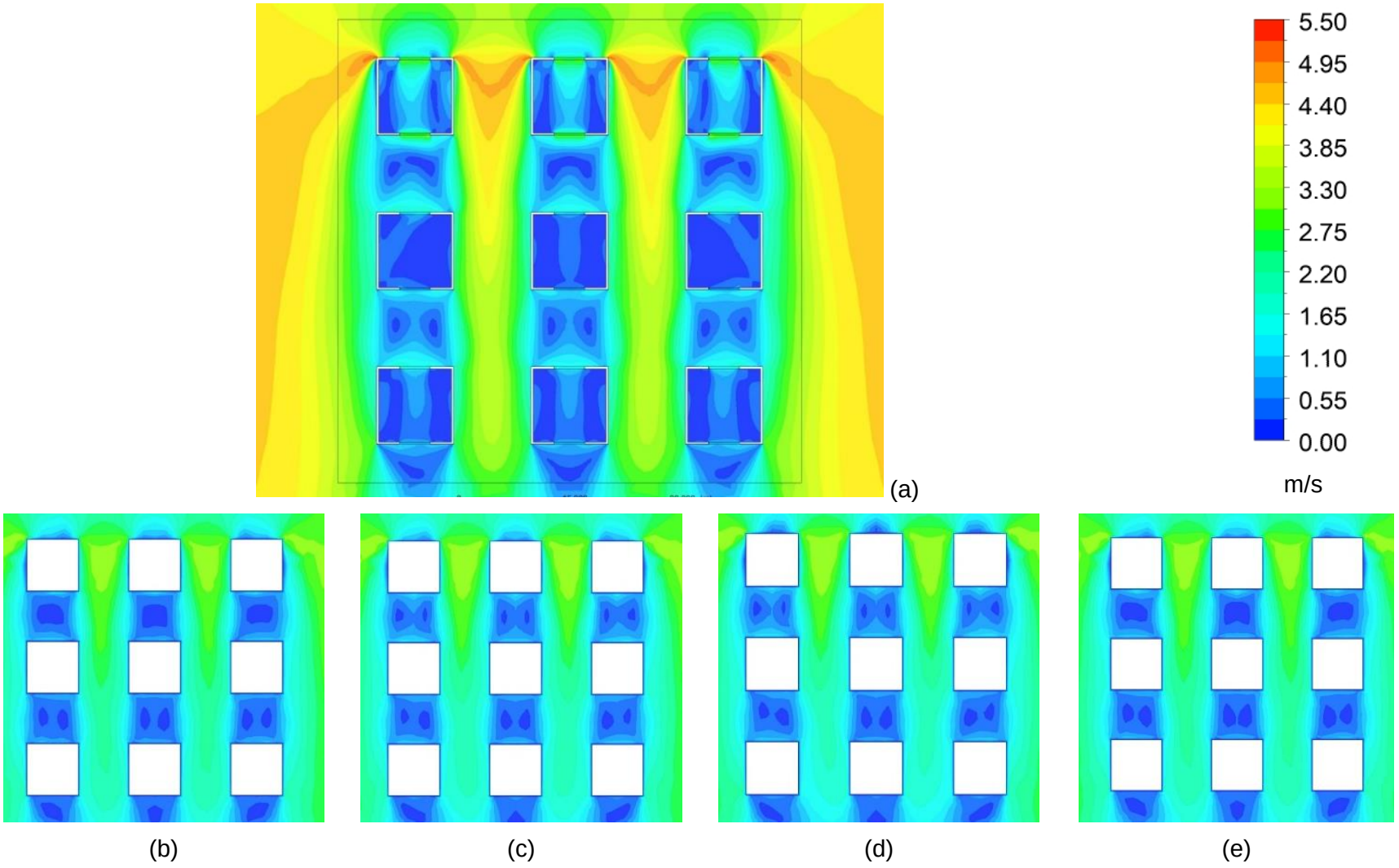

Figure 6-13 Comparison of velocity contours between a) CFD_f and CFD with b) mass-mass, c) velocity-pressure, d) pressure-pressure and e) velocity-velocity interface boundary conditions [86]

As seen in *Figure 6-13*, regardless of which boundary it is associated with, CFD has ubiquitously underestimated the velocity values. The underestimation also occurs in the upper stream area when the wind has not entered the target area. It is most likely caused by the different built-in algorithms (although the core functions are the same) of different simulation engines as different programs in this study handled CFD_f and CFD.

6.4.4. Representation of openings' local parameters

Table 6-4 provides the RMSE of four interface options representing different parameters, including pressure coefficient C_p, flow velocity U, pressure P, and mass flow rate $\dot{M}$ at all interfaces (opened windows). The velocity-velocity boundary shows a distinct advantage, especially in capturing the C_p and P patterns. The complex reverse flows error is considered as the primary source of error in P of pressure boundaries (velocity-pressure and pressure-pressure). The mass-mass boundary provides the same mass flowrate patterns for CFD as the assigned value (taken from CFD_f), and velocity boundaries (velocity-velocity and inlet boundaries of velocity-pressure) perform excellently in this aspect though without inputting mass flowrate values. In contrast, two options with pressure boundaries (pressure-pressure and outlet boundaries of velocity-pressure) fail to predict the mass flow rate at the openings. This failure can be even worse in non-isothermal cases where pressure boundaries would be very sensitive to the temperature field.

Table 6-4 Average RMSE of representing parameters at opening surfaces (interfaces) by CFD [86]

	mass-mass	velocity-pressure	pressure-pressure	velocity-velocity
C_p	12.960	27.773	36.470	0.658
U	0.139	0.147	0.409	0.104
P	3.322	6.951	9.033	0.655
$\dot{M}$	0	0.911	1.288	0.000

From all these explorations, the velocity-velocity option is recommended as the boundary type for CFD. Therefore, in this study, the transferred parameters are velocity components ($U_{(x,y,z)}$), turbulence kinetic energy k, and turbulence dissipation rate ε.

6.5. Runtime and convergence benefit

Although the accuracy is compromised by using CFD instead of CFD_f, the coupling CFD_f – CFD has considerably benefited the run time and computational cost. In the same isothermal scenario, the simulation of CFD only takes 1/28 of the runtime associated with CFD_f. The benefits of runtime conservation are even more apparent when non-isothermal conditions are considered. As seen in *Table 6-5*, in the first hour of the test day, the proposed CFD_f – CFD – BES takes considerably less time to complete one iteration than the CFDf–BES method (more than 1/70 in general). Moreover, it can be found that the proposed coupling method performed its advantages in faster convergence. At the same time, it only takes three iterations to converge comparing to 8 iterations by the conventional method. Therefore, the total saving in runtime becomes significant as it can be seen that the simulation using the proposed methods takes merely 1/195 of the runtime of CFD_f – CFD - BES.

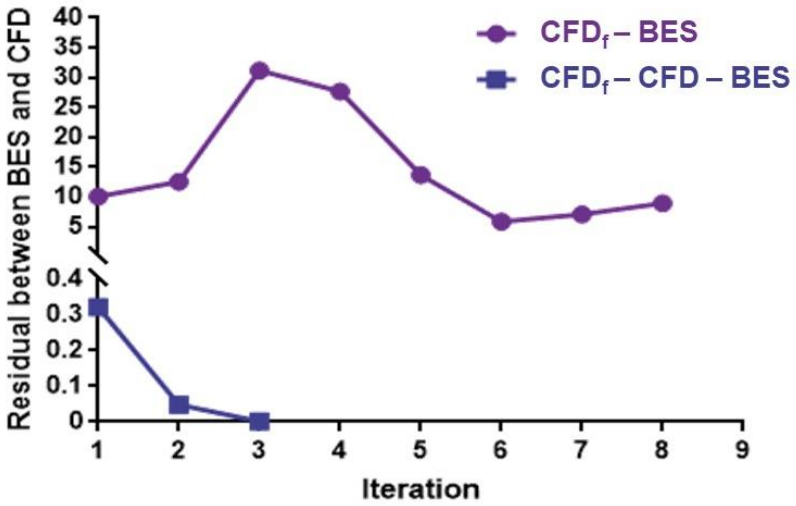

Figure 6-14 Plot of residuals of CHTC for every iterative calculation by CFD_f-BES and CFD_f-CFD-BES methods during the 1st hour of the test day [97]

Figure 6-14 shows the plot of residuals of CHTC by CFD domains between two continuous iterative calculations during the first hour of the day. The residuals achieved by the proposed CFD_f - CFD - BES method and conventional method are 0.0012 and 8.94, respectively. Thus, the proposed method approaches smoothly and stably to its convergence with a lower value. In contrast, the conventional CFD_f – BES method struggles to reach its convergence and fluctuates around a relatively high level of residuals. The challenge in convergence can be attributed to the intense calculation difficulty in processing high-resolution grids with complex environments. Furthermore, the error due to the poor convergence of the CFD_f – BES method may be transmitted and accumulated along with the iterations and cause concerns in the accuracy of the whole coupling method.

Table 6-5 Runtime of every iterative calculation by CFD_f-BES and CFD_f-CFD-BES methods for the 1st hour of the test day [97]

Iteration	CFD_f-BES	CFD_f-CFD-BES
iter-1	12:06:04	00:10:19
iter-2	11:14:34	00:10:26
iter-3	14:07:57	00:11:19
iter-4	11:53:02	Converged
iter-5	11:35:22	/
iter-6	12:55:11	/
iter-7	12:21:23	/
iter-8	12:38:40	/
	Converged	/
Total Runtime	98:52:14	0:32:04

The residuals between the two domains by CFD_f -- BES are fluctuating around 8 in 1st hour, around 16 in 2nd hour, and around 31 in 3rd hour. In contrast, the residuals by CFD_f – CFD - BES can quickly reach the criterion of 0.01.

Convergence between CFD and BES is achieved to a criterion of 0.01. However, sometimes it would be difficult to converge within ten iterations (e.g., 3rd hour of the test day); the criterion would then be extended to maintain the efficiency, as 0.1 in this study. *Figure 6-15* shows the number of iterations taken to get reliable results in each tested time-step.

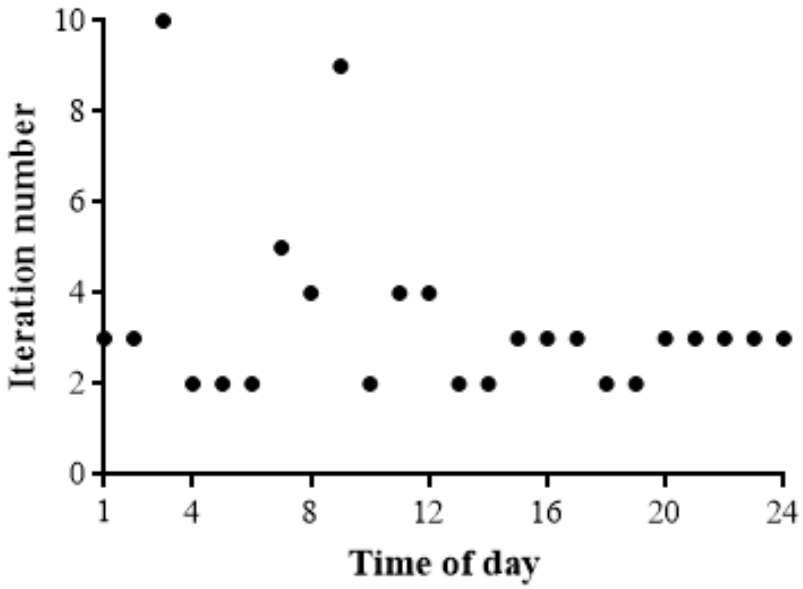

Figure 6-15 Iteration numbers to achieve convergence [97]

6.6. Comparison of stand-alone BES and coupling method

6.6.1. Zonal temperatures

Figure 6-16 shows the difference in zonal temperatures of the building in the center of the community (see B5 in *Figure 6-4*) provided by the proposed coupling and the stand-alone BES methods. The figure displays the results for all purging hours (1 a.m. – 6 a.m. and 7 p.m. – 12 p.m.) and two hours (7 a.m. and 8 a.m.) after the first purging period when the difference in the cooling simulation was still taking effect with the time lag. As for the other working hours, except the first two hours after the purging period, the temperature difference between the results of the two methods was negligible as the zones are under the control of the HVAC system. The positive values indicate that the DOE-2 algorithm (see *Eqn. 7* and *Eqn. 8*) underestimates the zonal temperatures. During the first purging period (1 a.m. – 6 a.m.), the magnitude of the temperature difference is much higher than that in the second purging

period (7 p.m. – 12 p.m.). As looking into the weather data, from 1 a.m. – 6 a.m., the approaching winds are from the north side; however, the approaching winds are from the south side from 7 p.m. – 12 p.m. Thereby, the accuracy of the DOE-2 algorithm is observed to be sensitive to the wind direction.

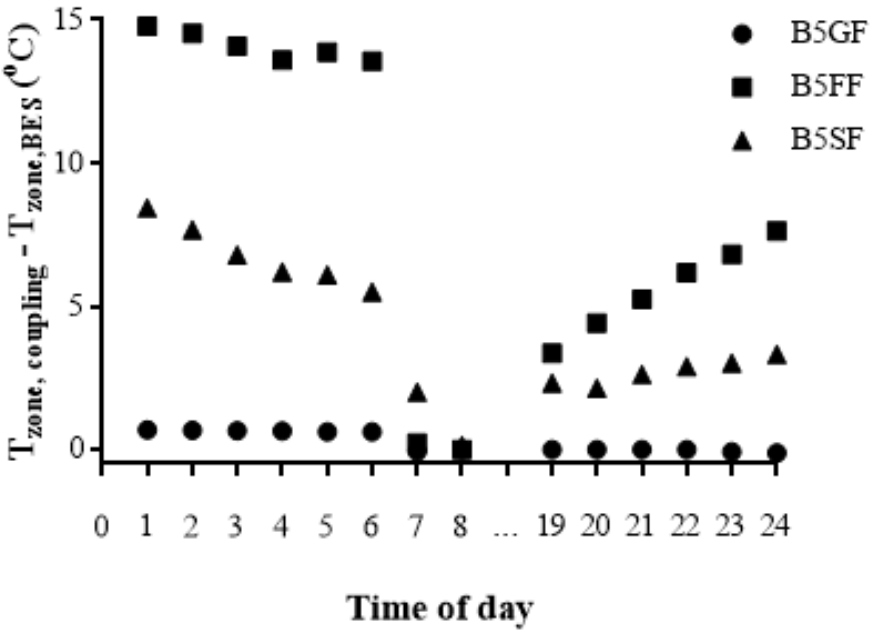

Figure 6-16 Difference of B5's zone temperature computed by the coupling and stand-alone BES methods [97]

From 1 a.m. to 6 a.m. and from 7 p.m. to 12 p.m., the top two floors are naturally ventilated while the ground floor (GF) is almost isolated from the environment. Since the temperature difference on the GF is only dependent on the update of CHTC, it is supposed to be lower than the other two temperature differences, and the simulation results approve that. Moreover, during the purging hours, the temperature difference on the first floor (FF) is found the highest. Even if the height difference is contributing, its influence is small. Thereby, it is taken aside. Taking FF as the benchmark (e.g., from 1 a.m. – 6 a.m.), the values of the second floor (SF) under both ventilation and convection conditions are approximately twice to three times those of FF (as seen from *Figure 6-16*). Significant differences are found between the GF and the top two floors, which means that the ventilation has played a larger heat exchange share than the convection part. The most significant difference between SF and FF is that SF contains the roof surface. This implies that the coupling method to update CHTC on the roof surface has compensated part

of the influence of the inclusion of natural ventilation. Because it has a significant influence on the roof surface temperature. This finding is confirmed by the fact that the most significant deviation occurs at the second floor (SF) at the 7th hour of the day when natural ventilation is deactivated, and the temperature difference on GF and first floor (FF) is minimal, as shown in *Figure 6-16*. It can also be drawn that the BES-only method has overestimated the volume of the natural ventilation.

6.6.2. Neighbourhood effect

EnergyPlus, or other BES tools, considers the effect of wind directions simply by dividing the walls into two categories of windward or leeward (as seen from *Eqn. 5*, *Eqn. 6*, *Eqn. 7*, and *Eqn. 8*). Thus, the difference between building and building is systematically ignored by the embedded CHTC algorithms of the BES tools. Therefore, the advantage of coupling CFD simulations is to improve the airflow modelling significantly and then improve the representation of the surrounding environment. *Figure 6-17* displays the standard deviation of CHTC at the exterior surfaces (categorized by different altitudes) in the neighbourhood environment. The standard deviations obtained by stand-alone BES are found relatively small, that the highest value is approximately 0.05, which means that the negligible neighbourhood effect is considered.

In contrast, the proposed dynamic coupling method has fully reflected the neighbourhood effect, as the apparent higher standard deviation can be explored, especially at the roof surfaces. For example, during the night-purging hours, the standard deviation of the roofs' CHTC by stand-alone BES is approximately 1.9E-04 while it is 2.2E+00 as obtained by the coupling method. However, this value is found in the working hours as 1.4E-05 by stand-alone BES and 4.4E+00 by the coupling method, respectively.

6.6.3. Total cooling load

Figure 6-18 demonstrates the cooling effect of the associated night purging strategy. The comparison is provided between the cases with mechanical ventilation by stand-alone BES and coupling CFD – BES methods and the

cases with night-purge cooling with day-time mechanical ventilation simulated by stand-alone BES and the proposed integrating methods. As can be found from the figure, there is a noticeable cooling load reduction from the cases with mechanical ventilation to those with night-purge cooling with the corresponding method. This approves the advantages of the night-purging strategy in saving cooling energy. The reduction of cooling load by the night-purging is observed to be smaller by the coupling methods than that of the BES-only method. It can be explained that the indoor spaces are under warmer conditions by using the proposed coupling method, though the working hours are simulated without the influence of natural ventilation. The difference of boundary conditions due to the time-lag effect has also been considered within the convection calculations. The total daily cooling loads of the community under night-purging scenarios by stand-alone BES and coupling CFD_f – CFD – BES methods are caudated as 1,466.8 kWh and 2,033.8 kWh, respectively. *Table 6-6* compares the community's total cooling loads of sealed and ventilated scenarios. The night purging strategy saved approximately 66% of the cooling load in the first two hours after closed windows with the BES-only method. Then the effect gradually weakened and became around 12-13% from the fourth hour until the second flushing time. However, there was no apparent change in the night purging strategy in saving cooling load when applying the coupling method. The effectiveness of saving cooling load peaked at the third hour (approximately 24%) and then became stable and maintained within 8%-18% (the variation range was wider than that using the BES-only method as partially contributed by amendment of convections).

In addition, the average standard deviation of the cooling loads of nines buildings is 1.79 by the BES only method compared to 2.01 calculated by the proposed coupling method.

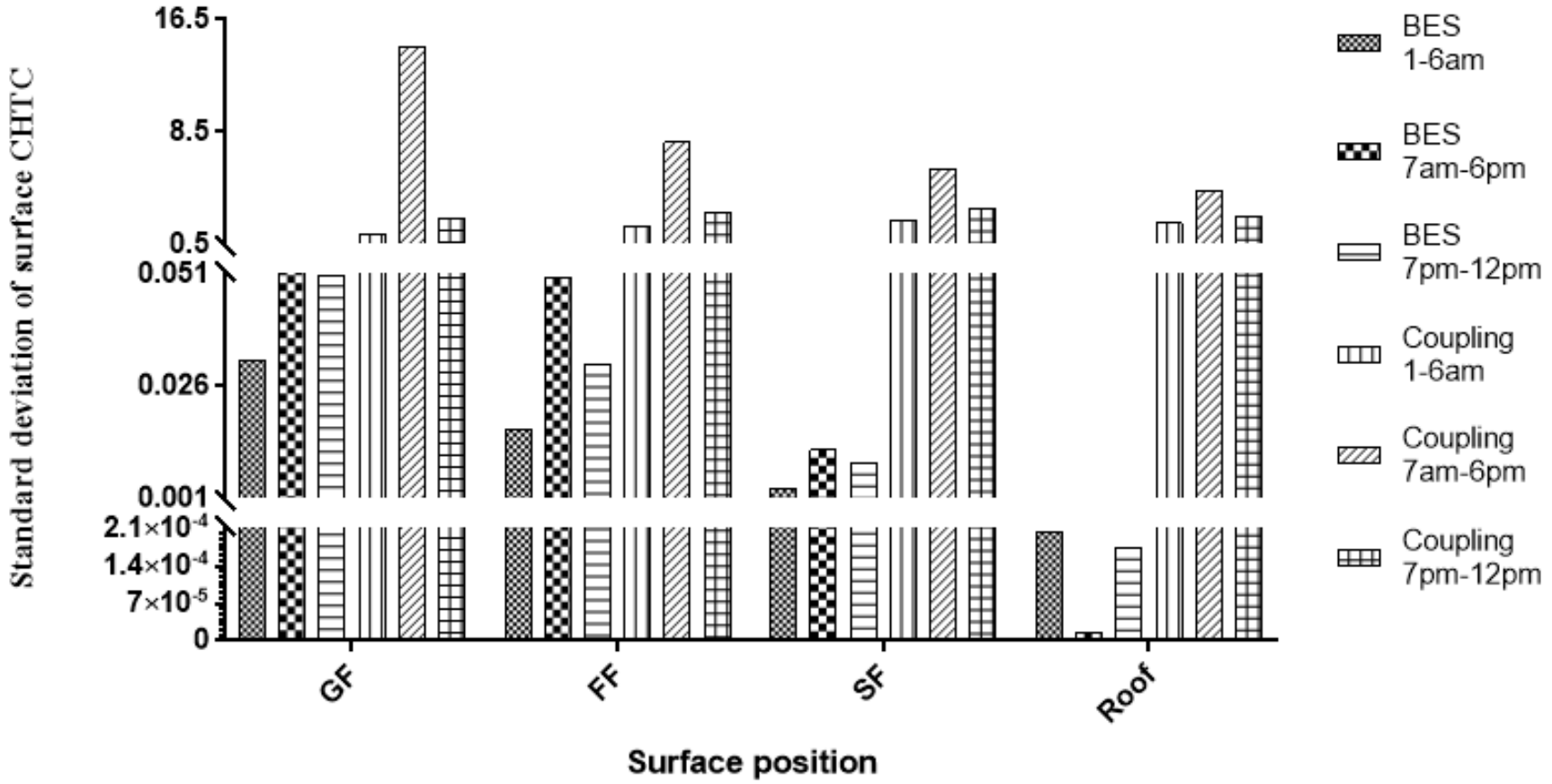

Figure 6-17 Standard deviation of surface CHTC by stand-alone BES and dynamic coupling method [97]

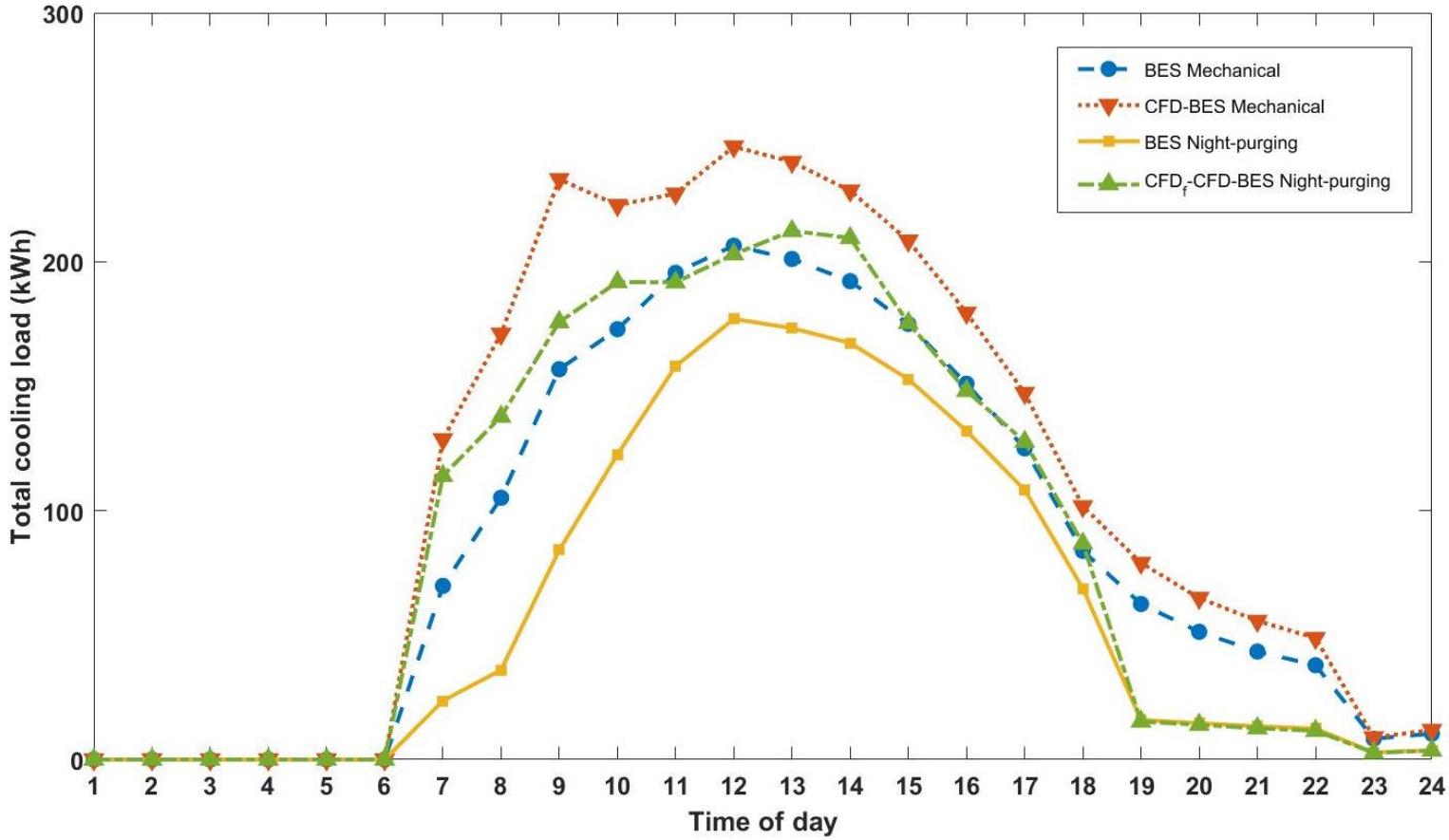

Figure 6-18 Total cooling load of the community throughout the test day [97]

Table 6-6 Hourly total cooling loads of the community calculated by different methods

Time of day	Total cooling load (kWh)			
	Mechanical ventilation		Night-purging ventilation	
	BES	CFD – BES	BES	CFD_f – CFD – BES
1-6	0	0	0	0
7	69.77	128.67	23.61	113.98
8	105.18	171.01	35.99	137.77
9	156.82	233.15	84.16	175.77
10	172.89	222.75	122.53	191.83
11	195.54	227.35	158.01	191.72
12	206.44	246.27	177.04	203.02
13	201.11	240.08	173.30	212.38
14	192.20	228.55	167.37	209.56
15	175.00	208.46	152.81	175.42
16	150.99	179.47	132.07	148.14
17	125.02	147.27	108.32	127.70
18	83.83	101.75	68.77	86.79
19	62.49	78.99	15.90	15.28
20	51.31	64.89	14.59	13.97
21	43.39	55.70	13.36	12.57
22	37.90	48.82	12.43	11.56
23	8.38	8.88	2.82	2.71
24	10.42	11.87	3.70	3.62

6.7. Summary

This chapter provides the approach of fully dynamic coupling for short-term modelling of natural ventilation scenarios. The key findings in this chapter are:

- In general, velocity-velocity is the best option out of four tested interface types for CFD to represent CFD_f. It gives the fastest processing. Its overall RMSE of local flow speed at 58 tested lines is found as 0.411 for scenarios of parallel wind with different wind speeds.

- The advantage of the velocity-velocity option is evident in capturing the flow patterns at the opening surfaces.

- The benefits of coupling CFD_f and CFD are proved with broadly conserved simulation time. For example, the fastest option velocity-velocity took only 1/28 of the time of the CFD_f model for isothermal cases, and 1/195 for non-isothermal cases.

- The coupling method is found to be effective in improving the inclusion of neighbourhood effect in energy modelling and the advantage of night-purge cooling in energy conservation is approved.

Chapter 7. MEDIUM-TERM TO LONG-TERM MODELLING

The microclimate around buildings is sensitive to their surrounding environment, including both weather conditions and urban morphology; The morphology characteristics have reported to significantly impact on the neighbourhoods' microclimate. Limitations in metamodel development in urban area hinders efforts to develop a universal algorithm for all morphological conditions in different cities, which implies on the necessity in development of flexible tools on the basis of each specific urban scenario. When targeting a specific urban scenario, the assessments can be further narrowed down to investigating the impact of local microclimate (including the impact of weather conditions and surrounding buildings' thermal performance).

As a compromise between the fully coupling and existing algorithms, virtual dynamic method is employed to develop datasets or metamodels of local CHTCs from the coupling results in different scenarios.

This chapter aims at developing a novel framework for virtual dynamic coupling of CFD and BES to improve local CHTC predictions from local microclimate using Artificial Neural Network for long-term building energy demand assessments.

General introduction of virtual dynamic coupling is presented in *Section 3.7*.

7.1. Framework for Medium-term to Long-term Modelling

Figure 7-1 illustrates a schematic of the flowchart for the proposed virtual dynamic method. Numbers in the flow chart with white backgrounds are the output or the dataset of a specific operation. Their results would be recalled being used in other processes with exact numbers but with navy backgrounds. The operation connected by dashed lines is optional to be operated in the algorithm.

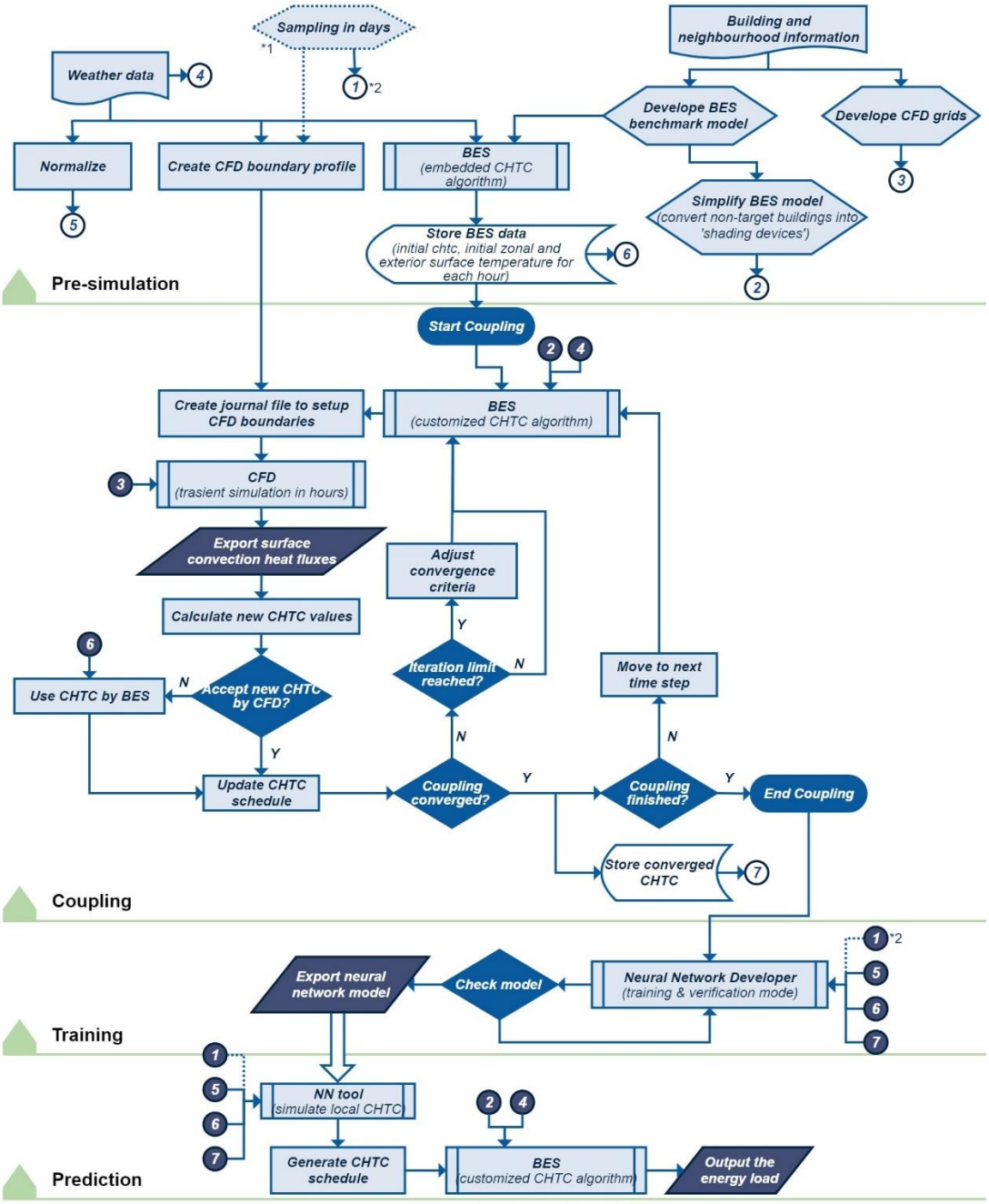

* Note: [1] shape by dashed lines are optional steps; [2] buttons with number are the stored data or results of the steps; those numbers in navy background are referred to those in white background with the corresponding numbers.

Figure 7-1 Schematic of flowchart of the proposed virtual dynamic coupling [89]

7.1.1. Simulation period definition

The whole test period is divided into two parts. The first part is when the coupling process is executed to obtain the training data (denoted as period-1). The second period is the remaining period after period-1, subtracted from the whole period, and it is denoted as period-2. There are two ways to determine period-1. As seen in *Figure 7-1*, there are two ways of specifying period-1. One

draws the training data from days in a regular order starting from the first day of the test period, naming the 'forward' method. The other uses sampling technique which selects days randomly out of the test period, naming the 'sampling' method. The data size depends on the size of the time-step during the coupling. In this study, the coupling was processed on an hourly basis. Thereby, every test day consisted of 24 groups of data.

7.1.2. Pre-simulation stage

Preparation of data is taken place at the preliminary stage. It includes the actions of creating the computational models for the BES and CFD domains, obtaining the initial guesses to start up the coupling, developing the boundary profile for CFD domain, and transforming parameters (e.g., normalizing the weather data to be used for the ANN training tool). As the proposed virtual coupling method is aimed for medium-/long-term simulations, simplifying the CFD model is necessary to moderate the complexity of the neighbourhood; thereby, the computational load can be controlled. Therefore, it is recommended to decide the target buildings first to focus on them rather than modelling the whole neighbourhood with all details. After distinguishing the target buildings from their surroundings, simplifications are then conducted through two aspects: simplifying the neighbourhood's geometries and identification of the coupling interfaces.

CFD and BES models are developed in accordance with the designs of buildings and neighbourhood, so that their geometries match each other. Therefore, the geometries of the investigated area would impact the flow field in the CFD domain. In contrast, its primary impact on the BES domain is reflected in the radiation algorithms (shadowing effect of surroundings).

In this stage, the convection on exterior surfaces is modelled using embedded algorithms in BES. The coupling interface between BES and CFD domains is placed merely at the exterior surfaces of the target buildings. As the initial guess to start the coupling process, the results on these interfaces are recorded. The CHTCs of surrounding buildings are not updated during the iterative process after the preliminary stage. However, they are still required to

be assigned as the boundary conditions into the CFD domain. Therefore, after obtaining the CHTC profiles of surrounding buildings for the entire test period, the surrounding buildings in BES are then converted into 'shading devices.' Besides the fixed profiles of surrounding buildings' CHTC and the initial guess of profiles of the target buildings' CHTC, zonal temperatures of all buildings are recorded at this stage to be used for the training of the Artificial Neural Network (ANN) tool in the later stage.

In this study, the normalization is executed to compute Z-score values for parameters of weather conditions, see *Eqn. 33*.

7.1.3. Coupling

A fully dynamic strategy is adopted for the coupling stage, which guarantees the convergence for iterative calculations related to each time step. As it has been discussed, only the target buildings' CHTCs would be processed and updated through iterative calculations. Unlike using embedded CHTC algorithms at the preliminary stage, the CHTCs of the target buildings are replaced with the values converted from the CFD results by applying *Eqn. 14*. The CFD results are then evaluated and filtered before being accepted by the BES side. Therefore, the convergence is determined by the average convective flux (q_c'') gap between two domains or the deviation between two iterations' variables within one domain (usually using T_s or q_c'' for BES whilst h^* or q_c'' for CFD). Thus, the criterion can be relatively loosened at a controlled pace for those time-steps when the iterative process encounters difficulties in the convergence. In addition, restriction of iteration numbers is required to avoid the algorithm being trapped in an infinite loop and to results in slow convergences or high-level fluctuations. The converged h^* of each time-step would then be recorded for later use in developing the ANN tool. The coupling loop ends after the simulation finishes for all period-1. The final data obtained from the coupling process together with the environmental information is forwarded to train the neural network tool. The details of the ANN tool are demonstrated in the following section.

7.1.4. Training

This study applied the feed-forward back propagate (BP) method to train the neural network to identify the non-linear relationship between the surrounding environment and the newly calculated surface convective heat transfer characteristic (h^*). There are multiple ANN tools to be developed for each surface of the target buildings. This means that $s+1$ ANN tools must be trained for the case with a single target building composed of s stories with regular features as the roof of the target building is considered at a different altitude from the other envelope surfaces.

In general, the input of the artificial neural network consists of:

1) the normalized meteorological parameters (including solar radiation, wind speed, and direction) in the format of Z-scores (see *Eqn. 33*),

2) the zone temperature of spaces in surrounding buildings, and

3) the difference between the target building's initial exterior-surface temperature and the ambient air temperature. The exterior surface temperature is estimated by BES' embedded algorithm, DOE-2. At the same time, the ambient air temperature is obtained at the same altitude as the centroids of surfaces calculated through *Eqn. 16*.

Figure 7-2 indicates the connections between the input and the output (h^*, targeting the values obtained from the coupling approach) inside the network. The arguments of the transfer function $f_{i,n}()$ within a neuro are computed by adding a bias $b_{i,n}$ to the sum of the weighted inputs to give the corresponding outputs ($a_{i,n}$), where the subscript i specifies the layer, and n specifies the neuron/element. In the feed-forward system, the inputs of the whole model consist of multiple parameters ($p_{l,k}$) and the weights between them.

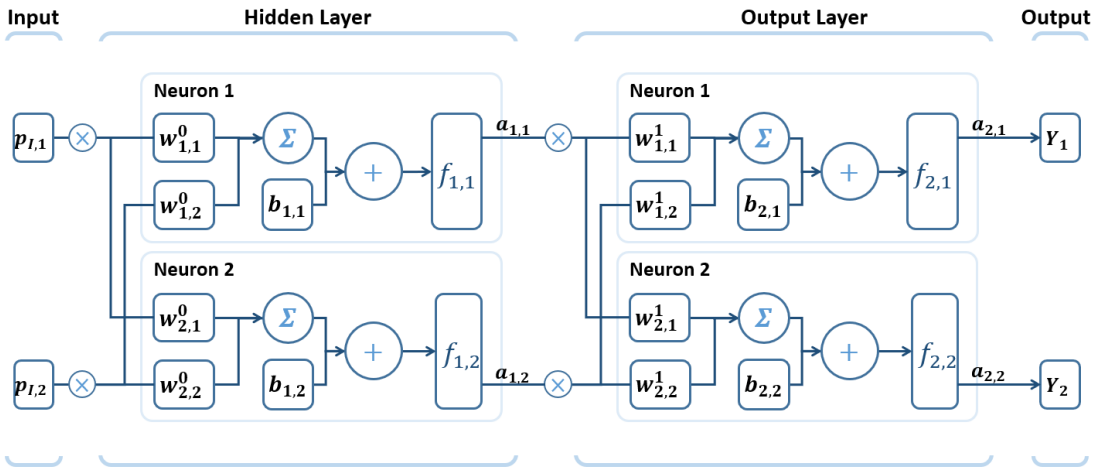

Figure 7-2 Structure of the neural network [89]

The first hidden layer is called input weights, while the inputs of other layers are referred to as the outputs from their previous layers a_{i-1}, which is weighted using the layer weights (denoted as $w_{d,sr}^{i}$), where the subscripts i specifies the source layer, d and sr indicate the destination and source element/neuron, respectively, that the corresponding weight is used to connect them. The number of neurons in the output layer depends on the number of output elements. This study created ten neurons in the hidden layer (a shallow neural network, which contains only one hidden layer). Therefore, the outputs of the tool Y_i in *Figure 7-2* can be evaluated through the following equation:

$$Y_i = f_{2,i}\left(\sum_j w_{i,j}^1 a_{1,j} + b_{2,i}\right) = f_{2,i}\left(\sum_j w_{i,j}^1 f_{1,j}\left(\sum_k w_{j,k}^0 p_{I,k} + b_{1,j}\right) + b_{2,i}\right) \quad \text{Eqn. 41)}$$

where i, j and k specifies the neuron/element.

As long as the feed-forward BP method is utilized, the inputs are processed in a forward path from the input layer through the hidden layer to reach the output layer. At the same time, the gradients of adjustments to the weights and biases of the layers are iterated. The propagation of this iterating process starts from the output layer and moves backward. The Levenberg-Marquardt algorithm is adopted as the training function in this study so that the minimum value of the performance judgment criterion is achieved for the tool's training stage. The

performance here is judged through the mean square error (MSE), see *Eqn. 38*. Hereon, o is the observation (drawn at the coupling stage) and the corresponding predictions by the developed ANN model Y is substituted as p. n presents the number of samples.

Moreover, the developed ANN model is checked through the adjusted determination coefficient (R^2, see *Eqn. 39*) and the fraction of predictions within a factor of two of observations ($FAC2$, see *Eqn. 37*) to confirm the quality of the developed ANN tool. Both R^2 and $FAC2$ are within the rage of 0 - 1 while a larger value for them can be assumed as a better fitting to the target values. A $FAC2$ of over 0.5 is claimed as a threshold of a good enough model [94].

7.1.5. Prediction

The developed ANN tools are employed at this step to predict the CHTC profiles for the exterior surfaces. The profiles are then substituted into BES's calculation of outdoor convective heat transfer and, therefore, to improve the energy demand assessment of BES for medium-/long-term simulations. The metric used to compare the performance of the tools is the relative discrepancy (e_r, see *Eqn. 34*) between the predictions and observations of the tool. The ANN results are applied to EnergyPlus through the schedules using bespoke code similar to that showing in *Appendix 5*.

7.2. Description of the Case Study

7.2.1. Case specification

The central building, B5, was selected as the target building in this study. Therefore, only B5 was modelled in detail, so it was divided into three zones according to its three stories. The centroids of the walls were placed at 1.70 m, 5.05 m, and 8.35 m above the ground for the ground floor, first floor, and second floor, respectively. Thereby, four tools (for each floor's walls and roof surfaces) were required to be trained and tested for this specific case study associated with the vertical surfaces on each floor and the roof. The

surrounding buildings were then simplified by merging all zones in each building into a single zone, as displayed in *Figure 7-3*.

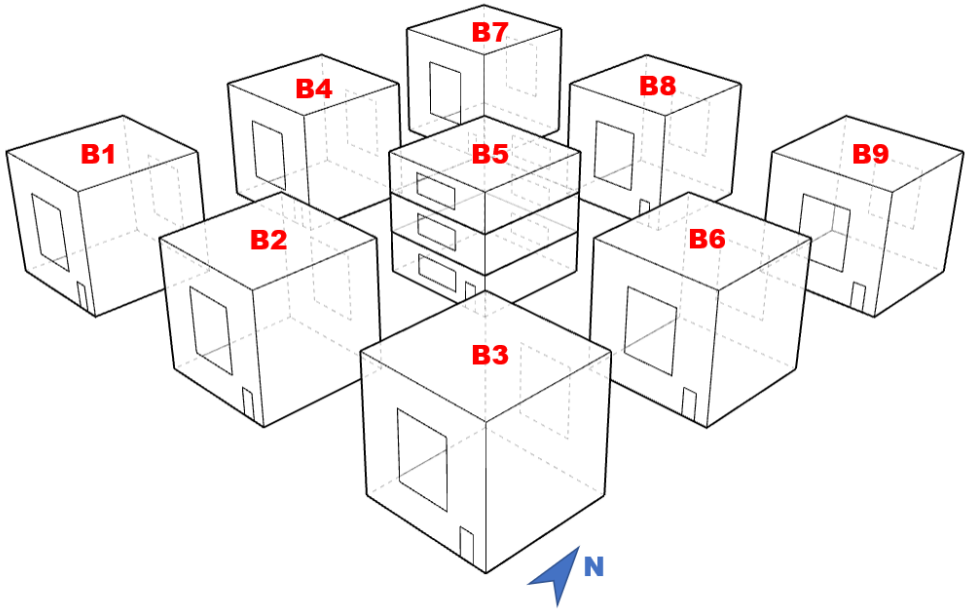

Figure 7-3 Simplified model for the medium-term – long-term virtual dynamic coupling

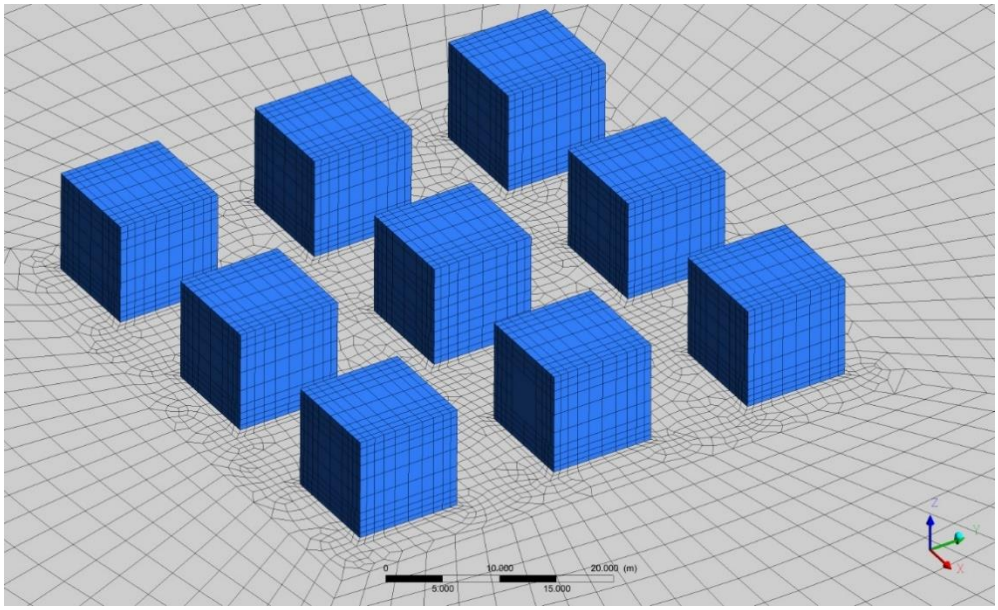

Figure 7-4 Final CFD model for medium-term to long-term simulations

The case study site was selected to be in Los Angeles, U.S., and the simulations were performed for a test period of one month (September in which the local hottest day occurs) regarded as the representative of a hot period. *Figure 7-5* shows the local hourly weather data in September, including ambient air temperature, wind speed and wind angle.

According to *Section 7.1.4*, $s+1$ tools should be developed. The target building B5 has three stories. Therefore, there were four ANN tools denoted as tool-a (for the vertical surfaces on the ground floor), tool-b (for the first floor), tool-c (for the second floor), and tool-d (for the roof surface) trained for the CHTC predictions of surfaces at the ground floor, first floor, second floor, and the roof, respectively.

7.2.2. Options of combination of period-1 and period-2

With the selected test period of 30 days, it was initially investigated to explore an adequate number of days for the coupling method to generate the required results for developing an accurate tool (period-1). For this purpose, the performance of the developed ANN tools should become independent when the number of used days increases. In other words, the study began with few days being modelled for the training of the ANN tools and the rest of the days being predicted using that tool. Here, '1+29' denotes that one day is used for the training, and then 29 days are predicted by the developed tools. Then, the process was following a sensitivity test about the length of period-1. So, seven combinations of period-1 and corresponding period-2 were investigated, including '1+29', '3+27', '5+25', '7+23', '10+20', '12+18', and '15+15'. Finally, all the tools were investigated by comparing their accuracy in the prediction of h^*.

7.3. Performance of Developed Tools for Different Surface Types

Four ANN tools (tool-a, tool-b, tool-c, and tool-d) were developed from the coupling results of the first 15 days of the simulated month (period-1 = 15). The performance of these tools is analysed to investigate their accuracy in this section.

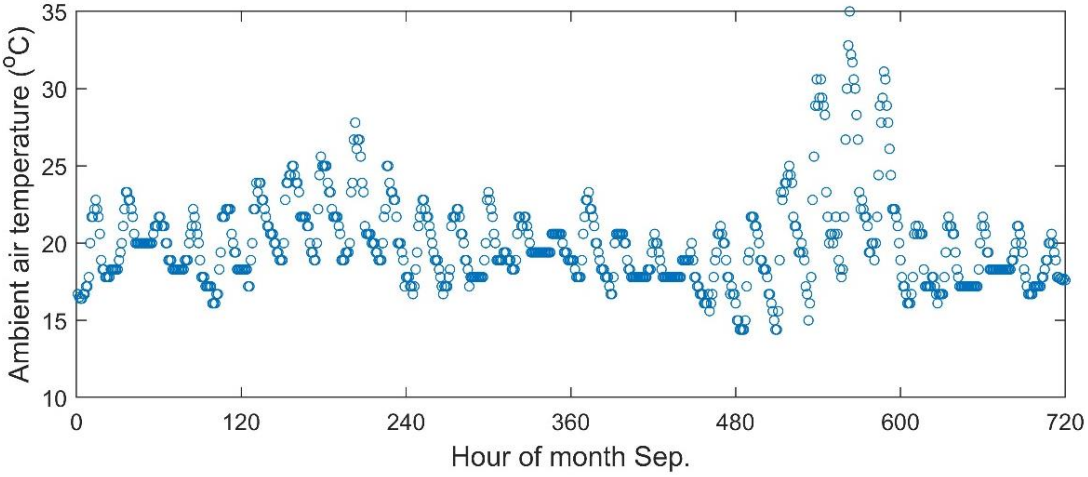

(a)

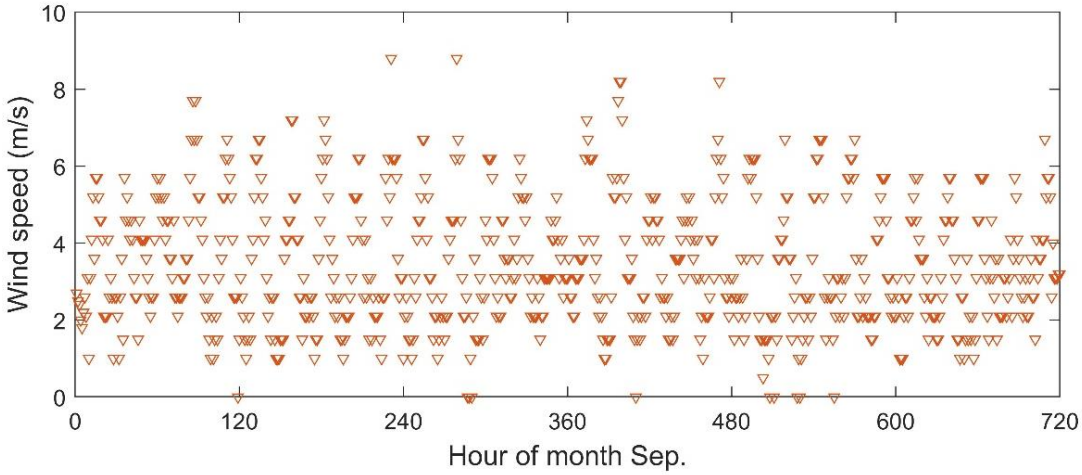

(b)

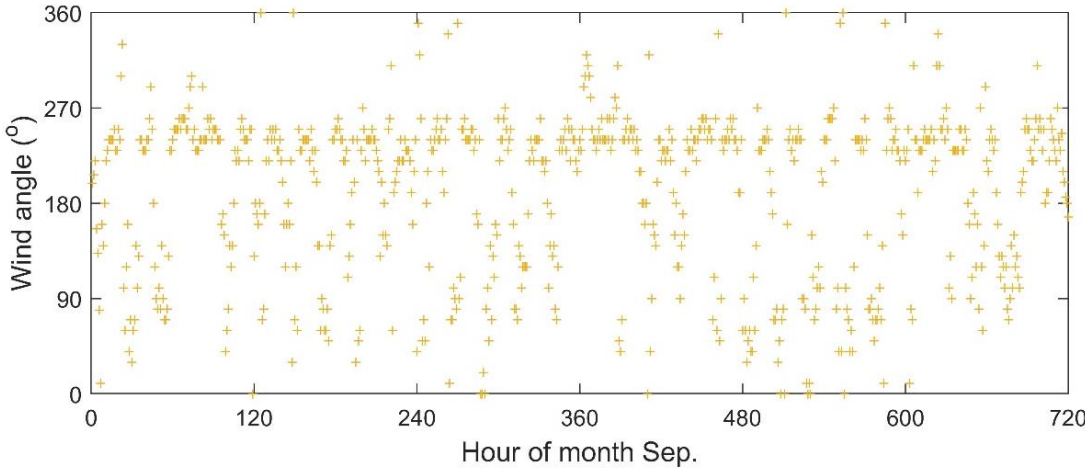

(c)

Figure 7-5 Hourly weather data, including a) air temperature, b) wind speed and c) wind angle) in September of Los Angeles [89]

There were two sets of input parameters for the neural network being tested as considering the potential factors, which may impact the local CHTCs. Both sets contained the meteorological information (including wind speed, wind direction, diffuse and direct solar radiations) and the temperature difference between the envelope surfaces and corresponding local ambient air ($T_{a,z}$ calculated from *Eqn. 16*). The difference between the two sets reveals that the inclusion of the zonal temperature of the surrounding buildings has a minimal impact on the results. The tools developed from these two sets are denoted as from method of 'inc. T_{zone}' and 'exc. T_{zone} '.

7.3.1. Performance of ANN tool-d for roof surfaces

It is found that, unlike the tools-a, b, and c (developed for the vertical surfaces), the tool-d (developed for the horizontal roof surface) encounters a struggle to learn the relationship between the inputs and outputs. The outputs of the trained tool-d fail to match the corresponding targets due to some extreme outliers in the target data. As displayed in *Figure 7-6*, a significant bias of output data is observed when the target h^* exceeds 50 (where a red threshold line is placed). At the same time, other output points against targets less than 50 gather around the diagonal line where output equals the target value. Based on this finding, the training data of tool-d are then filtered to exclude the outliers over 50, and the outputs of the new tool-d are then plotted in *Figure 7-7* against the targets. As it can be seen, the performance of the tool-d is improved significantly after excluding outliers as the gradient of the target-output fit line is increased to 0.729 from 0.096 (a unity gradient hints a good matching of outputs with the target data). Although the performance of tool-d is still not as good as tools a-c, whose fit line gradients can reach over 0.9, the training process is considered a successful one. A significant part of the discrepancy of tool-d may be explained by the weakness of the standard k - ε model in the representation of the flow separation near the roof surface. In other words, the limitations of CFD may introduce some irregular and case-sensitive noises into the coupling results, which makes it difficult for the ANN tool-d to learn these target data. However, even with this drawback, the k - ε model is still a

competitive choice considering its considerably lower computational cost and good performance.

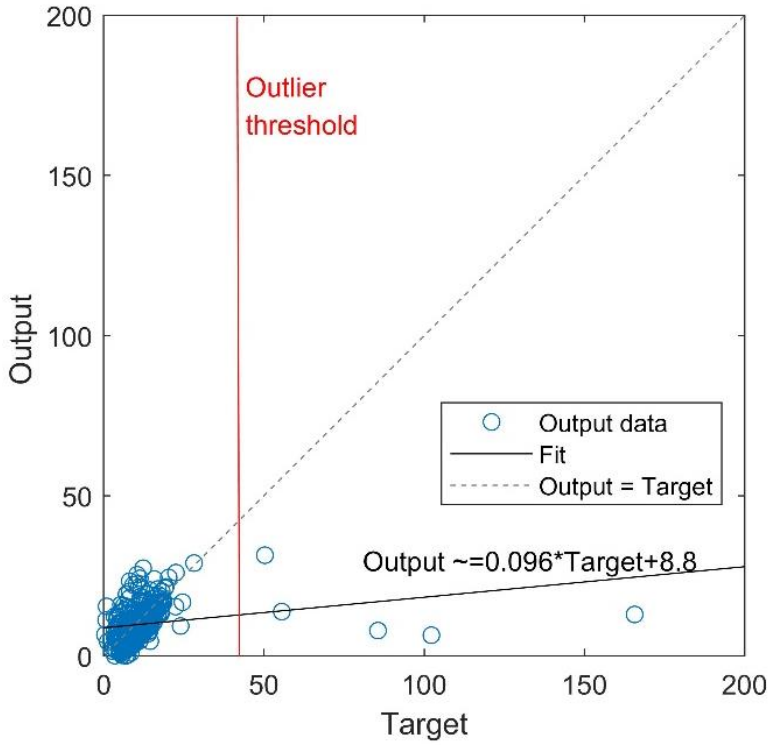

Figure 7-6 Comparisons between the target and the output of ANN tool-d (for the roof surface) developed from none-filtered target for roof surface during the training stage [89]

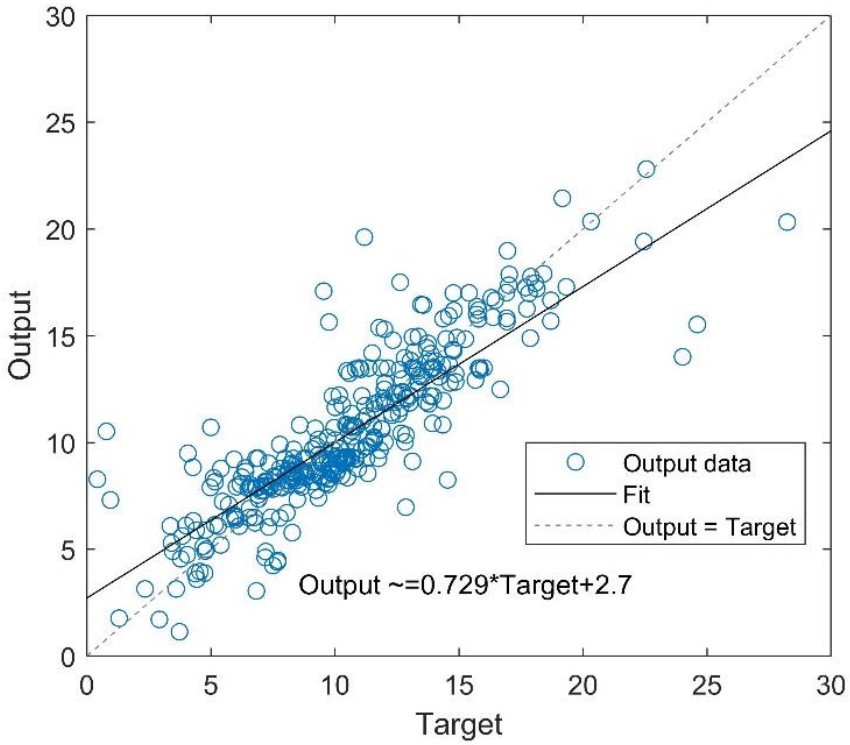

Figure 7-7 Comparisons between the target and the output of ANN tool-d (for the roof surface) developed from filtered target for roof surface during the training stage [89]

Table 7-1 Performance information of the developed ANN tools for different surfaces [89]

Position	e_r for the prediction stage as well as other metrics for the training stage							
	Surface orientation			South	East	North	West	Average
Ground floor	Prediction[1]	Tool-a	inc. T_{zone}	0.1220	0.1120	0.2505	0.1442	0.1572
			exc. T_{zone}	0.1244	0.1173	0.2153	0.1452	0.1505
		BES-only		0.4881	0.3801	0.3589	0.4757	0.4257
	Training[2]	inc. T_{zone}: R^2 = 0.9905, $FAC2$ = 0.9979, *MSE* = 0.5162 exc. T_{zone}: R^2 = 0.9900, $FAC2$ = 0.9993, *MSE* = 0.5420						
1st floor	Prediction	Tool-b	inc. T_{zone}	0.0813	0.0738	0.1255	0.0960	0.0941
			exc. T_{zone}	0.0710	0.0867	0.1165	0.1112	0.0963
		BES-only		0.4827	0.3698	0.3095	0.4444	0.4016
	Training	inc. T_{zone}: R^2 = 0.9938, $FAC2$ =1.0000, *MSE* = 0.5192 exc. T_{zone}: R^2 = 0.9955, $FAC2$ = 1.0000, *MSE* = 0.3841						
2nd floor	Prediction	Tool-c	inc. T_{zone}	0.0995	0.0710	0.1141	0.1205	0.1013
			exc. T_{zone}	0.1282	0.0867	0.1295	0.1341	0.1196
		BES-only		0.4914	0.3239	0.2908	0.4270	0.3833
	Training	inc. T_{zone}: R^2 = 0.9941, $FAC2$ =0.9993, *MSE* = 0.6489 exc. T_{zone}: R^2 = 0.9943, $FAC2$ = 1.0000, *MSE* = 0.6160						

Roof	Prediction	Tool-d	inc. T_{zone}	0.4200
			exc. T_{zone}	0.3734
		BES-only		0.4705
	Training	inc. T_{zone}: R^2 = 0.9944, $FAC2$ =1.0000, *MSE* = 0.6298 exc. T_{zone}: R^2 = 0.9462, $FAC2$ = 0.9444, *MSE* = 6.7398		

*Note: [1] the prediction is executed for period-2; [2] the training of tool uses the coupling data in period-1

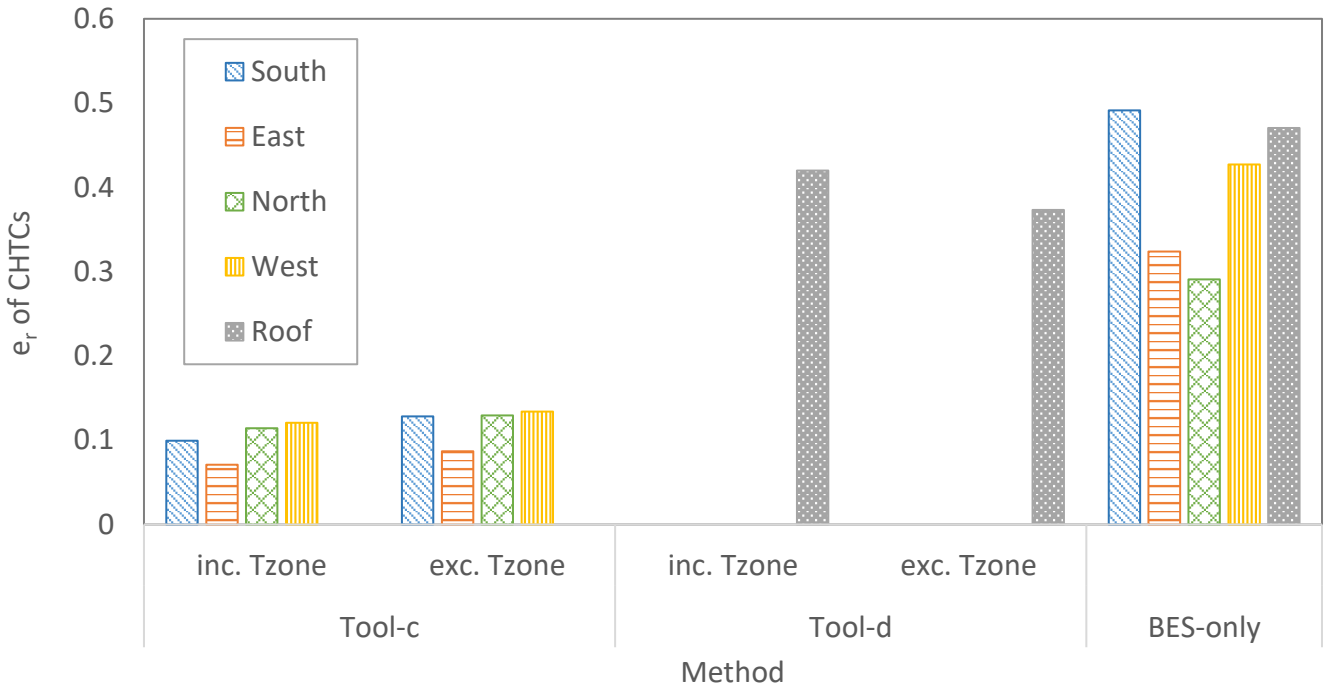

Figure 7-8 Relative discrepancy e_r of different methods' prediction compared to the fully dynamic coupling results of the local CHTCs over different surfaces [89]

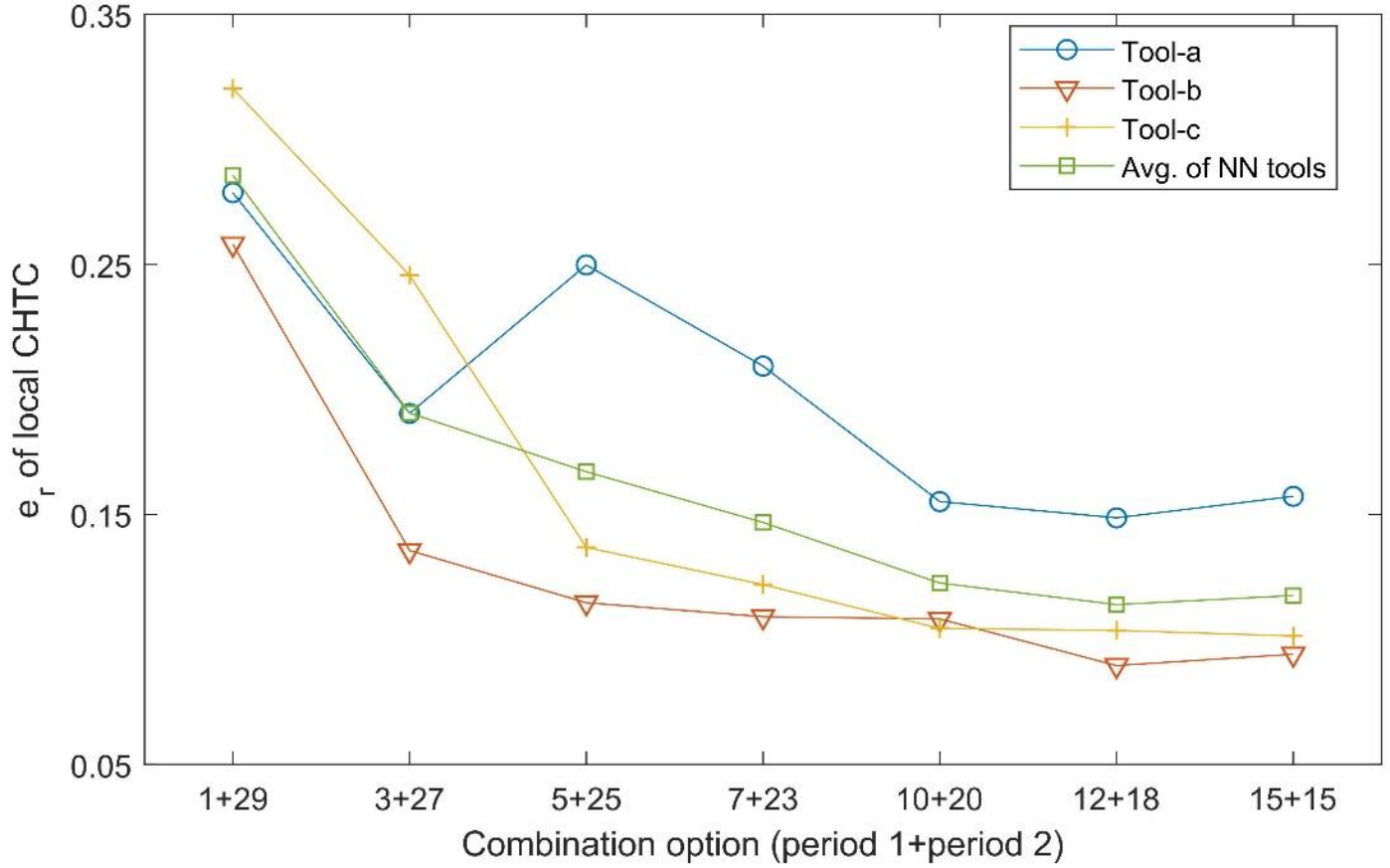

Figure 7-9 Relative discrepancy e_r of the predictions by ANN tools a-c using forward method for different combination options of period 1 + period 2 [89]

7.3.2. Performance of different tools

Table 7-1 demonstrates the relative discrepancy between the predicted local h during period-2 by the developed ANN tools and the results drawn from the DOE-2 algorithm within the BES package, hereon EnergyPlus. The values of R^2 are maintained over 0.99 except for the ANN tool-d developed from 'exc. T_{zone}'. The performance of the training process can be considered as good in terms of $FAC2$, being not less than 0.94.

In general, the predictions by tools developed from 'inc. T_{zone}' are observed to include a slight discrepancy in er in comparison to those from 'exc. T_{zone}'. The discrepancies at the vertical walls are less than 0.03, while for the roof surface, the discrepancy increases to approximately 0.05, which is still a very low number. The minor discrepancies mean that the impact of the surrounding buildings' thermal performance has a negligible impact on the local convective heat coefficients h^* of the target building in this case study. Considering the fact that the coupled model performs better than BES tools in predictions of the local CHTCs, utilization of the ANN tool would be preferable as it provides a significantly better match with the coupling results than BES-only tools at the vertical walls. The average reduction in e_r by using the tools a-c instead of the embedded BES algorithm is approximately 0.28. *Figure 7-8* shows an example plot of the developed tool-c's and tool-d's performance compared to the BES-only method. In general, the accuracies of tools a-c are satisfactory. However, there exist concerns for applying the proposed ANN tool-d on the roof surfaces. Thus, the rest of the result analysis is focused only on the vertical surfaces.

7.4. Effective Size of Period-1

The developed ANN tools are expected to predict medium-/long-term simulation. Therefore, finding the training data's adequate size (naming effective size of period-1) from the whole simulation period is essential. The judgment of 'effective size' is based on the prediction performance of the developed ANN tools to be whether further improved by adding the length of period-1 or not.

7.4.1. Forward method

The results in this section were obtained using the training set drawn by the forward method.

Table 7-2 e_r of local CHTC between the coupling results and the predictions by developed ANN tool and BES-only (embedded algorithm) for different combination options of period 1 and period 2 [89]

Position	Method	Combination option of test period (period 1+ period 2)						
		1+29	3+27	5+25	7+23	10+20	12+18	15+15
Ground floor	ANN tool a	0.2786	0.1904	0.2497	0.2093	0.1551	0.1486	0.1572
	BES only	0.4285	0.4284	0.4273	0.4250	0.4250	0.4242	0.4257
1st floor	ANN tool b	0.2581	0.1355	0.1147	0.1091	0.1081	0.0895	0.0941
	BES only	0.4044	0.4039	0.4041	0.4037	0.4037	0.4021	0.4016
2nd floor	ANN tool c	0.3203	0.2456	0.1367	0.1219	0.1044	0.1036	0.1013
	BES only	0.3863	0.3865	0.3865	0.3855	0.3848	0.3835	0.3833
Average	ANN tools	0.2857	0.1905	0.1670	0.1468	0.1225	0.1139	0.1175
	BES only	0.4064	0.4063	0.4060	0.4047	0.4045	0.4033	0.4035

Table 7-2 provides the change in relative discrepancy (e_r by the ANN tool and BES algorithm against the coupling results during period-2) with an incremental increase in period-1. The relative discrepancy between BES-only and the coupling results remains unchanged along with all combination options where the difference is less than 0.001. BES's embedded algorithm can understand this and ignore some factors, which could continuously impact the local CHTCs (e.g., the site's morphology). Evident reductions in e_r are observed until the length of period-1 reaches ten days. When period-1 exceeds ten days, the improvement in the prediction performance starts to be very marginal while the pace becomes less than 0.01. *Figure 7-9* displays the tendencies of different tools' performance improvement and different combination options of period-1 and period-2. Therefore, ten days is

considered the effective size for period-1 to properly train the ANN tools for a total of one month simulation for the investigated case study in this paper.

7.4.2. Sampling method

The results presented in this section were obtained using the training set drawn by sampling method. The sampling procedure in this study was based on Latin Hypercube Sampling (LHS) method, which is known as a stratified sampling technique [99]. The LHS selects the required n sample points by dividing the population evenly into n parts and then randomly picking one sample from each part to form the final sample group. As discussed in *Section 7.1.4*, the sampling process in this study was executed concerning test days. *Table 7-3* displays the selected sample groups according to different combination options.

Table 7-3 Selected samples for corresponding combination option

Combination option (period 1+ period 2)	**Selected sample group (day of month)**
1+29	20^{th}
3+27	3^{rd}, 14^{th} and 26^{th}
5+25	6^{th}, 11^{th}, 17^{th}, 22^{nd}, 29^{th}
7+23	1^{st}, 6^{th}, 9^{th}, 15^{th}, 19^{th}, 22^{nd}, 28^{th}
10+20	1^{st}, 4^{th}, 8^{th}, 11^{th}, 14^{th}, 16^{th}, 20^{th}, 24^{th}, 25^{th}, 27^{th}
12+18	3^{rd}, 5^{th}, 7^{th}, 9^{th}, 12^{th}, 13^{th}, 17^{th}, 19^{th}, 21^{st}, 22^{nd}, 25^{th}, 28^{th}
15+15	1^{st}, 3^{rd}, 5^{th}, 7^{th}, 9^{th}, 11^{th}, 13^{th}, 14^{th}, 16^{th}, 19^{th}, 22^{nd}, 23^{rd}, 24^{th}, 27^{th}, 28^{th}

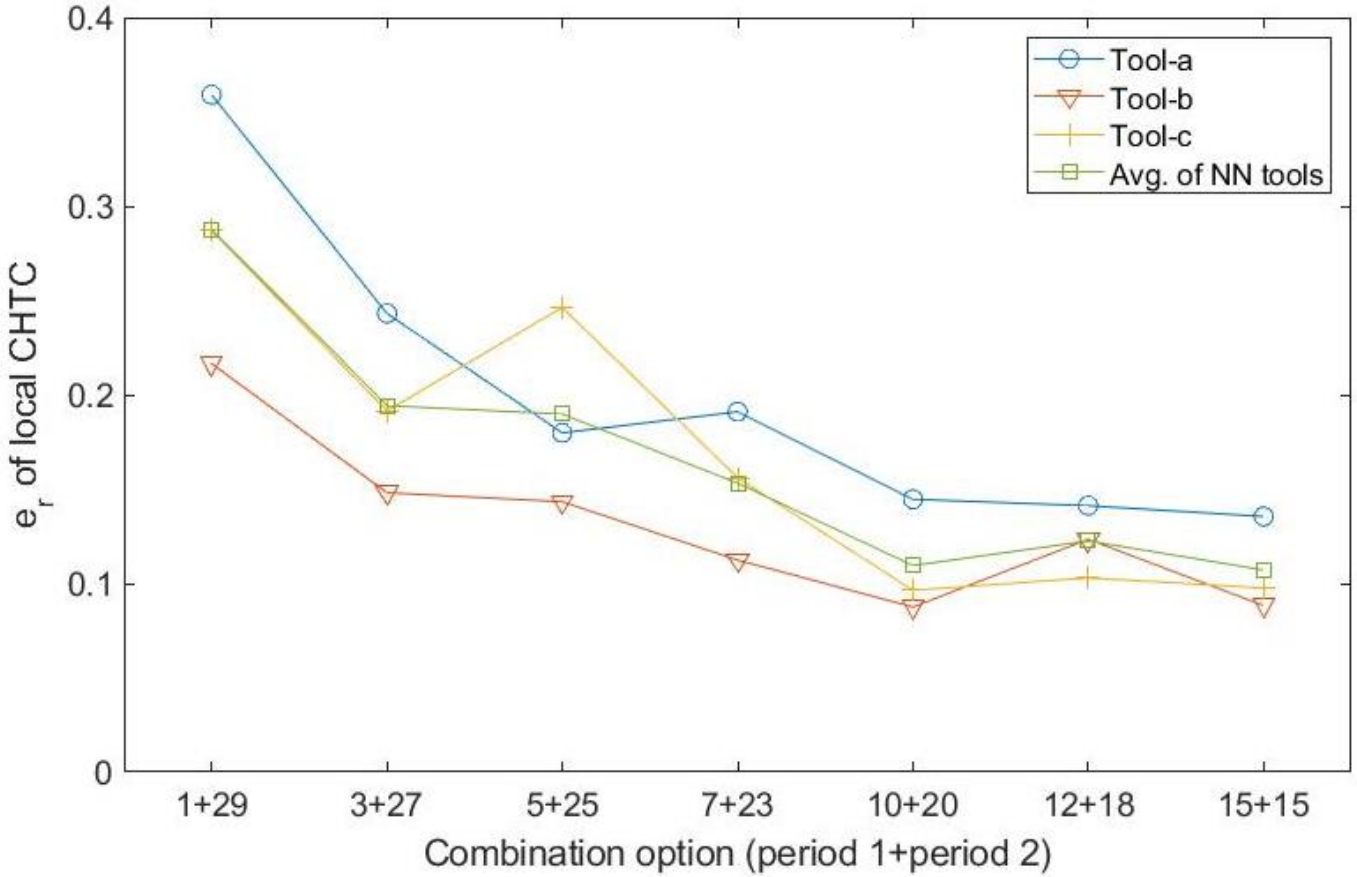

Figure 7-10 Relative discrepancy e_r of the predictions by ANN tools a-c using sampling method for different combination options of period 1 + period 2

Figure 7-10 shows the tendencies of performance improvement of different tools developed from the training set drawn by the sampling method. The improvement change becomes stable since the combination option of 10+20, which implies that ten days is the effective size. This finding reaches a consensus with that by the forward method in *Section 7.4.1*.

In statistics, the size of the sample (n_s) to properly reflect the population can be determined by the following equation:

$$n_s = \frac{n_p {z_c}^2 p_s(1-p_s)}{{\alpha_m}^2\left(n_p - 1\right) + {z_c}^2 p_s(1-p_s)} \qquad \text{Eqn. 42)}$$

where n_p is the population size, z_c is the critical value at a given confidence level (95 % as a common choice), which gives corresponding z_c = 1.96. p_s is the sample proportion typically taken as 0.5 to ensure the sample's representativeness. α_m is the margin error (assumed to be 0.05). Following such rule and considering the whole test period contains 720 hours) as the population, the sufficient sample size can be considered the required effective size of period-1 to train the ANN tool. Therefore, substituting the values into *Eqn. 42* gives a sample size of 251 hours (≈ 10.4 days), which is close to the obtained effective size of ten days.

7.5. Impact of Wind Direction and Wind Speed

As discovered in *Section 7.3.2*, the developed ANN tools perform differently at walls facing different directions. The most considerable reductions in the relative discrepancy of the local CHTCs compared to the coupling results are found at South and East walls. *Figure 7-11* shows how the performance of the ANN tools for different walls' predictions is improving with increasing period-1. As seen from this figure, predicting South walls' CHTC is poor when only one-day data is used for the training of the ANN tools. However, the relative discrepancy decreases sharply when period-1 gets expanded. At the same time, as an inverse observation, North walls improve along with the increase of days in period-1 least evidently.

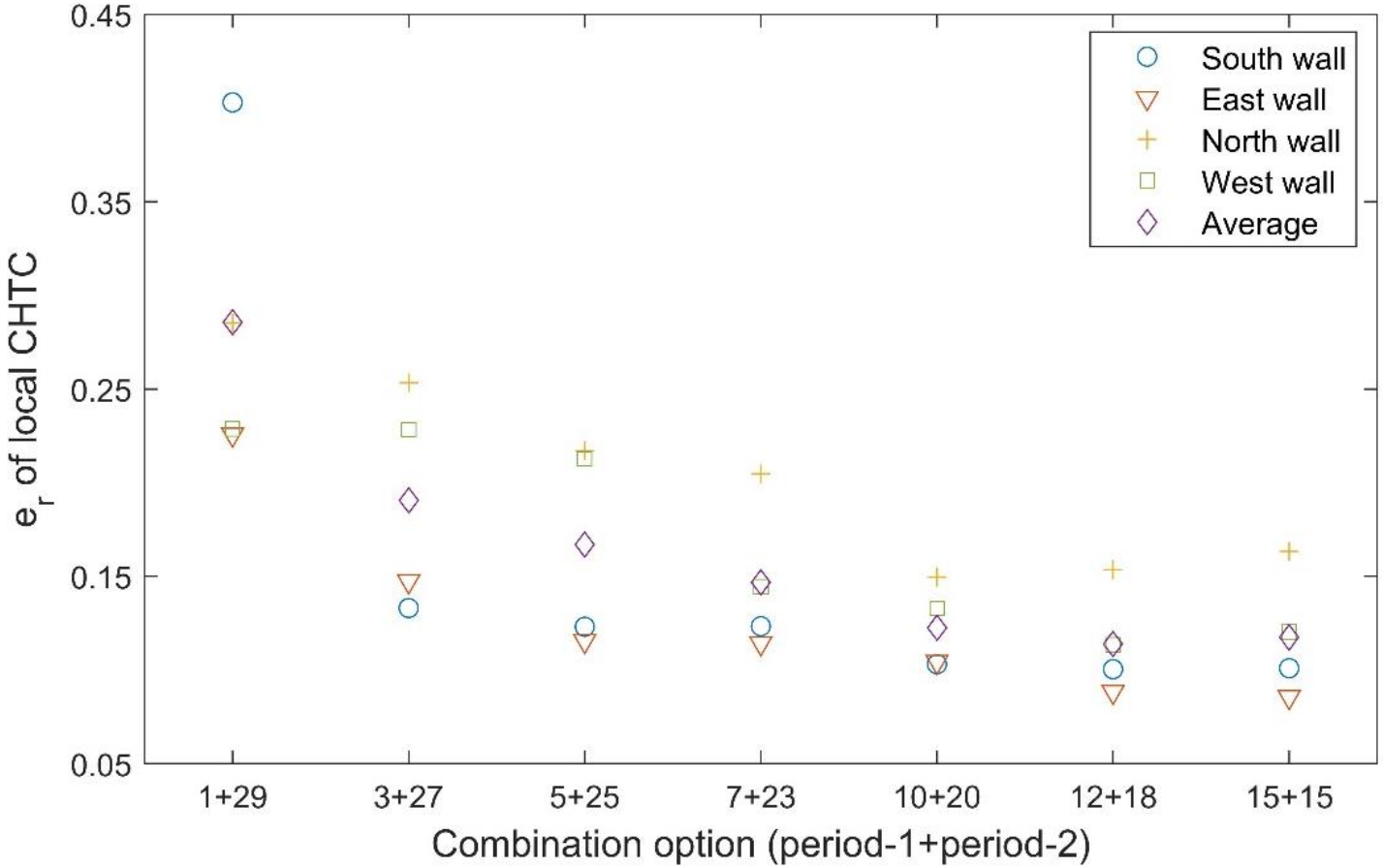

Figure 7-11 Relative discrepancy e_r of the predicted local CHTCs at walls, facing different directions for different combination options (period-1+ period-2) [89]

An analysis is provided to explore the impact of potential climatic factors (wind direction and related wind speed), as seen in *Figure 7-12*. The wind angles are categorised into four directions (South, East, West, and North), and every direction is divided into nine strips with an interval of 10 °. *Figure 7-12* demonstrates the frequencies of wind angles during the selected test period and the range and average values of wind speed at the corresponding hours. As discovered in *Figure 7-12*, though the frequency of winds from the West is much higher than those of other directions, their distributions are critically uneven. The winds from a relative negative angle (counter-clockwise from West) are much frequent than others within such direction. This increases the difficulty for the ANN tools to learn these characteristics properly. A similar pattern can be seen at North-direction, where the frequency of 'north direction wind' is the lowest among the four other directions. This implies that fewer data would be available to train the tools for scenarios with North-direction winds and adds difficulties for the ANN tools to learn from these data.

The general frequency of East-direction winds is similar to those of South-direction winds. Although the East-direction winds distribute more evenly in terms of angles, the prediction of East walls is not the one with the highest reduction in e_r. Unlike the South-direction winds, whose speeds are evenly distributed among the hours, some scenarios with East-direction winds encounter outliers of wind speeds. This is reflected in the average wind speed line, lying at a lower level within the whole wind speed range at some angles. Nonetheless, the average line for South-direction lies almost at the middle of the speed range. Hence, the outliers are understood to be unfriendly in the training process of the ANN tools.

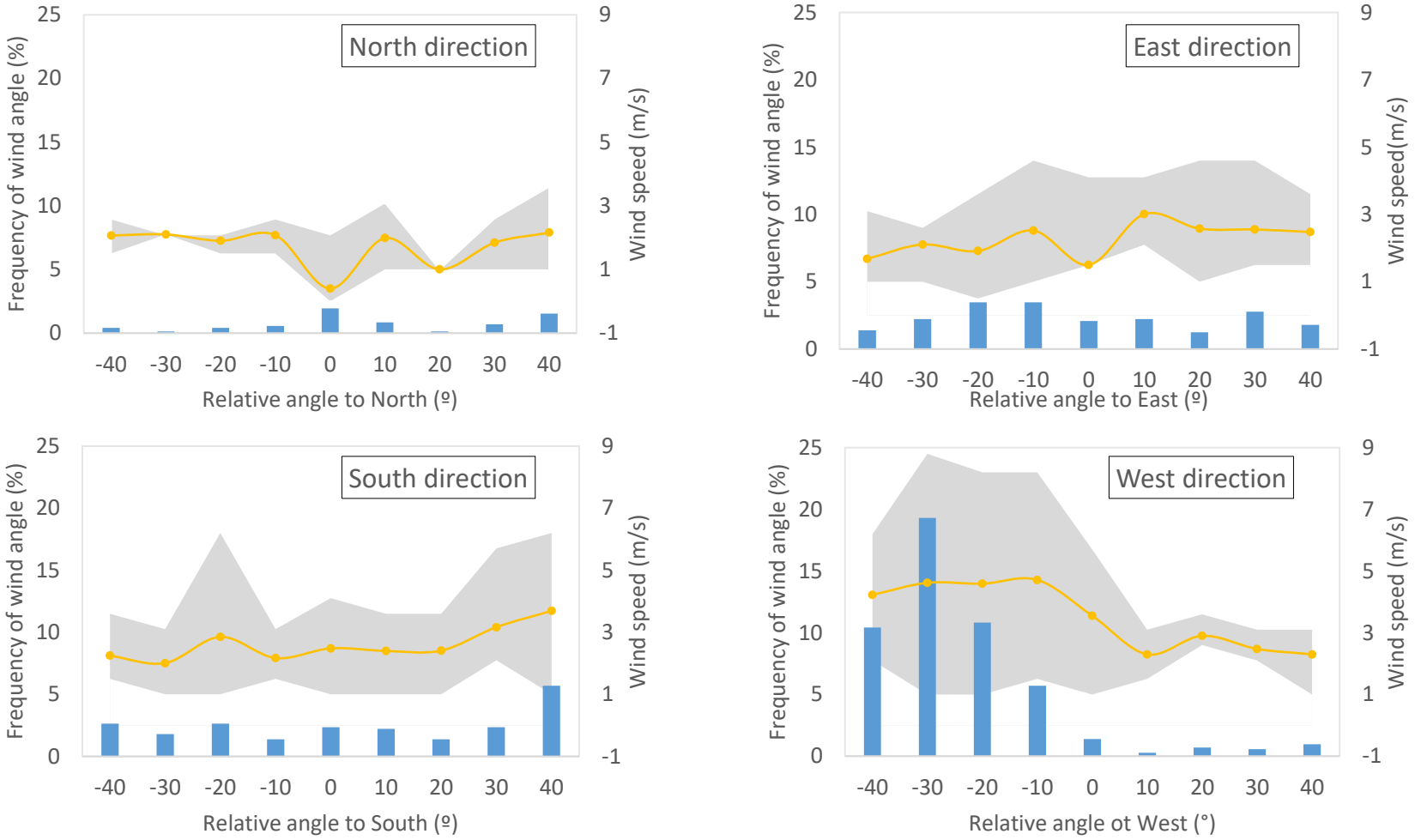

Figure 7-12 Occurrence frequency of wind angles in four directions and the associated wind speed at each specific direction [89]

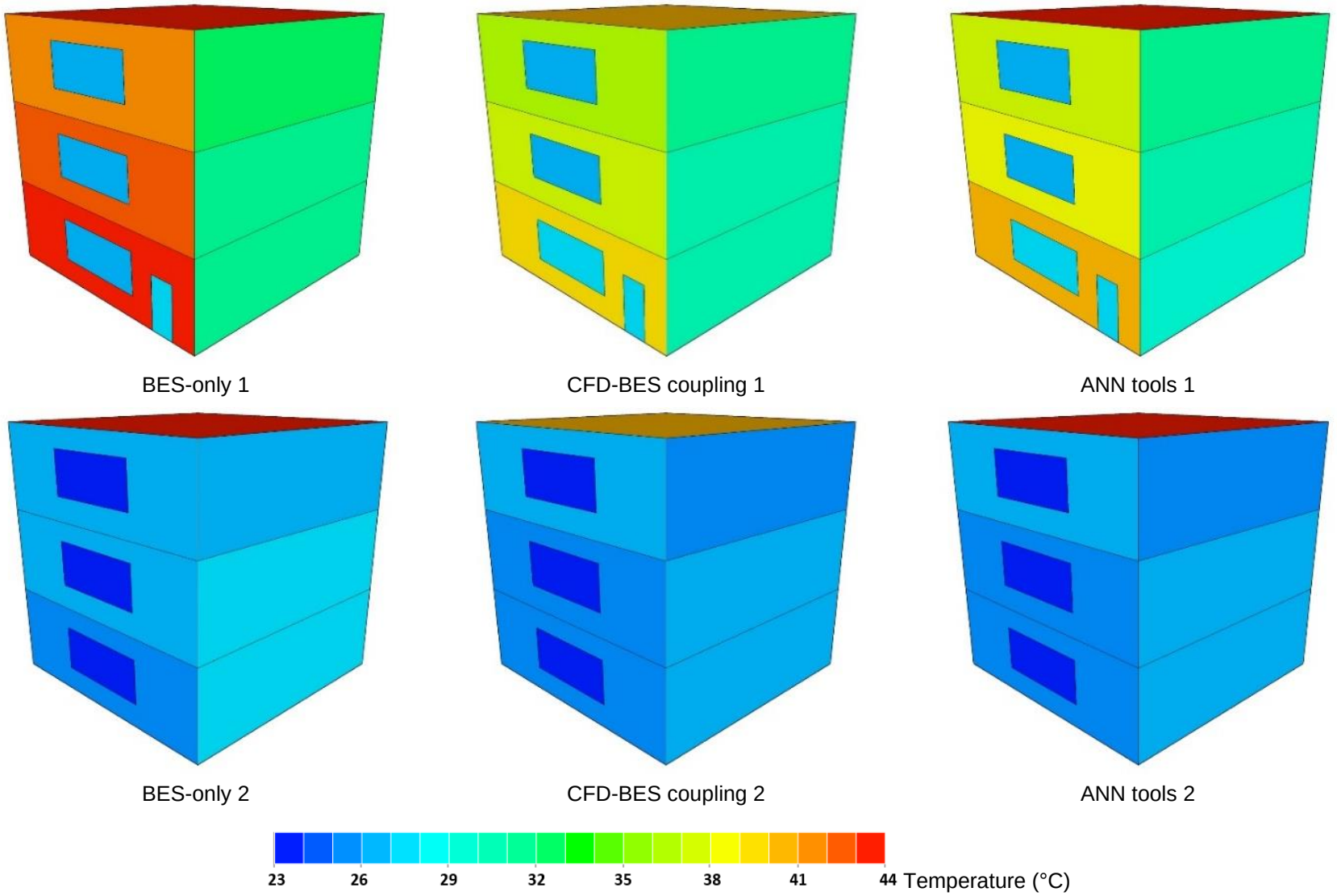

Figure 7-13 Comparison of surface temperatures calculated by different methods at 12 pm on 20th Sep., (row 1: southeast view; row 2 northwest view) [89]

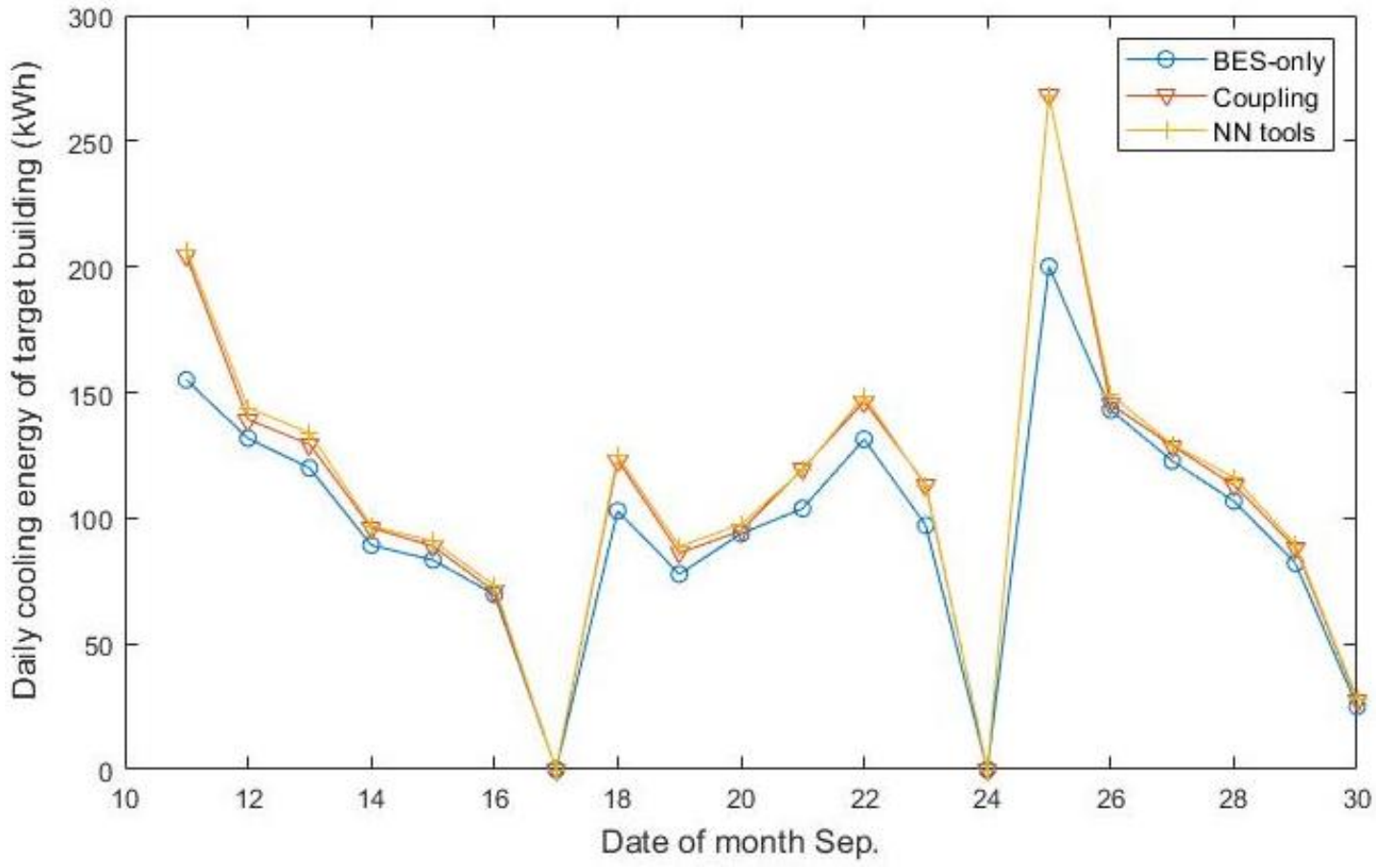

Figure 7-14 Comparison of the daily cooling energy of period-2 (11th – 30th Sep.) calculated by three different methods [89]

7.6. Comparison of Energy Simulation by Three Different Methods

Figure 7-13 shows an example comparison of temperature contours (at noon, 12 p.m., on 20th Sep) obtained by different modelling methods, including BES-only, BES-CFD coupling, and ANN tools. The surfaces temperatures calculated by the coupling method and ANN tools are lower than those of the BES-only method, especially on South facades where an evident difference can be observed. It is clear to see that the results calculated by the ANN tools are better matched to the coupling results than those provided by the BES-only method. As seen in *Figure 7-14*, a comparison is provided to discover the target buildings' cooling demand during period-2 (the prediction period) calculated by these three methods. In these 20 simulated days, there are two Sundays without any cooling energy demand. The cooling energy predicted from CHTCs by the ANN tools is found with a slight discrepancy of less than 0.02 compared to the values obtained from the coupling method. In contrast, the relative discrepancy between the cooling energy obtained by BES-only and coupling methods is approximately 0.1. Therefore, the prediction performance of the ANN tools is found to be satisfactory.

7.7. Computational Cost Benefits of The Proposed Framework

Each iteration of the dynamic coupling process takes approximately an average of 372.4 s CPU time. As it requires only ten-day coupling results to train the tool to predict the rest of the 20 days, specifically in this study, 264K s CPU time is spent to simulate the 10-day training data. This implies that the developed tool can save approximately 602K s CPU time. The computational cost would be, thus, reduced to 1/3 in the average. In general, every time step in this study (1-hour) requires an average of 3.2 iterations to reach convergence. The benefits can be different as the iterations of the coupling calculations required to achieve the convergence between CFD and BES can vary from a scenario to another one.

7.8. Summary

This chapter provides the approach of fully dynamic coupling for short-term modelling of natural ventilation scenarios. The key findings in this chapter are:

- It is found that 10 days can be considered as the effective size of period-1 for one-month simulation.

- The average accuracy of developed ANN tools reaches approximately 0.88.

- The proposed virtual dynamic coupling method can save about 2/3 of the computational time.

Chapter 8. CONCLUSIONS AND FURTHER WORK

8.1. Summary of The Work

.

This research aims to investigate the neighbourhood effect on the convection of buildings' exterior surfaces and enhance their presence in the local convective heat transfer coefficient format in building energy modelling. A practical and general framework for the coupling of CFD and BES tools is then developed.

The research starts with reviewing studies about the coupling technique of building energy simulation with computational fluid dynamics and the existing applications of the coupling method.

This research puts forward a general approach for combining BES and CFD tools, including developing the general external coupling framework, setting the bridge between two domains, and designing the case studies of applying the coupling method.

This research develops coupling frameworks for three different cases: the short-term sealed scenarios, the short-term ventilated scenarios, and the medium to long-term sealed scenarios. The model for short-term sealed scenarios is fundamental. Adding a hybrid indoor-outdoor CFD component to it gives the model for short-term ventilated scenarios. The key of CFD – CFD – BES model is transmitting the flow pattern at the opened fenestrations from dense hybrid grids to coarse indoor-only grids. Unlike the fully dynamic coupling used for short-term scenarios, virtual dynamic coupling is adopted for mid-term to long-term modelling. The virtual dynamic coupling is completed by integrating CFD and BES with the artificial neural network. Artificial neural

networks are trained to learn from fully dynamic modelling results and then deliver mid-term to long-term assessment predictions.

The case studies in this research are based on a simple city block consisting of nine buildings in a three-by-three array. All simulations are executed using the typical weather data of Los Angeles, U.S. The performance of these three models is analysed. Comparing the created coupling models and the BES-only model proves that the coupling CFD and BES helps to describe neighbourhoods' impact.

8.2. Conclusions

The main conclusions of this research are：

8.2.1. For short-term modelling of sealed scenarios

The coupling process aims to achieve a *good enough* agreement between the BES and CFD domains on convective heat flux values. In this study, the surface temperature (T_s) predicted by the BES tool and the CHTC (h^*) predicted by the CFD tool are the data shared between the two domains.

EnergyPlus uses a simplified local climate (the outdoor environment was considered homogeneous at a specific height) so it does not capture the vertical and horizontal air temperature distribution (impacted by local features, for example, the geometry and the neighbourhood) as accurately as the CFD domain. To achieve coherence results, EnergyPlus requires a more realistic convection coefficient, which CFD domain has the potential to modify it.

Convergence between the BES and CFD domains for a single time-step is identified by a residual criterion of T_s by the BES tool and h^* by the CFD tool. Initially, the residuals of T_s and h^* were set to be $<1\times10^{-3}$, but were increased to 1×10^{-2} to reduce the computational cost for some time-steps when convergence was not achieved within 20 iterations.

Fully dynamic coupling is realised by achieving convergence at each time-step of a simulation period. An analysis of an example hour during a test day shows that this coupling method can change the prediction of a building community's outdoor q_c'' by approximately 74 %. The prediction of hourly exterior convective energy is changed by over 64 % (including fenestration surfaces). Near-field buildings are shown to have a significant sheltering effect on others within the community. During the example hour, the standard deviation of q_c'' for all nine buildings increased by more than four times when compared to those predicted by the DOE-2 algorithm included in EnergyPlus.

The change in CHTC by the fully dynamic coupling model is found to be significant when compared to the algorithms used by EnergyPlus. The SimpleCombined and DOE-2 models are found to be the worst and the best algorithms, respectively, to capture the dynamic CHTC. Even with the best matching DOE-2 model, there is a 20 % difference in the daily average amendment of the CHTC.

All EnergyPlus embedded algorithms are found to underestimate the cooling load of the case study buildings. The largest gap in the daily energy demand is estimated to be 957 kWh predicted by the Adaptive model.

8.2.2. For short-term modelling of ventilated scenarios

The interfaces are placed at the openable windows on the first and second floors of nine buildings in a community. The buildings are naturally ventilated, so CFD_f shares the flow information at the opened surfaces to a CFD model with no indoor part.

Four options are investigated to find the appropriate boundary type for receiving the flow pattern from CFD_f, including mass flow inlet and outlet (mas-mass), velocity inlet with pressure outlet (velocity-pressure), pressure inlet and outlet (pressure-pressure), and velocity inlet and outlet (velocity-velocity). The proposed coupling method has been tested under the scenarios of winds at speeds of 4 m/s, 8 m/s and 16 m/s (wind angle = 0 °) and coming from

directions of 0 °, 22.5 °, 45 °, and 90 ° (U_{met}= 8 m/s) to study the impact of the inflow velocity magnitude and inflow angle. The main findings from these tests are:

- In general, velocity-velocity is the best option out of four tested interface types for CFD to represent CFD_f. It gives the fastest processing, making it preferable to be utilized in future coupling with other programs. Its overall RMSE of local flow speed at 58 tested lines is found as 0.411 (just slightly higher than the mass-mass option with 0.408 *RMSE*) for scenarios of parallel wind with different wind speeds. The advantage of the velocity-velocity option is evident in capturing the flow patterns at the opening surfaces. In contrast, the worst option is pressure-pressure, that the overall *RMSE* of 58 tested lines is approximately 0.428.

- 'OTO' layer, where horizontal lines between two adjacent rows of buildings are placed, is found to be the most challenging area to be represented due to the complexity of intertwining of the jet and breathing zones.

- As far as metric *FAC2* is considered, coupling the CFD_f - CFD method is *good enough* with each interface option. Underestimation of local velocity was found by each option. The sources of deviation between CFD and CFD_f can be mainly due to the reduction of resolution and different simulation engines. The impact of eliminating the indoor part is found as negligible.

- The impacts of inflow speed and inflow angle on CFD are found as non-linear. Therefore, the coupling of CFD_f and CFD is recommended for each particular scenario. The tendencies of *RMSE* by four interface options along with the change of inflow speed and inflow angle are very similar.

The concept of coupling of CFD_f and CFD is found to be feasible with obtaining acceptable velocity and mass flow rate fields in both models. The advantage in the conservation of runtime is considerable as it only takes less than 1/28 of the required time by replacing CFD_f with CFD model in each simulation. When

considering the non-isothermal scenarios, the strength of the proposed CFD_f – CFD – BES method becomes more obvious as it takes merely 1/195 of the runtime of that executed by CFD_f – BES method to complete the dynamic, iterative modelling.

The coupling method is found to be effective in improving the inclusion of neighbourhood effects in energy modelling. The roof surfaces are found as the place where the effect has been reflected strongest during the purging hours with a standard deviation of 1.7 in comparison to 0.00021 found by the stand-alone BES method. Furthermore, the standard deviations of the cooling load of nine buildings are 1.79 and 2.01 by stand-alone BES and the coupling methods, respectively.

8.2.3. For mid-term to long-term modelling

The surrounding buildings' zonal temperature is not important for the prediction of local CHTCs. The difference in the prediction accuracy of the tools by including or excluding this parameter is approximately 0.03.

It is found that ten days can be considered as the effective size of period-1 for a one-month simulation. The discrepancy between the predicted relative error by 10-day training of the period-1 and that of a longer period-1 is less than 0.01.

The performance of NN tools' predictions of differently oriented walls depends on the combination of the overall frequency of winds from that direction, the frequency distribution of wind angles within that specific wind direction, and the corresponding wind-speed distributions. Evenly distributed scenarios are better for NN tools to learn and can result in better accuracies.

The relative discrepancy of period-2's cooling energy predicted by the NN tools and coupling method is less than 0.02. The proposed method can save, on average, about 2/3 of the computational load for a one-month simulation.

8.3. Furter Work

The feasibility of the application of the proposed framework on more realistic scenarios is required to be investigated in future studies. Besides, further works are required to improve or seek an alternative way to predict the local CHTC on roof surfaces. Potentials of wider application of the coupled model with other tools need to be explored in further work.

BIBLIOGRAPHY

[1] "U.S. Energy Information Administration (EIA)," "International Energy Outlook 2021 with projections to 2050," 2021.

[2] "International Energy Agency (IEA)," "World Energy Outlook 2021," Paris, Oct. 2021.

[3] "Department for Business Energy & Industrial Strategy," "Energy Consumption in the UK 2021," Sep. 2021.

[4] C. A. Balaras, A. G. Gaglia, E. Georgopoulou, S. Mirasgedis, Y. Sarafidis, and D. P. Lalas, "European residential buildings and empirical assessment of the Hellenic building stock, energy consumption, emissions and potential energy savings," *Building and Environment*, vol. 42, no. 3, 2007, doi: 10.1016/j.buildenv.2005.11.001.

[5] E. Safirova, S. Houde, and W. Harrington, "Spatial Development and Energy Consumption," *SSRN Electronic Journal*, 2011, doi: 10.2139/ssrn.1087042.

[6] J. E. Cohen, "Human Population: The Next Half Century," *Science*, vol. 302, no. 5648. 2003. doi: 10.1126/science.1088665.

[7] C. O. R. Negrão, "Integration of computational fluid dynamics with building thermal and mass flow simulation," *Energy and Buildings*, vol. 27, no. 2, pp. 155–165, 1998, doi: https://doi.org/10.1016/S0378-7788(97)00036-4.

[8] J. A. Palyvos, "A survey of wind convection coefficient correlations for building envelope energy systems' modeling," *Applied Thermal Engineering*, vol. 28, no. 8, pp. 801–808, 2008, doi: https://doi.org/10.1016/j.applthermaleng.2007.12.005.

[9] M. G. Davies, *Building heat transfer*. 2006. doi: 10.1002/0470020555.

[10] A. de L. Vollaro, G. Galli, and A. Vallati, “CFD analysis of convective heat transfer coefficient on external surfaces of buildings,” *Sustainability (Switzerland)*, vol. 7, no. 7, 2015, doi: 10.3390/su7079088.

[11] M. G. Emmel, M. O. Abadie, and N. Mendes, “New external convective heat transfer coefficient correlations for isolated low-rise buildings,” *Energy and Buildings*, vol. 39, no. 3, 2007, doi: 10.1016/j.enbuild.2006.08.001.

[12] D. B. Crawley, J. W. Hand, M. Kummert, and B. T. Griffith, “Contrasting the capabilities of building energy performance simulation programs,” *Building and Environment*, vol. 43, no. 4, pp. 661–673, 2008, doi: https://doi.org/10.1016/j.buildenv.2006.10.027.

[13] S. Gilani, H. Montazeri, and B. Blocken, “CFD simulation of stratified indoor environment in displacement ventilation: Validation and sensitivity analysis,” *Building and Environment*, vol. 95, pp. 299–313, 2016, doi: https://doi.org/10.1016/j.buildenv.2015.09.010.

[14] M. Shirzadi, P. A. Mirzaei, and M. Naghashzadegan, “Development of an adaptive discharge coefficient to improve the accuracy of cross-ventilation airflow calculation in building energy simulation tools,” *Building and Environment*, vol. 127, pp. 277–290, 2018, doi: https://doi.org/10.1016/j.buildenv.2017.10.019.

[15] X. Wang and Y. Li, “Predicting urban heat island circulation using CFD,” *Building and Environment*, vol. 99, pp. 82–97, 2016, doi: https://doi.org/10.1016/j.buildenv.2016.01.020.

[16] C. O. R. Negrao, “Conflation of computational fluid dynamics and building thermal simulation.” Citeseer, 1995.

[17] D. B. Crawley, J. W. Hand, M. Kummert, and B. T. Griffith, “Contrasting the Capabilities of Building Energy Simulation Software tools. Energy Performance Simulation Software tools,” 2005.

[18] A. Almhafdy, N. Ibrahim, S. S. Ahmad, and J. Yahya, “Thermal Performance Analysis of Courtyards in a Hot Humid Climate Using Computational Fluid Dynamics CFD Method,” *Procedia - Social and Behavioral Sciences*, vol. 170, pp. 474–483, 2015, doi: https://doi.org/10.1016/j.sbspro.2015.01.012.

[19] P. S. Jahnkassim, “Energy strategies in the tropical context-the use of simulation tools in informing urban bioclimatic design in a malaysian highrise development-description and environmental study,” 2005.

[20] J. Van Der Veken, D. Saelens, G. Verbeeck, and H. Hens, “Comparison of steady-State and dynamic building energy simulation programs,” 2004.

[21] J. Clarke, *Energy simulation in building design*. 2007. doi: 10.4324/9780080505640.

[22] I. Beausoleil-Morrison, “The adaptive conflation of computational fluid dynamics with whole-building thermal simulation,” *Energy and Buildings*, vol. 34, no. 9, 2002, doi: 10.1016/S0378-7788(02)00061-0.

[23] M. Mirsadeghi, “Co-simulation of building energy simulation and computational fluid dynamics for whole-building heat, air and moisture engineering,” 2011.

[24] Z. Zhai and Q. Chen, “Solution characters of iterative coupling between energy simulation and CFD programs,” *Energy and Buildings*, vol. 35, no. 5, 2003, doi: 10.1016/S0378-7788(02)00156-1.

[25] Department of Energy U.S., “EnergyPlus 8.7 Engineering Reference,” 2016.

[26] A. Baskaran and A. Kashef, “Investigation of air flow around buildings using computational fluid dynamics techniques,” *Engineering Structures*, vol. 18, no. 11, 1996, doi: 10.1016/0141-0296(95)00154-9.

[27] B. Blocken, W. D. Janssen, and T. van Hooff, “CFD simulation for pedestrian wind comfort and wind safety in urban areas: General decision framework and case study for the Eindhoven University campus,” *Environmental Modelling and Software*, vol. 30, 2012, doi: 10.1016/j.envsoft.2011.11.009.

[28] M. Bady, S. Kato, Y. Ishida, H. Huang, and T. Takahashi, “Application of exceedance probability based on wind kinetic energy to evaluate the pedestrian level wind in dense urban areas,” *Building and Environment*, vol. 46, no. 9, 2011, doi: 10.1016/j.buildenv.2011.03.003.

[29] R. Ramponi, B. Blocken, L. B. de Coo, and W. D. Janssen, “CFD simulation of outdoor ventilation of generic urban configurations with different urban densities and equal and unequal street widths,” *Building and Environment*, vol. 92, 2015, doi: 10.1016/j.buildenv.2015.04.018.

[30] J. E. Flaherty, D. Stock, and B. Lamb, “Computational Fluid Dynamic Simulations of Plume Dispersion in Urban Oklahoma City,” *Journal of Applied Meteorology and Climatology*, vol. 46, no. 12, pp. 2110–2126, 2007, doi: 10.1175/2006JAMC1306.1.

[31] K.-M. Wai, C. Yuan, A. Lai, and P. K. N. Yu, “Relationship between pedestrian-level outdoor thermal comfort and building morphology in a high-density city,” *Science of The Total Environment*, vol. 708, p. 134516, 2020, doi: https://doi.org/10.1016/j.scitotenv.2019.134516.

[32] Y. Tominaga and T. Stathopoulos, “CFD modeling of pollution dispersion in a street canyon: Comparison between LES and RANS,” *Journal of Wind Engineering and Industrial Aerodynamics*, vol. 99, no. 4, 2011, doi: 10.1016/j.jweia.2010.12.005.

[33] M. Chavez, B. Hajra, T. Stathopoulos, and A. Bahloul, “Near-field pollutant dispersion in the built environment by CFD and wind tunnel simulations,” *Journal of Wind Engineering and Industrial Aerodynamics*, vol. 99, no. 4, 2011, doi: 10.1016/j.jweia.2011.01.003.

[34] E. Solazzo, S. Vardoulakis, and X. Cai, “A novel methodology for interpreting air quality measurements from urban streets using CFD modelling,” *Atmospheric Environment*, vol. 45, no. 29, 2011, doi: 10.1016/j.atmosenv.2011.05.022.

[35] P. Gousseau, B. Blocken, and G. J. F. van Heijst, “CFD simulation of pollutant dispersion around isolated buildings: On the role of convective and turbulent mass fluxes in the prediction accuracy,” *Journal of Hazardous Materials*, vol. 194, 2011, doi: 10.1016/j.jhazmat.2011.08.008.

[36] F. Haghighat and P. A. Mirzaei, “Impact of non-uniform urban surface temperature on pollution dispersion in urban areas,” *Building Simulation*, vol. 4, no. 3, 2011, doi: 10.1007/s12273-011-0035-6.

[37] P. A. Mirzaei and F. Haghighat, “Pollution removal effectiveness of the pedestrian ventilation system,” *Journal of Wind Engineering and Industrial Aerodynamics*, vol. 99, no. 1, 2011, doi: 10.1016/j.jweia.2010.10.007.

[38] H. kondo, K. Asahi, T. Tomizuka, and M. Suzuki, “Numerical analysis of diffusion around a suspended expressway by a multi-scale CFD model,” *Atmospheric Environment*, vol. 40, no. 16, 2006, doi: 10.1016/j.atmosenv.2006.01.012.

[39] Z. Tong, Y. Chen, and A. Malkawi, “Defining the Influence Region in neighborhood-scale CFD simulations for natural ventilation design,” *Applied Energy*, vol. 182, 2016, doi: 10.1016/j.apenergy.2016.08.098.

[40] M. Shirzadi, M. Naghashzadegan, and P. A. Mirzaei, “Improving the CFD modelling of cross-ventilation in highly-packed urban areas,” *Sustainable Cities and Society*, vol. 37, pp. 451–465, 2018, doi: https://doi.org/10.1016/j.scs.2017.11.020.

[41] M. Shirzadi, P. A. Mirzaei, M. Naghashzadegan, and Y. Tominaga, “Modelling enhancement of cross-ventilation in sheltered buildings using stochastic optimization,” *International Journal of Heat and Mass Transfer*, vol. 118, pp. 758–772, 2018, doi: https://doi.org/10.1016/j.ijheatmasstransfer.2017.10.107.

[42] M. F. King *et al.*, “Investigating the influence of neighbouring structures on natural ventilation potential of a full-scale cubical building using time-dependent CFD,” *Journal of Wind Engineering and Industrial Aerodynamics*, vol. 169, 2017, doi: 10.1016/j.jweia.2017.07.020.

[43] J. I. Peren, T. van Hooff, R. Ramponi, B. Blocken, and B. C. C. Leite, “Impact of roof geometry of an isolated leeward sawtooth roof building on cross-ventilation: Straight, concave, hybrid or convex?,” *Journal of Wind Engineering and Industrial Aerodynamics*, vol. 145, 2015, doi: 10.1016/j.jweia.2015.05.014.

[44] T. van Hooff, B. Blocken, and Y. Tominaga, “On the accuracy of CFD simulations of cross-ventilation flows for a generic isolated building: Comparison of RANS, LES and experiments,” *Building and Environment*, vol. 114, pp. 148–165, 2017, doi: https://doi.org/10.1016/j.buildenv.2016.12.019.

[45] D. Micallef, V. Buhagiar, and S. P. Borg, “Cross-ventilation of a room in a courtyard building,” *Energy and Buildings*, vol. 133, 2016, doi: 10.1016/j.enbuild.2016.09.053.

[46] L. J. Lo and A. Novoselac, “Effect of indoor buoyancy flow on wind-driven cross ventilation,” in *Building Simulation*, 2013, vol. 6, no. 1, pp. 69–79.

[47] Y. Tominaga, S. ichi Akabayashi, T. Kitahara, and Y. Arinami, “Air flow around isolated gable-roof buildings with different roof pitches: Wind tunnel experiments and CFD simulations,” *Building and Environment*, vol. 84, 2015, doi: 10.1016/j.buildenv.2014.11.012.

[48] P. Neofytou, A. G. Venetsanos, D. Vlachogiannis, J. G. Bartzis, and A. Scaperdas, “CFD simulations of the wind environment around an airport terminal building,” in *Environmental Modelling and Software*, 2006, vol. 21, no. 4. doi: 10.1016/j.envsoft.2004.08.011.

[49] B. Blocken, T. Stathopoulos, and J. Carmeliet, “CFD simulation of the atmospheric boundary layer: wall function problems,” *Atmospheric Environment*, vol. 41, no. 2, 2007, doi: 10.1016/j.atmosenv.2006.08.019.

[50] P. A. Mirzaei and J. Carmeliet, “Dynamical computational fluid dynamics modeling of the stochastic wind for application of urban studies,” *Building and Environment*, vol. 70, pp. 161–170, 2013, doi: https://doi.org/10.1016/j.buildenv.2013.08.014.

[51] R. Zhang, “Development and validation of a climatic CFD model to predict the surface temperature of building integrated photovoltaics,” The University of Nottingham, 2015.

[52] P. A. Mirzaei and F. Haghighat, “Approaches to study Urban Heat Island - Abilities and limitations,” *Building and Environment*, vol. 45, no. 10, 2010, doi: 10.1016/j.buildenv.2010.04.001.

[53] A. Mochida and I. Y. F. Lun, “Prediction of wind environment and thermal comfort at pedestrian level in urban area,” *Journal of Wind Engineering and Industrial Aerodynamics*, vol. 96, no. 10–11, 2008, doi: 10.1016/j.jweia.2008.02.033.

[54] Y. Tominaga *et al.*, “AIJ guidelines for practical applications of CFD to pedestrian wind environment around buildings,” *Journal of Wind*

Engineering and Industrial Aerodynamics, vol. 96, no. 10–11, pp. 1749–1761, 2008, doi: 10.1016/j.jweia.2008.02.058.

[55] J. Franke and A. Baklanov, *Best Practice Guideline for the CFD Simulation of Flows in the Urban Environment: COST Action 732 Quality Assurance and Improvement of Microscale Meteorological Models*. 2007.

[56] E. Djunaedy, J. L. M. Hensen, and M. G. L. C. Loomans, “External coupling between CFD and energy simulation: Implementation and validation,” in *ASHRAE Transactions*, 2005, vol. 111 PART 1.

[57] Z. Zhai, Q. Chen, J. H. Klems, and P. Haves, “Strayegies for Coupling Energy Simulation and Computational Fluid Dynamics Programs,” 2001.

[58] E. Djunaedy, J. L. M. Hensen, and M. G. L. C. Loomans, “Toward external coupling of building energy and airflow modeling programs,” in *ASHRAE Transactions*, 2003, vol. 109 PART 2.

[59] J. Srebric, Q. Chen, and L. R. Glicksman, “Coupled airflow and energy simulation program for indoor thermal environmental studies,” in *ASHRAE Transactions*, 2000, vol. 106.

[60] Z. J. Zhai and Q. Y. Chen, “Performance of coupled building energy and CFD simulations,” *Energy and Buildings*, vol. 37, no. 4, 2005, doi: 10.1016/j.enbuild.2004.07.001.

[61] Y. Q. Fan, T. Hayashi, and K. Ito, “Coupled simulation of BES-CFD and performance assessment of energy recovery ventilation system for office model,” *Journal of Central South University of Technology (English Edition)*, vol. 19, no. 3, 2012, doi: 10.1007/s11771-012-1049-7.

[62] Y. Fan and K. Ito, “Optimization of indoor environmental quality and ventilation load in office space by multilevel coupling of building energy simulation and computational fluid dynamics,” *Building Simulation*, vol. 7, no. 6, 2014, doi: 10.1007/s12273-014-0178-3.

[63] M. Gijón-Rivera, J. Xamán, G. Álvarez, and J. Serrano-Arellano, “Coupling CFD-BES Simulation of a glazed office with different types of windows in Mexico City,” *Building and Environment*, vol. 68, 2013, doi: 10.1016/j.buildenv.2013.06.005.

[64] A. Mochida, H. Yoshino, S. Miyauchi, and T. Mitamura, “Total analysis of cooling effects of cross-ventilation affected by microclimate around a building,” *Solar Energy*, vol. 80, no. 4, 2006, doi: 10.1016/j.solener.2005.08.014.

[65] Y. K. Yi and N. Feng, “Dynamic integration between building energy simulation (BES) and computational fluid dynamics (CFD) simulation for building exterior surface,” *Building Simulation*, vol. 6, no. 3. 2013. doi: 10.1007/s12273-013-0116-9.

[66] L. Malys, M. Musy, and C. Inard, “Microclimate and building energy consumption: Study of different coupling methods,” *Advances in Building Energy Research*, vol. 9, no. 2, 2015, doi: 10.1080/17512549.2015.1043643.

[67] S. Khoshdel Nikkho, M. Heidarinejad, J. Liu, and J. Srebric, “Quantifying the impact of urban wind sheltering on the building energy consumption,” *Applied Thermal Engineering*, vol. 116, 2017, doi: 10.1016/j.applthermaleng.2017.01.044.

[68] R. Zhang, K. P. Lam, S. chune Yao, and Y. Zhang, “Coupled EnergyPlus and computational fluid dynamics simulation for natural ventilation,” *Building and Environment*, vol. 68, 2013, doi: 10.1016/j.buildenv.2013.04.002.

[69] P. Shen and Z. Wang, “How neighborhood form influences building energy use in winter design condition: Case study of Chicago using CFD coupled simulation,” *Journal of Cleaner Production*, vol. 261, 2020, doi: 10.1016/j.jclepro.2020.121094.

[70] M. Barbason and S. Reiter, “Coupling building energy simulation and computational fluid dynamics: Application to a two-storey house in a temperate climate,” *Building and Environment*, vol. 75, 2014, doi: 10.1016/j.buildenv.2014.01.012.

[71] T. Hong, M. Lee, and J. Kim, “Analysis of Energy Consumption and Indoor Temperature Distributions in Educational Facility Based on CFD-BES Model,” in *Energy Procedia*, 2017, vol. 105. doi: 10.1016/j.egypro.2017.03.858.

[72] L. Wang and N. H. Wong, “Coupled simulations for naturally ventilated rooms between building simulation (BS) and computational fluid dynamics (CFD) for better prediction of indoor thermal environment,” *Building and Environment*, vol. 44, no. 1, 2009, doi: 10.1016/j.buildenv.2008.01.015.

[73] H. Kim, J. Haw, T. Kim, and S. B. Leigh, “Application of coupled simulation between bes-cfd for naturally ventilated residential buildings,” 2013.

[74] R. Zhang, P. A. Mirzaei, and B. Jones, “Development of a dynamic external CFD and BES coupling framework for application of urban neighbourhoods energy modelling,” *Building and Environment*, vol. 146, 2018, doi: 10.1016/j.buildenv.2018.09.006.

[75] R. Qin, D. Yan, X. Zhou, and Y. Jiang, “Research on a dynamic simulation method of atrium thermal environment based on neural network,” *Building and Environment*, vol. 50, 2012, doi: 10.1016/j.buildenv.2011.11.001.

[76] Y. K. Yi and A. M. Malkawi, “Site-specific optimal energy form generation based on hierarchical geometry relation,” *Automation in Construction*, vol. 26, 2012, doi: 10.1016/j.autcon.2012.05.004.

[77] M. Mirsadeghi, D. Cóstola, B. Blocken, and J. L. M. Hensen, “Review of external convective heat transfer coefficient models in building energy simulation programs: Implementation and uncertainty,” *Applied Thermal Engineering*, vol. 56, no. 1–2. 2013. doi: 10.1016/j.applthermaleng.2013.03.003.

[78] U. S. E. I. Administration, “International Energy Outlook (IEO) 2019, U. S. Energy Information Administration,” *U.S. Department of Energy*, vol. 44, no. 07, 2019.

[79] R. Zhang, Y. Gan, and P. A. Mirzaei, “A new regression model to predict BIPV cell temperature for various climates using a high-resolution CFD microclimate model,” *Advances in Building Energy Research*, pp. 1–23, Aug. 2019, doi: 10.1080/17512549.2019.1654917.

[80] J. Allegrini, V. Dorer, and J. Carmeliet, “Influence of morphologies on the microclimate in urban neighbourhoods,” *Journal of Wind Engineering and Industrial Aerodynamics*, vol. 144, 2015, doi: 10.1016/j.jweia.2015.03.024.

[81] R. Wei, D. Song, N. H. Wong, and M. Martin, “Impact of Urban Morphology Parameters on Microclimate,” in *Procedia Engineering*, 2016, vol. 169. doi: 10.1016/j.proeng.2016.10.017.

[82] J. W. Moon, “Performance of ANN-based predictive and adaptive thermal-control methods for disturbances in and around residential buildings,” *Building and Environment*, vol. 48, pp. 15–26, 2012, doi: https://doi.org/10.1016/j.buildenv.2011.06.005.

[83] N. K. Kandasamy, G. Karunagaran, C. Spanos, K. J. Tseng, and B.-H. Soong, “Smart lighting system using ANN-IMC for personalized lighting control and daylight harvesting,” *Building and Environment*, vol. 139, pp. 170–180, 2018, doi: https://doi.org/10.1016/j.buildenv.2018.05.005.

[84] T. Zhang, Y. Liu, Y. Rao, X. Li, and Q. Zhao, “Optimal design of building environment with hybrid genetic algorithm, artificial neural network, multivariate regression analysis and fuzzy logic controller,” *Building and Environment*, vol. 175, p. 106810, 2020, doi: https://doi.org/10.1016/j.buildenv.2020.106810.

[85] Architecture Institute of Japan, “Guidebook for CFD Predictions of Urban Wind Environment.” https://www.aij.or.jp/jpn/publish/cfdguide/index_e.htm (accessed Jan. 10, 2021).

[86] M. Deru *et al.*, “US Department of Energy commercial reference building models of the national building stock,” 2011.

[87] Department of Energy U.S., “Commercial Reference Buildings,” 2011. https://energy.gov/eere/buildings/commercial-reference-buildings (accessed Jul. 27, 2021).

[88] R. Zhang and P. A. Mirzaei, “CFD-CFD coupling: A novel method to develop a fast urban microclimate model,” *Journal of Building Physics*, Jul. 2020, doi: 10.1177/1744259120935921.

[89] B. E. (Brian E. Launder, *Lectures in mathematical models of turbulence [by] B. E. Launder and D. B. Spalding*. London, New York: Academic Press, 1972.

[90] R. Zhang, P. A. Mirzaei, and J. Carmeliet, “Prediction of the surface temperature of building-integrated photovoltaics: Development of a high accuracy correlation using computational fluid dynamics,” *Solar Energy*, vol. 147, 2017, doi: 10.1016/j.solener.2017.03.023.

[91] R. Zhang and P. A. Mirzaei, “Virtual dynamic coupling of computational fluid dynamics-building energy simulation-artificial intelligence: Case study of urban neighbourhood effect on buildings’ energy demand,”

Building and Environment, vol. 195, p. 107728, 2021, doi: https://doi.org/10.1016/j.buildenv.2021.107728.

[92] R. Zhang, P. A. Mirzaei, and B. Jones, “Development of a dynamic external CFD and BES coupling framework for application of urban neighbourhoods energy modelling,” *Building and Environment*, vol. 146, pp. 37–49, 2018, doi: https://doi.org/10.1016/j.buildenv.2018.09.006.

[93] Y. Tominaga and B. Blocken, “Wind tunnel experiments on cross-ventilation flow of a generic building with contaminant dispersion in unsheltered and sheltered conditions,” *Building and Environment*, vol. 92, pp. 452–461, 2015, doi: https://doi.org/10.1016/j.buildenv.2015.05.026.

[94] P. Gousseau, B. Blocken, and G. J. F. van Heijst, “Quality assessment of Large-Eddy Simulation of wind flow around a high-rise building: Validation and solution verification,” *Computers & Fluids*, vol. 79, pp. 120–133, 2013, doi: https://doi.org/10.1016/j.compfluid.2013.03.006.

[95] Y. Tominaga, “Flow around a high-rise building using steady and unsteady RANS CFD: Effect of large-scale fluctuations on the velocity statistics,” *Journal of Wind Engineering and Industrial Aerodynamics*, vol. 142, pp. 93–103, 2015, doi: https://doi.org/10.1016/j.jweia.2015.03.013.

[96] J. C. Chang and S. R. Hanna, “Air quality model performance evaluation,” *Meteorology and Atmospheric Physics*, vol. 87, no. 1, pp. 167–196, 2004, doi: 10.1007/s00703-003-0070-7.

[97] Y. et. al Tominaga, “Cross Comparisons of CFD Results of Wind Environment at Pedestrian Level around a High-rise Building and within a Building Complex,” *Journal of Asian Architecture and Building Engineering*, vol. 3, no. 1, pp. 63–70, 2004, doi: 10.3130/jaabe.3.63.

[98] A. Fluent, “Ansys Fluent 14.5 User’s Guide.” ANSYS, Inc. Canonsburg, PA, 2012.

[99] Cibse, *CIBSE guide C: reference data*. Routledge, 2007.

[100] I. Beausoleil-Morrison, “The adaptive coupling of heat and air flow modelling within dynamic whole-building simulation,” *Mechanical Engineering*, vol. Ph D, no. May, 2000.

[101] R. Zhang and P. A. Mirzaei, “Fast and dynamic urban neighbourhood energy simulation using CFDf-CFDc-BES coupling method,” *Sustainable Cities and Society*, p. 102545, Oct. 2020, doi: 10.1016/j.scs.2020.102545.

[102] K. Iyengar, *Sustainable architectural design: An overview*. Routledge, 2015.

[103] J. Indu and D. N. Kumar, “Making the Most of the Earth Observation Data Using Effective Sampling Techniques,” in *Sensitivity Analysis in Earth Observation Modelling*, Elsevier, 2017, pp. 257–272.

APPENDICES

Appendix 1 Bespoke code to update *IDF files, generate journals and check the convergence of the coupling

Following shows three main parts of the bespoke code to update *IDF files for EnergyPlus, generate journal files for Fluent and check the convergence of the iterative coupling process, respectively.

```
1.
%% IDF Updater
%This code assigns the new CHTCs from CFD from previous iteration
%to the *IDF file in EnergyPlus as Schedules for each surface.

%% Input data
f = load('Inputs.txt');
mdate = f(1);%mdate is the month of the test day
ddate = f(2);%ddate is the ?th day of the month
itime_no = f(3); %time of the test day
iter_no = f(4); %iteration number of the test hour
%% Make new directory
fn1 = strcat('time_',num2str(itime_no));
mkdir (fn1);
fn2 = strcat(fn1,'/iter_',num2str(iter_no),'.idf');
%new idf file for current iteration
fpath = fullfile('E:','AIJ_LA',fn2);
%original idf file with exterior CHTCs determined by DOE-2 method
ofpath = fullfile('E:','AIJ_LA','original.idf');
%% Update IDF
x = 9; %x is the number of target buildings
% Create array of cells of zone names
ARR_zname = cell(9,3);
for i = 1:1:9
    for j = 1:1:3
        ARR_zname(i,j)={char('B',num2str(i),num2str(j))};
    end
end
% Create new idf file
copyfile(ofpath,fpath);
if itime_no >1||iter_no >0
  % update the schedule of CHTCs
  [~] = sch_chtc(mdate,ddate,iter_no,fpath,itime_no,ARR_zname,x);
  % use user-defined CHTCs
Surface_convection_coefficients=CHTC(iter_no,fpath,itime_no,ARR_zn
ame,x);
End

function
[Schedule_chtc]=sch_chtc(mdate,ddate,iter_no,fpath,itime_no,ARR_zn
ame,x)
fidfsch_chtc = fopen(fpath,'a+');
chtc_1= read_pre(ARR_zname,x);
```

```
chtc_t = load('Convergence\newchtc.mat');
CHTC = chtc_t.chtc_bu;
for i = 1:1:x
  a = ARR_zname(i,:);
  a(cellfun(@isempty,a))=[];
  [~,m]=size(a);
  b = ARR_zname(i,:);
  for j=1:1:m
    c=chtc_1{i,j};
    d = CHTC{i,j};
    for k = 1:1:4
      fprintf(fidfsch_chtc,'Schedule:Compact,\n');
      fprintf(fidfsch_chtc,'%sS%d-CHTC-%d-%d,                    !-
name\n',b{1,j},k,itime_no,iter_no);
      fprintf(fidfsch_chtc,'Any Number,                 !- Schedule
Type Limits Name\n');
      fprintf(fidfsch_chtc,'Through:  %d/%d,               !-  Field
1\n',mdate,ddate-1);
      fprintf(fidfsch_chtc,'For: AllDays,           !- Field 2\n');
      fprintf(fidfsch_chtc,'Until: 21:00,           !- Field 3\n');
      fprintf(fidfsch_chtc,'0.1,                    !- Field 4\n');
      fprintf(fidfsch_chtc,'Until: 22:00,           !- Field 5\n');
      fprintf(fidfsch_chtc,'%1.3f,           !- Field 6\n',c(1,k));
      fprintf(fidfsch_chtc,'Until: 23:00,           !- Field 7\n');
      fprintf(fidfsch_chtc,'%1.3f,           !- Field 8\n',c(2,k));
      fprintf(fidfsch_chtc,'Until: 24:00,           !- Field 9\n');
      fprintf(fidfsch_chtc,'%1.3f,          !- Field 10\n',c(3,k));
      fprintf(fidfsch_chtc,'Through:  %d/%d,               !-  Field
11\n',mdate,ddate);
      fprintf(fidfsch_chtc,'For: AllDays,          !- Field 12\n');
      fprintf(fidfsch_chtc,'Until: 01:00,          !- Field 13\n');
      fprintf(fidfsch_chtc,'%1.3f,          !- Field 14\n',d(1,k));
      fprintf(fidfsch_chtc,'Until: 02:00,          !- Field 15\n');
      fprintf(fidfsch_chtc,'%1.3f,          !- Field 16\n',d(2,k));
      fprintf(fidfsch_chtc,'Until: 03:00,          !- Field 17\n');
      fprintf(fidfsch_chtc,'%1.3f,          !- Field 18\n',d(3,k));
      fprintf(fidfsch_chtc,'Until: 04:00,          !- Field 19\n');
      fprintf(fidfsch_chtc,'%1.3f,          !- Field 20\n',d(4,k));
      fprintf(fidfsch_chtc,'Until: 05:00,          !- Field 21\n');
      fprintf(fidfsch_chtc,'%1.3f,          !- Field 22\n',d(5,k));
      fprintf(fidfsch_chtc,'Until: 06:00,          !- Field 23\n');
      fprintf(fidfsch_chtc,'%1.3f,          !- Field 24\n',d(6,k));
      fprintf(fidfsch_chtc,'Until: 07:00,          !- Field 25\n');
      fprintf(fidfsch_chtc,'%1.3f,          !- Field 26\n',d(7,k));
      fprintf(fidfsch_chtc,'Until: 08:00,          !- Field 27\n');
      fprintf(fidfsch_chtc,'%1.3f,          !- Field 28\n',d(8,k));
      fprintf(fidfsch_chtc,'Until: 09:00,          !- Field 29\n');
      fprintf(fidfsch_chtc,'%1.3f,          !- Field 30\n',d(9,k));
      fprintf(fidfsch_chtc,'Until: 10:00,          !- Field 31\n');
      fprintf(fidfsch_chtc,'%1.3f,         !- Field 32\n',d(10,k));
      fprintf(fidfsch_chtc,'Until: 11:00,          !- Field 33\n');
      fprintf(fidfsch_chtc,'%1.3f,         !- Field 34\n',d(11,k));
      fprintf(fidfsch_chtc,'Until: 12:00,          !- Field 35\n');
      fprintf(fidfsch_chtc,'%1.3f,         !- Field 36\n',d(12,k));
      fprintf(fidfsch_chtc,'Until: 13:00,          !- Field 37\n');
      fprintf(fidfsch_chtc,'%1.3f,         !- Field 38\n',d(13,k));
      fprintf(fidfsch_chtc,'Until: 14:00,          !- Field 39\n');
      fprintf(fidfsch_chtc,'%1.3f,         !- Field 40\n',d(14,k));
      fprintf(fidfsch_chtc,'Until: 15:00,          !- Field 41\n');
      fprintf(fidfsch_chtc,'%1.3f,         !- Field 42\n',d(15,k));
      fprintf(fidfsch_chtc,'Until: 16:00,          !- Field 43\n');
```

```
        fprintf(fidfsch_chtc,'%1.3f,          !- Field 44\n',d(16,k));
        fprintf(fidfsch_chtc,'Until: 17:00,          !- Field 45\n');
        fprintf(fidfsch_chtc,'%1.3f,          !- Field 46\n',d(17,k));
        fprintf(fidfsch_chtc,'Until: 18:00,          !- Field 47\n');
        fprintf(fidfsch_chtc,'%1.3f,          !- Field 48\n',d(18,k));
        fprintf(fidfsch_chtc,'Until: 19:00,          !- Field 49\n');
        fprintf(fidfsch_chtc,'%1.3f,          !- Field 50\n',d(19,k));
        fprintf(fidfsch_chtc,'Until: 20:00,          !- Field 51\n');
        fprintf(fidfsch_chtc,'%1.3f,          !- Field 52\n',d(20,k));
        fprintf(fidfsch_chtc,'Until: 21:00,          !- Field 53\n');
        fprintf(fidfsch_chtc,'%1.3f,          !- Field 54\n',d(21,k));
        fprintf(fidfsch_chtc,'Until: 22:00,          !- Field 55\n');
        fprintf(fidfsch_chtc,'%1.3f,          !- Field 56\n',d(22,k));
        fprintf(fidfsch_chtc,'Until: 23:00,          !- Field 57\n');
        fprintf(fidfsch_chtc,'%1.3f,          !- Field 58\n',d(23,k));
        fprintf(fidfsch_chtc,'Until: 24:00,          !- Field 59\n');
        fprintf(fidfsch_chtc,'%1.3f,          !- Field 60\n',d(24,k));
        fprintf(fidfsch_chtc,'Through: 12/31,        !- Field 61\n');
        fprintf(fidfsch_chtc,'For: AllDays,          !- Field 62\n');
        fprintf(fidfsch_chtc,'Until: 24:00,          !- Field 63\n');
        fprintf(fidfsch_chtc,'0.1;                 !- Field 64\n\n');
        end
        if j == m
        fprintf(fidfsch_chtc,'Schedule:Compact,\n');
        fprintf(fidfsch_chtc,'%sR-CHTC-%d-%d,              !- Surface
Name\n',b{1,j},itime_no,iter_no);
        fprintf(fidfsch_chtc,'Any Number,                !- Schedule
Type Limits Name\n');
        fprintf(fidfsch_chtc,'Through:  %d/%d,               !- Field
1\n',mdate,ddate-1);
        fprintf(fidfsch_chtc,'For: AllDays,           !- Field 2\n');
        fprintf(fidfsch_chtc,'Until: 21:00,           !- Field 3\n');
        fprintf(fidfsch_chtc,'0.1,                    !- Field 4\n');
        fprintf(fidfsch_chtc,'Until: 22:00,           !- Field 5\n');
        fprintf(fidfsch_chtc,'%1.3f,           !- Field 6\n',c(1,5));
        fprintf(fidfsch_chtc,'Until: 23:00,           !- Field 7\n');
        fprintf(fidfsch_chtc,'%1.3f,           !- Field 8\n',c(2,5));
        fprintf(fidfsch_chtc,'Until: 24:00,           !- Field 9\n');
        fprintf(fidfsch_chtc,'%1.3f,          !- Field 10\n',c(3,5));
        fprintf(fidfsch_chtc,'Through:  %d/%d,               !- Field
11\n',mdate,ddate);
        fprintf(fidfsch_chtc,'For: AllDays,          !- Field 12\n');
        fprintf(fidfsch_chtc,'Until: 01:00,          !- Field 13\n');
        fprintf(fidfsch_chtc,'%1.3f,          !- Field 14\n',d(1,5));
        fprintf(fidfsch_chtc,'Until: 02:00,          !- Field 15\n');
        fprintf(fidfsch_chtc,'%1.3f,          !- Field 16\n',d(2,5));
        fprintf(fidfsch_chtc,'Until: 03:00,          !- Field 17\n');
        fprintf(fidfsch_chtc,'%1.3f,          !- Field 18\n',d(3,5));
        fprintf(fidfsch_chtc,'Until: 04:00,          !- Field 19\n');
        fprintf(fidfsch_chtc,'%1.3f,          !- Field 20\n',d(4,5));
        fprintf(fidfsch_chtc,'Until: 05:00,          !- Field 21\n');
        fprintf(fidfsch_chtc,'%1.3f,          !- Field 22\n',d(5,5));
        fprintf(fidfsch_chtc,'Until: 06:00,          !- Field 23\n');
        fprintf(fidfsch_chtc,'%1.3f,          !- Field 24\n',d(6,5));
        fprintf(fidfsch_chtc,'Until: 07:00,          !- Field 25\n');
        fprintf(fidfsch_chtc,'%1.3f,          !- Field 26\n',d(7,5));
        fprintf(fidfsch_chtc,'Until: 08:00,          !- Field 27\n');
        fprintf(fidfsch_chtc,'%1.3f,          !- Field 28\n',d(8,5));
        fprintf(fidfsch_chtc,'Until: 09:00,          !- Field 29\n');
        fprintf(fidfsch_chtc,'%1.3f,          !- Field 30\n',d(9,5));
        fprintf(fidfsch_chtc,'Until: 10:00,          !- Field 31\n');
```

```
      fprintf(fidfsch_chtc,'%1.3f,          !- Field 32\n',d(10,5));
      fprintf(fidfsch_chtc,'Until: 11:00,          !- Field 33\n');
      fprintf(fidfsch_chtc,'%1.3f,          !- Field 34\n',d(11,5));
      fprintf(fidfsch_chtc,'Until: 12:00,          !- Field 35\n');
      fprintf(fidfsch_chtc,'%1.3f,          !- Field 36\n',d(12,5));
      fprintf(fidfsch_chtc,'Until: 13:00,          !- Field 37\n');
      fprintf(fidfsch_chtc,'%1.3f,          !- Field 38\n',d(13,5));
      fprintf(fidfsch_chtc,'Until: 14:00,          !- Field 39\n');
      fprintf(fidfsch_chtc,'%1.3f,          !- Field 40\n',d(14,5));
      fprintf(fidfsch_chtc,'Until: 15:00,          !- Field 41\n');
      fprintf(fidfsch_chtc,'%1.3f,          !- Field 42\n',d(15,5));
      fprintf(fidfsch_chtc,'Until: 16:00,          !- Field 43\n');
      fprintf(fidfsch_chtc,'%1.3f,          !- Field 44\n',d(16,5));
      fprintf(fidfsch_chtc,'Until: 17:00,          !- Field 45\n');
      fprintf(fidfsch_chtc,'%1.3f,          !- Field 46\n',d(17,5));
      fprintf(fidfsch_chtc,'Until: 18:00,          !- Field 47\n');
      fprintf(fidfsch_chtc,'%1.3f,          !- Field 48\n',d(18,5));
      fprintf(fidfsch_chtc,'Until: 19:00,          !- Field 49\n');
      fprintf(fidfsch_chtc,'%1.3f,          !- Field 50\n',d(19,5));
      fprintf(fidfsch_chtc,'Until: 20:00,          !- Field 51\n');
      fprintf(fidfsch_chtc,'%1.3f,          !- Field 52\n',d(20,5));
      fprintf(fidfsch_chtc,'Until: 21:00,          !- Field 53\n');
      fprintf(fidfsch_chtc,'%1.3f,          !- Field 54\n',d(21,5));
      fprintf(fidfsch_chtc,'Until: 22:00,          !- Field 55\n');
      fprintf(fidfsch_chtc,'%1.3f,          !- Field 56\n',d(22,5));
      fprintf(fidfsch_chtc,'Until: 23:00,          !- Field 57\n');
      fprintf(fidfsch_chtc,'%1.3f,          !- Field 58\n',d(23,5));
      fprintf(fidfsch_chtc,'Until: 24:00,          !- Field 59\n');
      fprintf(fidfsch_chtc,'%1.3f,          !- Field 60\n',d(24,5));
      fprintf(fidfsch_chtc,'Through: 12/31,        !- Field 61\n');
      fprintf(fidfsch_chtc,'For: AllDays,          !- Field 62\n');
      fprintf(fidfsch_chtc,'Until: 24:00,          !- Field 63\n');
      fprintf(fidfsch_chtc,'0.1;                 !- Field 64\n\n');
      end
  end
end
    fclose(fidfsch_chtc);
Schedule_chtc = 1;

function[chtc_1] = read_pre(ARR_zname,x)
fr = load('prechtc.txt');
bindex = [1;2;3;4;5;6;7;8;9];
o = [1 0 1 0;1 0 1 0;1 0 1 0;1 0 1 0;1 0 1 0;1 0 1 0;1 0 1 0;1 0 1
0;1 0 1 0];
for i=1:1:x
    a = ARR_zname(i,:);
    [~,b]=size(a);
    n = o(i,:);
    n = n(n~=0);
    [~,nn] = size(n);
    sn(i,:)= nn*b+b*4+2;
end
for i= x:-1:1
    a = sn(i,:);
    b = a*(i-1)+2;
    n = o(i,:);
    n = n(n~=0);
    [~,nn] = size(n);
    m = o(i,:);
    c = ARR_zname(i,:);
    [~,d] = size(c);
```

```
    for j = d:-1:1
        rn = nn;
        for k = 4:-1:1
        if m(:,k) == 1
            rn = rn-1;
            e = a*(i-1)+(nn+4)*(j-1)+k+2+rn;
        end
        end
    end
end
for i =1:1:x
    a = ARR_zname(i,:);
    [~,b] = size(a);
    c = b*4*(i-1)+i;
    d = b*4*i+i;
    frr = fr(:,c:d);
    for j = 1:1:b
        e = 4*j-3;
        if j<b
         f = 4*j;
        else
         f = 4*j+1;
        end
        g = frr(:,e:f);
        chtc_1(i,j) = {g};
    end
end

function
[Surface_convection_coefficients]=CHTC(iter_no,fpath,itime_no,ARR_
zname,x)
fidfchtc = fopen(fpath,'a+');
fprintf(fidfchtc,'!-   ===  ALL OBJECTS IN CLASS:
SURFACEPROPERTY:CONVECTIONCOEFFICIENTS ===\n\n');
for i = 1:1:x
  a = ARR_zname(i,:);
  a(cellfun(@isempty,a)) =[];
  [~,m] = size(a);
  b = ARR_zname(i,:);
  for j = 1:1:m
     for k = 1:1:5
     if k < 5

fprintf(fidfchtc,'SurfaceProperty:ConvectionCoefficients,\n');
      fprintf(fidfchtc,'%sS%d,          !- Surface
Name\n',b{1,j},k);
      fprintf(fidfchtc,'Outside,                !- Convection
Coefficient 1 Location\n');
      fprintf(fidfchtc,'Schedule,               !- Convection
Coefficient 1 Type\n');
      fprintf(fidfchtc,',                       !- Convection
Coefficient 1 {W/m2-K}\n');
      fprintf(fidfchtc,'%sS%d-CHTC-%d-%d;       !- Convection
Coefficient 1 Schedule Name\n\n',b{1,j},k,itime_no,iter_no);
     elseif k == 5
      if j == m

fprintf(fidfchtc,'SurfaceProperty:ConvectionCoefficients,\n');
      fprintf(fidfchtc,'%sR,              !- Surface
Name\n',b{1,j});
```

```
      fprintf(fidfchtc,'Outside,                    !- Convection
Coefficient 1 Location\n');
      fprintf(fidfchtc,'Schedule,                   !- Convection
Coefficient 1 Type\n');
      fprintf(fidfchtc,',                           !- Convection
Coefficient 1 {W/m2-K}\n');
      fprintf(fidfchtc,'%sR-CHTC-%d-%d;             !- Convection
Coefficient 1 Schedule Name\n\n',b{1,j},itime_no,iter_no);
      end
     end
     end
  end
end
fclose(fidfchtc);
Surface_convection_coefficients = 1;


2.
%% Fluent Journal Generator
%This code is to generate the journal to be read in Fluent to
setup
%the boundary conditions, run the simulation and export the
results.
%This code also creates the weather profiles to present the
vertical
%profile of wind speed components and temperature.

%% Read the surface temperature from EnergyPlus results
[st_fs,st_bs,o,fname]=Surface_T(ARR_zname,x,iter_no, itime_no);
%% Read the weather data
[xf,yf,fin,fout,fsym,wf,~] = weather_profile(itime_no);
%% Make directories
stsave = fullfile('E:','AIJ_LA','FLUENT','journal');
hfsave = fullfile('E:','AIJ_LA','FLUENT','heat flux');
if iter_no == 0
mkdir(stsave,fname);
mkdir(hfsave,fname);
mkdir('FLUENT\casedata',fname);
end
sl = strcat('\');
readj = strcat(stsave,'\ReadJournal.jou');
%% Journal to read setup journal
pfname = strcat(stsave,'\',fname,'\','J_T',num2str(time),'-
',num2str(iter_no),'.jou');
frj = fopen(readj,'wt');
fprintf(frj,'"E:%sAIJ_LA%sFLUENT%sjournal%stime_%d%sJ_T%d-%d.jou"'
,sl,sl,sl,sl,sl,sl,sl,time,sl,time,iter_no);
fclose(frj);
%% Journal to set up the case (sc)
fsc = fopen(pfname,'wt');
fprintf(fsc,'file/read-case/"E:%sAIJ_LA%sFLUENT-
2%smesh%sm1.cas"\ny\n',sl,sl,sl,sl,sl,sl,sl);
fprintf(fsc,'file/read-profile/"E:%sAIJ_LA%sweather
profiles%sEps_%d.txt"\n',sl,sl,sl,sl,sl,sl,time);
fprintf(fsc,'file/read-profile/"E:%sAIJ_LA%sweather
profiles%sTa_%d.txt"\n',sl,sl,sl,sl,sl,sl,time);
fprintf(fsc,'file/read-profile/"E:%sAIJ_LA%sweather
profiles%sTke_%d.txt"\n',sl,sl,sl,sl,sl,sl,time);
fprintf(fsc,'file/read-profile/"E:%sAIJ_LA%sweather
profiles%sWs_%d.txt"\n',sl,sl,sl,sl,sl,sl,time);
for i = 1:1:4
```

```
    in = strcat(fin(i,1),fin(i,2));
    out = strcat(fout(i,1),fout(i,2));
    fprintf(fsc,'define/boundary-conditions/zone-type fetch%s
velocity-inlet\n',in);
    fprintf(fsc,'define/boundary-conditions/zone-type fetch%s
pressure-outlet\n',out);
    fprintf(fsc,'define/boundary-conditions/velocity-inlet fetch%s
y y y n vel%d velz-%d n 0 y n %1.3f n %1.3f n 0 y n ta%d taz-%d y
y n tke%d tkez-%d y n eps%d
epsz-%d\n',in,time,time,xf,yf,time,time,time,time,time,time);
    fprintf(fsc,'define/boundary-conditions/pressure-outlet
fetch%s y n 0 y n ta%d taz-%d y y n %1.3f n %1.3f n 0 y y n tke%d
tkez-%d y n eps%d epsz-%d n y n y n\n',out,time,time,-xf,-
yf,time,time,time,time);
end
for i = 1:1:8
    sym = strcat(fsym(i,1),fsym(i,2));
    fprintf(fsc,'define/boundary-conditions/wall fetch%s 0 n 0 n n
y n ta%d taz-%d n n n n 0 n 0.5 n 1\n',sym,time,time);
end
for i=1:1:x
    a = ARR_zname(i,:);
    [~,b] = size(a);
    for j = 1:1:b
        ss = 4*(j-1);
       for k = 1:1:4
          stt = st_bs(i,ss+k)+273.15;
          fprintf(fsc,'define/boundary-conditions/wall %sS%d 0 n 0
n n n %1.2f n n n n 0 n 0.5 n 1\n',strcat(a{j}),k,stt);
       end
    end
    srt = st_bs(i,b*4+1)+273.15;
    fprintf(fsc,'define/boundary-conditions/wall %sR 0 n 0 n n
n %1.2f n n n n 0 n 0.5 n 1\n',strcat(a{b}),srt);
end
for i = 1:1:x
    a = ARR_zname(i,:);
    [~,b]=size(a);
    n = o(i,:);
    n = n(n~=0);
    [~,nn]=size(n);
    m = o(i,:);
    for j = 1:1:b
        fss = 1+nn*(b-1);
        fss1 = fss;
        for k = 1:1:4
            if m (:,k)==1
              fss1 = fss1+1;
              fst = st_fs(i,fss1)+273.15;
              fprintf(fsc,'define/boundary-conditions/wall %sS%dW
0 n 0 n n n %1.2f n n n n 0 n 0.5 n 1\n',strcat(a{j}),k,fst);
            end
        end
    end
    sdt = st_fs(i,1);
    fprintf(fsc,'define/boundary-conditions/wall B%dD 0 n 0 n n
n %1.2f n n n n 0 n 0.5 n 1\n',i,sdt+273.15);
end
ini = strcat(fin(3,1),fin(3,2));
fprintf(fsc,'solve/initialize/compute-defaults/velocity-inlet
fetch%s \n',ini);
```

```
fprintf(fsc,'solve/initialize/initialize-flow\n');
fclose(fsc);
%%Journal to export heat flux
expj = strcat(stsave,'\Export.jou');
fexp = fopen(expj,'wt');
sid = '179  178 177 176 131 129 128 126 125 123 122 120 175 174
173 172 171 116 114 113 111 110 108 107 105 170 169 168 167 166
101 99  98  96  95  93  92  90  165 164 163 162 161 86  84  83  81
80  78  77  75  160 159 158 157 156 71  69  68  66  65  63  62  60
155 154 153 152 151 56  54  53  51  50  48  47  45  150 149 148
147 146 40  39  38  36  35  33  32  30  145 29  144 28  143 25  23
22  20  19  17  16  14  142 141 140 139 138 12  10  9   7   6   4
3   1   137';
fprintf(fexp,'report/surface-integrals/area-weighted-avg %s ()
heat-flux y "E:%sAIJ_LA%sFLUENT%sheat flux%stime_%d%sheat-
flux-%d.txt"\n',sid,sl,sl,sl,sl,sl,sl,sl,time,sl,iter_no);
fprintf(fexp,'file/write-case-data/
"E:%sAIJ_LA%sFLUENT%scasedata%stime_%d%sCdata-%d-%d.cas"\n',sl,sl,
sl,sl,sl,sl,sl,time,sl,time,iter_no);
fclose(fexp);


function
[st_fs,st_bs,o,fname]=Surface_T(x,ARR_zname,itime_no,iter_no)
loadf = input('Only load? ');
fname = strcat('time_',num2str(itime_no));
eresults = strcat('AIJ
IDF_2\',fname,'\iter_',num2str(iter_no),'.csv');
st = csvread(eresults,1,1);
o = [1 0 1 0;1 0 1 0;1 0 1 0;1 0 1 0;1 0 1 0;1 0 1 0;1 0 1 0;1 0 1
0;1 0 1 0];
ts = 0;
for i = 1:1:x
    a = ARR_zname(i,:);
    [~,b] = size(a);
    ln (:,i) = b;
    n = o(i,:);
    n = n(n~=0);
    [~,nn] = size(n);
    sn(i,:) = nn*b+b*7+1; %number of surfaces of each building
end
su = sum(sn);
sln = sum(ln);
b = su;
e = su;
for i=x:-1:1
    a = sn(i,:); %number of surfaces of building_i
    n = o(i,:);
    n = n(n~=0); %exclude surfaces without building
    [~,nn] = size(n); %number of windows on each floor of
building_i
    c = ARR_zname(i,:);
    [~,d] = size(c); %number of stories of building_i
    e = e-a;
    for j = d:-1:1
        f = e+(7+nn)*(j-1)+1;
        st(:,f+nn+7) = [];
        if j<d
            st(:,f+nn+6) = [];
        end
        st(:,f+nn+5) = [];
```

```
    end
end
conv_stsave = fullfile('E:','AIJ_LA','Convergence','Ts');
dname =
strcat(conv_stsave,'\',fname,'\Ts_iter_',num2str(iter_no),'.txt');
if loadf == 0
    if iter_no == 0
    mkdir(conv_stsave,fname);
    end
    dlmwrite(dname,st,'\t');
end
for i = 1:1:x
    a = ARR_zname(i,:);
    [~,b]=size(a);
    ln (:,i)=b;
    n = o(i,:);
    n = n(n~=0);
    [~,nn] = size(n);
    nsn(i,:) = nn*b+b*4+2; %number of surfaces of each building
end
nsu = sum(nsn);
b = nsu;
e = nsu;
y = max(ln);
st_bs = zeros(x,y*4+1);
for i = x:-1:1
    a = nsn(i,:); %number of surfaces of building_i
    b =  b-a+2; %position of door surface
    n = o(i,:);
    n = n(n~ = 0); %exclude surfaces without building
    [~,nn] = size(n); %number of windows on each floor of
building_i
    m = o(i,:);
    c = ARR_zname(i,:);
    [~,d]=size(c);
    wsn(i,:) = nn*d;
    e = e-a;
    for j = d:-1:1
        f  = e + (nn+4)*(j-1)+1;
        rn = nn;
        if j ==d
            sr = e+a;
            st_bs(i,d*4+1) = st(1,sr);
            st(:,sr)=[];
        end
      for k = 4:-1:1
        if m(:,k)==1
            rn = rn -1;
        end
        if j ==1 && k ==1
            sk = f;
          else
                sk = f+rn+k;
        end
         st_bs(i,4*(j-1)+k)=st(1,sk);
         st(:,sk)=[];
      end
    end
end
z = max(wsn);
st_fs = zeros(x,z+1);
```

```
[~,e]= size(st);
for i = x:-1:1
    c = ARR_zname(i,:);
    [~,d]=size(c);
    n = n(n~=0); %exclude surfaces without building
    [~,nn]=size(n); %number of windows on each floor of building_i
    a = nn*d+1;
    e = e-a;
    for j = d:-1:1
        for k =nn:-1:1
        st_fs(i,nn*(j-1)+1+k)=st(1,e+nn*(j-1)+1+k);
        st(:,e+1+nn*(j-1)+k)=[];
        end
        if j ==1
        st_fs(i,1)= st(1,e+1);
        st(:,e+1)=[];
        end
    end
end

function [xf,yf,fin,fout,fsym,wf]=weather_profile(itime_no)
load('weather.txt');
BHeight = [10;10;10;10;10;10;10;10;10];
z = max(BHeight);
zf = [0.05;0.1;0.15;0.25;0.35;0.5;0.75;1;1.25;1.5;1.75;2;3;4;5;6];
x = 0*zf;
y = 0*zf;
z = z*zf;
Ta = weather(itime_no,1);
v = weather(itime_no,2);
wd = weather(itime_no,3);
Tb = Ta+0.0065*6356000*1.5/(6356000+1.5);
Hz = 6356000*z./(6356000+z);
Taz = Tb-0.0065*Hz+273.15;
vz = v*(27.^0.14).*((z/460).^0.33);
Iz = 0.1*((z/460).^0.33);
kz = 1.5*((Iz.*vz).^2);
epsz = 0.3*0.33*kz.*(v/1.5).*((z/1.5).^(0.33-1));
fetch=['01';'02';'03';'04';'05';'06';'07';'08';'09';'10';'11';'12'
;'13';'14';'15';'16'];
if itime_no ==1
mkdir('weather profiles');
end
wf=fullfile('E:','AIJ_LA','weather profiles');
%% Air Temperature
fname = strcat(wf,'/','Ta_',num2str(itime_no),'.txt');
fat = fopen(fname,'wt');
fprintf(fat,'((ta%d point 16)\n(x\n',itime_no);
fprintf(fat,'%d\n',x);
fprintf(fat,')\n(y\n');
fprintf(fat,'%d\n',y);
fprintf(fat,')\n(z\n');
fprintf(fat,'%1.2f\n',z);
fprintf(fat,')\n(taz-%d\n',itime_no);
fprintf(fat,'%1.2f\n',Taz);
fprintf(fat,')\n)');
fclose(fat);
%% Wind Speed
fname = strcat(wf,'/','Ws_',num2str(itime_no),'.txt');
fws = fopen(fname,'wt');
fprintf(fws,'((vel%d point 16)\n(x\n',itime_no);
```

```
fprintf(fws,'%d\n',x);
fprintf(fws,')\n(y\n');
fprintf(fws,'%d\n',y);
fprintf(fws,')\n(z\n');
fprintf(fws,'%1.2f\n',z);
fprintf(fws,')\n(velz-%d\n',itime_no);
fprintf(fws,'%1.3f\n',vz);
fprintf(fws,')\n)');
fclose(fws);
% TKE
fname = strcat(wf,'/','Tke_',num2str(itime_no),'.txt');
ftke = fopen(fname,'wt');
fprintf(ftke,'((tke%d point 16)\n(x\n',itime_no);
fprintf(ftke,'%d\n',x);
fprintf(ftke,')\n(y\n');
fprintf(ftke,'%d\n',y);
fprintf(ftke,')\n(z\n');
fprintf(ftke,'%1.2f\n',z);
fprintf(ftke,')\n(tkez-%d\n',itime_no);
fprintf(ftke,'%1.3f\n',kz);
fprintf(ftke,')\n)');
fclose(ftke);
% Epsilon
fname = strcat(wf,'/','Eps_',num2str(itime_no),'.txt');
feps = fopen(fname,'wt');
fprintf(feps,'((eps%d point 16)\n(x\n',itime_no);
fprintf(feps,'%d\n',x);
fprintf(feps,')\n(y\n');
fprintf(feps,'%d\n',y);
fprintf(feps,')\n(z\n');
fprintf(feps,'%1.2f\n',z);
fprintf(feps,')\n(epsz-%d\n',itime_no);
fprintf(feps,'%1.3f\n',epsz);
fprintf(feps,')\n)');
fclose(feps);
%% Wind Direction
if (0<=wd&&wd<22.5)|| (180<=wd&&wd<202.5)
    if 0<=wd&&wd<22.5
    fin = ['15';'16';'01';'02'];
    fout = ['07';'08';'09';'10'];
    else
    fout = ['15';'16';'01';'02'];
    fin = ['07';'08';'09';'10'];
    end
elseif (22.5<=wd&&wd<45)|| (202.5<=wd&&wd<225)
    if 22.5<=wd&&wd<45
    fin = ['16';'01';'02';'03'];
    fout = ['08';'09';'10';'11'];
    else
    fout = ['16';'01';'02';'03'];
    fin = ['08';'09';'10';'11'];
    end
elseif (45<=wd&&wd<67.5)|| (225<=wd&&wd<247.5)
    if 45<=wd&&wd<67.5
    fin = ['01';'02';'03';'04'];
    fout = ['09';'10';'11';'12'];
    else
    fout = ['01';'02';'03';'04'];
    fin = ['09';'10';'11';'12'];
    end
elseif (67.5<=wd&&wd<90)|| (247.5<=wd&&wd<270)
```

```
    if 67.5<=wd&&wd<90
    fin = ['02';'03';'04';'05'];
    fout = ['10';'11';'12';'13'];
    else
    fout = ['02';'03';'04';'05'];
    fin = ['10';'11';'12';'13'];
    end
elseif (90<=wd&&wd<112.5)|| (270<=wd&&wd<292.5)
    if 90<=wd&&wd<112.5
    fin = ['03';'04';'05';'06'];
    fout = ['11';'12';'13';'14'];
    else
    fout = ['03';'04';'05';'06'];
    fin = ['11';'12';'13';'14'];
    end
elseif (112.5<=wd&&wd<135)|| (292.5<=wd&&wd<315)
    if 112.5<=wd&&wd<135
    fin = ['04';'05';'06';'07'];
    fout = ['12';'13';'14';'15'];
    else
    fout = ['04';'05';'06';'07'];
    fin = ['12';'13';'14';'15'];
    end
elseif (135<=wd&&wd<157.5)|| (315<=wd&&wd<337.5)
    if 135<=wd&&wd<157.5
    fin = ['05';'06';'07';'08'];
    fout = ['13';'14';'15';'16'];
    else
    fin = ['05';'06';'07';'08'];
    fout = ['13';'14';'15';'16'];
    end
else
    if 157.5<=wd&&wd<180
    fin = ['06';'07';'08';'09'];
    fout = ['14';'15';'16';'01'];
    else
    fout = ['06';'07';'08';'09'];
    fin = ['14';'15';'16';'01'];
    end
end
fsym = fetch;
for i = 1:1:4
fsym(strmatch(fin(i,:),fsym,'exact'),:)=[];
fsym(strmatch(fout(i,:),fsym,'exact'),:)=[];
end
xf = -sin(wd*pi/180);
yf = -cos(wd*pi/180);


3.
%% Convergence Checker
%This code is to calculate the new h* and check the convergence.

sheight = [3.4 3.3 3.3;3.4 3.3 3.3;3.4 3.3 3.3;3.4 3.3 3.3;3.4 3.3
3.3;3.4 3.3 3.3;3.4 3.3 3.3;3.4 3.3 3.3;3.4 3.3 3.3];
BHeight = [10;10;10;10;10;10;10;10;10];
load('weather.txt');
Ta = weather(:,1);
Tb = Ta+0.0065*6356000*1.5/(6356000+1.5);

%% Load the original chtc by EnergyPlus DOE-2
```

```
chtc_2 =preli(x,ARR_zname);
ff = strcat('E:\AIJ_LA\FLUENT\heat flux\',fname,'\heat-flux-
',num2str(iter_no),'.txt');
fhtc = fopen(ff,'r');
flux_s = textscan(fhtc,'%s');
flux_s = flux_s{1,1};
flux_s = flux_s(13:248,:);
fclose(fhtc);
for i=1:1:117
    fxs = flux_s{2*i};
    fxs = strcat(fxs);
    flux_l(i) = str2num(fxs);
end
for i =1:1:x
     a = ARR_zname(i,:);
    [~,b]=size(a);
    ln(:,i) = b;
    nst(:,i) = b*4+1;
end
ind = 0;
CHTC = chtc_2;
%% Check if the new h*s are within the range
for i = 1:1:x
    a = ARR_zname(i,:);
    [~,b]=size(a);
    sh = 0;
    nstp = nst(:,i);
    for j = 1:1:b
        sh = sheight(i,j)+sh;
        shc = sh - sheight(i,j)/2;
        Hsh = 6356000*shc./(6356000+shc);
        tas = Tb(itime_no)-0.0065*Hsh;
        dts = st_bs(i,4*j-3:4*j)-tas;
        schtc1 = chtc_2(i,j);
        schtc = schtc1{1,1};
        flux_z = flux_l(1,ind+4*j-3:ind+4*j);
        for k = 1:1:4
            if flux_z(k)/dts(k)<0.1
                schtc(itime_no,k) = 0.1;
            elseif flux_z(k)/dts(k)>10*schtc(itime_no,k)
            elseif flux_z(k)/dts(k)>1000
                schtc(itime_no,k) = 1000;
            else
        schtc(itime_no,k) = flux_z(k)/dts(k);
            end
        end
        if j == b
            rh = BHeight(i);
            Hrh = 6356000*rh./(6356000+rh);
            tar= Tb(itime_no)-0.0065*Hrh;
            dtr = st_bs(i,nstp)-tar;
            if flux_l(1,ind+nstp)/dtr<0.1
                schtc(itime_no,5)=0.1;
            elseif flux_l(1,ind+nstp)/dtr>10*schtc(itime_no,5)
            elseif flux_l(1,ind+nstp)/dtr>1000
                schtc(itime_no,5)=1000;
            else
                schtc(itime_no,5)= flux_l(1,ind+nstp)./dtr;
            end
        end
        schtc1 = {schtc};
```

```
        CHTC(i,j)=schtc1;
        chtc_bu (i,j) = schtc1;
    end
ind = ind + nstp;
end
convname = fullfile('E:','AIJ_LA','Convergence','chtc backup');
if iter_no ==0
    mkdir(convname,fname);
end
matsave =
strcat(convname,'\',fname,'\eg_',num2str(iter_no),'.mat');
chtcsave = strcat('updated_chtc.mat');
save(matsave,'chtc_bu');
%% Check if converged
if iter_no >0
[conv,iter_fix] = converged(convname,matsave,fname);
else
f = load('Inputs.txt');
finput = fopen('Inputs.txt','wt');
fprintf(finput,'%d\n%d\n%d\n%d\n',f(1),f(2),f(3)+1,f(4));
fclose(finput);
end
%% Number of iteration required to achive convergence
p = load('Convergence\Converged iteration.txt');
if iter_no>0 && iter_fix >0
    p(itime_no)=iter_fix;
    dlmwrite('Convergence\Converged iteration.txt',p,'\t');
end
%% Assign the obtained chtc for period before the 'time'
if itime_no>1
ac = load('Convergence\converged chtc.mat');
acn = ac.e;
ac1 = load(matsave);
acn1 = ac1.chtc_bu;
    for i = 1:1:x
    a = ARR_zname(i,:);
    [~,b]=size(a);
    for j = 1:1:b
        acc = acn{i,j};
        acc2 = acn1{i,j};
        for t = 1:1:itime_no-1
        if j <b
        mod = acc(t,1:4);
        acc2(t,1:4) = mod;
        else
        mod = acc(t,1:5);
        acc2(t,1:5) = mod;
        end
        end
        chtc_bu{i,j}=acc2;
    end
    end
end
save('Convergence\newchtc.mat','chtc_bu');

function [chtc_2]=preli(x,ARR_zname)
fr=load('prechtc1.txt');
bindex=[1;2;3;4;5;6;7;8;9];
o = [1 0 1 0;1 0 1 0;1 0 1 0;1 0 1 0;1 0 1 0;1 0 1 0;1 0 1 0;1 0 1
0;1 0 1 0];
ts=0;
```

```
for i=1:1:x
    a = ARR_zname(i,:);
    [~,b]=size(a);
    n = o(i,:);
    n = n(n~=0);
    [~,nn]=size(n);
    sn(i,:)=nn*b+b*4+2;
end
for i=x:-1:1
    a = sn(i,:);
    b = a*(i-1)+2;
    n = o(i,:);
    n = n(n~=0);
    [~,nn]=size(n);
    m = o(i,:);
    c = ARR_zname(i,:);
    [~,d]=size(c);
    for j = d:-1:1
        rn=nn;
        for k = 4:-1:1
        if m(:,k)==1
            rn=rn-1;
            e = a*(i-1)+(nn+4)*(j-1)+k+2+rn;
            fr(:,e)=[];
        end
        end
    end
    fr(:,b)=[];
end
for i =1:1:x
    a = ARR_zname(i,:);
    [~,b]=size(a);
    c = b*4*(i-1)+i;
    d = b*4*i+i;
    frr = fr(:,c:d);
    for j = 1:1:b
        e = 4*j-3;
        if j<b
         f = 4*j;
        else
         f=4*j+1;
        end
        g=frr(:,e:f);
        chtc_2(i,j)={g};
    end
end

function [conv,iter_fix] = converged(convname,matsave,fname)
f = load('Inputs.txt');
    mdate = f(1);
    ddate = f(2);
    itime_no = f(3);
    iter_no = f(4);
matsave_bf = strcat(convname,'\',fname,'\eg_',num2str(iter_no-
1),'.mat');
if itime_no > 1
    ebf = load('Convergence\converged chtc.mat','e');
    ebf = ebf.e;
end
a = load(matsave);
b = a.chtc_bu;
```

```
q = load(matsave_bf);
c = q.chtc_bu;
cal = 0;
[x,~]=size(c);
d = zeros(2,117);
e =b;
for i = 1:1:x
    xc = c(i,:);
    [~,y]= size(xc);
    for j = 1:1:y
        bb = b{i,j};
        cc = c{i,j};
        for k = 1:1:4
        d(1,cal+k)=bb(itime_no,k);
        d(2,cal+k)=cc(itime_no,k);
        end
        if j ==y
            d(1,cal+4*j+1)=bb(itime_no,5);
            d(2,cal+4*j+1)=cc(itime_no,5);
        end
    end
    cal = cal+4*j+1;
end

if itime_no>1
 b = a.chtc_bu;
  for i = 1:1:x
      xc = b(i,:);
      [~,y]= size(xc);
      for j = 1:1:y
          ee = ebf{i,j};
          bb = b{i,j};
          for t = 1:1:itime_no
             if t < itime_no
             for k = 1:1:4
               c1(t,k)=ee(t,k);
             end
             if j==y
               c1(t,5)=ee(t,5);
             end
             else
               for k = 1:1:4
               c1(t,k)=bb(t,k);
               end
             if j==y
               c1(t,5)=bb(t,5);
             end
             end
          end
          e{i,j} = c1;
      end
   end
end
res = mean(d(1,:)-d(2,:));
res = abs(res);
iter_fix =0;
if res <0.001
    conv = 1;
    iter_fix = iter_no;
    iter_no =0;
    itime_no = itime_no+1;
```

```
    save('Convergence\converged chtc.mat','e');
elseif iter_no >19&&res<0.01
    conv = 1;
    iter_fix = iter_no;
    iter_no =0;
    itime_no = itime_no+1;
    save('Convergence\converged chtc.mat','e')
else
    conv = 0;
    iter_no = iter_no + 1;
end
finput = fopen('Inputs.txt','wt');
fprintf(finput,'%d\n%d\n%d\n%d\n',f(1),f(2),f(3)+1,f(4));
fclose(finput);
display(res);
```

Appendix 2 Test points of AIJ Case C

Table Appx. -1 provides the coordinates of 120 test points (as displayed in *Figure 3-2*).

Table Appx. -1 Coordinates of 120 test points for AIJ Case C

point	position[m]			point	position[m]		
	X	Y	Z		X	Y	Z
4	-0.15	-0.10	0.02	70	0.15	0.10	0.02
5	-0.15	-0.05	0.02	71	0.15	0.05	0.02
6	-0.15	0.00	0.02	72	0.15	0.00	0.02
7	-0.15	0.05	0.02	73	0.15	-0.05	0.02
8	-0.15	0.10	0.02	74	0.15	-0.10	0.02
9	-0.15	0.15	0.02	75	0.15	-0.15	0.02
10	-0.15	0.20	0.02	76	0.15	-0.20	0.02
11	-0.15	0.25	0.02	77	0.15	-0.25	0.02
12	-0.15	0.30	0.02	78	0.15	-0.30	0.02
13	-0.20	-0.10	0.02	79	0.20	0.10	0.02
14	-0.20	-0.05	0.02	80	0.20	0.05	0.02
15	-0.20	0.00	0.02	81	0.20	0.00	0.02
16	-0.20	0.05	0.02	82	0.20	-0.05	0.02
17	-0.20	0.10	0.02	83	0.20	-0.10	0.02
18	-0.20	0.15	0.02	84	0.20	-0.15	0.02
19	-0.20	0.20	0.02	85	0.20	-0.20	0.02
20	-0.20	0.25	0.02	86	0.20	-0.25	0.02
21	-0.20	0.30	0.02	87	0.20	-0.30	0.02
22	-0.25	-0.10	0.02	88	0.25	0.10	0.02
23	-0.25	-0.05	0.02	89	0.25	0.05	0.02
24	-0.25	0.00	0.02	90	0.25	0.00	0.02
25	-0.25	0.05	0.02	91	0.25	-0.05	0.02
26	-0.25	0.10	0.02	92	0.25	-0.10	0.02
27	-0.25	0.15	0.02	93	0.25	-0.15	0.02
28	-0.25	0.20	0.02	94	0.25	-0.20	0.02
29	-0.25	0.25	0.02	95	0.25	-0.25	0.02
30	-0.25	0.30	0.02	96	0.25	-0.30	0.02
31	-0.30	0.15	0.02	97	0.30	-0.15	0.02
32	-0.30	0.20	0.02	98	0.30	-0.20	0.02
33	-0.30	0.25	0.02	99	0.30	-0.25	0.02

38	0.05	-0.15	0.02	103	-0.10	0.15	0.02
39	0.00	-0.15	0.02	104	-0.05	0.15	0.02
40	-0.05	-0.15	0.02	105	0.00	0.15	0.02
41	-0.10	-0.15	0.02	106	0.05	0.15	0.02
42	-0.15	-0.15	0.02	107	0.10	0.15	0.02
43	-0.20	-0.15	0.02	108	0.15	0.15	0.02
44	-0.25	-0.15	0.02	109	0.20	0.15	0.02
45	-0.30	-0.15	0.02	110	0.25	0.15	0.02
47	0.05	-0.20	0.02	111	0.30	0.15	0.02
48	0.00	-0.20	0.02	112	-0.10	0.20	0.02
49	-0.05	-0.20	0.02	113	-0.05	0.20	0.02
50	-0.10	-0.20	0.02	114	0.00	0.20	0.02
51	-0.15	-0.20	0.02	115	0.05	0.20	0.02
52	-0.20	-0.20	0.02	116	0.10	0.20	0.02
53	-0.25	-0.20	0.02	117	0.15	0.20	0.02
54	-0.30	-0.20	0.02	118	0.20	0.20	0.02
56	0.05	-0.25	0.02	119	0.25	0.20	0.02
57	0.00	-0.25	0.02	120	0.30	0.20	0.02
58	-0.05	-0.25	0.02	121	-0.10	0.25	0.02
59	-0.10	-0.25	0.02	122	-0.05	0.25	0.02
60	-0.15	-0.25	0.02	123	0.00	0.25	0.02
61	-0.20	-0.25	0.02	124	0.05	0.25	0.02
62	-0.25	-0.25	0.02	125	0.10	0.25	0.02
63	-0.30	-0.25	0.02	126	0.15	0.25	0.02
64	-0.15	-0.30	0.02	127	0.20	0.25	0.02
65	-0.20	-0.30	0.02	128	0.25	0.25	0.02
66	-0.25	-0.30	0.02	129	0.30	0.25	0.02
67	0.10	-0.15	0.02	130	0.15	0.30	0.02
68	0.10	-0.20	0.02	131	0.20	0.30	0.02
69	0.10	-0.25	0.02	132	0.25	0.30	0.02

Appendix 3 Names of exterior surfaces in coupling models

Table Appx. -2 provides a list of names of building exterior surfaces where information is shared between CFD and BES domains in coupling process.

Table Appx. -2 List of building exterior surfaces' names

Surface name	Position	Surface name	Position
Walls			
B11S1	South wall on the ground floor of B1	B32S1	South wall on the 1st floor of B3
B11S2	East wall on the ground floor of B1	B32S2	East wall on the 1st floor of B3
B11S3	North wall on the ground floor of B1	B32S3	North wall on the 1st floor of B3
B11S4	West wall on the ground floor of B1	B32S4	West wall on the 1st floor of B3
B12S1	South wall on the 1st floor of B1	B33S1	South wall on the 2nd floor of B3
B12S2	East wall on the 1st floor of B1	B33S2	East wall on the 2nd floor of B3
B12S3	North wall on the 1st floor of B1	B33S3	North wall on the 2nd floor of B3
B12S4	West wall on the 1st floor of B1	B41S1	South wall on the ground floor of B4
B13S1	South wall on the 2nd floor of B1	B41S2	East wall on the ground floor of B4
B13S2	East wall on the 2nd floor of B1	B41S3	North wall on the ground floor of B4
B13S3	North wall on the 2nd floor of B1	B41S4	West wall on the ground floor of B4
B13S4	West wall on the 2nd floor of B1	B42S1	South wall on the 1st floor of B4
B21S1	South wall on the ground floor of B2	B42S2	East wall on the 1st floor of B4
B21S2	East wall on the ground floor of B2	B42S3	North wall on the 1st floor of B4
B21S3	North wall on the ground floor of B2	B42S4	West wall on the 1st floor of B4
B21S4	West wall on the ground floor of B2	B43S1	South wall on the 2nd floor of B4
B22S1	South wall on the 1st floor of B2	B43S2	East wall on the 2nd floor of B4
B22S2	East wall on the 1st floor of B2	B43S3	North wall on the 2nd floor of B4
B22S3	North wall on the 1st floor of B2	B43S4	West wall on the 2nd floor of B4
B22S4	West wall on the 1st floor of B2	B51S1	South wall on the ground floor of B5
B23S1	South wall on the 2nd floor of B2	B51S2	East wall on the ground floor of B5
B23S2	East wall on the 2nd floor of B2	B51S3	North wall on the ground floor of B5
B23S3	North wall on the 2nd floor of B2	B51S4	West wall on the ground floor of B5
B23S4	West wall on the 2nd floor of B2	B52S1	South wall on the 1st floor of B5

B31S1	South wall on the ground floor of B2	B52S2	East wall on the 1st floor of B5
B31S2	East wall on the ground floor of B2	B52S3	North wall on the 1st floor of B5
B31S3	North wall on the ground floor of B2	B52S4	West wall on the 1st floor of B5
B31S4	West wall on the ground floor of B2	B53S1	South wall on the 2nd floor of B5
B53S2	East wall on the 2nd floor of B5	B73S4	West wall on the 2nd floor of B7
B53S3	North wall on the 2nd floor of B5	B81S1	South wall on the ground floor of B8
B53S4	West wall on the 2nd floor of B5	B81S2	East wall on the ground floor of B8
B61S1	South wall on the ground floor of B6	B81S3	North wall on the ground floor of B8
B61S2	East wall on the ground floor of B6	B81S4	West wall on the ground floor of B8
B61S3	North wall on the ground floor of B6	B82S1	South wall on the 1st floor of B8
B61S4	West wall on the ground floor of B6	B82S2	East wall on the 1st floor of B8
B62S1	South wall on the 1st floor of B6	B82S3	North wall on the 1st floor of B8
B62S2	East wall on the 1st floor of B6	B82S4	West wall on the 1st floor of B8
B62S3	North wall on the 1st floor of B6	B83S1	South wall on the 2nd floor of B8
B62S4	West wall on the 1st floor of B6	B83S2	East wall on the 2nd floor of B8
B63S1	South wall on the 2nd floor of B6	B83S3	North wall on the 2nd floor of B8
B63S2	East wall on the 2nd floor of B6	B83S4	West wall on the 2nd floor of B8
B63S3	North wall on the 2nd floor of B6	B91S1	South wall on the ground floor of B9
B63S4	West wall on the 2nd floor of B6	B91S2	East wall on the ground floor of B9
B71S1	South wall on the ground floor of B7	B91S3	North wall on the ground floor of B9
B71S2	East wall on the ground floor of B7	B91S4	West wall on the ground floor of B9
B71S3	North wall on the ground floor of B7	B92S1	South wall on the 1st floor of B9
B71S4	West wall on the ground floor of B7	B92S2	East wall on the 1st floor of B9
B72S1	South wall on the 1st floor of B7	B92S3	North wall on the 1st floor of B9
B72S2	East wall on the 1st floor of B7	B92S4	West wall on the 1st floor of B9
B72S3	North wall on the 1st floor of B1	B93S1	South wall on the 2nd floor of B9
B72S4	West wall on the 1st floor of B1	B93S2	East wall on the 2nd floor of B9
B73S1	South wall on the 2nd floor of B1	B93S3	North wall on the 2nd floor of B9
B73S2	East wall on the 2nd floor of B1	B93S4	West wall on the 2nd floor of B9
B73S3	North wall on the 2nd floor of B1		

Fenestrations

B1D	Entrance door of B1	B5D	Entrance door of B5
B11S1W	Window on B11S1W	B51S1W	Window on B51S1W
B11S3W	Window on B11S3W	B51S3W	Window on B51S3W

B12S1W	Window on B12S1W	B52S1W	Window on B52S1W
B12S3W	Window on B12S3W	B52S3W	Window on B52S3W
B13S1W	Window on B13S1W	B53S1W	Window on B53S1W
B13S3W	Window on B14S3W	B53S3W	Window on B54S3W
B2D	Entrance door of B2	B6D	Entrance door of B6
B21S1W	Window on B21S1W	B61S1W	Window on B61S1W
B21S3W	Window on B21S3W	B61S3W	Window on B61S3W
B22S1W	Window on B22S1W	B62S1W	Window on B62S1W
B22S3W	Window on B22S3W	B62S3W	Window on B62S3W
B23S1W	Window on B23S1W	B63S1W	Window on B63S1W
B23S3W	Window on B24S3W	B63S3W	Window on B64S3W
B3D	Entrance door of B3	B7D	Entrance door of B7
B31S1W	Window on B31S1W	B71S1W	Window on B71S1W
B31S3W	Window on B31S3W	B71S3W	Window on B71S3W
B32S1W	Window on B32S1W	B72S1W	Window on B72S1W
B32S3W	Window on B32S3W	B72S3W	Window on B72S3W
B33S1W	Window on B33S1W	B73S1W	Window on B73S1W
B33S3W	Window on B34S3W	B73S3W	Window on B74S3W
B4D	Entrance door of B4	B8D	Entrance door of B8
B41S1W	Window on B41S1W	B81S1W	Window on B81S1W
B41S3W	Window on B41S3W	B81S3W	Window on B81S3W
B42S1W	Window on B42S1W	B82S1W	Window on B82S1W
B42S3W	Window on B42S3W	B82S3W	Window on B82S3W
B43S1W	Window on B43S1W	B83S1W	Window on B83S1W
B43S3W	Window on B44S3W	B83S3W	Window on B84S3W
B9D	Entrance door of B9	B92S3W	Window on B92S3W
B91S1W	Window on B91S1W	B93S1W	Window on B93S1W
B91S3W	Window on B91S3W	B93S3W	Window on B94S3W
B92S1W	Window on B92S1W		

Roofs

B13R (B11R)	Roof of B1	B63R (B61R)	Roof of B6
B23R (B21R)	Roof of B2	B73R (B71R)	Roof of B7

B33R (B31R)	Roof of B3	B83R (B81R)	Roof of B8
B43R (B41R)	Roof of B4	B93R (B91R)	Roof of B9
B53R	Roof of B5		

Appendix 4 EnergyPlus *IDF file for short-term modelling of sealed B5 without applying the coupling method

The followings are the contents of the original EnergyPlus *IDF file for the example case of short-term sealed buildings without applying the coupled CHTCs. Therefore, only B5 among nine buildings is provided in this appendix rather than all for concise.

```
!-Generator IDFEditor 1.49
!-Option SortedOrder

!-NOTE: All comments with '!-' are ignored by the IDFEditor and are generated automatically.
!-     Use '!' comments if they need to be retained when using the IDFEditor.

!-   === ALL OBJECTS IN CLASS: VERSION ===Version,
    8.7;                                    !- Version Identifier

!-        ===     ALL     OBJECTS     IN     CLASS: SIMULATIONCONTROL ===
SimulationControl,
    No,                     !- Do Zone Sizing Calculation
    No,                     !- Do System Sizing Calculation
    No,                     !- Do Plant Sizing Calculation
    No,                     !- Run Simulation for Sizing Periods
    Yes;                    !- Run Simulation for Weather File Run Periods

!-   === ALL OBJECTS IN CLASS: BUILDING ===
Building,
    Untitled,                               !- Name
    0.0,                                    !- North Axis {deg}
    City,                                   !- Terrain
    0.04,                   !- Loads Convergence Tolerance Value
    0.4,                    !- Temperature Convergence Tolerance Value {deltaC}
    FullInteriorAndExterior,        !- Solar Distribution
    25,                     !- Maximum Number of Warmup Days
    6;                      !- Minimum Number of Warmup Days

!-        ===     ALL     OBJECTS     IN     CLASS: SHADOWCALCULATION ===
ShadowCalculation,
    AverageOverDaysInFrequency,     !- Calculation Method
    1,                              !- Calculation Frequency
    15000;                  !- Maximum Figures in Shadow Overlap Calculations

!-        ===ALL     OBJECTS     IN     CLASS: SURFACECONVECTIONALGORITHM:INSIDE ===
SurfaceConvectionAlgorithm:Inside,
    TARP;                                   !- Algorithm

!-        ===     ALL     OBJECTS     IN     CLASS: SURFACECONVECTIONALGORITHM:OUTSIDE ===
SurfaceConvectionAlgorithm:Outside,
    DOE-2;                                  !- Algorithm

!-        ===     ALL     OBJECTS     IN     CLASS: HEATBALANCEALGORITHM ===
HeatBalanceAlgorithm,
    ConductionTransferFunction,     !- Algorithm
    200,    !- Surface Temperature Upper Limit {C}
    0.1,    !- Minimum Surface Convection Heat Transfer Coefficient Value {W/m2-K}
    1000;   !- Maximum Surface Convection Heat Transfer Coefficient Value {W/m2-K}

!-   === ALL OBJECTS IN CLASS: TIMESTEP ===
Timestep,
    1;                      !- Number of Timesteps per Hour

!-        ===     ALL     OBJECTS     IN     CLASS: SITE:LOCATION ===
Site:Location,
    USA CA-LOS ANGELES,                     !- Name
    33.92,                          !- Latitude {deg}
    -118.40,                        !- Longitude {deg}
    -8.00,                          !- Time Zone {hr}
    32;                             !- Elevation {m}

!-        ===     ALL     OBJECTS     IN     CLASS: SIZINGPERIOD:DESIGNDAY ===
SizingPeriod:DesignDay,
    LA Ann Summer,                          !- Name
    8,                                      !- Month
    21,                             !- Day of Month
    SummerDesignDay,                        !- Day Type
    25.5,   !- Maximum Dry-Bulb Temperature {C}
    6,      !- Daily Dry-Bulb Temperature Range {deltaC}
    DefaultMultipliers,     !- Dry-Bulb Temperature Range Modifier Type
    ,       !- Dry-Bulb Temperature Range Modifier Day Schedule Name
    Wetbulb,                !- Humidity Condition Type
    21.1,   !- Wetbulb or DewPoint at Maximum Dry-Bulb {C}
    ,   !- Humidity Condition Day Schedule Name
    ,       !- Humidity Ratio at Maximum Dry-Bulb {kgWater/kgDryAir}
    ,       !- Enthalpy at Maximum Dry-Bulb {J/kg}
```

```
   ,!- Daily Wet-Bulb Temperature Range {deltaC}
   100941,                 !- Barometric Pressure {Pa}
   4.2,                    !- Wind Speed {m/s}
   250,                    !- Wind Direction {deg}
   No,                     !- Rain Indicator
   No,                     !- Snow Indicator
   No,              !- Daylight Saving Time Indicator
   ASHRAEClearSky,      !- Solar Model Indicator
   ,                !- Beam Solar Day Schedule Name
   ,              !- Diffuse Solar Day Schedule Name
   ,         !- ASHRAE Clear Sky Optical Depth for
Beam Irradiance (taub) {dimensionless}
   ,         !- ASHRAE Clear Sky Optical Depth for
Diffuse Irradiance (taud) {dimensionless}
   1;                      !- Sky Clearness

SizingPeriod:DesignDay,
   LA Ann Winter,          !- Name
   1,                      !- Month
   21,                     !- Day of Month
   WinterDesignDay,        !- Day Type
   6.6,      !- Maximum Dry-Bulb Temperature {C}
   0,          !- Daily Dry-Bulb Temperature Range
{deltaC}
   DefaultMultipliers,      !- Dry-Bulb Temperature
Range Modifier Type
   ,       !- Dry-Bulb Temperature Range Modifier
Day Schedule Name
   Wetbulb,              !- Humidity Condition Type
   6.6,         !- Wetbulb or DewPoint at Maximum
Dry-Bulb {C}
   ,     !- Humidity Condition Day Schedule Name
   ,          !- Humidity Ratio at Maximum Dry-Bulb
{kgWater/kgDryAir}
   ,         !- Enthalpy at Maximum Dry-Bulb {J/kg}
   ,           !- Daily Wet-Bulb Temperature Range
{deltaC}
   100941,              !- Barometric Pressure {Pa}
   2.5,                 !- Wind Speed {m/s}
   80,                  !- Wind Direction {deg}
   No,                  !- Rain Indicator
   No,                  !- Snow Indicator
   No,              !- Daylight Saving Time Indicator
   ASHRAEClearSky,      !- Solar Model Indicator
   ,                !- Beam Solar Day Schedule Name
   ,              !- Diffuse Solar Day Schedule Name
   ,         !- ASHRAE Clear Sky Optical Depth for
Beam Irradiance (taub) {dimensionless}
   ,         !- ASHRAE Clear Sky Optical Depth for
Diffuse Irradiance (taud) {dimensionless}
   0;                      !- Sky Clearness

!-  === ALL OBJECTS IN CLASS: RUNPERIOD
===
RunPeriod,
   runtime,                !- Name
   9,                      !- Begin Month
   24,                     !- Begin Day of Month
   9,                      !- End Month
   25,                     !- End Day of Month
   UseWeatherFile,  !- Day of Week for Start Day
   No,              !- Use Weather File Holidays and
Special Days
   No,          !- Use Weather File Daylight Saving
Period
   No,              !- Apply Weekend Holiday Rule
   Yes,          !- Use Weather File Rain Indicators
   Yes,     !- Use Weather File Snow Indicators
   1.0000;    !- Number of Times Runperiod to be
Repeated

!-        ===        ALL        OBJECTS        IN        CLASS:
RUNPERIODCONTROL:SPECIALDAYS ===
RunPeriodControl:SpecialDays,
   New Years Day,          !- Name
   January 1,              !- Start Date
   1,                      !- Duration {days}
   Holiday;                !- Special Day Type

RunPeriodControl:SpecialDays,
   Veterans Day,           !- Name
   November 11,            !- Start Date
   1,                      !- Duration {days}
   Holiday;                !- Special Day Type

RunPeriodControl:SpecialDays,
   Christmas,              !- Name
   December 25,            !- Start Date
   1,                      !- Duration {days}
   Holiday;                !- Special Day Type

RunPeriodControl:SpecialDays,
   Independence Day,       !- Name
   July 4,                 !- Start Date
   1,                      !- Duration {days}
   Holiday;                !- Special Day Type

RunPeriodControl:SpecialDays,
   MLK Day,                !- Name
   3rd Monday in January,  !- Start Date
   1,                      !- Duration {days}
   Holiday;                !- Special Day Type

RunPeriodControl:SpecialDays,
   Presidents Day,         !- Name
   3rd Monday in February, !- Start Date
   1,                      !- Duration {days}
   Holiday;                !- Special Day Type

RunPeriodControl:SpecialDays,
   Memorial Day,           !- Name
   Last Monday in May,     !- Start Date
   1,                      !- Duration {days}
   Holiday;                !- Special Day Type

RunPeriodControl:SpecialDays,
   Labor Day,              !- Name
   1st Monday in September,!- Start Date
   1,                      !- Duration {days}
   Holiday;                !- Special Day Type

RunPeriodControl:SpecialDays,
   Columbus Day,           !- Name
   2nd Monday in October,  !- Start Date
   1,                      !- Duration {days}
   Holiday;                !- Special Day Type

RunPeriodControl:SpecialDays,
   Thanksgiving,           !- Name
```

```
   4th Thursday in November,      !- Start Date
   1,                             !- Duration {days}
   Holiday;                       !- Special Day Type

!-   ===   ALL   OBJECTS   IN   CLASS:
SITE:GROUNDTEMPERATURE:BUILDINGSUR
FACE ===
Site:GroundTemperature:BuildingSurface,
   20.133,     !- January Ground Temperature {C}
   20.114,     !- February Ground Temperature {C}
   20.098,     !- March Ground Temperature {C}
   20.195,     !- April Ground Temperature {C}
   20.555,     !- May Ground Temperature {C}
   20.958,     !- June Ground Temperature {C}
   22.367,     !- July Ground Temperature {C}
   22.7,       !- August Ground Temperature {C}
   22.775, !- September Ground Temperature {C}
   21.957,     !- October Ground Temperature {C}
   20.592,  !- November Ground Temperature {C}
   20.216;  !- December Ground Temperature {C}

!-   ===   ALL   OBJECTS   IN   CLASS:
SITE:WATERMAINSTEMPERATURE ===
Site:WaterMainsTemperature,
   Correlation,                   !- Calculation Method
   ,                              !- Temperature Schedule Name
   16.64,          !- Annual Average Outdoor Air
Temperature {C}
   6.8;         !- Maximum Difference In Monthly
Average Outdoor Air Temperatures {deltaC}

!-   ===   ALL   OBJECTS   IN   CLASS:
SCHEDULETYPELIMITS ===
ScheduleTypeLimits,
   Any Number;                    !- Name

ScheduleTypeLimits,
   Fraction,                      !- Name
   0.0,                        !- Lower Limit Value
   1.0,                        !- Upper Limit Value
   CONTINUOUS;                 !- Numeric Type

ScheduleTypeLimits,
   Temperature,                   !- Name
   -60,                        !- Lower Limit Value
   200,                        !- Upper Limit Value
   CONTINUOUS;                 !- Numeric Type

ScheduleTypeLimits,
   On/Off,                        !- Name
   0,                          !- Lower Limit Value
   1,                          !- Upper Limit Value
   DISCRETE;                   !- Numeric Type

ScheduleTypeLimits,
   Control Type,                  !- Name
   0,                          !- Lower Limit Value
   4,                          !- Upper Limit Value
   DISCRETE;                   !- Numeric Type

ScheduleTypeLimits,
   Humidity,                      !- Name
   10,                         !- Lower Limit Value
   90,                         !- Upper Limit Value
   CONTINUOUS;                 !- Numeric Type

!-   ===   ALL   OBJECTS   IN   CLASS:
SCHEDULE:COMPACT ===
Schedule:Compact,
   OFF_EQP_SCH,                   !- Name
   Fraction,       !- Schedule Type Limits Name
   Through: 12/31,                !- Field 1
   For:Weekdays,                  !- Field 2
   Until: 08:00,                  !- Field 3
   0.4,                           !- Field 4
   Until: 12:00,                  !- Field 5
   0.9,                           !- Field 6
   Until: 13:00,                  !- Field 7
   0.8,                           !- Field 8
   Until: 17:00,                  !- Field 9
   0.9,                           !- Field 10
   Until: 18:00,                  !- Field 11
   0.5,                           !- Field 12
   Until: 24:00,                  !- Field 13
   0.4,                           !- Field 14
   For:Saturday,                  !- Field 15
   Until: 06:00,                  !- Field 16
   0.3,                           !- Field 17
   Until: 08:00,                  !- Field 18
   0.4,                           !- Field 19
   Until: 12:00,                  !- Field 20
   0.5,                           !- Field 21
   Until: 17:00,                  !- Field 22
   0.35,                          !- Field 23
   Until: 24:00,                  !- Field 24
   0.3,                           !- Field 25
   For:SummerDesignDay,           !- Field 26
   Until: 24:00,                  !- Field 27
   1,                             !- Field 28
   For:WinterDesignDay,           !- Field 29
   Until: 24:00,                  !- Field 30
   0,                             !- Field 31
   For AllOtherDays,              !- Field 32
   Until: 24:00,                  !- Field 33
   0.3;                           !- Field 34

Schedule:Compact,
   OFF_LIGHT_SCH,                 !- Name
   Fraction,       !- Schedule Type Limits Name
   Through: 12/31,                !- Field 1
   For:Weekdays,                  !- Field 2
   Until: 05:00,                  !- Field 3
   0.05,                          !- Field 4
   Until: 07:00,                  !- Field 5
   0.1,                           !- Field 6
   Until: 08:00,                  !- Field 7
   0.2,                           !- Field 8
   Until: 17:00,                  !- Field 9
   0.9,                           !- Field 10
   Until: 18:00,                  !- Field 11
   0.5,                           !- Field 12
   Until: 20:00,                  !- Field 13
   0.3,                           !- Field 14
   Until: 22:00,                  !- Field 15
   0.2,                           !- Field 16
   Until: 23:00,                  !- Field 17
   0.1,                           !- Field 18
   Until: 24:00,                  !- Field 19
   0.05,                          !- Field 20
```

```
   For:Saturday,                    !- Field 21
   Until: 06:00,                    !- Field 22
   0.05,                            !- Field 23
   Until: 08:00,                    !- Field 24
   0.1,                             !- Field 25
   Until: 12:00,                    !- Field 26
   0.3,                             !- Field 27
   Until: 17:00,                    !- Field 28
   0.15,                            !- Field 29
   Until: 24:00,                    !- Field 30
   0.05,                            !- Field 31
   For:SummerDesignDay,             !- Field 32
   Until: 24:00,                    !- Field 33
   1,                               !- Field 34
   For:WinterDesignDay,             !- Field 35
   Until: 24:00,                    !- Field 36
   0,                               !- Field 37
   For AllOtherDays,                !- Field 38
   Until: 24:00,                    !- Field 39
   0.05;                            !- Field 40

Schedule:Compact,
   OFF_CLOTHING_SCH,                !- Name
   Any Number,     !- Schedule Type Limits Name
   Through: 04/30,                  !- Field 1
   For: AllDays,                    !- Field 2
   Until: 24:00,                    !- Field 3
   1,                               !- Field 4
   Through: 09/30,                  !- Field 5
   For: AllDays,                    !- Field 6
   Until: 24:00,                    !- Field 7
   0.5,                             !- Field 8
   Through: 12/31,                  !- Field 9
   For: AllDays,                    !- Field 10
   Until: 24:00,                    !- Field 11
   1;                               !- Field 12

Schedule:Compact,
   OFF_OCC_SCH,                     !- Name
   Fraction,          !- Schedule Type Limits Name
   Through: 12/31,                  !- Field 1
   For:Weekdays,                    !- Field 2
   Until: 06:00,                    !- Field 3
   0,                               !- Field 4
   Until: 07:00,                    !- Field 5
   0.1,                             !- Field 6
   Until: 08:00,                    !- Field 7
   0.2,                             !- Field 8
   Until: 12:00,                    !- Field 9
   0.95,                            !- Field 10
   Until: 13:00,                    !- Field 11
   0.5,                             !- Field 12
   Until: 17:00,                    !- Field 13
   0.95,                            !- Field 14
   Until: 18:00,                    !- Field 15
   0.3,                             !- Field 16
   Until: 20:00,                    !- Field 17
   0.1,                             !- Field 18
   Until: 24:00,                    !- Field 19
   0.05,                            !- Field 20
   For:Saturday,                    !- Field 21
   Until: 06:00,                    !- Field 22
   0,                               !- Field 23
   Until: 08:00,                    !- Field 24
   0.1,                             !- Field 25
   Until: 12:00,                    !- Field 26
   0.3,                             !- Field 27
   Until: 17:00,                    !- Field 28
   0.1,                             !- Field 29
   Until: 24:00,                    !- Field 30
   0,                               !- Field 31
   For:SummerDesignDay,             !- Field 32
   Until: 06:00,                    !- Field 33
   0,                               !- Field 34
   Until: 22:00,                    !- Field 35
   1,                               !- Field 36
   Until: 24:00,                    !- Field 37
   0.05,                            !- Field 38
   For AllOtherDays,                !- Field 39
   Until: 24:00,                    !- Field 40
   0;                               !- Field 41

Schedule:Compact,
   OFF_HTGSETP_SCH,                 !- Name
   Temperature,    !- Schedule Type Limits Name
   THROUGH: 12/31,                  !- Field 1
   FOR:Weekdays,                    !- Field 2
   UNTIL: 06:00,                    !- Field 3
   15.6,                            !- Field 4
   UNTIL: 22:00,                    !- Field 5
   21,                              !- Field 6
   UNTIL: 24:00,                    !- Field 7
   15.6,                            !- Field 8
   For:Saturday,                    !- Field 9
   UNTIL: 06:00,                    !- Field 10
   15.6,                            !- Field 11
   UNTIL: 18:00,                    !- Field 12
   21,                              !- Field 13
   UNTIL: 24:00,                    !- Field 14
   15.6,                            !- Field 15
   FOR:WinterDesignDay,             !- Field 16
   UNTIL: 24:00,                    !- Field 17
   21,                              !- Field 18
   FOR: AllOtherDays,               !- Field 19
   UNTIL: 24:00,                    !- Field 20
   15.6;                            !- Field 21

Schedule:Compact,
   OFF_CLGSETP_SCH,                 !- Name
   Temperature,    !- Schedule Type Limits Name
   THROUGH: 12/31,                  !- Field 1
   FOR:Weekdays SummerDesignDay,    !- Field 2
   UNTIL: 06:00,                    !- Field 3
   26.7,                            !- Field 4
   UNTIL: 22:00,                    !- Field 5
   24,                              !- Field 6
   UNTIL:24:00,                     !- Field 7
   26.7,                            !- Field 8
   For:Saturday,                    !- Field 9
   UNTIL: 06:00,                    !- Field 10
   26.7,                            !- Field 11
   UNTIL: 18:00,                    !- Field 12
   24,                              !- Field 13
   UNTIL: 24:00,                    !- Field 14
   26.7,                            !- Field 15
   FOR: AllOtherDays,               !- Field 16
   UNTIL: 24:00,                    !- Field 17
   26.7;                            !- Field 18
```

```
Schedule:Compact,
   Report_Sch,                              !- Name
   On/Off,          !- Schedule Type Limits Name
   Through: 9/24,                           !- Field 1
   For: AllDays,                            !- Field 2
   Until: 24:00,                            !- Field 3
   0,                                       !- Field 4
   Through: 9/25,                           !- Field 5
   For: AllDays,                            !- Field 6
   Until: 1:00,                             !- Field 7
   1,                                       !- Field 8
   Until: 24:00,                            !- Field 9
   0,                                       !- Field 10
   Through: 12/31,                          !- Field 11
   For: AllDays,                            !- Field 12
   Until: 24:00,                            !- Field 13
   0;                                       !- Field 14

Schedule:Compact,
   Prechtc_Sch,                             !- Name
   On/Off,          !- Schedule Type Limits Name
   Through: 9/24,                           !- Field 1
   For: AllDays,                            !- Field 2
   Until: 21:00,                            !- Field 3
   0,                                       !- Field 4
   Until: 24:00,                            !- Field 5
   1,                                       !- Field 6
   Through: 12/31,                          !- Field 7
   For: AllDays,                            !- Field 8
   Until: 24:00,                            !- Field 9
   0;                                       !- Field 10

Schedule:Compact,
   ALWAYS_ON,                               !- Name
   On/Off,          !- Schedule Type Limits Name
   Through: 12/31,                          !- Field 1
   For: AllDays,                            !- Field 2
   Until: 24:00,                            !- Field 3
   1;                                       !- Field 4

Schedule:Compact,
   ACTIVITY_SCH,                            !- Name
   Any Number,    !- Schedule Type Limits Name
   Through: 12/31,                          !- Field 1
   For: AllDays,                            !- Field 2
   Until: 24:00,                            !- Field 3
   120;                                     !- Field 4

Schedule:Compact,
   WORK_EFF_SCH,                            !- Name
   Fraction,        !- Schedule Type Limits Name
   Through: 12/31,                          !- Field 1
   For: AllDays,                            !- Field 2
   Until: 24:00,                            !- Field 3
   0.0;                                     !- Field 4

Schedule:Compact,
   AIR_VELO_SCH,                            !- Name
   Any Number,    !- Schedule Type Limits Name
   Through: 12/31,                          !- Field 1
   For: AllDays,                            !- Field 2
   Until: 24:00,                            !- Field 3
   0.2;                                     !- Field 4

Schedule:Compact,
   Dual Zone Control Type Sched,            !- Name
   Control Type,  !- Schedule Type Limits Name
   Through: 12/31,                          !- Field 1
   For: AllDays,                            !- Field 2
   Until: 24:00,                            !- Field 3
   4;                                       !- Field 4

Schedule:Compact,
   HVACOperationSchd,                       !- Name
   On/Off,          !- Schedule Type Limits Name
   Through: 12/31,                          !- Field 1
   FOR:Weekdays SummerDesignDay,            !- Field 2
   Until: 06:00,                            !- Field 3
   0,                                       !- Field 4
   Until: 22:00,                            !- Field 5
   1,                                       !- Field 6
   Until: 24:00,                            !- Field 7
   0,                                       !- Field 8
   FOR:Saturday WinterDesignDay,            !- Field 9
   Until: 06:00,                            !- Field 10
   0,                                       !- Field 11
   Until: 18:00,                            !- Field 12
   1,                                       !- Field 13
   Until: 24:00,                            !- Field 14
   0,                                       !- Field 15
   For AllOtherDays,                        !- Field 16
   Until: 24:00,                            !- Field 17
   0;                                       !- Field 18

!-   === ALL OBJECTS IN CLASS: MATERIAL ===
Material,
   Wall Insulation,                         !- Name
   MediumRough,                             !- Roughness
   0.0365394788793098,                      !- Thickness {m}
   0.049,                                   !- Conductivity {W/m-K}
   265.0000,                                !- Density {kg/m3}
   836.8000,                                !- Specific Heat {J/kg-K}
   0.9000,                                  !- Thermal Absorptance
   0.7000,                                  !- Solar Absorptance
   0.7000;                                  !- Visible Absorptance

Material,
   NonRes Insulation,                       !- Name
   MediumRough,                             !- Roughness
   0.234129751336427,                       !- Thickness {m}
   0.049,                                   !- Conductivity {W/m-K}
   265.0000,                                !- Density {kg/m3}
   836.8000,                                !- Specific Heat {J/kg-K}
   0.9000,                                  !- Thermal Absorptance
   0.7000,                                  !- Solar Absorptance
   0.7000;                                  !- Visible Absorptance

Material,
   Std Wood 6inch,                          !- Name
   MediumSmooth,                            !- Roughness
   0.15,                                    !- Thickness {m}
   0.12,                                    !- Conductivity {W/m-K}
   540.0000,                                !- Density {kg/m3}
   1210,                                    !- Specific Heat {J/kg-K}
   0.9000000,                               !- Thermal Absorptance
   0.7000000,                               !- Solar Absorptance
   0.7000000;                               !- Visible Absorptance
```

```
Material,
    Wood Siding,                !- Name
    MediumSmooth,               !- Roughness
    0.0100,                     !- Thickness {m}
    0.1100,                     !- Conductivity {W/m-K}
    544.6200,                   !- Density {kg/m3}
    1210.0000,                  !- Specific Heat {J/kg-K}
    0.9000,                     !- Thermal Absorptance
    0.7800,                     !- Solar Absorptance
    0.7800;                     !- Visible Absorptance

Material,
    1/2IN Gypsum,               !- Name
    Smooth,                     !- Roughness
    0.0127,                     !- Thickness {m}
    0.1600,                     !- Conductivity {W/m-K}
    784.9000,                   !- Density {kg/m3}
    830.0000,                   !- Specific Heat {J/kg-K}
    0.9000,                     !- Thermal Absorptance
    0.9200,                     !- Solar Absorptance
    0.9200;                     !- Visible Absorptance

Material,
    1IN Stucco,                 !- Name
    Smooth,                     !- Roughness
    0.0253,                     !- Thickness {m}
    0.6918,                     !- Conductivity {W/m-K}
    1858.0000,                  !- Density {kg/m3}
    837.0000,                   !- Specific Heat {J/kg-K}
    0.9000,                     !- Thermal Absorptance
    0.9200,                     !- Solar Absorptance
    0.9200;                     !- Visible Absorptance

Material,
    8IN CONCRETE HW,            !- Name
    Rough,                      !- Roughness
    0.2032,                     !- Thickness {m}
    1.3110,                     !- Conductivity {W/m-K}
    2240.0000,                  !- Density {kg/m3}
    836.8000,                   !- Specific Heat {J/kg-K}
    0.9000,                     !- Thermal Absorptance
    0.7000,                     !- Solar Absorptance
    0.7000;                     !- Visible Absorptance

Material,
    Metal Siding,               !- Name
    Smooth,                     !- Roughness
    0.0015,                     !- Thickness {m}
    44.9600,                    !- Conductivity {W/m-K}
    7688.8600,                  !- Density {kg/m3}
    410.0000,                   !- Specific Heat {J/kg-K}
    0.9000,                     !- Thermal Absorptance
    0.2000,                     !- Solar Absorptance
    0.2000;                     !- Visible Absorptance

Material,
    HW CONCRETE,                !- Name
    Rough,                      !- Roughness
    0.1016,                     !- Thickness {m}
    1.3110,                     !- Conductivity {W/m-K}
    2240.0000,                  !- Density {kg/m3}
    836.8000,                   !- Specific Heat {J/kg-K}
    0.9000,                     !- Thermal Absorptance
    0.7000,                     !- Solar Absorptance
    0.7000;                     !- Visible Absorptance

Material,
    Roof Membrane,              !- Name
    VeryRough,                  !- Roughness
    0.0095,                     !- Thickness {m}
    0.1600,                     !- Conductivity {W/m-K}
    1121.2900,                  !- Density {kg/m3}
    1460.0000,                  !- Specific Heat {J/kg-K}
    0.9000,                     !- Thermal Absorptance
    0.7000,                     !- Solar Absorptance
    0.7000;                     !- Visible Absorptance

Material,
    Metal Decking,              !- Name
    MediumSmooth,               !- Roughness
    0.0015,                     !- Thickness {m}
    45.0060,                    !- Conductivity {W/m-K}
    7680.0000,                  !- Density {kg/m3}
    418.4000,                   !- Specific Heat {J/kg-K}
    0.9000,                     !- Thermal Absorptance
    0.7000,                     !- Solar Absorptance
    0.3000;                     !- Visible Absorptance

Material,
    Metal Roofing,              !- Name
    MediumSmooth,               !- Roughness
    0.0015,                     !- Thickness {m}
    45.0060,                    !- Conductivity {W/m-K}
    7680.0000,                  !- Density {kg/m3}
    418.4000,                   !- Specific Heat {J/kg-K}
    0.9000,                     !- Thermal Absorptance
    0.7000,                     !- Solar Absorptance
    0.3000;                     !- Visible Absorptance

Material,
    MAT-CC05 4 HW CONCRETE,     !- Name
    Rough,                      !- Roughness
    0.1016,                     !- Thickness {m}
    1.3110,                     !- Conductivity {W/m-K}
    2240.0000,                  !- Density {kg/m3}
    836.8000,                   !- Specific Heat {J/kg-K}
    0.9000,                     !- Thermal Absorptance
    0.7000,                     !- Solar Absorptance
    0.7000;                     !- Visible Absorptance

Material,
    Std AC02,                   !- Name
    MediumSmooth,               !- Roughness
    1.2700000E-02,              !- Thickness {m}
    5.7000000E-02,              !- Conductivity {W/m-K}
    288.0000,                   !- Density {kg/m3}
    1339.000,                   !- Specific Heat {J/kg-K}
    0.9000000,                  !- Thermal Absorptance
    0.7000000,                  !- Solar Absorptance
    0.2000000;                  !- Visible Absorptance

!-   === ALL OBJECTS IN CLASS: MATERIAL:NOMASS ===
Material:NoMass,
    CP02 CARPET PAD,            !- Name
    VeryRough,                  !- Roughness
    0.2165,          !- Thermal Resistance {m2-K/W}
    0.9000,                     !- Thermal Absorptance
    0.7000,                     !- Solar Absorptance
```

```
   0.8000;                  !- Visible Absorptance

Material:NoMass,
   MAT-AIR-WALL,            !- Name
   Rough,                   !- Roughness
   0.2079491,    !- Thermal Resistance {m2-K/W}
   0.9,                     !- Thermal Absorptance
   0.7;                     !- Solar Absorptance

!-   === ALL OBJECTS IN CLASS: WINDOWMATERIAL:SIMPLEGLAZINGSYSTEM ===
WindowMaterial:SimpleGlazingSystem,
   NonRes Fixed Assembly Window,    !- Name
   3.23646,                 !- U-Factor {W/m2-K}
   0.25;            !- Solar Heat Gain Coefficient

!-   === ALL OBJECTS IN CLASS: CONSTRUCTION ===
Construction,
   Exterior Floor,                  !- Name
   HW CONCRETE,             !- Outside Layer
   CP02 CARPET PAD;                 !- Layer 2

Construction,
   Exterior Wall,                   !- Name
   1IN Stucco,              !- Outside Layer
   8IN Concrete HW,                 !- Layer 2
   Wall Insulation,                 !- Layer 3
   1/2IN Gypsum;                    !- Layer 4

Construction,
   Interior Floor,                  !- Name
   1/2IN Gypsum,            !- Outside Layer
   NonRes Insulation,               !- Layer 2
   1/2IN Gypsum;                    !- Layer 3

Construction,
   Interior Ceiling,                !- Name
   1/2IN Gypsum,            !- Outside Layer
   NonRes Insulation,               !- Layer 2
   1/2IN Gypsum;                    !- Layer 3

Construction,
   Exterior Roof,                   !- Name
   Roof Membrane,           !- Outside Layer
   Metal Decking;                   !- Layer 2

Construction,
   Exterior Window,                 !- Name
   NonRes Fixed Assembly Window;  !- Outside Layer

Construction,
   InteriorFurnishings,             !- Name
   Std Wood 6inch;          !- Outside Layer

!-   === ALL OBJECTS IN CLASS: GLOBALGEOMETRYRULES ===
GlobalGeometryRules,
   UpperLeftCorner,    !- Starting Vertex Position
   Counterclockwise,    !- Vertex Entry Direction
   Relative,            !- Coordinate System
   Relative;       !- Daylighting Reference Point Coordinate System


!-  === ALL OBJECTS IN CLASS: ZONE ===
Zone,
   B51,                             !- Name
   0.0,          !- Direction of Relative North {deg}
   -5.0,                    !- X Origin {m}
   -5.0,                    !- Y Origin {m}
   0.0,                     !- Z Origin {m}
   ,                                !- Type
   1,                       !- Multiplier
   autocalculate,           !- Ceiling Height {m}
   autocalculate,           !- Volume {m3}
   autocalculate,           !- Floor Area {m2}
   ,           !- Zone Inside Convection Algorithm
   ,          !- Zone Outside Convection Algorithm
   Yes;                     !- Part of Total Floor Area

Zone,
   B52,                             !- Name
   0.0,          !- Direction of Relative North {deg}
   -5.0,                    !- X Origin {m}
   -5.0,                    !- Y Origin {m}
   3.4,                     !- Z Origin {m}
   ,                                !- Type
   1,                       !- Multiplier
   autocalculate,           !- Ceiling Height {m}
   autocalculate,           !- Volume {m3}
   autocalculate,           !- Floor Area {m2}
   ,           !- Zone Inside Convection Algorithm
   ,          !- Zone Outside Convection Algorithm
   Yes;                     !- Part of Total Floor Area

Zone,
   B53,                             !- Name
   0.0,          !- Direction of Relative North {deg}
   -5.0,                    !- X Origin {m}
   -5.0,                    !- Y Origin {m}
   6.7,                     !- Z Origin {m}
   ,                                !- Type
   1,                       !- Multiplier
   autocalculate,           !- Ceiling Height {m}
   autocalculate,           !- Volume {m3}
   autocalculate,           !- Floor Area {m2}
   ,           !- Zone Inside Convection Algorithm
   ,          !- Zone Outside Convection Algorithm
   Yes;                     !- Part of Total Floor Area

!-   === ALL OBJECTS IN CLASS: BUILDINGSURFACE:DETAILED ===
BuildingSurface:Detailed,
   B51S1,                           !- Name
   Wall,                            !- Surface Type
   Exterior Wall,           !- Construction Name
   B51,                             !- Zone Name
   Outdoors,       !- Outside Boundary Condition
   ,         !- Outside Boundary Condition Object
   SunExposed,                      !- Sun Exposure
   WindExposed,             !- Wind Exposure
   ,                        !- View Factor to Ground
   4,                       !- Number of Vertices
   0.00,                    !- Vertex 1 X-coordinate {m}
   0.00,                    !- Vertex 1 Y-coordinate {m}
   3.40,                    !- Vertex 1 Z-coordinate {m}
```

```
    0.00,                   !- Vertex 2 X-coordinate {m}
    0.00,                   !- Vertex 2 Y-coordinate {m}
    0.00,                   !- Vertex 2 Z-coordinate {m}
    10.00,                  !- Vertex 3 X-coordinate {m}
    0.00,                   !- Vertex 3 Y-coordinate {m}
    0.00,                   !- Vertex 3 Z-coordinate {m}
    10.00,                  !- Vertex 4 X-coordinate {m}
    0.00,                   !- Vertex 4 Y-coordinate {m}
    3.40;                   !- Vertex 4 Z-coordinate {m}

BuildingSurface:Detailed,
    B51S2,                                  !- Name
    Wall,                                   !- Surface Type
    Exterior Wall,                          !- Construction Name
    B51,                                    !- Zone Name
    Outdoors,               !- Outside Boundary Condition
    ,                       !- Outside Boundary Condition Object
    SunExposed,                             !- Sun Exposure
    WindExposed,                            !- Wind Exposure
    ,                                       !- View Factor to Ground
    4,                                      !- Number of Vertices
    10.00,                  !- Vertex 1 X-coordinate {m}
    0.00,                   !- Vertex 1 Y-coordinate {m}
    3.40,                   !- Vertex 1 Z-coordinate {m}
    10.00,                  !- Vertex 2 X-coordinate {m}
    0.00,                   !- Vertex 2 Y-coordinate {m}
    0.00,                   !- Vertex 2 Z-coordinate {m}
    10.00,                  !- Vertex 3 X-coordinate {m}
    10.00,                  !- Vertex 3 Y-coordinate {m}
    0.00,                   !- Vertex 3 Z-coordinate {m}
    10.00,                  !- Vertex 4 X-coordinate {m}
    10.00,                  !- Vertex 4 Y-coordinate {m}
    3.40;                   !- Vertex 4 Z-coordinate {m}

BuildingSurface:Detailed,
    B51S3,                                  !- Name
    Wall,                                   !- Surface Type
    Exterior Wall,                          !- Construction Name
    B51,                                    !- Zone Name
    Outdoors,               !- Outside Boundary Condition
    ,                       !- Outside Boundary Condition Object
    SunExposed,                             !- Sun Exposure
    WindExposed,                            !- Wind Exposure
    ,                                       !- View Factor to Ground
    4,                                      !- Number of Vertices
    10.00,                  !- Vertex 1 X-coordinate {m}
    10.00,                  !- Vertex 1 Y-coordinate {m}
    3.40,                   !- Vertex 1 Z-coordinate {m}
    10.00,                  !- Vertex 2 X-coordinate {m}
    10.00,                  !- Vertex 2 Y-coordinate {m}
    0.00,                   !- Vertex 2 Z-coordinate {m}
    0.00,                   !- Vertex 3 X-coordinate {m}
    10.00,                  !- Vertex 3 Y-coordinate {m}
    0.00,                   !- Vertex 3 Z-coordinate {m}
    0.00,                   !- Vertex 4 X-coordinate {m}
    10.00,                  !- Vertex 4 Y-coordinate {m}
    3.40;                   !- Vertex 4 Z-coordinate {m}

BuildingSurface:Detailed,
    B51S4,                                  !- Name
    Wall,                                   !- Surface Type
    Exterior Wall,                          !- Construction Name
    B51,                                    !- Zone Name
    Outdoors,               !- Outside Boundary Condition
    ,                       !- Outside Boundary Condition Object
    SunExposed,                             !- Sun Exposure
    WindExposed,                            !- Wind Exposure
    ,                                       !- View Factor to Ground
    4,                                      !- Number of Vertices
    0.00,                   !- Vertex 1 X-coordinate {m}
    10.00,                  !- Vertex 1 Y-coordinate {m}
    3.40,                   !- Vertex 1 Z-coordinate {m}
    0.00,                   !- Vertex 2 X-coordinate {m}
    10.00,                  !- Vertex 2 Y-coordinate {m}
    0.00,                   !- Vertex 2 Z-coordinate {m}
    0.00,                   !- Vertex 3 X-coordinate {m}
    0.00,                   !- Vertex 3 Y-coordinate {m}
    0.00,                   !- Vertex 3 Z-coordinate {m}
    0.00,                   !- Vertex 4 X-coordinate {m}
    0.00,                   !- Vertex 4 Y-coordinate {m}
    3.40;                   !- Vertex 4 Z-coordinate {m}

BuildingSurface:Detailed,
    B51R,                                   !- Name
    Ceiling,                                !- Surface Type
    Interior Ceiling,                       !- Construction Name
    B51,                                    !- Zone Name
    Surface,                !- Outside Boundary Condition
    B52F,                   !- Outside Boundary Condition Object
    NoSun,                                  !- Sun Exposure
    NoWind,                                 !- Wind Exposure
    ,                                       !- View Factor to Ground
    4,                                      !- Number of Vertices
    10.00,                  !- Vertex 1 X-coordinate {m}
    10.00,                  !- Vertex 1 Y-coordinate {m}
    3.40,                   !- Vertex 1 Z-coordinate {m}
    0.00,                   !- Vertex 2 X-coordinate {m}
    10.00,                  !- Vertex 2 Y-coordinate {m}
    3.40,                   !- Vertex 2 Z-coordinate {m}
    0.00,                   !- Vertex 3 X-coordinate {m}
    0.00,                   !- Vertex 3 Y-coordinate {m}
    3.40,                   !- Vertex 3 Z-coordinate {m}
    10.00,                  !- Vertex 4 X-coordinate {m}
    0.00,                   !- Vertex 4 Y-coordinate {m}
    3.40;                   !- Vertex 4 Z-coordinate {m}

BuildingSurface:Detailed,
    B51F,                                   !- Name
    Floor,                                  !- Surface Type
    Exterior Floor,                         !- Construction Name
    B51,                                    !- Zone Name
    Ground,                 !- Outside Boundary Condition
    ,                       !- Outside Boundary Condition Object
    NoSun,                                  !- Sun Exposure
    NoWind,                                 !- Wind Exposure
    0.0,                    !- View Factor to Ground
    4,                                      !- Number of Vertices
    10.00,                  !- Vertex 1 X-coordinate {m}
    10.00,                  !- Vertex 1 Y-coordinate {m}
    0.00,                   !- Vertex 1 Z-coordinate {m}
    10.00,                  !- Vertex 2 X-coordinate {m}
    0.00,                   !- Vertex 2 Y-coordinate {m}
    0.00,                   !- Vertex 2 Z-coordinate {m}
    0.00,                   !- Vertex 3 X-coordinate {m}
    0.00,                   !- Vertex 3 Y-coordinate {m}
    0.00,                   !- Vertex 3 Z-coordinate {m}
    0.00,                   !- Vertex 4 X-coordinate {m}
    10.00,                  !- Vertex 4 Y-coordinate {m}
    0.00;                   !- Vertex 4 Z-coordinate {m}
```

```
BuildingSurface:Detailed,
    B52S1,                    !- Name
    Wall,                     !- Surface Type
    Exterior Wall,            !- Construction Name
    B52,                      !- Zone Name
    Outdoors,                 !- Outside Boundary Condition
    ,                         !- Outside Boundary Condition Object
    SunExposed,               !- Sun Exposure
    WindExposed,              !- Wind Exposure
    ,                         !- View Factor to Ground
    4,                        !- Number of Vertices
    0.00,                     !- Vertex 1 X-coordinate {m}
    0.00,                     !- Vertex 1 Y-coordinate {m}
    3.30,                     !- Vertex 1 Z-coordinate {m}
    0.00,                     !- Vertex 2 X-coordinate {m}
    0.00,                     !- Vertex 2 Y-coordinate {m}
    0.00,                     !- Vertex 2 Z-coordinate {m}
    10.00,                    !- Vertex 3 X-coordinate {m}
    0.00,                     !- Vertex 3 Y-coordinate {m}
    0.00,                     !- Vertex 3 Z-coordinate {m}
    10.00,                    !- Vertex 4 X-coordinate {m}
    0.00,                     !- Vertex 4 Y-coordinate {m}
    3.30;                     !- Vertex 4 Z-coordinate {m}

BuildingSurface:Detailed,
    B52S2,                    !- Name
    Wall,                     !- Surface Type
    Exterior Wall,            !- Construction Name
    B52,                      !- Zone Name
    Outdoors,                 !- Outside Boundary Condition
    ,                         !- Outside Boundary Condition Object
    SunExposed,               !- Sun Exposure
    WindExposed,              !- Wind Exposure
    ,                         !- View Factor to Ground
    4,                        !- Number of Vertices
    10.00,                    !- Vertex 1 X-coordinate {m}
    0.00,                     !- Vertex 1 Y-coordinate {m}
    3.30,                     !- Vertex 1 Z-coordinate {m}
    10.00,                    !- Vertex 2 X-coordinate {m}
    0.00,                     !- Vertex 2 Y-coordinate {m}
    0.00,                     !- Vertex 2 Z-coordinate {m}
    10.00,                    !- Vertex 3 X-coordinate {m}
    10.00,                    !- Vertex 3 Y-coordinate {m}
    0.00,                     !- Vertex 3 Z-coordinate {m}
    10.00,                    !- Vertex 4 X-coordinate {m}
    10.00,                    !- Vertex 4 Y-coordinate {m}
    3.30;                     !- Vertex 4 Z-coordinate {m}

BuildingSurface:Detailed,
    B52S3,                    !- Name
    Wall,                     !- Surface Type
    Exterior Wall,            !- Construction Name
    B52,                      !- Zone Name
    Outdoors,                 !- Outside Boundary Condition
    ,                         !- Outside Boundary Condition Object
    SunExposed,               !- Sun Exposure
    WindExposed,              !- Wind Exposure
    ,                         !- View Factor to Ground
    4,                        !- Number of Vertices
    10.00,                    !- Vertex 1 X-coordinate {m}
    10.00,                    !- Vertex 1 Y-coordinate {m}
    3.30,                     !- Vertex 1 Z-coordinate {m}
    10.00,                    !- Vertex 2 X-coordinate {m}
    10.00,                    !- Vertex 2 Y-coordinate {m}
    0.00,                     !- Vertex 2 Z-coordinate {m}
    0.00,                     !- Vertex 3 X-coordinate {m}
    10.00,                    !- Vertex 3 Y-coordinate {m}
    0.00,                     !- Vertex 3 Z-coordinate {m}
    0.00,                     !- Vertex 4 X-coordinate {m}
    10.00,                    !- Vertex 4 Y-coordinate {m}
    3.30;                     !- Vertex 4 Z-coordinate {m}

BuildingSurface:Detailed,
    B52S4,                    !- Name
    Wall,                     !- Surface Type
    Exterior Wall,            !- Construction Name
    B52,                      !- Zone Name
    Outdoors,                 !- Outside Boundary Condition
    ,                         !- Outside Boundary Condition Object
    SunExposed,               !- Sun Exposure
    WindExposed,              !- Wind Exposure
    ,                         !- View Factor to Ground
    4,                        !- Number of Vertices
    0.00,                     !- Vertex 1 X-coordinate {m}
    10.00,                    !- Vertex 1 Y-coordinate {m}
    3.30,                     !- Vertex 1 Z-coordinate {m}
    0.00,                     !- Vertex 2 X-coordinate {m}
    10.00,                    !- Vertex 2 Y-coordinate {m}
    0.00,                     !- Vertex 2 Z-coordinate {m}
    0.00,                     !- Vertex 3 X-coordinate {m}
    0.00,                     !- Vertex 3 Y-coordinate {m}
    0.00,                     !- Vertex 3 Z-coordinate {m}
    0.00,                     !- Vertex 4 X-coordinate {m}
    0.00,                     !- Vertex 4 Y-coordinate {m}
    3.30;                     !- Vertex 4 Z-coordinate {m}

BuildingSurface:Detailed,
    B52R,                     !- Name
    Ceiling,                  !- Surface Type
    Interior Ceiling,         !- Construction Name
    B52,                      !- Zone Name
    Surface,                  !- Outside Boundary Condition
    B53F,                     !- Outside Boundary Condition Object
    NoSun,                    !- Sun Exposure
    NoWind,                   !- Wind Exposure
    ,                         !- View Factor to Ground
    4,                        !- Number of Vertices
    10.00,                    !- Vertex 1 X-coordinate {m}
    10.00,                    !- Vertex 1 Y-coordinate {m}
    3.30,                     !- Vertex 1 Z-coordinate {m}
    0.00,                     !- Vertex 2 X-coordinate {m}
    10.00,                    !- Vertex 2 Y-coordinate {m}
    3.30,                     !- Vertex 2 Z-coordinate {m}
    0.00,                     !- Vertex 3 X-coordinate {m}
    0.00,                     !- Vertex 3 Y-coordinate {m}
    3.30,                     !- Vertex 3 Z-coordinate {m}
    10.00,                    !- Vertex 4 X-coordinate {m}
    0.00,                     !- Vertex 4 Y-coordinate {m}
    3.30;                     !- Vertex 4 Z-coordinate {m}

BuildingSurface:Detailed,
    B52F,                     !- Name
    Floor,                    !- Surface Type
    Interior Floor,           !- Construction Name
    B52,                      !- Zone Name
    Surface,                  !- Outside Boundary Condition
    B51R,                     !- Outside Boundary Condition Object
    NoSun,                    !- Sun Exposure
```

```
    NoWind,                  !- Wind Exposure
    0.0,                     !- View Factor to Ground
    4,                       !- Number of Vertices
    10.00,                   !- Vertex 1 X-coordinate {m}
    10.00,                   !- Vertex 1 Y-coordinate {m}
    0.00,                    !- Vertex 1 Z-coordinate {m}
    10.00,                   !- Vertex 2 X-coordinate {m}
    0.00,                    !- Vertex 2 Y-coordinate {m}
    0.00,                    !- Vertex 2 Z-coordinate {m}
    0.00,                    !- Vertex 3 X-coordinate {m}
    0.00,                    !- Vertex 3 Y-coordinate {m}
    0.00,                    !- Vertex 3 Z-coordinate {m}
    0.00,                    !- Vertex 4 X-coordinate {m}
    10.00,                   !- Vertex 4 Y-coordinate {m}
    0.00;                    !- Vertex 4 Z-coordinate {m}

BuildingSurface:Detailed,
    B53S1,                   !- Name
    Wall,                    !- Surface Type
    Exterior Wall,           !- Construction Name
    B53,                     !- Zone Name
    Outdoors,                !- Outside Boundary Condition
    ,                        !- Outside Boundary Condition Object
    SunExposed,              !- Sun Exposure
    WindExposed,             !- Wind Exposure
    ,                        !- View Factor to Ground
    4,                       !- Number of Vertices
    0.00,                    !- Vertex 1 X-coordinate {m}
    0.00,                    !- Vertex 1 Y-coordinate {m}
    3.30,                    !- Vertex 1 Z-coordinate {m}
    0.00,                    !- Vertex 2 X-coordinate {m}
    0.00,                    !- Vertex 2 Y-coordinate {m}
    0.00,                    !- Vertex 2 Z-coordinate {m}
    10.00,                   !- Vertex 3 X-coordinate {m}
    0.00,                    !- Vertex 3 Y-coordinate {m}
    0.00,                    !- Vertex 3 Z-coordinate {m}
    10.00,                   !- Vertex 4 X-coordinate {m}
    0.00,                    !- Vertex 4 Y-coordinate {m}
    3.30;                    !- Vertex 4 Z-coordinate {m}

BuildingSurface:Detailed,
    B53S2,                   !- Name
    Wall,                    !- Surface Type
    Exterior Wall,           !- Construction Name
    B53,                     !- Zone Name
    Outdoors,                !- Outside Boundary Condition
    ,                        !- Outside Boundary Condition Object
    SunExposed,              !- Sun Exposure
    WindExposed,             !- Wind Exposure
    ,                        !- View Factor to Ground
    4,                       !- Number of Vertices
    10.00,                   !- Vertex 1 X-coordinate {m}
    0.00,                    !- Vertex 1 Y-coordinate {m}
    3.30,                    !- Vertex 1 Z-coordinate {m}
    10.00,                   !- Vertex 2 X-coordinate {m}
    0.00,                    !- Vertex 2 Y-coordinate {m}
    0.00,                    !- Vertex 2 Z-coordinate {m}
    10.00,                   !- Vertex 3 X-coordinate {m}
    10.00,                   !- Vertex 3 Y-coordinate {m}
    0.00,                    !- Vertex 3 Z-coordinate {m}
    10.00,                   !- Vertex 4 X-coordinate {m}
    10.00,                   !- Vertex 4 Y-coordinate {m}
    3.30;                    !- Vertex 4 Z-coordinate {m}

BuildingSurface:Detailed,
    B53S3,                   !- Name
    Wall,                    !- Surface Type
    Exterior Wall,           !- Construction Name
    B53,                     !- Zone Name
    Outdoors,                !- Outside Boundary Condition
    ,                        !- Outside Boundary Condition Object
    SunExposed,              !- Sun Exposure
    WindExposed,             !- Wind Exposure
    ,                        !- View Factor to Ground
    4,                       !- Number of Vertices
    10.00,                   !- Vertex 1 X-coordinate {m}
    10.00,                   !- Vertex 1 Y-coordinate {m}
    3.30,                    !- Vertex 1 Z-coordinate {m}
    10.00,                   !- Vertex 2 X-coordinate {m}
    10.00,                   !- Vertex 2 Y-coordinate {m}
    0.00,                    !- Vertex 2 Z-coordinate {m}
    0.00,                    !- Vertex 3 X-coordinate {m}
    10.00,                   !- Vertex 3 Y-coordinate {m}
    0.00,                    !- Vertex 3 Z-coordinate {m}
    0.00,                    !- Vertex 4 X-coordinate {m}
    10.00,                   !- Vertex 4 Y-coordinate {m}
    3.30;                    !- Vertex 4 Z-coordinate {m}

BuildingSurface:Detailed,
    B53S4,                   !- Name
    Wall,                    !- Surface Type
    Exterior Wall,           !- Construction Name
    B53,                     !- Zone Name
    Outdoors,                !- Outside Boundary Condition
    ,                        !- Outside Boundary Condition Object
    SunExposed,              !- Sun Exposure
    WindExposed,             !- Wind Exposure
    ,                        !- View Factor to Ground
    4,                       !- Number of Vertices
    0.00,                    !- Vertex 1 X-coordinate {m}
    10.00,                   !- Vertex 1 Y-coordinate {m}
    3.30,                    !- Vertex 1 Z-coordinate {m}
    0.00,                    !- Vertex 2 X-coordinate {m}
    10.00,                   !- Vertex 2 Y-coordinate {m}
    0.00,                    !- Vertex 2 Z-coordinate {m}
    0.00,                    !- Vertex 3 X-coordinate {m}
    0.00,                    !- Vertex 3 Y-coordinate {m}
    0.00,                    !- Vertex 3 Z-coordinate {m}
    0.00,                    !- Vertex 4 X-coordinate {m}
    0.00,                    !- Vertex 4 Y-coordinate {m}
    3.30;                    !- Vertex 4 Z-coordinate {m}

BuildingSurface:Detailed,
    B53R,                    !- Name
    Roof,                    !- Surface Type
    Exterior Roof,           !- Construction Name
    B53,                     !- Zone Name
    Outdoors,                !- Outside Boundary Condition
    ,                        !- Outside Boundary Condition Object
    SunExposed,              !- Sun Exposure
    WindExposed,             !- Wind Exposure
    ,                        !- View Factor to Ground
    4,                       !- Number of Vertices
    10.00,                   !- Vertex 1 X-coordinate {m}
    10.00,                   !- Vertex 1 Y-coordinate {m}
    3.30,                    !- Vertex 1 Z-coordinate {m}
    0.00,                    !- Vertex 2 X-coordinate {m}
    10.00,                   !- Vertex 2 Y-coordinate {m}
    3.30,                    !- Vertex 2 Z-coordinate {m}
```

```
    0.00,                   !- Vertex 3 X-coordinate {m}
    0.00,                   !- Vertex 3 Y-coordinate {m}
    3.30,                   !- Vertex 3 Z-coordinate {m}
    10.00,                  !- Vertex 4 X-coordinate {m}
    0.00,                   !- Vertex 4 Y-coordinate {m}
    3.30;                   !- Vertex 4 Z-coordinate {m}

BuildingSurface:Detailed,
    B53F,                                   !- Name
    Floor,                                  !- Surface Type
    Interior Floor,                 !- Construction Name
    B53,                                    !- Zone Name
    Surface,                !- Outside Boundary Condition
    B52R,   !- Outside Boundary Condition Object
    NoSun,                                  !- Sun Exposure
    NoWind,                                 !- Wind Exposure
    0.0,                            !- View Factor to Ground
    4,                                      !- Number of Vertices
    10.00,                  !- Vertex 1 X-coordinate {m}
    10.00,                  !- Vertex 1 Y-coordinate {m}
    0.00,                   !- Vertex 1 Z-coordinate {m}
    10.00,                  !- Vertex 2 X-coordinate {m}
    0.00,                   !- Vertex 2 Y-coordinate {m}
    0.00,                   !- Vertex 2 Z-coordinate {m}
    0.00,                   !- Vertex 3 X-coordinate {m}
    0.00,                   !- Vertex 3 Y-coordinate {m}
    0.00,                   !- Vertex 3 Z-coordinate {m}
    0.00,                   !- Vertex 4 X-coordinate {m}
    10.00,                  !- Vertex 4 Y-coordinate {m}
    0.00;                   !- Vertex 4 Z-coordinate {m}

!-   ===   ALL   OBJECTS   IN   CLASS:
FENESTRATIONSURFACE:DETAILED ===
FenestrationSurface:Detailed,
    B5D,                                    !- Name
    GlassDoor,                              !- Surface Type
    Exterior Window,                !- Construction Name
    B51S1,                  !- Building Surface Name
    ,       !- Outside Boundary Condition Object
    ,                               !- View Factor to Ground
    ,                               !- Shading Control Name
    ,                       !- Frame and Divider Name
    ,                                       !- Multiplier
    4,                                      !- Number of Vertices
    7.99,                   !- Vertex 1 X-coordinate {m}
    0.00,                   !- Vertex 1 Y-coordinate {m}
    2.13,                   !- Vertex 1 Z-coordinate {m}
    7.99,                   !- Vertex 2 X-coordinate {m}
    0.00,                   !- Vertex 2 Y-coordinate {m}
    0.00,                   !- Vertex 2 Z-coordinate {m}
    8.99,                   !- Vertex 3 X-coordinate {m}
    0.00,                   !- Vertex 3 Y-coordinate {m}
    0.00,                   !- Vertex 3 Z-coordinate {m}
    8.99,                   !- Vertex 4 X-coordinate {m}
    0.00,                   !- Vertex 4 Y-coordinate {m}
    2.13;                   !- Vertex 4 Z-coordinate {m}

FenestrationSurface:Detailed,
    B51S1W,                                 !- Name
    Window,                                 !- Surface Type
    Exterior Window,                !- Construction Name
    B51S1,                  !- Building Surface Name
    ,       !- Outside Boundary Condition Object
    ,                               !- View Factor to Ground
    ,                               !- Shading Control Name
    ,                       !- Frame and Divider Name
    ,                                       !- Multiplier
    4,                                      !- Number of Vertices
    3.02,                   !- Vertex 1 X-coordinate {m}
    0.00,                   !- Vertex 1 Y-coordinate {m}
    2.60,                   !- Vertex 1 Z-coordinate {m}
    3.02,                   !- Vertex 2 X-coordinate {m}
    0.00,                   !- Vertex 2 Y-coordinate {m}
    0.90,                   !- Vertex 2 Z-coordinate {m}
    6.98,                   !- Vertex 3 X-coordinate {m}
    0.00,                   !- Vertex 3 Y-coordinate {m}
    0.90,                   !- Vertex 3 Z-coordinate {m}
    6.98,                   !- Vertex 4 X-coordinate {m}
    0.00,                   !- Vertex 4 Y-coordinate {m}
    2.60;                   !- Vertex 4 Z-coordinate {m}

FenestrationSurface:Detailed,
    B52S1W,                                 !- Name
    Window,                                 !- Surface Type
    Exterior Window,                !- Construction Name
    B52S1,                  !- Building Surface Name
    ,       !- Outside Boundary Condition Object
    ,                               !- View Factor to Ground
    ,                               !- Shading Control Name
    ,                       !- Frame and Divider Name
    ,                                       !- Multiplier
    4,                                      !- Number of Vertices
    3.02,                   !- Vertex 1 X-coordinate {m}
    0.00,                   !- Vertex 1 Y-coordinate {m}
    2.55,                   !- Vertex 1 Z-coordinate {m}
    3.02,                   !- Vertex 2 X-coordinate {m}
    0.00,                   !- Vertex 2 Y-coordinate {m}
    0.90,                   !- Vertex 2 Z-coordinate {m}
    6.98,                   !- Vertex 3 X-coordinate {m}
    0.00,                   !- Vertex 3 Y-coordinate {m}
    0.90,                   !- Vertex 3 Z-coordinate {m}
    6.98,                   !- Vertex 4 X-coordinate {m}
    0.00,                   !- Vertex 4 Y-coordinate {m}
    2.55;                   !- Vertex 4 Z-coordinate {m}

FenestrationSurface:Detailed,
    B53S1W,                                 !- Name
    Window,                                 !- Surface Type
    Exterior Window,                !- Construction Name
    B53S1,                  !- Building Surface Name
    ,       !- Outside Boundary Condition Object
    ,                               !- View Factor to Ground
    ,                               !- Shading Control Name
    ,                       !- Frame and Divider Name
    ,                                       !- Multiplier
    4,                                      !- Number of Vertices
    3.02,                   !- Vertex 1 X-coordinate {m}
    0.00,                   !- Vertex 1 Y-coordinate {m}
    2.55,                   !- Vertex 1 Z-coordinate {m}
    3.02,                   !- Vertex 2 X-coordinate {m}
    0.00,                   !- Vertex 2 Y-coordinate {m}
    0.90,                   !- Vertex 2 Z-coordinate {m}
    6.98,                   !- Vertex 3 X-coordinate {m}
    0.00,                   !- Vertex 3 Y-coordinate {m}
    0.90,                   !- Vertex 3 Z-coordinate {m}
    6.98,                   !- Vertex 4 X-coordinate {m}
    0.00,                   !- Vertex 4 Y-coordinate {m}
    2.55;                   !- Vertex 4 Z-coordinate {m}
```

```
FenestrationSurface:Detailed,
   B51S3W,                  !- Name
   Window,                  !- Surface Type
   Exterior Window,         !- Construction Name
   B51S3,                   !- Building Surface Name
   ,                        !- Outside Boundary Condition Object
   ,                        !- View Factor to Ground
   ,                        !- Shading Control Name
   ,                        !- Frame and Divider Name
   ,                        !- Multiplier
   4,                       !- Number of Vertices
   6.98,                    !- Vertex 1 X-coordinate {m}
   10.00,                   !- Vertex 1 Y-coordinate {m}
   2.60,                    !- Vertex 1 Z-coordinate {m}
   6.98,                    !- Vertex 2 X-coordinate {m}
   10.00,                   !- Vertex 2 Y-coordinate {m}
   0.90,                    !- Vertex 2 Z-coordinate {m}
   3.02,                    !- Vertex 3 X-coordinate {m}
   10.00,                   !- Vertex 3 Y-coordinate {m}
   0.90,                    !- Vertex 3 Z-coordinate {m}
   3.02,                    !- Vertex 4 X-coordinate {m}
   10.00,                   !- Vertex 4 Y-coordinate {m}
   2.60;                    !- Vertex 4 Z-coordinate {m}

FenestrationSurface:Detailed,
   B52S3W,                  !- Name
   Window,                  !- Surface Type
   Exterior Window,         !- Construction Name
   B52S3,                   !- Building Surface Name
   ,                        !- Outside Boundary Condition Object
   ,                        !- View Factor to Ground
   ,                        !- Shading Control Name
   ,                        !- Frame and Divider Name
   ,                        !- Multiplier
   4,                       !- Number of Vertices
   6.98,                    !- Vertex 1 X-coordinate {m}
   10.00,                   !- Vertex 1 Y-coordinate {m}
   2.55,                    !- Vertex 1 Z-coordinate {m}
   6.98,                    !- Vertex 2 X-coordinate {m}
   10.00,                   !- Vertex 2 Y-coordinate {m}
   0.90,                    !- Vertex 2 Z-coordinate {m}
   3.02,                    !- Vertex 3 X-coordinate {m}
   10.00,                   !- Vertex 3 Y-coordinate {m}
   0.90,                    !- Vertex 3 Z-coordinate {m}
   3.02,                    !- Vertex 4 X-coordinate {m}
   10.00,                   !- Vertex 4 Y-coordinate {m}
   2.55;                    !- Vertex 4 Z-coordinate {m}

FenestrationSurface:Detailed,
   B53S3W,                  !- Name
   Window,                  !- Surface Type
   Exterior Window,         !- Construction Name
   B53S3,                   !- Building Surface Name
   ,                        !- Outside Boundary Condition Object
   ,                        !- View Factor to Ground
   ,                        !- Shading Control Name
   ,                        !- Frame and Divider Name
   ,                        !- Multiplier
   4,                       !- Number of Vertices
   6.98,                    !- Vertex 1 X-coordinate {m}
   10.00,                   !- Vertex 1 Y-coordinate {m}
   2.55,                    !- Vertex 1 Z-coordinate {m}
   6.98,                    !- Vertex 2 X-coordinate {m}
   10.00,                   !- Vertex 2 Y-coordinate {m}
   0.90,                    !- Vertex 2 Z-coordinate {m}
   3.02,                    !- Vertex 3 X-coordinate {m}
   10.00,                   !- Vertex 3 Y-coordinate {m}
   0.90,                    !- Vertex 3 Z-coordinate {m}
   3.02,                    !- Vertex 4 X-coordinate {m}
   10.00,                   !- Vertex 4 Y-coordinate {m}
   2.55;                    !- Vertex 4 Z-coordinate {m}

!-   ===   ALL   OBJECTS   IN   CLASS:
INTERNALMASS ===
InternalMass,
   B51_Internal Mass,       !- Name
   InteriorFurnishings,     !- Construction Name
   B51,                     !- Zone Name
   200.00;                  !- Surface Area {m2}

InternalMass,
   B52_Internal Mass,       !- Name
   InteriorFurnishings,     !- Construction Name
   B52,                     !- Zone Name
   200.00;                  !- Surface Area {m2}

InternalMass,
   B53_Internal Mass,       !- Name
   InteriorFurnishings,     !- Construction Name
   B53,                     !- Zone Name
   200.00;                  !- Surface Area {m2}

!-  === ALL OBJECTS IN CLASS: PEOPLE ===
People,
   B51 People,              !- Name
   B51,                     !- Zone or ZoneList Name
   OFF_OCC_SCH,             !- Number of People
Schedule Name
   Area/Person,  !- Number of People Calculation
Method
   ,                        !- Number of People
   ,     !- People per Zone Floor Area {person/m2}
   18.58,                   !- Zone Floor Area per Person
{m2/person}
   0.3,                     !- Fraction Radiant
   AUTOCALCULATE,  !- Sensible Heat Fraction
   ACTIVITY_SCH,       !- Activity Level Schedule
Name
   ,  !- Carbon Dioxide Generation Rate {m3/s-W}
   No,   !- Enable ASHRAE 55 Comfort Warnings
   ZoneAveraged,!- Mean Radiant Temperature
Calculation Type
   ,       !- Surface Name/Angle Factor List Name
   WORK_EFF_SCH,            !- Work Efficiency
Schedule Name
   ClothingInsulationSchedule,     !- Clothing
Insulation Calculation Method
   ,       !- Clothing Insulation Calculation Method
Schedule Name
   OFF_CLOTHING_SCH,   !- Clothing Insulation
Schedule Name
   AIR_VELO_SCH,        !- Air Velocity Schedule
Name
   Fanger;       !- Thermal Comfort Model 1 Type

People,
   B52 People,              !- Name
   B52,                     !- Zone or ZoneList Name
```

```
   OFF_OCC_SCH,              !- Number of People Schedule Name
   Area/Person,  !- Number of People Calculation Method
   ,                         !- Number of People
   ,     !- People per Zone Floor Area {person/m2}
   18.58,            !- Zone Floor Area per Person {m2/person}
   0.3,                      !- Fraction Radiant
   AUTOCALCULATE,  !- Sensible Heat Fraction
   ACTIVITY_SCH,     !- Activity Level Schedule Name
   ,  !- Carbon Dioxide Generation Rate {m3/s-W}
   No,   !- Enable ASHRAE 55 Comfort Warnings
   ZoneAveraged,  !- Mean Radiant Temperature Calculation Type
   ,       !- Surface Name/Angle Factor List Name
   WORK_EFF_SCH,             !- Work Efficiency Schedule Name
   ClothingInsulationSchedule,     !- Clothing Insulation Calculation Method
   ,       !- Clothing Insulation Calculation Method Schedule Name
   OFF_CLOTHING_SCH,   !- Clothing Insulation Schedule Name
   AIR_VELO_SCH,       !- Air Velocity Schedule Name
   Fanger;       !- Thermal Comfort Model 1 Type

People,
   B53 People,                     !- Name
   B53,                  !- Zone or ZoneList Name
   OFF_OCC_SCH,              !- Number of People Schedule Name
   Area/Person,  !- Number of People Calculation Method
   ,                         !- Number of People
   ,     !- People per Zone Floor Area {person/m2}
   18.58,            !- Zone Floor Area per Person {m2/person}
   0.3,                      !- Fraction Radiant
   AUTOCALCULATE,  !- Sensible Heat Fraction
   ACTIVITY_SCH,     !- Activity Level Schedule Name
   ,  !- Carbon Dioxide Generation Rate {m3/s-W}
   No,   !- Enable ASHRAE 55 Comfort Warnings
   ZoneAveraged,  !- Mean Radiant Temperature Calculation Type
   ,       !- Surface Name/Angle Factor List Name
   WORK_EFF_SCH,             !- Work Efficiency Schedule Name
   ClothingInsulationSchedule,     !- Clothing Insulation Calculation Method
   ,       !- Clothing Insulation Calculation Method Schedule Name
   OFF_CLOTHING_SCH,   !- Clothing Insulation Schedule Name
   AIR_VELO_SCH,       !- Air Velocity Schedule Name
   Fanger;       !- Thermal Comfort Model 1 Type

!-  ===  ALL OBJECTS IN CLASS: LIGHTS ===
Lights,
   B51_Lights,                     !- Name
   B51,                  !- Zone or ZoneList Name
   OFF_LIGHT_SCH,            !- Schedule Name
   Watts/Area,           !- Design Level Calculation Method
   ,                         !- Lighting Level {W}
   10.76,     !- Watts per Zone Floor Area {W/m2}
   ,                         !- Watts per Person {W/person}
   0.0000,                   !- Return Air Fraction
   0.7000,                   !- Fraction Radiant
   0.2000,                   !- Fraction Visible
   1.0000,                   !- Fraction Replaceable
   General,                  !- End-Use Subcategory
   No;       !- Return Air Fraction Calculated from Plenum Temperature

Lights,
   B52_Lights,                     !- Name
   B52,                  !- Zone or ZoneList Name
   OFF_LIGHT_SCH,            !- Schedule Name
   Watts/Area,           !- Design Level Calculation Method
   ,                         !- Lighting Level {W}
   10.76,     !- Watts per Zone Floor Area {W/m2}
   ,                         !- Watts per Person {W/person}
   0.0000,                   !- Return Air Fraction
   0.7000,                   !- Fraction Radiant
   0.2000,                   !- Fraction Visible
   1.0000,                   !- Fraction Replaceable
   General,                  !- End-Use Subcategory
   No;       !- Return Air Fraction Calculated from Plenum Temperature

Lights,
   B53_Lights,                     !- Name
   B53,                  !- Zone or ZoneList Name
   OFF_LIGHT_SCH,            !- Schedule Name
   Watts/Area,           !- Design Level Calculation Method
   ,                         !- Lighting Level {W}
   10.76,     !- Watts per Zone Floor Area {W/m2}
   ,                         !- Watts per Person {W/person}
   0.0000,                   !- Return Air Fraction
   0.7000,                   !- Fraction Radiant
   0.2000,                   !- Fraction Visible
   1.0000,                   !- Fraction Replaceable
   General,                  !- End-Use Subcategory
   No;       !- Return Air Fraction Calculated from Plenum Temperature

!-  ===  ALL OBJECTS IN CLASS: ELECTRICEQUIPMENT ===
ElectricEquipment,
   B51_PlugMisc_Equip,             !- Name
   B51,                  !- Zone or ZoneList Name
   OFF_EQP_SCH,              !- Schedule Name
   Watts/Area,           !- Design Level Calculation Method
   ,                         !- Design Level {W}
   10.76,     !- Watts per Zone Floor Area {W/m2}
   ,                         !- Watts per Person {W/person}
   0.0000,                   !- Fraction Latent
   0.5000,                   !- Fraction Radiant
   0.0000,                   !- Fraction Lost
   MiscPlug;                 !- End-Use Subcategory
```

```
ElectricEquipment,
   B52_PlugMisc_Equip,                  !- Name
   B52,                     !- Zone or ZoneList Name
   OFF_EQP_SCH,             !- Schedule Name
   Watts/Area,           !- Design Level Calculation
Method
   ,                                    !- Design Level {W}
   10.76,     !- Watts per Zone Floor Area {W/m2}
   ,                  !- Watts per Person {W/person}
   0.0000,                              !- Fraction Latent
   0.5000,                              !- Fraction Radiant
   0.0000,                                !- Fraction Lost
   MiscPlug;                !- End-Use Subcategory

ElectricEquipment,
   B53_PlugMisc_Equip,                  !- Name
   B53,                     !- Zone or ZoneList Name
   OFF_EQP_SCH,             !- Schedule Name
   Watts/Area,           !- Design Level Calculation
Method
   ,                                    !- Design Level {W}
   10.76,     !- Watts per Zone Floor Area {W/m2}
   ,                  !- Watts per Person {W/person}
   0.0000,                              !- Fraction Latent
   0.5000,                              !- Fraction Radiant
   0.0000,                                !- Fraction Lost
   MiscPlug;                !- End-Use Subcategory

!-   ===   ALL   OBJECTS   IN   CLASS:
EXTERIOR:LIGHTS ===
Exterior:Lights,
   Exterior Facade Lighting,            !- Name
   ALWAYS_ON,               !- Schedule Name
   2303,                    !- Design Level {W}
   AstronomicalClock,          !- Control Option
   Exterior Facade Lighting;          !- End-Use
Subcategory

!-   ===   ALL   OBJECTS   IN   CLASS:
DESIGNSPECIFICATION:OUTDOORAIR ===
DesignSpecification:OutdoorAir,
   B51 DSOA,                            !- Name
   Flow/Person,             !- Outdoor Air Method
   0.01;          !- Outdoor Air Flow per Person
{m3/s-person}

DesignSpecification:OutdoorAir,
   B52 DSOA,                            !- Name
   Flow/Person,             !- Outdoor Air Method
   0.01;          !- Outdoor Air Flow per Person
{m3/s-person}

DesignSpecification:OutdoorAir,
   B53 DSOA,                            !- Name
   Flow/Person,             !- Outdoor Air Method
   0.01;          !- Outdoor Air Flow per Person
{m3/s-person}

!-   ===   ALL   OBJECTS   IN   CLASS:
ZONECONTROL:THERMOSTAT ===
ZoneControl:Thermostat,
   B51 Thermostat,                      !- Name
   B51,                     !- Zone or ZoneList Name
   Dual Zone Control Type Sched,  !- Control Type
Schedule Name
   ThermostatSetpoint:DualSetpoint,  !- Control 1
Object Type
   OFF DualSPSched;           !- Control 1 Name

ZoneControl:Thermostat,
   B52 Thermostat,                      !-
Name
   B52,                     !- Zone or ZoneList Name
   Dual Zone Control Type Sched,  !- Control Type
Schedule Name
   ThermostatSetpoint:DualSetpoint,  !- Control 1
Object Type
   OFF DualSPSched;           !- Control 1 Name

ZoneControl:Thermostat,
   B53 Thermostat,                      !- Name
   B53,                     !- Zone or ZoneList Name
   Dual Zone Control Type Sched,  !- Control Type
Schedule Name
   ThermostatSetpoint:DualSetpoint,  !- Control 1
Object Type
   OFF DualSPSched;           !- Control 1 Name

!-   ===   ALL   OBJECTS   IN   CLASS:
THERMOSTATSETPOINT:DUALSETPOINT
===
ThermostatSetpoint:DualSetpoint,
   OFF DualSPSched,                     !- Name
   OFF_HTGSETP_SCH,     !- Heating Setpoint
Temperature Schedule Name
   OFF_CLGSETP_SCH;     !- Cooling Setpoint
Temperature Schedule Name

!-   ===   ALL   OBJECTS   IN   CLASS:
ZONEHVAC:IDEALLOADSAIRSYSTEM ===
ZoneHVAC:IdealLoadsAirSystem,
   B51 HVAC,                            !- Name
   OFF_OCC_SCH,         !- Availability Schedule
Name
   B51 Supply Inlet,       !- Zone Supply Air Node
Name
   B51 Exhaust, !- Zone Exhaust Air Node Name
   40,                  !- Maximum Heating Supply Air
Temperature {C}
   14,                  !- Minimum Cooling Supply Air
Temperature {C}
   0.0156,           !- Maximum Heating Supply Air
Humidity Ratio {kgWater/kgDryAir}
   0.01,  !- Minimum Cooling Supply Air Humidity
Ratio {kgWater/kgDryAir}
   NoLimit,                             !- Heating Limit
   ,       !- Maximum Heating Air Flow Rate {m3/s}
   ,    !- Maximum Sensible Heating Capacity {W}
   NoLimit,                             !- Cooling Limit
   ,       !- Maximum Cooling Air Flow Rate {m3/s}
   ,         !- Maximum Total Cooling Capacity {W}
   ,           !- Heating Availability Schedule Name
   ,           !- Cooling Availability Schedule Name
   ConstantSupplyHumidityRatio,         !-
Dehumidification Control Type
   0.7,                 !- Cooling Sensible Heat Ratio
{dimensionless}
```

```
   ConstantSupplyHumidityRatio,              !-
Humidification Control Type
   B51 DSOA,     !- Design Specification Outdoor
Air Object Name
   ,                         !- Outdoor Air Inlet Node Name
   None,   !- Demand Controlled Ventilation Type
   NoEconomizer,       !- Outdoor Air Economizer
Type
   None,                     !- Heat Recovery Type
   0.7,    !- Sensible Heat Recovery Effectiveness
{dimensionless}
   0.65;    !- Latent Heat Recovery Effectiveness
{dimensionless}

ZoneHVAC:IdealLoadsAirSystem,
   B52 HVAC,                              !- Name
   OFF_OCC_SCH,        !- Availability Schedule
Name
   B52 Supply Inlet,       !- Zone Supply Air Node
Name
   B52 Exhaust, !- Zone Exhaust Air Node Name
   40,                 !- Maximum Heating Supply Air
Temperature {C}
   14,                 !- Minimum Cooling Supply Air
Temperature {C}
   0.0156,          !- Maximum Heating Supply Air
Humidity Ratio {kgWater/kgDryAir}
   0.01,               !- Minimum Cooling Supply Air
Humidity Ratio {kgWater/kgDryAir}
   NoLimit,                        !- Heating Limit
   ,       !- Maximum Heating Air Flow Rate {m3/s}
   ,    !- Maximum Sensible Heating Capacity {W}
   NoLimit,                        !- Cooling Limit
   ,       !- Maximum Cooling Air Flow Rate {m3/s}
   ,         !- Maximum Total Cooling Capacity {W}
   ,           !- Heating Availability Schedule Name
   ,           !- Cooling Availability Schedule Name
   ConstantSupplyHumidityRatio,              !-
Dehumidification Control Type
   0.7,                !- Cooling Sensible Heat Ratio
{dimensionless}
   ConstantSupplyHumidityRatio,              !-
Humidification Control Type
   B52 DSOA,     !- Design Specification Outdoor
Air Object Name
   ,                         !- Outdoor Air Inlet Node Name
   None,   !- Demand Controlled Ventilation Type
   NoEconomizer,       !- Outdoor Air Economizer
Type
   None,                     !- Heat Recovery Type
   0.7,    !- Sensible Heat Recovery Effectiveness
{dimensionless}
   0.65;    !- Latent Heat Recovery Effectiveness
{dimensionless}

ZoneHVAC:IdealLoadsAirSystem,
   B53 HVAC,                              !- Name
   OFF_OCC_SCH,        !- Availability Schedule
Name
   B53 Supply Inlet,       !- Zone Supply Air Node
Name
   B53 Exhaust, !- Zone Exhaust Air Node Name
   40,                 !- Maximum Heating Supply Air
Temperature {C}
   14,                 !- Minimum Cooling Supply Air
Temperature {C}
   0.0156,          !- Maximum Heating Supply Air
Humidity Ratio {kgWater/kgDryAir}
   0.01,               !- Minimum Cooling Supply Air
Humidity Ratio {kgWater/kgDryAir}
   NoLimit,                        !- Heating Limit
   ,       !- Maximum Heating Air Flow Rate {m3/s}
   ,    !- Maximum Sensible Heating Capacity {W}
   NoLimit,                        !- Cooling Limit
   ,       !- Maximum Cooling Air Flow Rate {m3/s}
   ,         !- Maximum Total Cooling Capacity {W}
   ,           !- Heating Availability Schedule Name
   ,           !- Cooling Availability Schedule Name
   ConstantSupplyHumidityRatio,              !-
Dehumidification Control Type
   0.7,                !- Cooling Sensible Heat Ratio
{dimensionless}
   ConstantSupplyHumidityRatio,              !-
Humidification Control Type
   B53 DSOA,!- Design Specification Outdoor Air
Object Name
   ,                         !- Outdoor Air Inlet Node Name
   None,   !- Demand Controlled Ventilation Type
   NoEconomizer,       !- Outdoor Air Economizer
Type
   None,                     !- Heat Recovery Type
   0.7,    !- Sensible Heat Recovery Effectiveness
{dimensionless}
   0.65;    !- Latent Heat Recovery Effectiveness
{dimensionless}

!-   ===   ALL   OBJECTS   IN   CLASS:
ZONEHVAC:EQUIPMENTLIST ===
ZoneHVAC:EquipmentList,
   B51 HVAC Equipment,                    !- Name
   ZoneHVAC:IdealLoadsAirSystem,    !- Zone
Equipment 1 Object Type
   B51 HVAC,          !- Zone Equipment 1 Name
   1,       !- Zone Equipment 1 Cooling Sequence
   1;      !- Zone Equipment 1 Heating or No-Load
Sequence

ZoneHVAC:EquipmentList,
   B52 HVAC Equipment,                    !- Name
   ZoneHVAC:IdealLoadsAirSystem,    !- Zone
Equipment 1 Object Type
   B52 HVAC,          !- Zone Equipment 1 Name
   1,       !- Zone Equipment 1 Cooling Sequence
   1;      !- Zone Equipment 1 Heating or No-Load
Sequence

ZoneHVAC:EquipmentList,
   B53 HVAC Equipment,                    !- Name
   ZoneHVAC:IdealLoadsAirSystem,    !- Zone
Equipment 1 Object Type
   B53 HVAC,          !- Zone Equipment 1 Name
   1,       !- Zone Equipment 1 Cooling Sequence
   1;      !- Zone Equipment 1 Heating or No-Load
Sequence

!-   ===   ALL   OBJECTS   IN   CLASS:
ZONEHVAC:EQUIPMENTCONNECTIONS ===
ZoneHVAC:EquipmentConnections,
```

```
   B51,                          !- Zone Name
B51 HVAC Equipment,      !- Zone Conditioning
Equipment List Name
   B51 Supply Inlet,        !- Zone Air Inlet Node or
NodeList Name
   B51 Exhaust,        !- Zone Air Exhaust Node or
NodeList Name
   B51 Zone Air Node,     !- Zone Air Node Name
   B51 Return Outlet;      !- Zone Return Air Node
Name

ZoneHVAC:EquipmentConnections,
   B52,                          !- Zone Name
   B52 HVAC Equipment,     !- Zone Conditioning
Equipment List Name
   B52 Supply Inlet,        !- Zone Air Inlet Node or
NodeList Name
   B52 Exhaust,        !- Zone Air Exhaust Node or
NodeList Name
   B52 Zone Air Node,     !- Zone Air Node Name
   B52 Return Outlet;      !- Zone Return Air Node
Name

ZoneHVAC:EquipmentConnections,
   B53,                          !- Zone Name
   B53 HVAC Equipment,     !- Zone Conditioning
Equipment List Name
   B53 Supply Inlet,        !- Zone Air Inlet Node or
NodeList Name
   B53 Exhaust,        !- Zone Air Exhaust Node or
NodeList Name
   B53 Zone Air Node,     !- Zone Air Node Name
   B53 Return Outlet;      !- Zone Return Air Node
Name

!-        ===        ALL        OBJECTS        IN        CLASS:
OUTPUT:VARIABLEDICTIONARY ===
Output:VariableDictionary,
   regular;                      !- Key Field

!-        ===        ALL        OBJECTS        IN        CLASS:
OUTPUTCONTROL:TABLE:STYLE ===
OutputControl:Table:Style,
   Tab,                          !- Column Separator
   JtoKWH;                       !- Unit Conversion

!-        ===        ALL        OBJECTS        IN        CLASS:
OUTPUTCONTROL:REPORTINGTOLERANCE
S ===
OutputControl:ReportingTolerances,
   0.556,   !- Tolerance for Time Heating Setpoint
Not Met {deltaC}
   0.556;   !- Tolerance for Time Cooling Setpoint
Not Met {deltaC}

!-        ===        ALL        OBJECTS        IN        CLASS:
OUTPUT:VARIABLE ===
Output:Variable,
   *,                            !- Key Value
   Surface Outside Face Temperature,     !-
Variable Name
   Hourly,                       !- Reporting Frequency
   Report_Sch;                   !- Schedule Name

!-        ===        ALL        OBJECTS        IN        CLASS:
ENVIRONMENTALIMPACTFACTORS ===
EnvironmentalImpactFactors,
   0.663,                !- District Heating Efficiency
   4.18,                 !- District Cooling COP {W/W}
   0.585,                !- Steam Conversion Efficiency
   80.7272,  !- Total Carbon Equivalent Emission
Factor From N2O {kg/kg}
   6.2727,    !- Total Carbon Equivalent Emission
Factor From CH4 {kg/kg}
   0.2727;    !- Total Carbon Equivalent Emission
Factor From CO2 {kg/kg}
```

Appendix 5 Additional content to EnergyPlus *IDF file to apply the new CHTCs from CFD among iterations during the coupling process

The followings are the additional contents to the *IDF file in *Appendix 4* to accept new CHTCs for each surface of B5 during the coupling process.

```
!-   === ALL OBJECTS IN CLASS: SURFACEPROPERTY:CONVECTIONCOEFFICIENTS ===
SurfaceProperty:ConvectionCoefficients,
    B51S1,                   !- Surface Name
    Outside,   !- Convection Coefficient 1 Location
    Schedule,      !- Convection Coefficient 1 Type
    ,          !- Convection Coefficient 1 {W/m2-K}
    B51S1-CHTC-12-2;!- Convection Coefficient 1 Schedule Name

SurfaceProperty:ConvectionCoefficients,
    B51S2,                   !- Surface Name
    Outside,   !- Convection Coefficient 1 Location
    Schedule,      !- Convection Coefficient 1 Type
    ,          !- Convection Coefficient 1 {W/m2-K}
    B51S2-CHTC-12-2;!- Convection Coefficient 1 Schedule Name

SurfaceProperty:ConvectionCoefficients,
    B51S3,                   !- Surface Name
    Outside,   !- Convection Coefficient 1 Location
    Schedule,      !- Convection Coefficient 1 Type
    ,          !- Convection Coefficient 1 {W/m2-K}
    B51S3-CHTC-12-2;!- Convection Coefficient 1 Schedule Name

SurfaceProperty:ConvectionCoefficients,
    B51S4,                   !- Surface Name
    Outside,   !- Convection Coefficient 1 Location
    Schedule,      !- Convection Coefficient 1 Type
    ,          !- Convection Coefficient 1 {W/m2-K}
    B51S4-CHTC-12-2;!- Convection Coefficient 1 Schedule Name

SurfaceProperty:ConvectionCoefficients,
    B52S1,                   !- Surface Name
    Outside,   !- Convection Coefficient 1 Location
    Schedule,      !- Convection Coefficient 1 Type
    ,          !- Convection Coefficient 1 {W/m2-K}
    B52S1-CHTC-12-2;!- Convection Coefficient 1 Schedule Name

SurfaceProperty:ConvectionCoefficients,
    B52S2,                   !- Surface Name
    Outside,   !- Convection Coefficient 1 Location
    Schedule,      !- Convection Coefficient 1 Type
    ,          !- Convection Coefficient 1 {W/m2-K}
    B52S2-CHTC-12-2;!- Convection Coefficient 1 Schedule Name

SurfaceProperty:ConvectionCoefficients,
    B52S3,                   !- Surface Name
    Outside,   !- Convection Coefficient 1 Location
    Schedule,      !- Convection Coefficient 1 Type
    ,          !- Convection Coefficient 1 {W/m2-K}
    B52S3-CHTC-12-2;!- Convection Coefficient 1 Schedule Name

SurfaceProperty:ConvectionCoefficients,
    B52S4,                   !- Surface Name
    Outside,   !- Convection Coefficient 1 Location
    Schedule,      !- Convection Coefficient 1 Type
    ,          !- Convection Coefficient 1 {W/m2-K}
    B52S4-CHTC-12-2;!- Convection Coefficient 1 Schedule Name

SurfaceProperty:ConvectionCoefficients,
    B53S1,                   !- Surface Name
    Outside,   !- Convection Coefficient 1 Location
    Schedule,      !- Convection Coefficient 1 Type
    ,          !- Convection Coefficient 1 {W/m2-K}
    B53S1-CHTC-12-2;!- Convection Coefficient 1 Schedule Name

SurfaceProperty:ConvectionCoefficients,
    B53S2,                   !- Surface Name
    Outside,   !- Convection Coefficient 1 Location
    Schedule,      !- Convection Coefficient 1 Type
    ,          !- Convection Coefficient 1 {W/m2-K}
    B53S2-CHTC-12-2;!- Convection Coefficient 1 Schedule Name

SurfaceProperty:ConvectionCoefficients,
    B53S3,                   !- Surface Name
    Outside,   !- Convection Coefficient 1 Location
    Schedule,      !- Convection Coefficient 1 Type
    ,          !- Convection Coefficient 1 {W/m2-K}
    B53S3-CHTC-12-2;!- Convection Coefficient 1 Schedule Name

SurfaceProperty:ConvectionCoefficients,
    B53S4,                   !- Surface Name
    Outside,   !- Convection Coefficient 1 Location
    Schedule,      !- Convection Coefficient 1 Type
    ,          !- Convection Coefficient 1 {W/m2-K}
    B53S4-CHTC-12-2;!- Convection Coefficient 1 Schedule Name

SurfaceProperty:ConvectionCoefficients,
    B53R,                    !- Surface Name
    Outside,   !- Convection Coefficient 1 Location
    Schedule,      !- Convection Coefficient 1 Type
    ,          !- Convection Coefficient 1 {W/m2-K}
```

```
   B53R-CHTC-12-2;  !- Convection Coefficient 1 Schedule Name

*Following objects would be added to the class of schedule '!-  ===  ALL OBJECTS IN CLASS: SCHEDULE:COMPACT ==='.

Schedule:Compact,
   B51S1-CHTC-12-2,                 !- Name
   Any Number,    !- Schedule Type Limits Name
   Through: 9/24,                   !- Field 1
   For: AllDays,                    !- Field 2
   Until: 21:00,                    !- Field 3
   0.1,                             !- Field 4
   Until: 22:00,                    !- Field 5
   3.686,                           !- Field 6
   Until: 23:00,                    !- Field 7
   4.183,                           !- Field 8
   Until: 24:00,                    !- Field 9
   3.716,                           !- Field 10
   Through: 9/25,                   !- Field 11
   For: AllDays,                    !- Field 12
   Until: 01:00,                    !- Field 13
   6.164,                           !- Field 14
   Until: 02:00,                    !- Field 15
   3.917,                           !- Field 16
   Until: 03:00,                    !- Field 17
   3.568,                           !- Field 18
   Until: 04:00,                    !- Field 19
   3.152,                           !- Field 20
   Until: 05:00,                    !- Field 21
   3.226,                           !- Field 22
   Until: 06:00,                    !- Field 23
   3.127,                           !- Field 24
   Until: 07:00,                    !- Field 25
   2.525,                           !- Field 26
   Until: 08:00,                    !- Field 27
   3.215,                           !- Field 28
   Until: 09:00,                    !- Field 29
   3.370,                           !- Field 30
   Until: 10:00,                    !- Field 31
   10.042,                          !- Field 32
   Until: 11:00,                    !- Field 33
   9.544,                           !- Field 34
   Until: 12:00,                    !- Field 35
   6.498,                           !- Field 36
   Until: 13:00,                    !- Field 37
   5.867,                           !- Field 38
   Until: 14:00,                    !- Field 39
   6.239,                           !- Field 40
   Until: 15:00,                    !- Field 41
   6.223,                           !- Field 42
   Until: 16:00,                    !- Field 43
   6.174,                           !- Field 44
   Until: 17:00,                    !- Field 45
   5.433,                           !- Field 46
   Until: 18:00,                    !- Field 47
   4.484,                           !- Field 48
   Until: 19:00,                    !- Field 49
   4.193,                           !- Field 50
   Until: 20:00,                    !- Field 51
   3.774,                           !- Field 52
   Until: 21:00,                    !- Field 53
   3.472,                           !- Field 54
   Until: 22:00,                    !- Field 55
   3.689,                           !- Field 56
   Until: 23:00,                    !- Field 57
   3.449,                           !- Field 58
   Until: 24:00,                    !- Field 59
   3.461,                           !- Field 60
   Through: 12/31,                  !- Field 61
   For: AllDays,                    !- Field 62
   Until: 24:00,                    !- Field 63
   0.1;                             !- Field 64

Schedule:Compact,
   B51S2-CHTC-12-2,                 !- Name
   Any Number,    !- Schedule Type Limits Name
   Through: 9/24,                   !- Field 1
   For: AllDays,                    !- Field 2
   Until: 21:00,                    !- Field 3
   0.1,                             !- Field 4
   Until: 22:00,                    !- Field 5
   3.343,                           !- Field 6
   Until: 23:00,                    !- Field 7
   3.904,                           !- Field 8
   Until: 24:00,                    !- Field 9
   3.011,                           !- Field 10
   Through: 9/25,                   !- Field 11
   For: AllDays,                    !- Field 12
   7.600,                           !- Field 14
   Until: 02:00,                    !- Field 15
   3.233,                           !- Field 16
   Until: 03:00,                    !- Field 17
   2.836,                           !- Field 18
   Until: 04:00,                    !- Field 19
   2.823,                           !- Field 20
   Until: 05:00,                    !- Field 21
   2.931,                           !- Field 22
   Until: 06:00,                    !- Field 23
   2.384,                           !- Field 24
   Until: 07:00,                    !- Field 25
   2.049,                           !- Field 26
   Until: 08:00,                    !- Field 27
   2.327,                           !- Field 28
   Until: 09:00,                    !- Field 29
   2.668,                           !- Field 30
   Until: 10:00,                    !- Field 31
   6.592,                           !- Field 32
   Until: 11:00,                    !- Field 33
   7.558,                           !- Field 34
   Until: 12:00,                    !- Field 35
   4.614,                           !- Field 36
   Until: 13:00,                    !- Field 37
   5.303,                           !- Field 38
   Until: 14:00,                    !- Field 39
   5.454,                           !- Field 40
   Until: 15:00,                    !- Field 41
   5.419,                           !- Field 42
   Until: 16:00,                    !- Field 43
   5.428,                           !- Field 44
   Until: 17:00,                    !- Field 45
   4.916,                           !- Field 46
   Until: 18:00,                    !- Field 47
   4.204,                           !- Field 48
   Until: 19:00,                    !- Field 49
   4.067,                           !- Field 50
   Until: 20:00,                    !- Field 51
   3.711,                           !- Field 52
```

```
   Until: 21:00,                    !- Field 53
   3.016,                           !- Field 54
   Until: 22:00,                    !- Field 55
   3.309,                           !- Field 56
   Until: 23:00,                    !- Field 57
   3.484,                           !- Field 58
   Until: 24:00,                    !- Field 59
   3.515,                           !- Field 60
   Through: 12/31,                  !- Field 61
   For: AllDays,                    !- Field 62
   Until: 24:00,                    !- Field 63
   0.1;                             !- Field 64

Schedule:Compact,
   B51S3-CHTC-12-2,                 !- Name
   Any Number,     !- Schedule Type Limits Name
   Through: 9/24,                   !- Field 1
   For: AllDays,                    !- Field 2
   Until: 21:00,                    !- Field 3
   0.1,                             !- Field 4
   Until: 22:00,                    !- Field 5
   3.080,                           !- Field 6
   Until: 23:00,                    !- Field 7
   3.691,                           !- Field 8
   Until: 24:00,                    !- Field 9
   2.744,                           !- Field 10
   Through: 9/25,                   !- Field 11
   For: AllDays,                    !- Field 12
   Until: 01:00,                    !- Field 13
   6.346,                           !- Field 14
   Until: 02:00,                    !- Field 15
   3.000,                           !- Field 16
   Until: 03:00,                    !- Field 17
   2.554,                           !- Field 18
   Until: 04:00,                    !- Field 19
   2.549,                           !- Field 20
   Until: 05:00,                    !- Field 21
   2.703,                           !- Field 22
   Until: 06:00,                    !- Field 23
   2.055,                           !- Field 24
   Until: 07:00,                    !- Field 25
   2.245,                           !- Field 26
   Until: 08:00,                    !- Field 27
   2.558,                           !- Field 28
   Until: 09:00,                    !- Field 29
   2.932,                           !- Field 30
   Until: 10:00,                    !- Field 31
   6.531,                           !- Field 32
   Until: 11:00,                    !- Field 33
   6.754,                           !- Field 34
   Until: 12:00,                    !- Field 35
   8.408,                           !- Field 36
   Until: 13:00,                    !- Field 37
   4.607,                           !- Field 38
   Until: 14:00,                    !- Field 39
   5.112,                           !- Field 40
   Until: 15:00,                    !- Field 41
   5.163,                           !- Field 42
   Until: 16:00,                    !- Field 43
   5.223,                           !- Field 44
   Until: 17:00,                    !- Field 45
   4.715,                           !- Field 46
   Until: 18:00,                    !- Field 47
   3.988,                           !- Field 48
   Until: 19:00,                    !- Field 49
   3.833,                           !- Field 50
   Until: 20:00,                    !- Field 51
   3.447,                           !- Field 52
   Until: 21:00,                    !- Field 53
   3.148,                           !- Field 54
   Until: 22:00,                    !- Field 55
   3.469,                           !- Field 56
   Until: 23:00,                    !- Field 57
   3.244,                           !- Field 58
   Until: 24:00,                    !- Field 59
   3.301,                           !- Field 60
   Through: 12/31,                  !- Field 61
   For: AllDays,                    !- Field 62
   Until: 24:00,                    !- Field 63
   0.1;                             !- Field 64

Schedule:Compact,
   B51S4-CHTC-12-2,                 !- Name
   Any Number,     !- Schedule Type Limits Name
   Through: 9/24,                   !- Field 1
   For: AllDays,                    !- Field 2
   Until: 21:00,                    !- Field 3
   0.1,                             !- Field 4
   Until: 22:00,                    !- Field 5
   3.805,                           !- Field 6
   Until: 23:00,                    !- Field 7
   4.269,                           !- Field 8
   Until: 24:00,                    !- Field 9
   3.467,                           !- Field 10
   Through: 9/25,                   !- Field 11
   For: AllDays,                    !- Field 12
   Until: 01:00,                    !- Field 13
   5.086,                           !- Field 14
   Until: 02:00,                    !- Field 15
   3.699,                           !- Field 16
   Until: 03:00,                    !- Field 17
   3.327,                           !- Field 18
   Until: 04:00,                    !- Field 19
   3.311,                           !- Field 20
   Until: 05:00,                    !- Field 21
   3.396,                           !- Field 22
   Until: 06:00,                    !- Field 23
   2.857,                           !- Field 24
   Until: 07:00,                    !- Field 25
   2.601,                           !- Field 26
   Until: 08:00,                    !- Field 27
   2.056,                           !- Field 28
   Until: 09:00,                    !- Field 29
   2.685,                           !- Field 30
   Until: 10:00,                    !- Field 31
   8.922,                           !- Field 32
   Until: 11:00,                    !- Field 33
   9.380,                           !- Field 34
   Until: 12:00,                    !- Field 35
   5.403,                           !- Field 36
   Until: 13:00,                    !- Field 37
   4.739,                           !- Field 38
   Until: 14:00,                    !- Field 39
   5.524,                           !- Field 40
   Until: 15:00,                    !- Field 41
   5.863,                           !- Field 42
   Until: 16:00,                    !- Field 43
   6.096,                           !- Field 44
   Until: 17:00,                    !- Field 45
```

```
    5.275,                   !- Field 46
    Until: 18:00,            !- Field 47
    4.279,                   !- Field 48
    Until: 19:00,            !- Field 49
    3.951,                   !- Field 50
    Until: 20:00,            !- Field 51
    3.492,                   !- Field 52
    Until: 21:00,            !- Field 53
    3.166,                   !- Field 54
    Until: 22:00,            !- Field 55
    3.805,                   !- Field 56
    Until: 23:00,            !- Field 57
    3.164,                   !- Field 58
    Until: 24:00,            !- Field 59
    3.197,                   !- Field 60
    Through: 12/31,          !- Field 61
    For: AllDays,            !- Field 62
    Until: 24:00,            !- Field 63
    0.1;                     !- Field 64

Schedule:Compact,
    B52S1-CHTC-12-2,         !- Name
    Any Number,    !- Schedule Type Limits Name
    Through: 9/24,           !- Field 1
    For: AllDays,            !- Field 2
    Until: 21:00,            !- Field 3
    0.1,                     !- Field 4
    Until: 22:00,            !- Field 5
    4.284,                   !- Field 6
    Until: 23:00,            !- Field 7
    5.133,                   !- Field 8
    Until: 24:00,            !- Field 9
    4.139,                   !- Field 10
    Through: 9/25,           !- Field 11
    For: AllDays,            !- Field 12
    Until: 01:00,            !- Field 13
    6.507,                   !- Field 14
    Until: 02:00,            !- Field 15
    4.427,                   !- Field 16
    Until: 03:00,            !- Field 17
    3.983,                   !- Field 18
    Until: 04:00,            !- Field 19
    3.589,                   !- Field 20
    Until: 05:00,            !- Field 21
    3.657,                   !- Field 22
    Until: 06:00,            !- Field 23
    3.414,                   !- Field 24
    Until: 07:00,            !- Field 25
    2.776,                   !- Field 26
    Until: 08:00,            !- Field 27
    3.676,                   !- Field 28
    Until: 09:00,            !- Field 29
    3.818,                   !- Field 30
    Until: 10:00,            !- Field 31
    11.256,                  !- Field 32
    Until: 11:00,            !- Field 33
    10.698,                  !- Field 34
    Until: 12:00,            !- Field 35
    7.737,                   !- Field 36
    Until: 13:00,            !- Field 37
    7.170,                   !- Field 38
    Until: 14:00,            !- Field 39
    7.682,                   !- Field 40
    Until: 15:00,            !- Field 41
    7.665,                   !- Field 42
    Until: 16:00,            !- Field 43
    7.626,                   !- Field 44
    Until: 17:00,            !- Field 45
    6.549,                   !- Field 46
    Until: 18:00,            !- Field 47
    5.135,                   !- Field 48
    Until: 19:00,            !- Field 49
    4.891,                   !- Field 50
    Until: 20:00,            !- Field 51
    4.324,                   !- Field 52
    Until: 21:00,            !- Field 53
    3.864,                   !- Field 54
    Until: 22:00,            !- Field 55
    4.260,                   !- Field 56
    Until: 23:00,            !- Field 57
    3.849,                   !- Field 58
    Until: 24:00,            !- Field 59
    3.863,                   !- Field 60
    Through: 12/31,          !- Field 61
    For: AllDays,            !- Field 62
    Until: 24:00,            !- Field 63
    0.1;                     !- Field 64

Schedule:Compact,
    B52S2-CHTC-12-2,         !- Name
    Any Number,    !- Schedule Type Limits Name
    Through: 9/24,           !- Field 1
    For: AllDays,            !- Field 2
    Until: 21:00,            !- Field 3
    0.1,                     !- Field 4
    Until: 22:00,            !- Field 5
    4.064,                   !- Field 6
    Until: 23:00,            !- Field 7
    4.967,                   !- Field 8
    Until: 24:00,            !- Field 9
    3.565,                   !- Field 10
    Through: 9/25,           !- Field 11
    For: AllDays,            !- Field 12
    Until: 01:00,            !- Field 13
    7.991,                   !- Field 14
    Until: 02:00,            !- Field 15
    3.931,                   !- Field 16
    Until: 03:00,            !- Field 17
    3.376,                   !- Field 18
    Until: 04:00,            !- Field 19
    3.366,                   !- Field 20
    Until: 05:00,            !- Field 21
    3.455,                   !- Field 22
    Until: 06:00,            !- Field 23
    2.726,                   !- Field 24
    Until: 07:00,            !- Field 25
    2.437,                   !- Field 26
    Until: 08:00,            !- Field 27
    2.971,                   !- Field 28
    Until: 09:00,            !- Field 29
    3.536,                   !- Field 30
    Until: 10:00,            !- Field 31
    7.263,                   !- Field 32
    Until: 11:00,            !- Field 33
    7.820,                   !- Field 34
    Until: 12:00,            !- Field 35
    5.162,                   !- Field 36
    Until: 13:00,            !- Field 37
    6.304,                   !- Field 38
```

```
    Until: 14:00,                 !- Field 39
    6.535,                        !- Field 40
    Until: 15:00,                 !- Field 41
    6.503,                        !- Field 42
    Until: 16:00,                 !- Field 43
    6.507,                        !- Field 44
    Until: 17:00,                 !- Field 45
    5.830,                        !- Field 46
    Until: 18:00,                 !- Field 47
    4.864,                        !- Field 48
    Until: 19:00,                 !- Field 49
    4.747,                        !- Field 50
    Until: 20:00,                 !- Field 51
    4.309,                        !- Field 52
    Until: 21:00,                 !- Field 53
    3.543,                        !- Field 54
    Until: 22:00,                 !- Field 55
    4.005,                        !- Field 56
    Until: 23:00,                 !- Field 57
    3.970,                        !- Field 58
    Until: 24:00,                 !- Field 59
    3.997,                        !- Field 60
    Through: 12/31,               !- Field 61
    For: AllDays,                 !- Field 62
    Until: 24:00,                 !- Field 63
    0.1;                          !- Field 64

Schedule:Compact,
    B52S3-CHTC-12-2,              !- Name
    Any Number,    !- Schedule Type Limits Name
    Through: 9/24,                !- Field 1
    For: AllDays,                 !- Field 2
    Until: 21:00,                 !- Field 3
    0.1,                          !- Field 4
    Until: 22:00,                 !- Field 5
    3.839,                        !- Field 6
    Until: 23:00,                 !- Field 7
    4.796,                        !- Field 8
    Until: 24:00,                 !- Field 9
    3.333,                        !- Field 10
    Through: 9/25,                !- Field 11
    For: AllDays,                 !- Field 12
    Until: 01:00,                 !- Field 13
    8.626,                        !- Field 14
    Until: 02:00,                 !- Field 15
    3.722,                        !- Field 16
    Until: 03:00,                 !- Field 17
    3.114,                        !- Field 18
    Until: 04:00,                 !- Field 19
    3.110,                        !- Field 20
    Until: 05:00,                 !- Field 21
    3.241,                        !- Field 22
    Until: 06:00,                 !- Field 23
    2.397,                        !- Field 24
    Until: 07:00,                 !- Field 25
    2.831,                        !- Field 26
    Until: 08:00,                 !- Field 27
    3.206,                        !- Field 28
    Until: 09:00,                 !- Field 29
    3.492,                        !- Field 30
    Until: 10:00,                 !- Field 31
    6.098,                        !- Field 32
    Until: 11:00,                 !- Field 33
    4.999,                        !- Field 34
    Until: 12:00,                 !- Field 35
    6.789,                        !- Field 36
    Until: 13:00,                 !- Field 37
    6.281,                        !- Field 38
    Until: 14:00,                 !- Field 39
    6.244,                        !- Field 40
    Until: 15:00,                 !- Field 41
    6.283,                        !- Field 42
    Until: 16:00,                 !- Field 43
    6.328,                        !- Field 44
    Until: 17:00,                 !- Field 45
    5.651,                        !- Field 46
    Until: 18:00,                 !- Field 47
    4.663,                        !- Field 48
    Until: 19:00,                 !- Field 49
    4.530,                        !- Field 50
    Until: 20:00,                 !- Field 51
    4.060,                        !- Field 52
    Until: 21:00,                 !- Field 53
    3.656,                        !- Field 54
    Until: 22:00,                 !- Field 55
    4.078,                        !- Field 56
    Until: 23:00,                 !- Field 57
    3.738,                        !- Field 58
    Until: 24:00,                 !- Field 59
    3.788,                        !- Field 60
    Through: 12/31,               !- Field 61
    For: AllDays,                 !- Field 62
    Until: 24:00,                 !- Field 63
    0.1;                          !- Field 64

Schedule:Compact,
    B52S4-CHTC-12-2,              !- Name
    Any Number,    !- Schedule Type Limits Name
    Through: 9/24,                !- Field 1
    For: AllDays,                 !- Field 2
    Until: 21:00,                 !- Field 3
    0.1,                          !- Field 4
    Until: 22:00,                 !- Field 5
    4.413,                        !- Field 6
    Until: 23:00,                 !- Field 7
    5.062,                        !- Field 8
    Until: 24:00,                 !- Field 9
    3.980,                        !- Field 10
    Through: 9/25,                !- Field 11
    For: AllDays,                 !- Field 12
    Until: 01:00,                 !- Field 13
    6.420,                        !- Field 14
    Until: 02:00,                 !- Field 15
    4.285,                        !- Field 16
    Until: 03:00,                 !- Field 17
    3.822,                        !- Field 18
    Until: 04:00,                 !- Field 19
    3.808,                        !- Field 20
    Until: 05:00,                 !- Field 21
    3.881,                        !- Field 22
    Until: 06:00,                 !- Field 23
    3.226,                        !- Field 24
    Until: 07:00,                 !- Field 25
    3.001,                        !- Field 26
    Until: 08:00,                 !- Field 27
    2.845,                        !- Field 28
    Until: 09:00,                 !- Field 29
    3.282,                        !- Field 30
    Until: 10:00,                 !- Field 31
```

```
    9.746,                   !- Field 32
    Until: 11:00,            !- Field 33
    10.522,                  !- Field 34
    Until: 12:00,            !- Field 35
    6.502,                   !- Field 36
    Until: 13:00,            !- Field 37
    6.364,                   !- Field 38
    Until: 14:00,            !- Field 39
    7.165,                   !- Field 40
    Until: 15:00,            !- Field 41
    7.406,                   !- Field 42
    Until: 16:00,            !- Field 43
    7.600,                   !- Field 44
    Until: 17:00,            !- Field 45
    6.645,                   !- Field 46
    Until: 18:00,            !- Field 47
    5.072,                   !- Field 48
    Until: 19:00,            !- Field 49
    4.772,                   !- Field 50
    Until: 20:00,            !- Field 51
    4.163,                   !- Field 52
    Until: 21:00,            !- Field 53
    3.672,                   !- Field 54
    Until: 22:00,            !- Field 55
    4.387,                   !- Field 56
    Until: 23:00,            !- Field 57
    3.662,                   !- Field 58
    Until: 24:00,            !- Field 59
    3.689,                   !- Field 60
    Through: 12/31,          !- Field 61
    For: AllDays,            !- Field 62
    Until: 24:00,            !- Field 63
    0.1;                     !- Field 64

Schedule:Compact,
    B53S1-CHTC-12-2,                 !- Name
    Any Number,     !- Schedule Type Limits Name
    Through: 9/24,           !- Field 1
    For: AllDays,            !- Field 2
    Until: 21:00,            !- Field 3
    0.1,                     !- Field 4
    Until: 22:00,            !- Field 5
    4.653,                   !- Field 6
    Until: 23:00,            !- Field 7
    5.712,                   !- Field 8
    Until: 24:00,            !- Field 9
    4.359,                   !- Field 10
    Through: 9/25,           !- Field 11
    For: AllDays,            !- Field 12
    6.170,                   !- Field 14
    Until: 02:00,            !- Field 15
    4.720,                   !- Field 16
    Until: 03:00,            !- Field 17
    4.220,                   !- Field 18
    Until: 04:00,            !- Field 19
    3.874,                   !- Field 20
    Until: 05:00,            !- Field 21
    3.936,                   !- Field 22
    Until: 06:00,            !- Field 23
    3.566,                   !- Field 24
    Until: 07:00,            !- Field 25
    2.921,                   !- Field 26
    Until: 08:00,            !- Field 27
    3.930,                   !- Field 28
    Until: 09:00,            !- Field 29
    4.088,                   !- Field 30
    Until: 10:00,            !- Field 31
    12.334,                  !- Field 32
    Until: 11:00,            !- Field 33
    11.426,                  !- Field 34
    Until: 12:00,            !- Field 35
    7.810,                   !- Field 36
    Until: 13:00,            !- Field 37
    8.008,                   !- Field 38
    Until: 14:00,            !- Field 39
    8.603,                   !- Field 40
    Until: 15:00,            !- Field 41
    8.587,                   !- Field 42
    Until: 16:00,            !- Field 43
    8.553,                   !- Field 44
    Until: 17:00,            !- Field 45
    7.279,                   !- Field 46
    Until: 18:00,            !- Field 47
    5.586,                   !- Field 48
    Until: 19:00,            !- Field 49
    5.360,                   !- Field 50
    Until: 20:00,            !- Field 51
    4.698,                   !- Field 52
    Until: 21:00,            !- Field 53
    4.135,                   !- Field 54
    Until: 22:00,            !- Field 55
    4.639,                   !- Field 56
    Until: 23:00,            !- Field 57
    4.122,                   !- Field 58
    Until: 24:00,            !- Field 59
    4.136,                   !- Field 60
    Through: 12/31,          !- Field 61
    For: AllDays,            !- Field 62
    Until: 24:00,            !- Field 63
    0.1;                     !- Field 64

Schedule:Compact,
    B53S2-CHTC-12-2,                 !- Name
    Any Number,     !- Schedule Type Limits Name
    Through: 9/24,           !- Field 1
    For: AllDays,            !- Field 2
    Until: 21:00,            !- Field 3
    0.1,                     !- Field 4
    Until: 22:00,            !- Field 5
    4.501,                   !- Field 6
    Until: 23:00,            !- Field 7
    5.602,                   !- Field 8
    Until: 24:00,            !- Field 9
    3.894,                   !- Field 10
    Through: 9/25,           !- Field 11
    For: AllDays,            !- Field 12
    Until: 01:00,            !- Field 13
    11.498,                  !- Field 14
    Until: 02:00,            !- Field 15
    4.383,                   !- Field 16
    Until: 03:00,            !- Field 17
    3.732,                   !- Field 18
    Until: 04:00,            !- Field 19
    3.719,                   !- Field 20
    Until: 05:00,            !- Field 21
    3.795,                   !- Field 22
    Until: 06:00,            !- Field 23
    2.948,                   !- Field 24
    Until: 07:00,            !- Field 25
```

```
    2.671,                   !- Field 26
    Until: 08:00,            !- Field 27
    3.867,                   !- Field 28
    Until: 09:00,            !- Field 29
    4.588,                   !- Field 30
    Until: 10:00,            !- Field 31
    6.723,                   !- Field 32
    Until: 11:00,            !- Field 33
    6.435,                   !- Field 34
    Until: 12:00,            !- Field 35
    4.721,                   !- Field 36
    Until: 13:00,            !- Field 37
    6.897,                   !- Field 38
    Until: 14:00,            !- Field 39
    7.170,                   !- Field 40
    Until: 15:00,            !- Field 41
    7.140,                   !- Field 42
    Until: 16:00,            !- Field 43
    7.142,                   !- Field 44
    Until: 17:00,            !- Field 45
    6.379,                   !- Field 46
    Until: 18:00,            !- Field 47
    5.279,                   !- Field 48
    Until: 19:00,            !- Field 49
    5.163,                   !- Field 50
    Until: 20:00,            !- Field 51
    4.676,                   !- Field 52
    Until: 21:00,            !- Field 53
    3.910,                   !- Field 54
    Until: 22:00,            !- Field 55
    4.465,                   !- Field 56
    Until: 23:00,            !- Field 57
    4.267,                   !- Field 58
    Until: 24:00,            !- Field 59
    4.290,                   !- Field 60
    Through: 12/31,          !- Field 61
    For: AllDays,            !- Field 62
    Until: 24:00,            !- Field 63
    0.1;                     !- Field 64

Schedule:Compact,
    B53S3-CHTC-12-2,         !- Name
    Any Number,    !- Schedule Type Limits Name
    Through: 9/24,           !- Field 1
    For: AllDays,            !- Field 2
    Until: 21:00,            !- Field 3
    0.1,                     !- Field 4
    Until: 22:00,            !- Field 5
    4.268,                   !- Field 6
    Until: 23:00,            !- Field 7
    5.431,                   !- Field 8
    Until: 24:00,            !- Field 9
    3.650,                   !- Field 10
    Through: 9/25,           !- Field 11
    For: AllDays,            !- Field 12
    Until: 01:00,            !- Field 13
    11.828,                  !- Field 14
    Until: 02:00,            !- Field 15
    4.168,                   !- Field 16
    Until: 03:00,            !- Field 17
    3.456,                   !- Field 18
    Until: 04:00,            !- Field 19
    3.448,                   !- Field 20
    Until: 05:00,            !- Field 21
    3.567,                   !- Field 22
    Until: 06:00,            !- Field 23
    2.575,                   !- Field 24
    Until: 07:00,            !- Field 25
    3.180,                   !- Field 26
    Until: 08:00,            !- Field 27
    3.619,                   !- Field 28
    Until: 09:00,            !- Field 29
    3.842,                   !- Field 30
    Until: 10:00,            !- Field 31
    5.029,                   !- Field 32
    Until: 11:00,            !- Field 33
    4.710,                   !- Field 34
    Until: 12:00,            !- Field 35
    7.194,                   !- Field 36
    Until: 13:00,            !- Field 37
    7.285,                   !- Field 38
    Until: 14:00,            !- Field 39
    6.891,                   !- Field 40
    Until: 15:00,            !- Field 41
    6.926,                   !- Field 42
    Until: 16:00,            !- Field 43
    6.965,                   !- Field 44
    Until: 17:00,            !- Field 45
    6.200,                   !- Field 46
    Until: 18:00,            !- Field 47
    5.072,                   !- Field 48
    Until: 19:00,            !- Field 49
    4.938,                   !- Field 50
    Until: 20:00,            !- Field 51
    4.415,                   !- Field 52
    Until: 21:00,            !- Field 53
    3.950,                   !- Field 54
    Until: 22:00,            !- Field 55
    4.424,                   !- Field 56
    Until: 23:00,            !- Field 57
    4.021,                   !- Field 58
    Until: 24:00,            !- Field 59
    4.065,                   !- Field 60
    Through: 12/31,          !- Field 61
    For: AllDays,            !- Field 62
    Until: 24:00,            !- Field 63
    0.1;                     !- Field 64

Schedule:Compact,
    B53S4-CHTC-12-2,         !- Name
    Any Number,    !- Schedule Type Limits Name
    Through: 9/24,           !- Field 1
    For: AllDays,            !- Field 2
    Until: 21:00,            !- Field 3
    0.1,                     !- Field 4
    Until: 22:00,            !- Field 5
    4.772,                   !- Field 6
    Until: 23:00,            !- Field 7
    5.512,                   !- Field 8
    Until: 24:00,            !- Field 9
    4.274,                   !- Field 10
    Through: 9/25,           !- Field 11
    For: AllDays,            !- Field 12
    Until: 01:00,            !- Field 13
    6.591,                   !- Field 14
    Until: 02:00,            !- Field 15
    4.647,                   !- Field 16
    Until: 03:00,            !- Field 17
    4.135,                   !- Field 18
```

```
Until: 04:00,                !- Field 19
4.118,                       !- Field 20
Until: 05:00,                !- Field 21
4.179,                       !- Field 22
Until: 06:00,                !- Field 23
3.461,                       !- Field 24
Until: 07:00,                !- Field 25
3.249,                       !- Field 26
Until: 08:00,                !- Field 27
3.243,                       !- Field 28
Until: 09:00,                !- Field 29
3.611,                       !- Field 30
Until: 10:00,                !- Field 31
10.960,                      !- Field 32
Until: 11:00,                !- Field 33
13.130,                      !- Field 34
Until: 12:00,                !- Field 35
8.781,                       !- Field 36
Until: 13:00,                !- Field 37
7.359,                       !- Field 38
Until: 14:00,                !- Field 39
8.183,                       !- Field 40
Until: 15:00,                !- Field 41
8.380,                       !- Field 42
Until: 16:00,                !- Field 43
8.542,                       !- Field 44
Until: 17:00,                !- Field 45
7.453,                       !- Field 46
Until: 18:00,                !- Field 47
5.890,                       !- Field 48
Until: 19:00,                !- Field 49
5.436,                       !- Field 50
Until: 20:00,                !- Field 51
4.687,                       !- Field 52
Until: 21:00,                !- Field 53
4.078,                       !- Field 54
Until: 22:00,                !- Field 55
4.769,                       !- Field 56
Until: 23:00,                !- Field 57
4.036,                       !- Field 58
Until: 24:00,                !- Field 59
4.051,                       !- Field 60
Through: 12/31,              !- Field 61
For: AllDays,                !- Field 62
Until: 24:00,                !- Field 63
0.1;                         !- Field 64

Schedule:Compact,
  B53R-CHTC-12-2,            !- Name
  Any Number,                !- Schedule Type Limits Name
  Through: 9/24,             !- Field 1
  For: AllDays,              !- Field 2
  Until: 21:00,              !- Field 3
  0.1,                       !- Field 4
  Until: 22:00,              !- Field 5
  7.441,                     !- Field 6
  Until: 23:00,              !- Field 7
  10.009,                    !- Field 8
  Until: 24:00,              !- Field 9
  6.044,                     !- Field 10
  Through: 9/25,             !- Field 11
  For: AllDays,              !- Field 12
  Until: 01:00,              !- Field 13
  7.657,                     !- Field 14
  Until: 02:00,              !- Field 15
  7.195,                     !- Field 16
  Until: 03:00,              !- Field 17
  5.805,                     !- Field 18
  Until: 04:00,              !- Field 19
  5.795,                     !- Field 20
  Until: 05:00,              !- Field 21
  5.837,                     !- Field 22
  Until: 06:00,              !- Field 23
  4.197,                     !- Field 24
  Until: 07:00,              !- Field 25
  4.187,                     !- Field 26
  Until: 08:00,              !- Field 27
  5.779,                     !- Field 28
  Until: 09:00,              !- Field 29
  5.648,                     !- Field 30
  Until: 10:00,              !- Field 31
  10.045,                    !- Field 32
  Until: 11:00,              !- Field 33
  10.170,                    !- Field 34
  Until: 12:00,              !- Field 35
  8.050,                     !- Field 36
  Until: 13:00,              !- Field 37
  12.660,                    !- Field 38
  Until: 14:00,              !- Field 39
  13.763,                    !- Field 40
  Until: 15:00,              !- Field 41
  13.789,                    !- Field 42
  Until: 16:00,              !- Field 43
  13.829,                    !- Field 44
  Until: 17:00,              !- Field 45
  11.392,                    !- Field 46
  Until: 18:00,              !- Field 47
  7.988,                     !- Field 48
  Until: 19:00,              !- Field 49
  8.740,                     !- Field 50
  Until: 20:00,              !- Field 51
  7.197,                     !- Field 52
  Until: 21:00,              !- Field 53
  5.866,                     !- Field 54
  Until: 22:00,              !- Field 55
  7.216,                     !- Field 56
  Until: 23:00,              !- Field 57
  5.951,                     !- Field 58
  Until: 24:00,              !- Field 59
  5.965,                     !- Field 60
  Through: 12/31,            !- Field 61
  For: AllDays,              !- Field 62
  Until: 24:00,              !- Field 63
  0.1;                       !- Field 64
```